UNIVERSITY OF OKLAHOMA

GRADUATE COLLEGE

# NOVEL BIOMARKER DISTRIBUTIONS IN THE CHESTERIAN LIMESTONE OF THE ANADARKO BASIN, OKLAHOMA

A THESIS

SUBMITTED TO THE GRADUATE FACULTY

in partial fulfillment of the requirements for the

Degree of

MASTER OF SCIENCE

By

MATTHEW KEVIN WOOD
Norman, Oklahoma
2017

NOVEL BIOMARKER DISTRIBUTIONS IN THE CHESTERIAN LIMESTONE OF THE ANADARKO BASIN, OKLAHOMA

A THESIS APPROVED FOR THE
CONOCOPHILLIPS SCHOOL OF GEOLOGY AND GEOPHYSICS

BY

_____
Dr. Roger M. Slatt, Chair

_____
Dr. R. Paul Philp

_____
Dr. Michael H. Engel

For Valene,

Thank you for everything

## Acknowledgements

Completing my M.S. thesis has been my single greatest academic achievement to date and was only possible through the help and support of many people over the past two years.

First, I would like to acknowledge and thank my advisor, Dr. R. Paul Philp, for his help in providing me with the necessary understanding of organic geochemistry and for encouraging me to dive into the literature to learn more. Also for his guidance with preparing and interpreting the samples used in this thesis, and for his help in refining the writing of this thesis to where it is today.

I would also like to thank Dr. Roger Slatt and Dr. Michael Engel for being on my committee and especially Dr. Slatt for serving as my committee chair. Their feedback and encouragement has been very helpful throughout the past two years.

I would like to thank Dr. Thanh Nguyen for his help with the preliminary work on the study area and for helping me better understand the lab techniques used in preparing the samples. Mr. Jon Allen and Mr. Larry Hyde were also invaluable with their constant attention to the lab and for teaching me the processes needed to produce the results presented in this thesis.

The members of the Organic Geochemistry Group were also a great asset over the past two years. I'm grateful for their encouragement and for their company in the seemingly endless trenches of schoolwork.

The faculty and staff of the ConocoPhillips School of Geology and Geophysics were a major part of my experience at the University of Oklahoma. I'm grateful for the time put into their courses and for their help with increasing my education. The geology

office staff were also very helpful and cheerful; I never failed to get a smile and encouragement whenever I was in the office.

I am indebted to my family for all of their support and encouragement throughout my studies. In particular I want to thank my wonderful wife, Valene, for her support and time. The past two years included many late nights completing course work and working on this thesis and her constant support was invaluable during them. I also want to thank her for her help with our two boys, Alden and Edmund. I love you.

# Table of Contents

## List of Tables

## List of Figures

## Abstract

18α(H)-Oleanane is a biomarker that is proposed to be derived from β-amyrin, which is produced by angiosperm plants. As such, the presence of 18α(H)-oleanane is often used as an indicator that the petroleum source is of Cretaceous age or younger. Pre-Cretaceous occurrences of 18α(H)-oleanane are rare but have been identified. 18α(H)-Oleanane, as well as an aromatic degradation product of β-amyrin, 1,2,7-trimethylnaphthalene, have been tentatively identified in the Chesterian Limestone in the Anadarko Basin in northwest Oklahoma. The presence of these compounds suggests the presence of either angiosperms themselves or another plant group capable of synthesizing precursors of oleanane and oleanane-type compounds in the depositional environment. The present study analyzed 26 source rocks from the Chesterian Limestone and 14 oil samples from other Mississippian Limestones in the Anadarko Basin. The observed tentative distribution of 18α(H)-oleanane and 1,2,7-trimethylnaphthalene in the Chesterian Limestone are presented and possible explanations for the presence of these compounds are discussed.

Unusual distributions of 17α(H)-diahopanes and 9,15-dimethyl-25,27-bisnorhopanes (another series of rearranged hopanes) are also observed in the source rock samples. Both series of rearranged hopanes closely co-vary with each other, which is likely because of their similar structures and suggests that they have similar formation processes. The rearranged hopanes are thermally more stable than the regular hopanes and are known to increase in concentration with increasing maturity. The tricyclic terpanes are also thermally more stable than the regular hopanes and are observed in unusually high abundances in the study area and even dominate the regular hopanes in

three source rock samples and in six oil samples from the study area. The corresponding 17α(H)-diahopane/17α(H)-hopane values suggest that thermal maturity plays a role in the increased abundance of the tricyclic terpanes.

The distributions of rearranged hopanes and tricyclic terpanes suggests that the oils in the Mississippian Limestones in the Anadarko Basin are not sourced from the underlying Woodford Shale. This is further confirmed by the observed presence and distribution of head-to-head isoprenoids in both the source rock and the oil samples used in the present study.

# 1. Introduction

## 1.1. Primary Purpose and Objectives

### *1.1.1. 18α(H)-Oleanane*

Oleanane is a plant derived triterpenoid and acts as a biomarker for angiosperm plants. Oleanane is frequently used to interpret both the source and age of a crude oil. There are two isomers of oleanane, 18α(H)-oleanane and 18β(H)-oleanane (Caccialanza and Riva, 1987; Riva et al., 1988). Separation of the two oleanane isomers is difficult, which caused the 18β(H)-oleanane isomer to be identified after the 18α(H)-oleanane isomer (Caccialanza and Riva, 1987). Thermal maturity also preferentially increases 18α(H)-oleanane over 18β(H)-oleanane (Riva et al., 1988). Because of the reduction of 18β(H)-oleanane with increasing thermal maturity and because the lab procedures applied in the present study would not have separated 18α(H)-oleanane and 18β(H)-oleanane, only the 18α(H)-oleanane isomer will be referenced in the remainder of this study.

18α(H)-Oleanane is formed by diagenetic and catagenetic alteration of the angiosperm triterpenoid β-amyrin and as such the presence of 18α(H)-oleanane in a crude oil indicates that the source includes higher plant material. Furthermore, since the fossil record indicates that angiosperms evolved in the early Cretaceous, their presence generally indicates that the crude oil is of Cretaceous or younger age (Figure 1; Ekweozor and Udo, 1988; Riva et al., 1988; Molodwan et al., 1994). The lack of 18α(H)-oleanane in a crude oil does not necessarily indicate that the sample is older than the Cretaceous because the preservation of 18α(H)-oleanane is highly susceptible to the conditions of the depositional environment. Murray et al. (1997) showed that 18α(H)-oleanane is enhanced in a crude oil when the initial plant material comes into

contact with seawater during early diagenesis. Contact with seawater helps reduce skeletal alteration and aromatization of 18α(H)-oleanane which occurs readily in freshwater conditions. Crude oils with low abundance of 18α(H)-oleanane are sometimes difficult to interpret due to the possible presence of compounds that are similar to 18α(H)-oleanane and that may co-elute with 18α(H)-oleanane on non-specialized gas chromatography columns. Such compounds include various $C_{30}$ hopanes, demethylated hopanes, and lupane (Alberdi and López, 2000; Nytoft et al., 2002; Taylor et al., 2005). Due to the possibility of compounds co-eluting with 18α(H)-oleanane and the difficulty in separating 18α(H)-oleanane from such compounds, it is important to note that the current identification of 18α(H)-oleanane in the samples from the Anadarko Basin presented in this study is tentative.

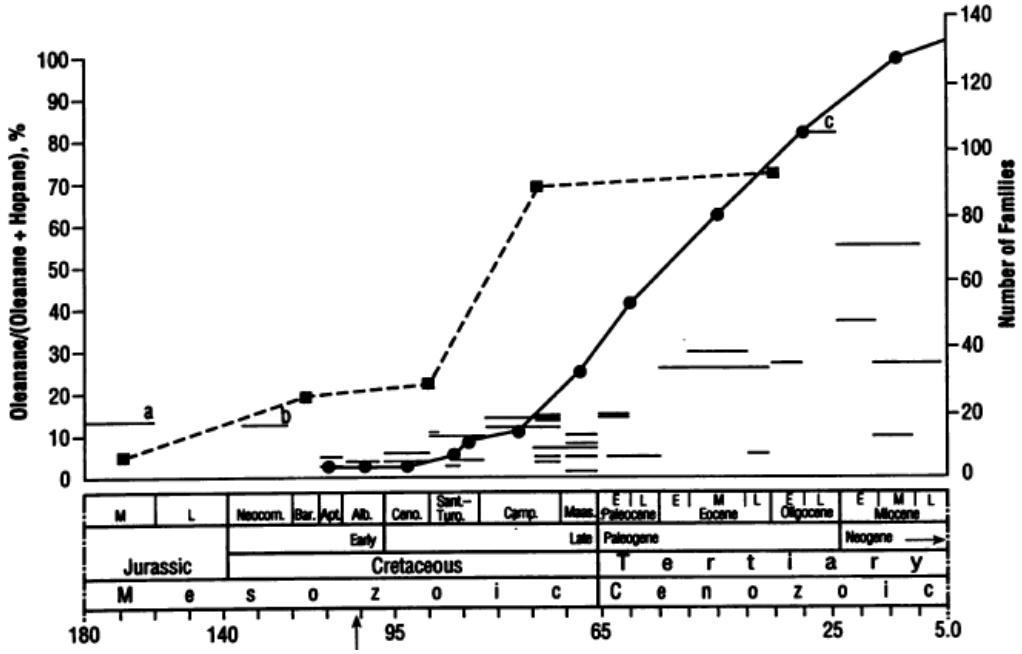


***Figure 1.*** *Plot from Moldowan et al. (1994) displaying the relative frequency of data indicative of angiosperms. The dashed line represents the occurrence of oleanane within the detectable limits set for their study and the solid line represents fossil pollens that can be assigned to angiosperm plant families. Note that fossil evidence for angiosperms begins in the Cretaceous and that both fossil and geochemical evidence increase dramatically in frequency after/during the Late Cretaceous.*

### *1.1.2. Oleanoids*

The formation of 18α(H)-oleanane represents only a small portion of the compounds that can be derived from degradation of β-amyrin (Murray et al., 1997; Chattopadhyay and Dutta, 2014). An abbreviated summary of the compounds that can be formed by diagenetic processes of β-amyrin and other related angiosperm compounds is shown in Figure 2. The pathways that form 18α(H)-oleanane, and the other saturate oleanane-type compounds, are dominated by aromatic pathways in terrestrial environments and include formation of 1,2,5-and 1,2,7-trimethylnaphthalene and 1,2,5,6-

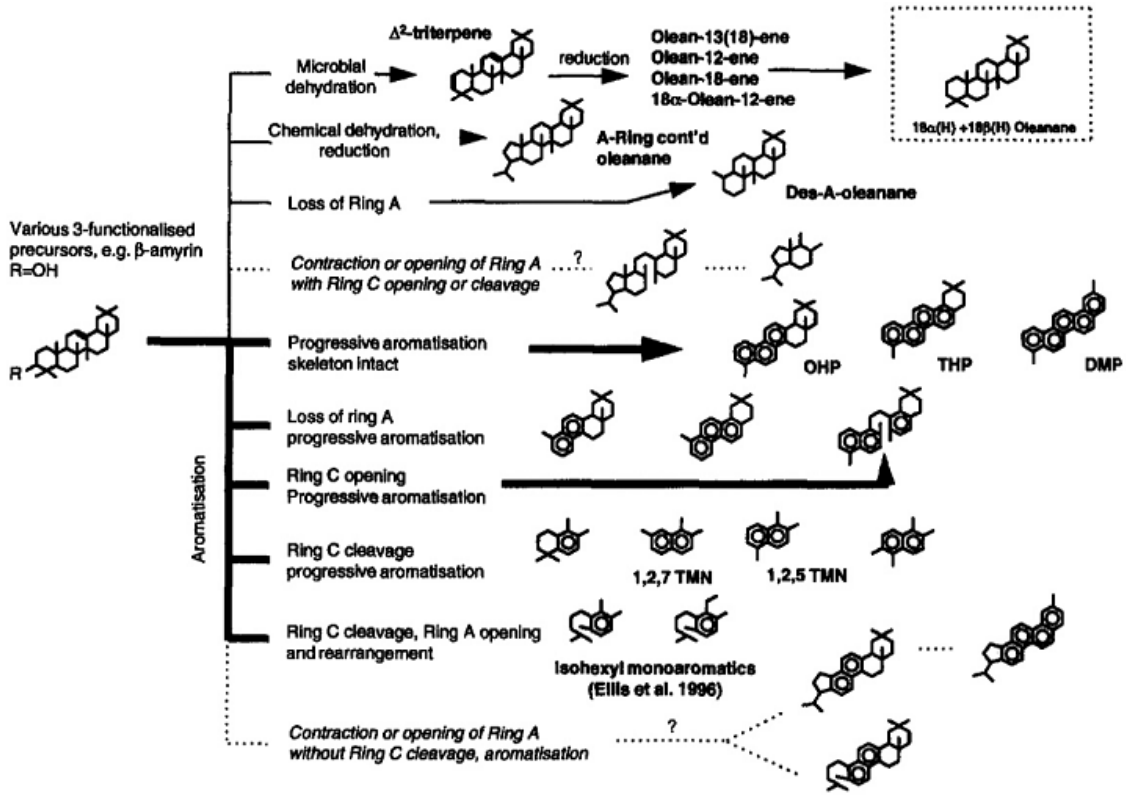


***Figure 2.*** *Illustration from Murray et al., (1997) displaying an abbreviated selection of compounds that form by degradation of β-amyrin. Bolded lines indicate the dominate pathways in terrestrial environments and the dashed lines indicate theoretical compounds that have not yet been identified in a sample. Notice that oleanane and the other saturated degradation products are not favored in terrestrial settings.*

tetramethylnaphthalene. While all three of these compounds can be formed by degradation of β-amyrin, 1,2,5-trimethylnaphthalene and 1,2,5,6-tetramethylnaphthalene are also known to be formed from other, non-angiosperm, compounds (Figure 3; Thomas, 1969; Carman and Craig, 1971; Armstroff et al., 2006;

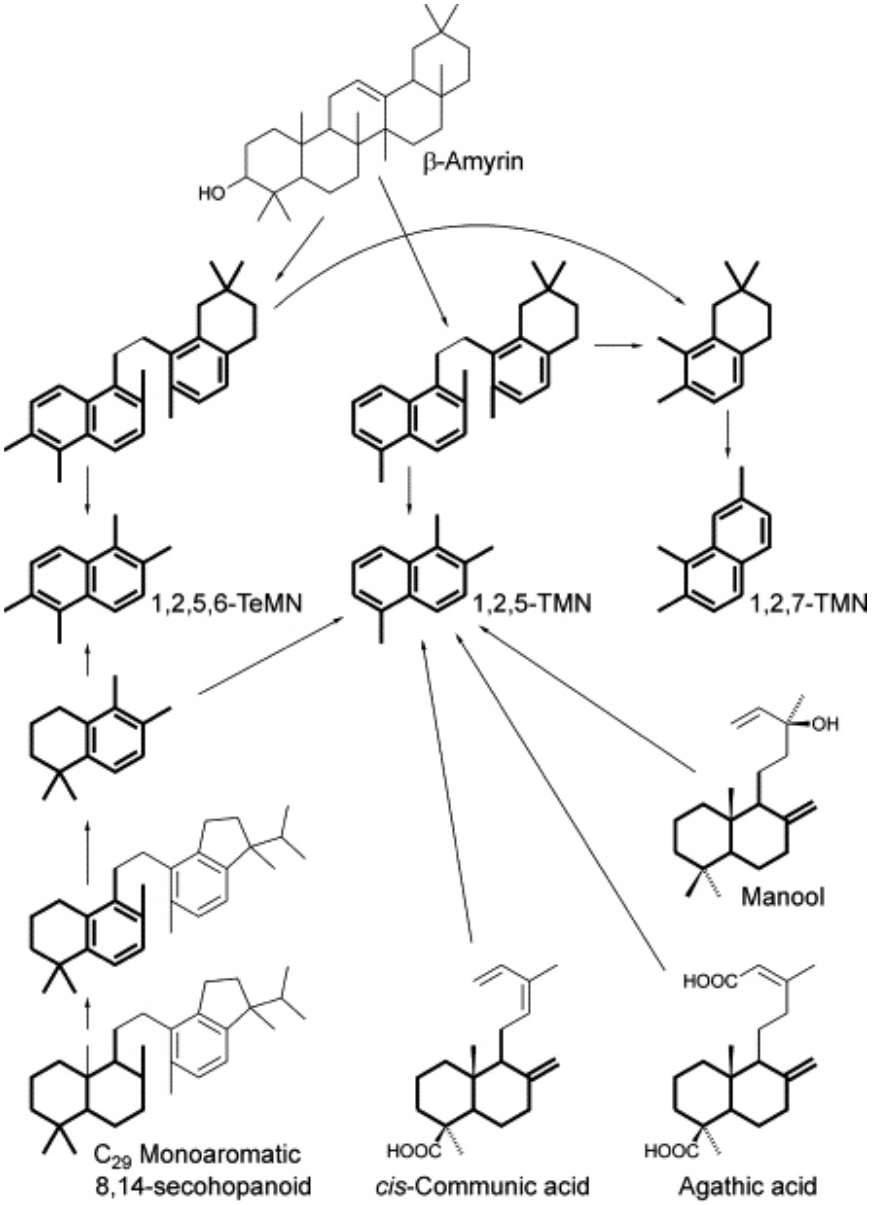


***Figure 3.*** *Diagram from Armstroff et al. (2006) illustrating some of the known pathways for synthesizing alkylnaphthalene compounds that indicate higher plant organic matter input. Note that 1,2,5,6-tetramehtylnaphthalene and 1,2,5-trimethylnaphthalene have multiple known precursors, whereas 1,2,7-trimethylnaphthalene is only derived from degradation of β-amyrin.*

Asif and Fazeelat, 2012). 1,2,7-Trimethylnaphthalene, as far as is currently known, can only be formed by degradation of β-amyrin via C-ring cleavage of the β-amyrin skeleton and aromatization of the D and E rings (the A and B rings form 1,2,5-trimethylnaphthalene) (Figure 3; Strachan et al., 1988; Heppenheimer et al., 1992; Armstroff et al., 2006). Because it is proposed that 1,2,7-trimethylnaphthalene can only be formed by degradation of β-amyrin, it is often used as a marker for angiosperm plants in the same manner as the oleananes (Püttmann and Villar, 1987; Strachan et al., 1988; Asif and Fazeelat, 2012). It is difficult to use absolute abundance levels of 1,2,7-trimethylnaphthalene due to maturity-driven isomerization reactions that can shift 1,2,7-trimethylnaphthalene to 1,3,7- trimethylnaphthalene and these reactions begin to occur at lower maturity levels than those at which 18α(H)-oleanane is affected by increasing thermal maturity (Strachan et al., 1988; Armstroff et al., 2006).

### *1.1.3. Preliminary Results*

A study on the distribution of the tricyclic terpanes in the Mississippian Limestones (specifically the Chesterian Limestone) in the Anadarko Basin was done by Kim and Philp (1999). The saturate and aromatic fractions of the source rock samples used by Kim and Philp (1999) were still available and during further analysis 18α(H)-oleanane was tentatively identified in low abundance in three saturate fractions, two from the Flint core and one from the Jacob Betz core (star icons in Figure 8). 1,2,7-Trimethylnaphthalene was also identified in the same three samples as well as other samples from this study. Because 18α(H)-oleanane was in low abundance, and unexpected, it was further confirmed by gas chromatography/mass spectrometry/mass spectrometry (GC/MS/MS) analysis, interpreting the 412 to 191 and 412 to 369 parent-

daughter transitions. The 412 to 191 transition was selected because 18α(H)-oleanane has a molecular mass of 412 and 191 is its dominate fragment ion. Lupane co-elutes with 18α(H)-oleanane and also has a molecular mass of 412 and a dominant 191 fragment ion. However, lupane also has a 369 fragment ion that 18α(H)-oleanane does not produce, thus interpreting both the 412 to 191 and the 412 to 369 parent-daughter transitions was necessary to further confirm the presence of 18α(H)-oleanane. A co-injection was also done with an oil from Malaysia that was known to contain a high abundance of 18α(H)-oleanane (Figure 4). Both the GC/MS/MS and the co-injection analysis indicated that 18α(H)-oleanane was present in the Chesterian Limestone. The identification of 18α(H)-oleanane and 1,2,7-trimethylnaphthalene in the Chesterian Limestone was unexpected and did not agree with the current understanding of how 18α(H)-oleanane and oleanoid compounds are formed and where/when they are to be found. The purpose of the present study was to conduct additional source rock sampling within the Chesterian Limestone in the Anadarko Basin near the Flint and Jacob Betz cores with the objective of determining if 18α(H)-oleanane and 1,2,7-trimethylnaphthalene are present in the additional samples and if so, to identify a preliminary distribution of these compounds within the Anadarko Basin.

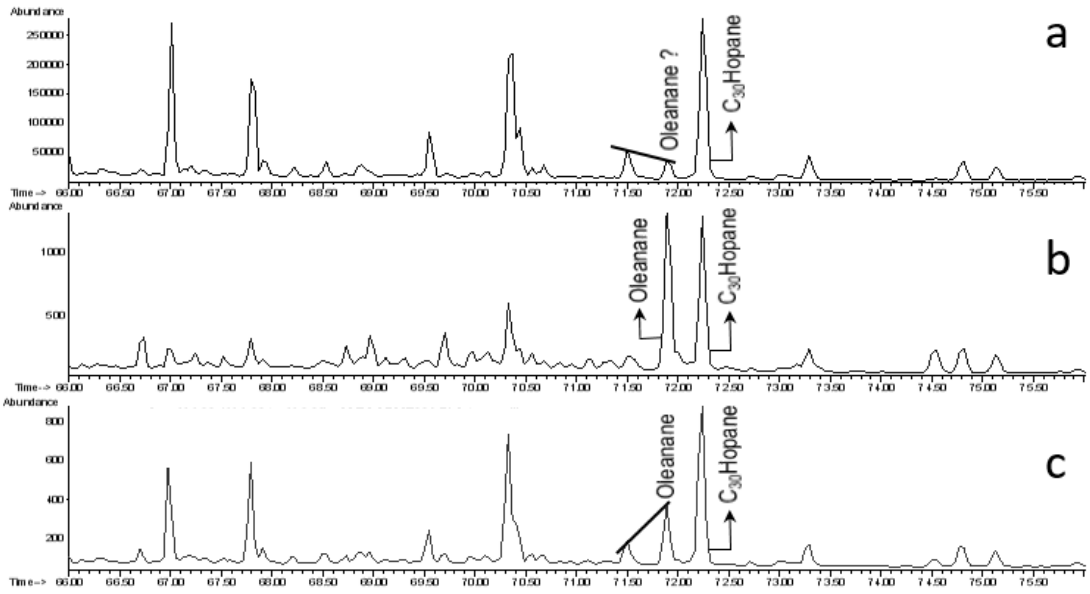


***Figure 4.*** *M/z 191 chromatograms illustrating preliminary identification of 18α(H)-oleanane by co-injection. (a) shows the Chesterian Limestone source rock sample containing the peak suspected to be 18α(H)-oleanane. (b) shows a Malaysian oil known to contain a high abundance of 18α(H)-oleanane relative to the $C_{30}$ hopane. (c) shows the co-injection of a and b (3:1). The relative increase in abundance of the suspect peak between a and c indicates that the suspect peak matches the 18α(H)-oleanane peak in the Malaysian oil.*

## 1.2. Additional Biomarker Analysis

The samples used in the present study were also analyzed for the presence of other biomarkers; including tricyclic terpanes, diahopanes, and 9,15-dimethyl-25,27-bisnorhopanes (an additional series of rearranged hopanes).

Previous studies have shown an unusually high abundance of tricyclic terpanes in the Mississippian aged rocks of the Anadarko Basin (Wang, 1993; Kim and Philp, 1999; Pearson, 2016). This distribution is also observed to varying degrees in the source rock and oil samples used in this study. Potential linkages of this unusual distribution to thermal maturity were also observed and will be discussed below.

17α(H)-Diahopane is another compound that exhibited an unusual distribution in the study area. Initially observed by Philp and Gilbert (1986), 17α(H)-diahopane was later identified in further detail through NMR techniques and determined to be a member of a series of rearranged hopanes by Moldowan et al. (1991). The formation of diahopanes requires clay minerals to be present and is typically associated with significant input of terrestrial organic matter (Volkman et al., 1983; Philp and Gilbert, 1986; Moldowan et al., 1991). It is unusual for carbonate depositional systems to contain significant levels of diahopane and thus it was unexpected to observe relatively high abundances of diahopanes throughout the source rock and oil samples used in this study on the Chesterian Limestone. Similar abundances of 9,15-dimethyl-25,27-bisnorhopanes were also observed throughout the study area. Both the diahopanes and the 9,15-dimethyl-25,27-bisnorhopanes have been reported to be widely distributed in the overlying Springer Group and Morrow Formation (Wang, 1993; Sumer Gorenekli, 2017). The 9,15-dimethyl-25,27-bisnorhopanes are an additional series of rearranged hopanes which were previously identified as the early eluting series of rearranged hopanes (Killops and Howell, 1991; Telnæs et al., 1992; Farrimond and Telnæs 1996) the structure of this series was later identified by Nytoft et al. (2007) and named the 9,15-dimethyl-25,27-bisnorhopanes.

The distribution of the n-alkanes and the isoprenoids were also analyzed and used to determine aspects of the depositional environment. The presence of an unidentified, unusual aromatic compound which is observed to elute between the methylphenanthrene isomer pairs in the gas chromatogram of the aromatic fractions is

also reported. This unknown compound was selected because of its unusual location in the gas chromatograms of the aromatic fractions of the source rock samples.

### 1.3. Geologic Background of the Chesterian Limestone

The Anadarko Basin is located in west-central Oklahoma and is one of the major geologic provinces of Oklahoma (Figure 5). The Anadarko Basin is bounded to the west and the north by the Anadarko Shelf, and to the east by the Anadarko Shelf and the Nemaha Uplift. The Anadarko Basin abuts to the Ardmore Basin to the southeast and is bounded by the Wichita Uplift (Amarillo Uplift in Texas) to the south and southwest (Johnson, 1989; Charpentier, 2001).

The Anadarko Basin is one of deepest Paleozoic basins in North America, with sediment accumulations up to 40,000 feet thick in the deeper portions of the basin (Johnson, 1989). The Anadarko Basin is asymmetric with the basin axis running northwest, paralleling the Amarillo-Wichita Uplift which acts as the southern border of

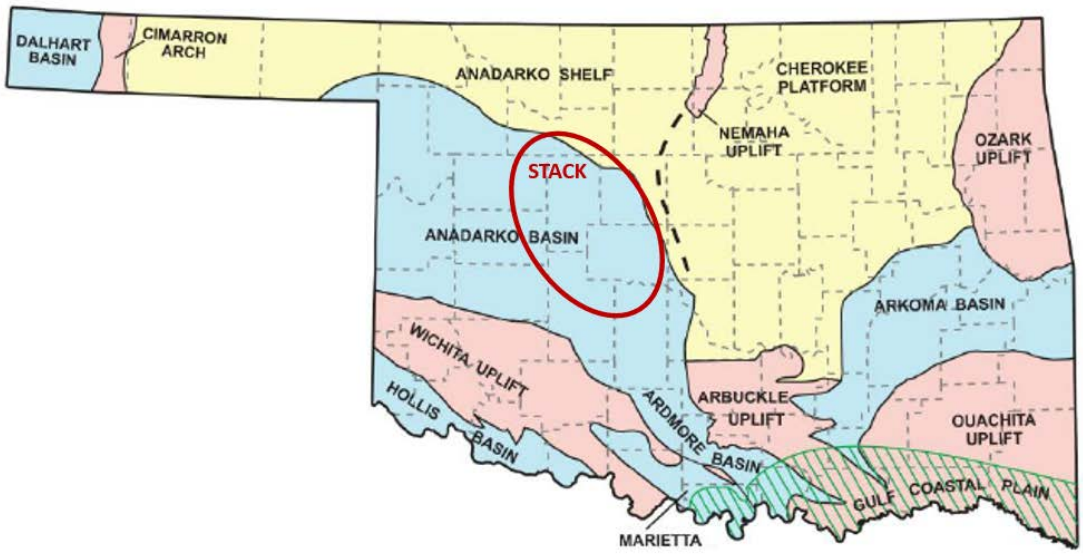


***Figure 5.*** *Geologic provinces of Oklahoma. The Anadarko Basin is located in the west central portion of the state. The STACK production area is approximated by the red oval. Modified from Johnson (2008).*

the basin. The steep limb of the basin is adjacent to the Amarillo-Wichita Uplift (Figure 6). The earliest development of the Anadarko Basin began with the formation of the South Oklahoma Aulacogen, which was an epicontinental sea formed by the abandoned arm of a major triple junction rift system that was active during the late Precambrian through the early Cambrian (Johnson, 1989; Cardott and Caplin, 1993). The principal tectonic events of the basin occurred during the Wichita orogeny, from the late Morrowan until early Desmoinesian (Rascoe and Adler, 1983; Johnson, 1989).

The Anadarko Basin contains numerous hydrocarbon producing intervals, with thick, dark shales of primarily Devonian and early Mississippian age forming the primary hydrocarbon source intervals (Johnson, 1989). This region is called the STACK

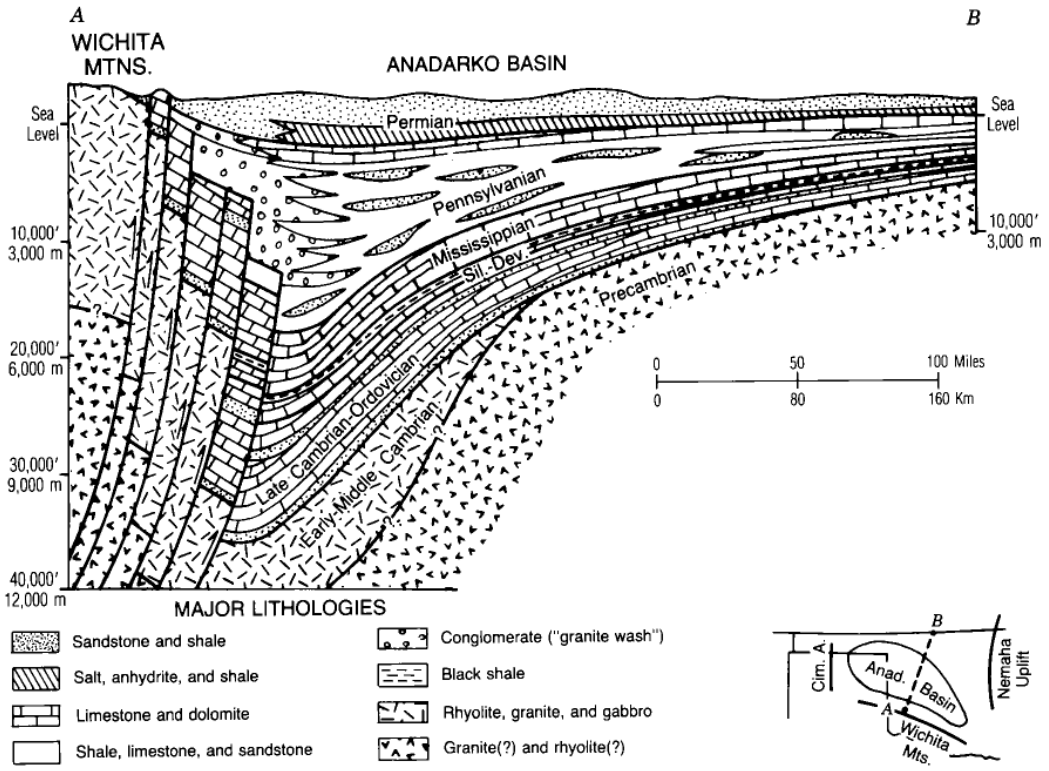


***Figure 6.*** *Generalized cross section of the Anadarko Basin illustrating the asymmetric nature of the basin and the deep depocenter along its southern margin. Also note the relatively conformable stratigraphy of the Mississippian Limestones (Johnson, 1989).*

(Sooner Trend (oil field) Anadarko (basin) Canadian and Kingfisher(counties)) and has been an active region for hydrocarbon exploration for decades, with particular emphasis being placed on the prolific Woodford Shale (Slatt et al., 2011). The Woodford Shale is overlain by the Mississippian Limestones, of which the Chesterian Limestone is the uppermost interval (Figure 7).

The Chesterian Limestone has been characterized as a shallow marine platform carbonate deposit (Hendrickson et al., 2001), interbedded with calcareous, grey shale beds (Peace and Forgotson, 1991) which have been suggested to have a mixed sedimentary and volcanic origin (Weaver, 1958). The Chesterian Limestone thins depositionally basinward and reaches its thinnest point along its southern boundary where the carbonate platform was progressively drowned as the Springer Group sands and black shales transgressed northward over the backstepping Chesterian facies (Peace and Forgotson, 1991). The Chesterian Limestone is overlain by the Pennsylvanian Springer Group and Morrow Formation and overlays the Mississippian Meramec Formation (Figure 7).

As mentioned previously, the Chesterian Limestone is one of the intervals in the STACK area of the Anadarko Basin which historically has been thought to have received the majority of its hydrocarbon content from the underlying Woodford Shale. The biomarker analysis presented in the present study may provide additional insight into a better understanding of the source of the hydrocarbons in the Anadarko Basin; particularly in recognizing differences between hydrocarbons sourced from the Woodford Shale and hydrocarbons sourced from the Mississippian Limestone(s), particularly from within the Chesterian interval.

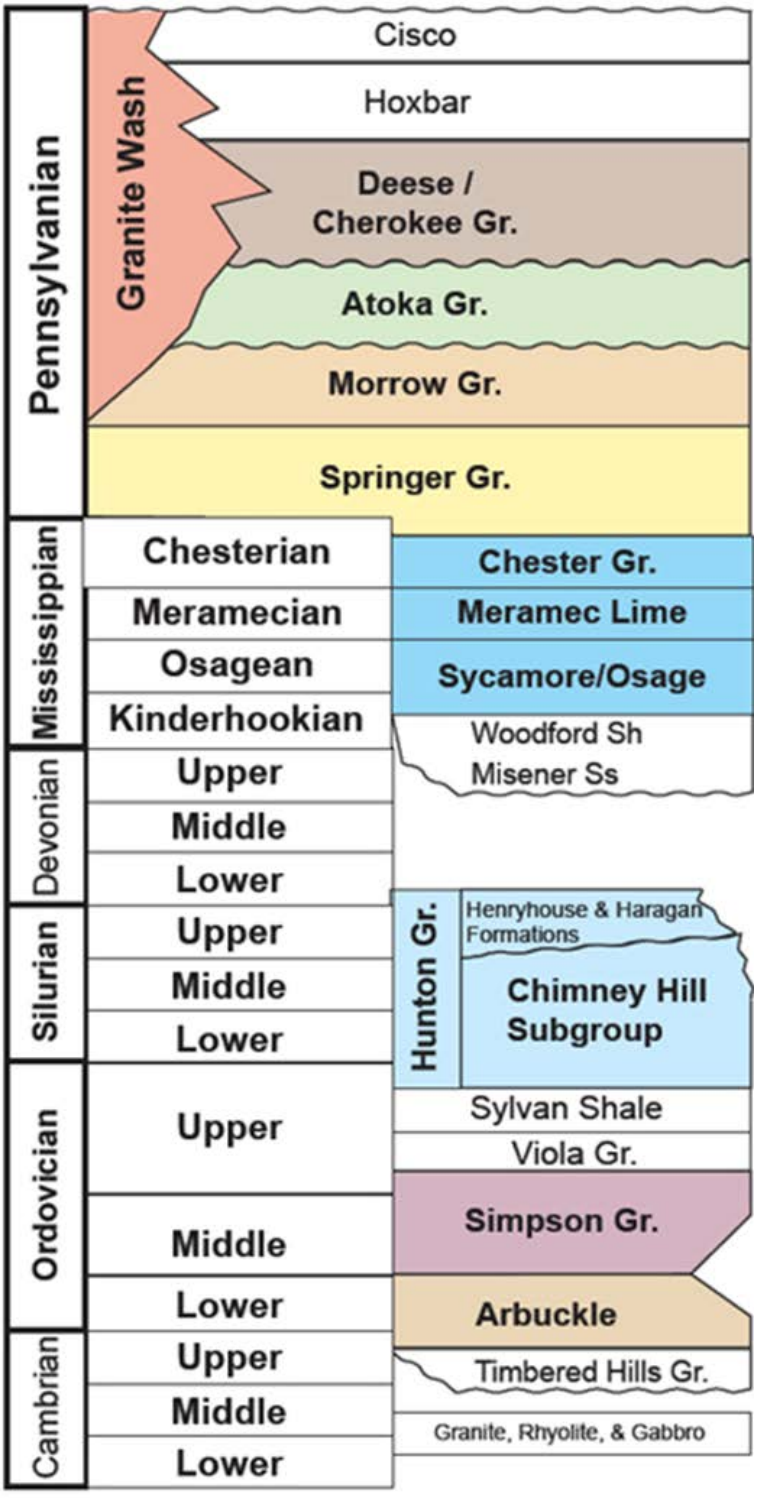


***Figure 7.*** *Generalized stratigraphic column of the Anadarko Basin from Rose (2004).*

# 2. Methodology

## 2.1. Sample Data Sets

### *2.1.1. Sample Locations*

There are three groups of samples for this project. The first sample group is from the work of a previous M.S. thesis by Dongwon Kim (Kim and Philp, 1999), the samples used from this study were from the Flint and Jacob Betz cores (star icons on Figure 8). The second sample group includes 26 source rock samples selected from six cores at the Oklahoma Petroleum Information Center (OPIC) (yellow icons in Figure 8). The third sample group includes 14 oil samples from within the Anadarko Basin with Mississippian targets below the Chesterian Limestone. Because of proprietary reasons the oil samples are not included on any maps.

### *2.1.2. Sample Selection*

Source rock sampling was done to determine the presence or absence of 18α(H)-oleanane and oleanane-type compounds within the Chesterian Limestone in the Anadarko Basin. A total of 26 source rock samples were selected from the Oklahoma Petroleum Information Center (OPIC) core library based on sampling availability in the Chesterian interval and on geographic proximity to the Flint and Jacob Betz cores from Kim and Philp (1999). Well log interpretations were done to correlate the depths of the samples where 18α(H)-oleanane was tentatively identified from the Flint and Jacob Betz cores to the other Chesterian cores available through OPIC. Sampling locations were based on these well log correlations and additional sampling was done in intervals appearing to have relatively higher organic content.

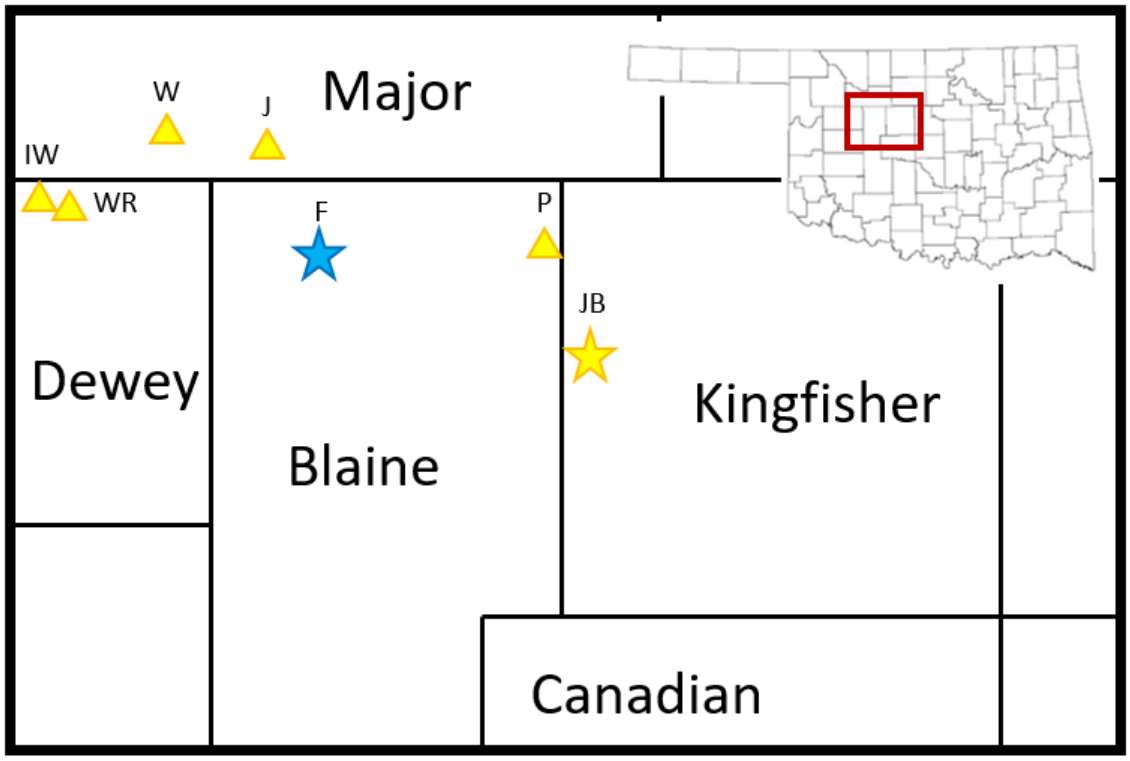


***Figure 8.*** *Map showing locations of the samples used in this study. The two star icons represent the cores from Kim and Philp (1999) that were reinterpreted and were tentatively found to contain 18α(H)-oleanane. The yellow icons indicate the cores where further source rock sampling was conducted for this study. The Jacob Betz well (yellow star) was sampled from in both studies. IW=Ivan Ward 3-4 core; WR=White Rabbit 2-3 core; W=Wilmott 1 core; J=W. H. Janzen 1 core; F=Flint 1-34 core; P=Pavlu 1 core; JB=Jacob Betz 1 core. The oil samples are not shown because of proprietary reasons.*

## 2.2. Experimental

### *2.2.1. Sample Preparation*

The source rock samples were washed with Neutrad labware detergent and water to remove marker and other surface contaminants. After the initial wash they were rinsed with deionized water and methanol, followed by dichloromethane to remove any water and foreign organic material. The samples were allowed to air dry in atmospheric conditions for at least 24 hours prior to crushing and then pulverized to 40 mesh powder using a ceramic mortar and pestle.

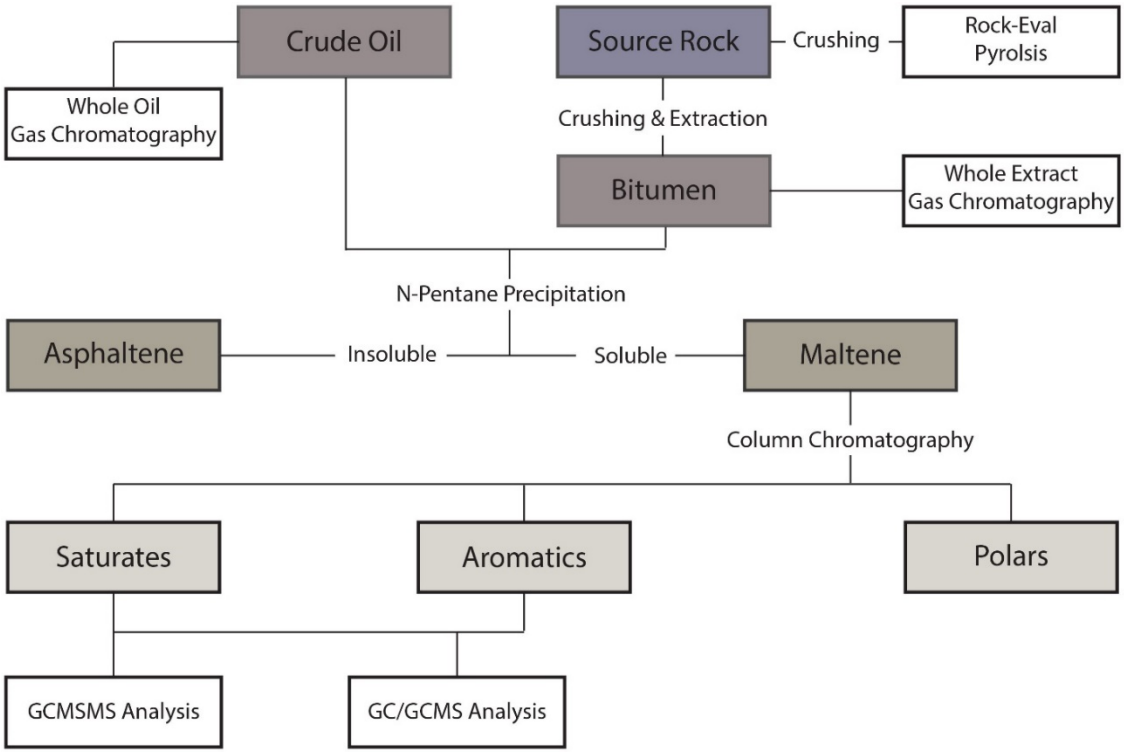


***Figure 9.*** *Schematic workflow of the lab procedure used in this study.*

### *2.2.2. Extraction*

Organic material was extracted from the source rock samples using a soxhlet extraction method. Approximately 50g of powdered sample was placed in a cellulose thimble, pre-extracted for at least 18 hours and the sample extraction was run for at least 24 hours. Both processes used a 1:1 mixture of dichloromethane (DCM) and methanol (MeOH) solvent. A ball of rolled copper thread was also pre-extracted and used to remove any elemental sulfur from the sample. The resulting extract was rotary evaporated using a Yamato Hi tec RE-51 Rotary Evaporator and attached BM-51 water bath. The sample extracts were then transferred to a pre-weighed 20 mL vial using DCM and blown to dryness under nitrogen stream using an Organomation Meyer N-Evap Model 112 Analytical Evaporator. The resulting extract weight was measured

using a R200D Sartorius Analytical Balance and the amount of extract recovered from each source rock sample is given in Table 1.

### *2.2.3. Asphaltene Separation*

Using minimal DCM (> 5mL) the sample extracts were transferred to a 50mL centrifuge tube and an excess of n-pentane added, dropwise for approximately the first 5 mL, then more rapidly until it reached the shoulder of the centrifuge tube. The sample was placed in a freezer for at least 8 hours and then centrifuged using a Damon Model K Centrifuge. The supernatant liquid in the centrifuge tube was decanted into a round bottle, and the remaining precipitated asphaltene was transferred to a 4mL vial using DCM. The asphaltenes were dried under nitrogen stream and weighed. The maltenes (extract minus the asphaltenes) were rotary evaporated to remove the pentane, then transferred to a 4mL vial using DCM and dried under nitrogen stream and the weights were measured. Asphaltenes were also isolated from the oils using at least 150mg of each oil. Yields from all samples are given in Table 1. Samples that contained low amounts of extract (less than 35mg) were not de-asphalted to prevent additional loss of material. Samples WR8348 and J7798 were already de-asphalted before this limit was applied (Table 1).

| Sample Name | Extract (mg) | Asphaltene (mg) | Maltene (mg) |
|---|---|---|---|
| **WR8318** | 44.81 | 2.81 | 30.86 |
| **WR8322** | 50.31 | 5.67 | 43.63 |
| **WR8342** | 71.39 | 7.18 | 22.69 |
| **WR8348** | 13.76 | 0.94 | 10.92 |
| **WR8364** | 78.50 | 3.67 | 15.85 |
| **J7781** | 2.55 | * | 0.79 |
| **J7788** | 3.96 | * | 2.77 |
| **J7798** | 5.22 | 3.24 | 1.93 |
| **J7816** | 7.45 | * | 7.21 |
| **P7785** | 110.71 | 56.05 | 47.11 |
| **W8147** | 11.96 | * | 7.49 |
| **W8148** | 7.49 | * | 3.20 |
| **W8150** | 45.57 | 18.04 | 25.48 |
| **W8155** | 8.45 | * | 3.68 |
| **W8156** | 16.41 | * | 14.98 |
| **IW8317** | 43.70 | 1.90 | 9.80 |
| **IW8320** | 22.29 | * | 17.20 |
| **IW8330** | 14.50 | * | 10.24 |
| **IW8334** | 56.00 | 2.08 | 45.79 |
| **IW8335** | 38.62 | 3.06 | 30.92 |
| **IW8339** | 21.94 | * | 21.09 |
| **IW8365** | 130.94 | 28.69 | 76.68 |
| **IW8406** | 11.70 | * | 10.49 |
| **JB7868** | 5.95 | * | 5.51 |
| **JB7889** | 33.49 | * | 12.28 |
| **JB7912** | 266.08 | 6.64 | 222.27 |
| **Oil 1 **** | 182 | 0.00 | 70.16 |
| **Oil 2** | 192 | 0.00 | 105.91 |
| **Oil 3** | 153 | 0.00 | 88.07 |
| **Oil 4** | 171 | 0.00 | 64.75 |
| **Oil 5** | 219 | 0.00 | 135.60 |
| **Oil 6** | 180 | 0.00 | 101.90 |
| **Oil 7** | 201 | 0.00 | 128.82 |
| **Oil 8** | 207 | 0.00 | 121.29 |
| **Oil 9** | 179 | 0.00 | 92.11 |
| **Oil 10** | 192 | 0.00 | 132.15 |
| **Oil 11** | 204 | 0.00 | 110.39 |
| **Oil 12** | 235 | 0.00 | 152.70 |
| **Oil 13** | 180 | 0.00 | 89.83 |
| **Oil 14** | 184 | 0.00 | 85.31 |

***Table 1.*** *Total extracts recovered from source rock extraction (value given for oil samples is the initial amount of crude oil). Amount of asphaltenes separated from the extract or crude oil and the resulting total maltene per sample. Resulting maltene weight was also impacted by loss of volatiles from the crude oil and the removal of copper oxide from the extracts.*
** indicates that there was not enough extract to de-asphalt the sample.*

### *2.2.4. Column Chromatography*

The maltenes were diluted to a known concentration by adding DCM (200µL for the source rock extracts and 600µL for the oil samples) and the amount to be used for fractionation was transferred to a separate 4 mL vial and blown to dryness under nitrogen stream. Column chromatography was used to fractionate the samples into saturate, aromatic, and NSO (polar) fractions. Two column sizes were used to accommodate different sample amounts (Table 2). Both column chromatography methods were designed by Dr. Thanh Nguyen and were determined to be equivalent methods. The columns were packed in a Kimble 5 3/4" monster pipette with A540-3 alumina adsorption 80-200 mesh powder (1.8g and 3.8g for smaller and larger sample amounts respectively) and pre-extracted glass wool as a support at the base of the column. The column was wetted and cleaned using excess hexane. The maltenes (approximately 9mg and 17mg maltenes for the smaller and larger column sizes respectively) were dissolved in hexane (150-200µL) and allowed to fully infiltrate the top of the alumina column. Hexane (4.5mL and 8.5mL for respective column sizes) was used to elute the saturate fraction; a 7:3 mixture of hexane and DCM (18mL and 25mL for respective column sizes) was used to elute the aromatic fraction; and finally, a 98:2 mixture of chloroform and methanol (18mL and 25mL for respective column sizes) was used to elute the NSO (polar) fraction. Excess solvent was removed by rotary evaporation from each fraction and the remainder was transferred via DCM to a 4mL vial. Each fraction was dried under nitrogen stream and weighed.

Some samples were fractionated from whole extracts. These were extracts that were determined to not have enough material to de-asphalt (less than 35 mg total

extract) but did have enough material to load a column for fractionation (at least 8 mg total extract). These samples are marked in Table 2 with ** but also show a value for the amount fractionated.

It is also important to note that the majority of the source rock samples contained material that was dissolved by DCM (which was used to prepare the maltenes and extracts for fractionation) but that was not dissolved by hexane (which was used to load the sample onto the column). This resulted in a residue that was not introduced to the column but was included in the initial amount prepared for the column. To account for this difference the residue was dried and weighed, and this weight was subtracted from the amount prepared to get the amount fractionated (Table 2). The percentages shown in Table 3 are calculated from the amount fractionated, not the amount prepared. The extracts that were not de-asphalted contained higher residue amounts than the extracts that were de-asphalted, suggesting that the residue was composed of asphaltenes and other high molecular weight or polar compounds. The oil samples did not leave any residue.

### *2.2.5. Molecular Sieve*

The saturate fractions of samples JB7912 and Oil 7 were selected for molecular sieving. The molecular sieve was done by packing a glass pipette with UOP brand S-115 powder molecular sieves. Pre-extracted glass wool was used as a support at the base of the pipette. The molecular sieves were washed with excess pentane. The saturate fraction was dissolved in pentane and introduced to the molecular sieves. Air flow was applied to the top of the pipette to push the saturate fraction and excess pentane through the molecular sieves. The sample was collected in a 4 mL vial and was

| Sample Name | Total maltene (mg) | Amount prepared (mg) | Amount fractionated (mg) | Column size |
|---|---|---|---|---|
| **WR8318** | 30.86 | 9.49 | 8.89 | S |
| **WR8322** | 43.63 | 7.74 | 7.14 | S |
| **WR8342** | 6.01 | * | * | * |
| **WR8348** | 10.92 | 9.02 | 8.19 | S |
| **WR8364** | 15.85 | 8.77 | 7.02 | S |
| **J7781** | 0.79 ** | * | * | * |
| **J7788** | 2.77 ** | * | * | * |
| **J7798** | 1.93 | * | * | * |
| **J7816** | 7.21 ** | * | * | * |
| **P7785** | 47.11 | 18.08 | 18.04 | L |
| **W8147** | 7.49 ** | * | * | * |
| **W8148** | 3.2 ** | * | * | * |
| **W8150** | 25.48 | 17.09 | 12.26 | L |
| **W8155** | 3.68 ** | * | * | * |
| **W8156** | 14.98 ** | 9.01 | 6.20 | S |
| **IW8317** | 9.80 | 8.08 | 5.96 | S |
| **IW8320** | 17.2 ** | 9.29 | 5.33 | S |
| **IW8330** | 10.24 ** | 7.93 | 3.63 | S |
| **IW8334** | 45.79 | 17.89 | 17.75 | L |
| **IW8335** | 30.92 | 16.65 | 15.77 | L |
| **IW8339** | 21.09 ** | 17.23 | 10.25 | L |
| **IW8365** | 76.68 | 17.96 | 16.79 | L |
| **IW8406** | 10.49 ** | 7.87 | 5.96 | S |
| **JB7868** | 5.51 ** | * | * | * |
| **JB7889** | 12.28 ** | 8.64 | 7.16 | S |
| **JB7912** | 222.27 | 18.49 | 18.09 | L |
| **Oil 1** | 88 | 8.17 | 8.17 | S |
| **Oil 2** | 65 | 7.87 | 7.87 | S |
| **Oil 3** | 70 | 8.52 | 8.52 | S |
| **Oil 4** | 121 | 8.01 | 8.01 | S |
| **Oil 5** | 110 | 7.83 | 7.83 | S |
| **Oil 6** | 92 | 8.26 | 8.26 | S |
| **Oil 7** | 85 | 7.88 | 7.88 | S |
| **Oil 8** | 90 | 7.58 | 7.58 | S |
| **Oil 9** | 153 | 7.07 | 7.07 | S |
| **Oil 10** | 102 | 8.70 | 8.70 | S |
| **Oil 11** | 106 | 8.38 | 8.38 | S |
| **Oil 12** | 136 | 7.33 | 7.33 | S |
| **Oil 13** | 132 | 7.33 | 7.33 | S |
| **Oil 14** | 129 | 9.11 | 9.11 | S |

***Table 2.*** *Total maltenes recovered from extraction of source rock samples and weights of maltene used for fractionation of the sample. Column size used for each sample. S=smaller column size (approximately 9 mg of maltene) L=larger column size (approximately 17 mg of maltene). * indicates that the maltene was not fractionated. ** indicates that the sample remained as a whole extract, not enough material to de-asphalt.*

blown to dryness under nitrogen stream. The recovered sample was then weighed, diluted in DCM and run under the same analysis program as the other saturate fractions.

### *2.2.6. Gas Chromatography (GC)*

Gas chromatography was used for a preliminary analysis of the saturate and aromatic fractions. Total extracts from source rocks that did not contain enough material to fractionate were also screened using GC (Table 2) as well as the whole oils. All samples were diluted to 3mg/mL in DCM and analyzed using an Agilent 6890 GC fitted with a DB-5MS silica column (60m length 0.32mm diameter serial number 8859113). The injection was splitless with a temperature program starting at 40°C, the initial temperature was held for 1.5 minutes, then ramped to 300 °C at 4°C per minute. The final temperature was held for 14.0 minutes with a total time of 80.5 minutes. Helium was used as the carrier gas at a constant flow of 1.4 mL/min.

### *2.2.7. Gas Chromatography/Mass Spectrometry (GC/MS)*

Gas chromatography/mass spectrometry was performed using an Agilent 7890A GC fitted with a DB-5MS silica column (60m x 250µm x 0.25µm, serial number USF674011H) interfaced to an Agilent 5975C XL MSD mass spectrometer. The temperature program initially held at an initial temperature of 40°C for 1.5 minutes, then ramped at 4°C per minute to 300°C and held there for 34 minutes for a total run time of 100.5 minutes. The injection method was splitless with a helium flow rate of 1.4 mL/min. Saturate and aromatic fractions, as well as total extracts for samples that were not fractionated and whole oils were analyzed by GC/MS at a concentration of 3mg/mL in DCM.

#### *2.2.8. Gas Chromatography/Mass Spectrometry/Mass Spectrometry (GC/MS/MS)*

Select saturate fractions were analyzed using GC/MS/MS using a Thermo Scientific Trace 1310 gas chromatograph coupled with a TSQ 8000 triple quadrupole mass spectrometer. The initial GC temperature program was 40°C for 1.50 minutes then ramped at 4°C per minute up to 300°C and held for 34 minutes using helium as carrier gas. The MS transfer line and the ion source were held at 300°C and argon was used as the collision gas.

## 3. Results

### 3.1. Fraction Yields

Yields from the fractionation of the source rock and oil samples are shown in Table 3. The source rock samples typically had a higher aromatic and polar content than the oil samples, which had a higher saturate content. The observed fraction yields are consistent with previous studies which have reported that the asphaltenes and other high molecular weight compounds are preferentially retained in the source rock when oil is expelled (Dahl and Speers, 1986; Wilhelms and Larter, 1994a; Wilhelms and Larter, 1994b, Hunt, 1996). The process of preferentially retaining the higher molecular weight compounds in the source rock has been called natural deasphalting (Hunt, 1996) and has been observed to cause up to a 60 wt% difference in asphaltene content between a source rock and its expelled oil (Wilhelms and Larter, 1994a; 1994b). Natural deasphalting is likely the cause of the oils in the Anadarko Basin containing fewer asphaltenes, (Table 1) aromatic and polar compounds (Table 3) than the source rocks.

| Sample Name | SAT (mg) | ARO (mg) | NSO (mg) | % SAT | % ARO | % NSO |
|---|---|---|---|---|---|---|
| **WR8318** | 4.85 | 1.46 | 1.21 | 54.6 | 16.4 | 13.6 |
| **WR8322** | 3.51 | 1.29 | 1.01 | 49.2 | 18.1 | 14.1 |
| **WR8342** | * | * | * | * | * | * |
| **WR8348** | 6.36 | 1.66 | 1.28 | 77.7 | 20.3 | 15.6 |
| **WR8364** | 4.34 | 1.15 | 0.68 | 61.8 | 16.4 | 9.7 |
| **J7781** | * | * | * | * | * | * |
| **J7788** | * | * | * | * | * | * |
| **J7798** | * | * | * | * | * | * |
| **J7816** | * | * | * | * | * | * |
| **P7785** | 14.50 | 2.18 | 1.61 | 80.4 | 12.1 | 8.9 |
| **W8147** | * | * | * | * | * | * |
| **W8148** | * | * | * | * | * | * |
| **W8150** | 4.89 | 4.13 | 2.01 | 39.9 | 33.7 | 16.4 |
| **W8155** | * | * | * | * | * | * |
| **W8156** | 3.11 | 1.05 | 0.95 | 50.2 | 16.9 | 15.3 |
| **IW8317** | 2.26 | 1.49 | 1.06 | 37.9 | 25.0 | 17.8 |
| **IW8320** | 2.53 | 1.23 | 0.90 | 47.5 | 23.1 | 16.9 |
| **IW8330** | 1.57 | 1.24 | 0.69 | 43.3 | 34.2 | 19.0 |
| **IW8334** | 10.65 | 2.05 | 2.17 | 60.0 | 11.5 | 12.2 |
| **IW8335** | 10.62 | 2.21 | 2.39 | 67.3 | 14.0 | 15.2 |
| **IW8339** | 5.43 | 2.10 | 1.58 | 53.0 | 20.5 | 15.4 |
| **IW8365** | 9.44 | 2.07 | 2.59 | 56.2 | 12.3 | 15.4 |
| **IW8406** | 3.11 | 1.41 | 1.11 | 52.2 | 23.7 | 18.6 |
| **JB7868** | * | * | * | * | * | * |
| **JB7889** | 4.35 | 0.99 | 0.96 | 60.8 | 13.8 | 13.4 |
| **JB7912** | 15.05 | 1.60 | 1.61 | 83.2 | 8.8 | 8.9 |
| **Oil 1** | 7.01 | 0.68 | 0.12 | 82.3 | 8.0 | 1.4 |
| **Oil 2** | 6.71 | 1.08 | 0.25 | 83.6 | 13.4 | 3.1 |
| **Oil 3** | 6.93 | 0.70 | 0.19 | 84.8 | 8.6 | 2.3 |
| **Oil 4** | 7.10 | 0.63 | 0.00 | 90.2 | 8.0 | 0.0 |
| **Oil 5** | 5.16 | 0.87 | 0.48 | 75.3 | 12.7 | 7.0 |
| **Oil 6** | 6.97 | 1.15 | 0.38 | 80.1 | 13.2 | 4.4 |
| **Oil 7** | 7.97 | 1.41 | 0.36 | 90.5 | 16.0 | 4.1 |
| **Oil 8** | 6.96 | 0.61 | 0.04 | 86.9 | 7.6 | 0.5 |
| **Oil 9** | 6.35 | 1.02 | 0.14 | 76.9 | 12.3 | 1.7 |
| **Oil 10** | 5.79 | 1.29 | 0.13 | 79.0 | 17.6 | 1.8 |
| **Oil 11** | 5.35 | 1.19 | 0.12 | 68.3 | 15.2 | 1.5 |
| **Oil 12** | 5.54 | 1.00 | 0.23 | 78.4 | 14.1 | 3.3 |
| **Oil 13** | 6.59 | 0.61 | 0.00 | 86.9 | 8.0 | 0.0 |
| **Oil 14** | 6.39 | 0.70 | 0.04 | 89.1 | 9.8 | 0.6 |

***Table 3.*** *Amount of saturate, aromatic, and polar fractions recovered for each sample. Samples showing an * were not fractionated, and thus had no yield value. Percentages are of the total maltene fractionated.*

## 3.2. Biomarker Analysis

### *3.2.1. 18α(H)-Oleanane and Oleanane-Type Compounds*

#### *3.2.1.1. 18α(H)-Oleanane*

18α(H)-Oleanane is a biomarker for angiosperm plants and is formed from the leaf wax compound β-amyrin (Ekweozor and Udo, 1988; Moldowan et al., 1994; Murray et al., 1997; Nytoft et al., 2002; Armstroff et al., 2006). Both the source rock and the oil samples were analyzed for the presence of 18α(H)-oleanane by interpretation of the *m/z* 191 chromatogram of the saturate fraction (whole extract for source rock samples with insufficient extract weight to be fractionated). 18α(H)-Oleanane was tentatively found to be present in three source rock samples from the Pavlu and Jacob Betz cores (Figure 10). The remaining source rock samples and all of the oil samples did not indicate the presence of 18α(H)-oleanane.

#### *3.2.1.2. Alkylnaphthalenes*

As mentioned previously, there is a wide variety of aromatic oleanoid compounds that may be formed during diagenesis of β-amyrin and/or degradation of oleanane and oleanane-type compounds (Figure 2). These include some of the methylnaphthalenes, specifically 1,2,5-and 1,2,7-trimethylnaphthalene and 1,2,5,6-tetramethylnaphthalene (Murray et al., 1997). All three of these compounds were identified in each of the source rock and oil samples used in the present study (Figure 11 and Table 4). It was decided to focus on 1,2,7- trimethylnaphthalene due to both 1,2,5- trimethylnaphthalene and 1,2,5,6-tetramethylnaphthalene having multiple precursors that the observed presence of these compounds may be attributed to (Strachan et al., 1988; Armstroff et al., 2006).

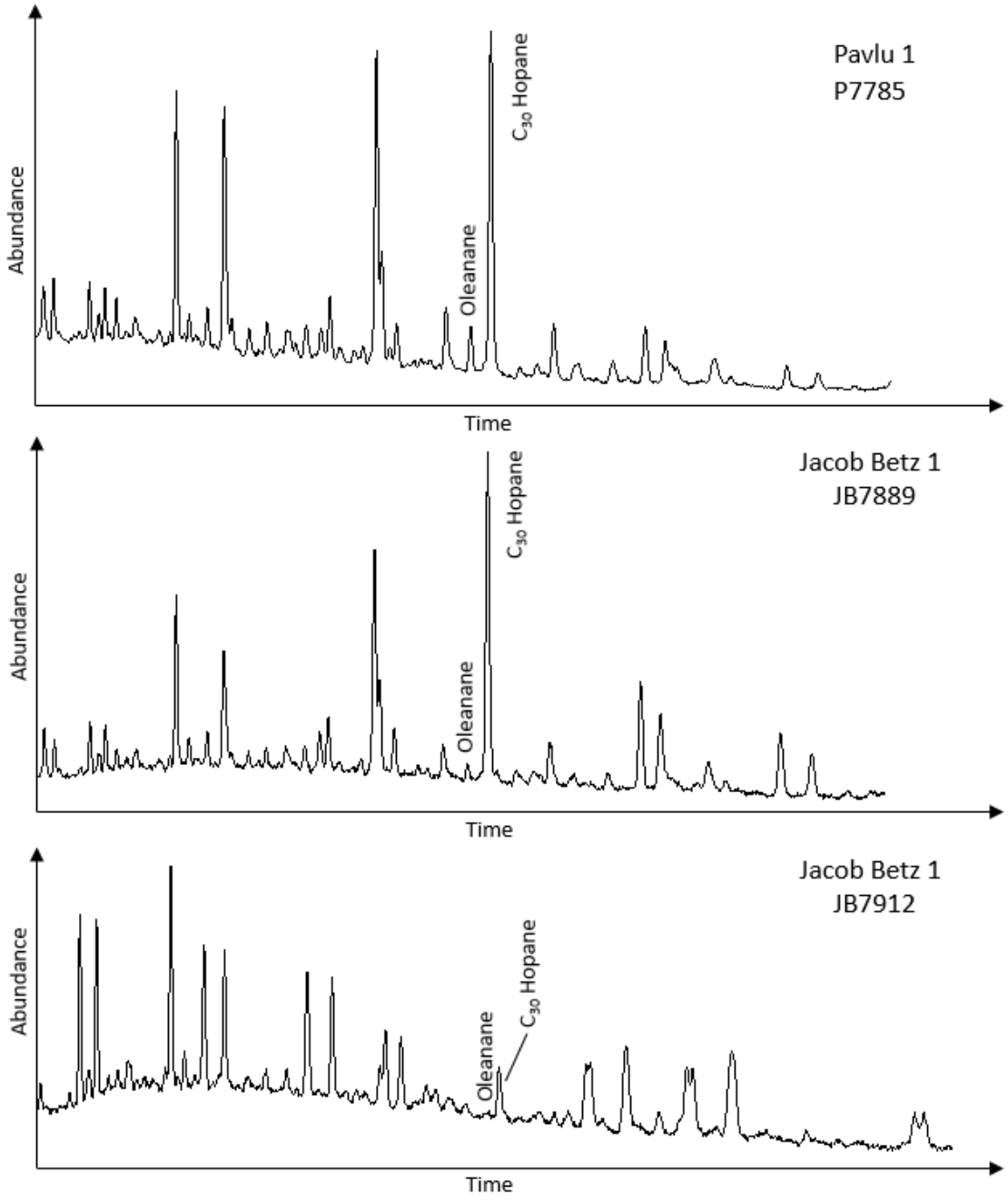


***Figure 10.*** *M/z 191 chromatograms showing the three source rock samples in which 18α(H)-oleanane was tentatively identified.*

Relative abundance of the ten trimethylnaphthalene isomers identified in the Mississippian Limestone, as well as relevant ratios, are presented in Table 5 as percentages of the total trimethylnaphthalenes. Strachan et al. (1988) observed that as maturity increases the 1,2,5- and 1,2,7- trimethylnaphthalene isomers shift to the 1,3,6- and 1,3,7- trimethylnaphthalene isomers; the proposed pathway for these isomer shifts is shown in Figure 12. The 1,2,5-trimethylnaphthalene /1,3,6-trimethylnaphthalene and 1,2,7-trimethylnaphthalene /1,3,7-trimethylnaphthalene ratios account for the changes observed with increasing maturity. Strachan et al. (1988) used the 1,3,6 and 1,3,7 isomers because they were determined to be the most stable isomers in sediments. A logarithmic plot, after the plot in Strachan et al. (1988), of the above mentioned ratios is shown in Figure 13 which allows for assessment of the input of trimethylnaphthalenes in a depositional environment. The dashed lines in Figure 13 are for comparison and are the same lines used by Strachan et al. (1988) in their plot. Referring to the dashed lines as quadrant divisions Strachan et al. (1988) described the lower left quadrant as representing samples that either had little to no input from higher plants or contained input from higher plants but under conditions where aromatization of higher plant compounds was a minor process, thus producing low abundances of 1,2,5- and 1,2,7-trimethylnaphthalene.

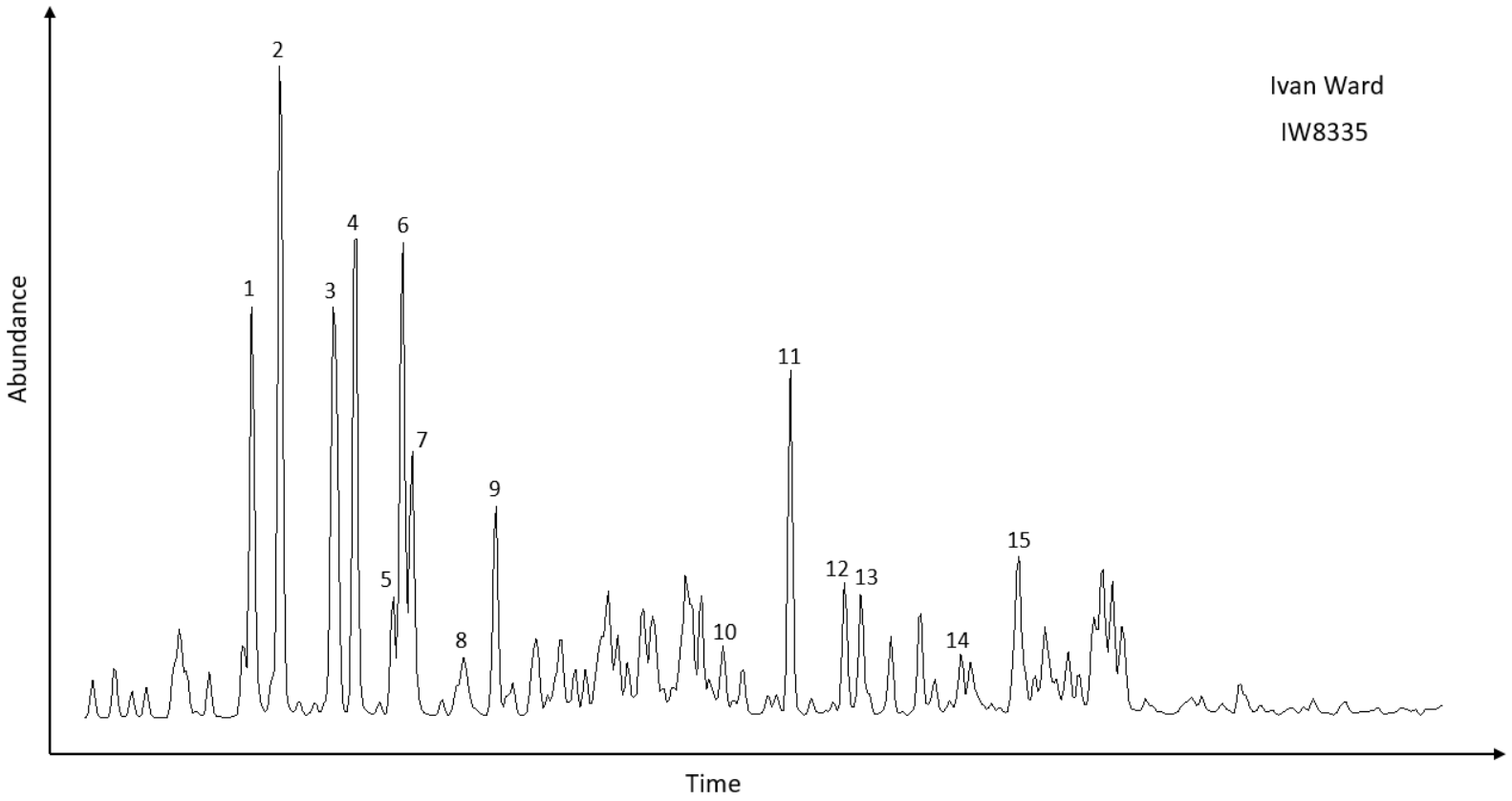


***Figure 11.*** *M/z 170 + 184 chromatogram showing the distribution of tri- and tetramethylnaphthalenes. This sample is representative of the distribution of these compounds in all samples used in this study. Compound names for numbered peaks are shown in Table 4. See Appendix B for the m/z 170 chromatograms for all samples from the present study.*

| Peak Number | Compound Name |
|---|---|
| 1 | 1,3,7-Trimethylnaphthalene |
| 2 | 1,3,6-Trimethylnaphthalene |
| 3 | 1,3,5- + 1,4,6-Trimethylnaphthalene |
| 4 | 2,3,6-Trimethylnaphthalene |
| 5 | 1,2,7-Trimethylnaphthalene |
| 6 | 1,6,7-Trimethylnaphthalene |
| 7 | 1,2,6-Trimethylnaphthalene |
| 8 | 1,2,4-Trimethylnaphthalene |
| 9 | 1,2,5-Trimethylnaphthalene |
| 10 | 1,3,5,7-Tetramethylnaphthalene |
| 11 | Cadalene |
| 12 | 1,2,4,6- + 1,2,4,7- + 1,4,6,7-Tetramethylnaphthalene |
| 13 | 1,2,5,7-Tetramethylnaphthalene |
| 14 | 1,2,3,6-Tetramethylnaphthalene |
| 15 | 1,2,5,6- + 1,2,3,5-Tetramethylnaphthalene |

***Table 4.*** *Peak identification of alkylnaphthalenes in Figure 11.*

| Sample | a | b | c | d | e | f | g | h | i | j | k |
|---|---|---|---|---|---|---|---|---|---|---|---|
| **WR8318** | 14.7 | 23.4 | 13.0 | 19.7 | 3.2 | 14.4 | 5.7 | 1.2 | 4.8 | 0.21 | 0.22 |
| **WR8322** | 14.5 | 22.1 | 12.3 | 20.1 | 3.2 | 13.9 | 7.0 | 1.6 | 5.4 | 0.24 | 0.22 |
| **WR8342** | 13.8 | 21.2 | 12.9 | 18.9 | 3.9 | 14.2 | 7.1 | 1.4 | 6.7 | 0.31 | 0.29 |
| **WR8348** | 13.2 | 19.6 | 15.4 | 16.6 | 4.2 | 14.9 | 7.6 | 1.4 | 7.0 | 0.36 | 0.32 |
| **WR8364** | 13.2 | 18.7 | 10.5 | 20.4 | 4.8 | 15.5 | 9.1 | 1.3 | 6.4 | 0.34 | 0.37 |
| **J7781** | 11.6 | 17.8 | 12.9 | 17.0 | 4.5 | 15.0 | 8.6 | 2.2 | 10.3 | 0.58 | 0.39 |
| **J7788** | 13.1 | 20.3 | 11.2 | 21.5 | 3.7 | 14.5 | 6.9 | 1.4 | 7.3 | 0.36 | 0.29 |
| **J7798** | 11.3 | 19.3 | 10.9 | 20.5 | 4.1 | 15.6 | 8.4 | 1.3 | 8.5 | 0.44 | 0.36 |
| **J7816** | 11.9 | 20.5 | 11.9 | 18.1 | 3.9 | 16.0 | 7.9 | 1.6 | 8.3 | 0.41 | 0.33 |
| **P7785** | 14.0 | 20.0 | 14.3 | 16.2 | 4.0 | 13.7 | 7.5 | 2.5 | 7.9 | 0.40 | 0.28 |
| **W8147** | 11.4 | 20.1 | 12.5 | 17.8 | 3.8 | 16.8 | 7.0 | 1.9 | 8.7 | 0.43 | 0.33 |
| **W8148** | 11.7 | 18.7 | 11.7 | 17.9 | 4.4 | 16.3 | 8.3 | 2.3 | 8.7 | 0.47 | 0.38 |
| **W8150** | 11.2 | 18.3 | 12.6 | 17.0 | 4.6 | 15.9 | 8.9 | 2.6 | 8.8 | 0.48 | 0.41 |
| **W8155** | 13.4 | 22.2 | 13.4 | 15.8 | 4.3 | 13.5 | 7.6 | 2.3 | 7.6 | 0.34 | 0.33 |
| **W8156** | 12.0 | 19.8 | 10.6 | 21.9 | 4.3 | 15.7 | 7.6 | 1.4 | 6.8 | 0.34 | 0.36 |
| **IW8317** | 12.6 | 20.2 | 12.6 | 17.7 | 4.2 | 15.3 | 8.3 | 1.6 | 7.4 | 0.37 | 0.33 |
| **IW8320** | 12.1 | 20.7 | 13.5 | 16.2 | 4.0 | 15.5 | 8.5 | 1.8 | 7.7 | 0.37 | 0.33 |
| **IW8330** | 11.6 | 17.5 | 11.3 | 20.1 | 4.1 | 16.8 | 9.3 | 1.7 | 7.7 | 0.44 | 0.35 |
| **IW8334** | 13.3 | 22.1 | 13.4 | 16.3 | 3.7 | 14.9 | 8.0 | 1.6 | 6.7 | 0.30 | 0.28 |
| **IW8335** | 13.5 | 21.4 | 13.5 | 15.7 | 3.9 | 15.5 | 8.4 | 1.4 | 6.8 | 0.32 | 0.29 |
| **IW8339** | 12.3 | 22.0 | 11.8 | 18.9 | 3.9 | 14.5 | 8.0 | 1.4 | 7.1 | 0.32 | 0.32 |
| **IW8365** | 13.1 | 22.3 | 12.5 | 21.7 | 3.1 | 14.4 | 6.6 | 1.3 | 5.0 | 0.23 | 0.23 |
| **IW8406** | 14.9 | 21.4 | 14.5 | 15.3 | 4.2 | 13.6 | 8.0 | 1.7 | 6.5 | 0.30 | 0.28 |
| **JB7868** | 14.6 | 21.4 | 12.1 | 19.6 | 4.2 | 13.0 | 6.7 | 1.9 | 6.5 | 0.30 | 0.29 |
| **JB7889** | 13.5 | 20.5 | 10.8 | 22.5 | 4.0 | 13.5 | 7.7 | 1.5 | 6.0 | 0.29 | 0.30 |
| **JB7912** | 10.9 | 15.5 | 17.6 | 14.7 | 4.3 | 19.6 | 7.0 | 2.1 | 8.3 | 0.54 | 0.39 |
| **Oil 1** | 18.7 | 24.7 | 14.8 | 15.9 | 2.8 | 12.7 | 5.1 | 1.6 | 3.7 | 0.15 | 0.15 |
| **Oil 2** | 18.4 | 24.5 | 14.2 | 16.8 | 3.7 | 11.0 | 5.8 | 1.7 | 4.0 | 0.16 | 0.20 |
| **Oil 3** | 20.2 | 25.5 | 14.2 | 17.1 | 2.5 | 11.5 | 4.9 | 1.3 | 2.9 | 0.11 | 0.13 |
| **Oil 4** | 20.6 | 29.4 | 13.7 | 17.2 | 2.1 | 10.1 | 3.8 | 1.1 | 2.1 | 0.07 | 0.10 |
| **Oil 5** | 16.3 | 22.9 | 14.2 | 15.7 | 4.4 | 11.8 | 7.0 | 2.0 | 5.7 | 0.25 | 0.27 |
| **Oil 6** | 18.5 | 24.6 | 14.4 | 16.5 | 3.3 | 11.8 | 5.3 | 1.8 | 3.9 | 0.16 | 0.18 |
| **Oil 7** | 15.3 | 22.5 | 14.2 | 15.8 | 4.7 | 11.4 | 7.6 | 2.1 | 6.4 | 0.29 | 0.31 |
| **Oil 8** | 16.6 | 26.2 | 13.1 | 18.9 | 2.2 | 13.1 | 5.0 | 1.5 | 3.4 | 0.13 | 0.13 |
| **Oil 9** | 16.0 | 24.0 | 13.2 | 17.7 | 3.6 | 12.5 | 6.3 | 2.1 | 4.6 | 0.19 | 0.23 |
| **Oil 10** | 14.8 | 20.9 | 16.2 | 13.1 | 4.7 | 11.8 | 8.7 | 2.4 | 7.3 | 0.35 | 0.32 |
| **Oil 11** | 15.8 | 22.1 | 15.0 | 17.7 | 3.8 | 11.7 | 6.8 | 2.2 | 4.9 | 0.22 | 0.24 |
| **Oil 12** | 16.3 | 22.9 | 13.9 | 17.2 | 4.1 | 11.6 | 6.7 | 2.0 | 5.4 | 0.24 | 0.25 |
| **Oil 13** | 18.5 | 25.7 | 13.6 | 16.1 | 3.3 | 12.1 | 5.5 | 1.5 | 3.7 | 0.14 | 0.18 |
| **Oil 14** | 19.8 | 24.7 | 14.1 | 16.9 | 3.0 | 11.5 | 4.9 | 1.8 | 3.4 | 0.14 | 0.15 |

***Table 5.*** *Relative abundances of trimethylnaphthalene isomers expressed as percentages of the total trimethylnaphthalenes. (a) 1,3,7-trimethylnaphthalene (b) 1,3,6-trimethylnaphthalene (c) 1,3,5- + 1,4,6- trimethylnaphthalene (d) 2,3,6- trimethylnaphthalene (e) 1,2,7-trimethylnaphthalene (f) 1,6,7- trimethylnaphthalene (g) 1,2,6- trimethylnaphthalene (h) 1,2,4-trimethylnaphthalene (i) 1,2,5- trimethylnaphthalene (j) 1,2,5- trimethylnaphthalene/1,3,6-trimethylnaphthalene, which is used to account for maturity impacts for 1,2,5-trimethylnaphthalene (k) 1,2,7- trimethylnaphthalene/1,3,7- trimethylnaphthalene, which is used to account for maturity impacts for 1,2,7- trimethylnaphthalene.*

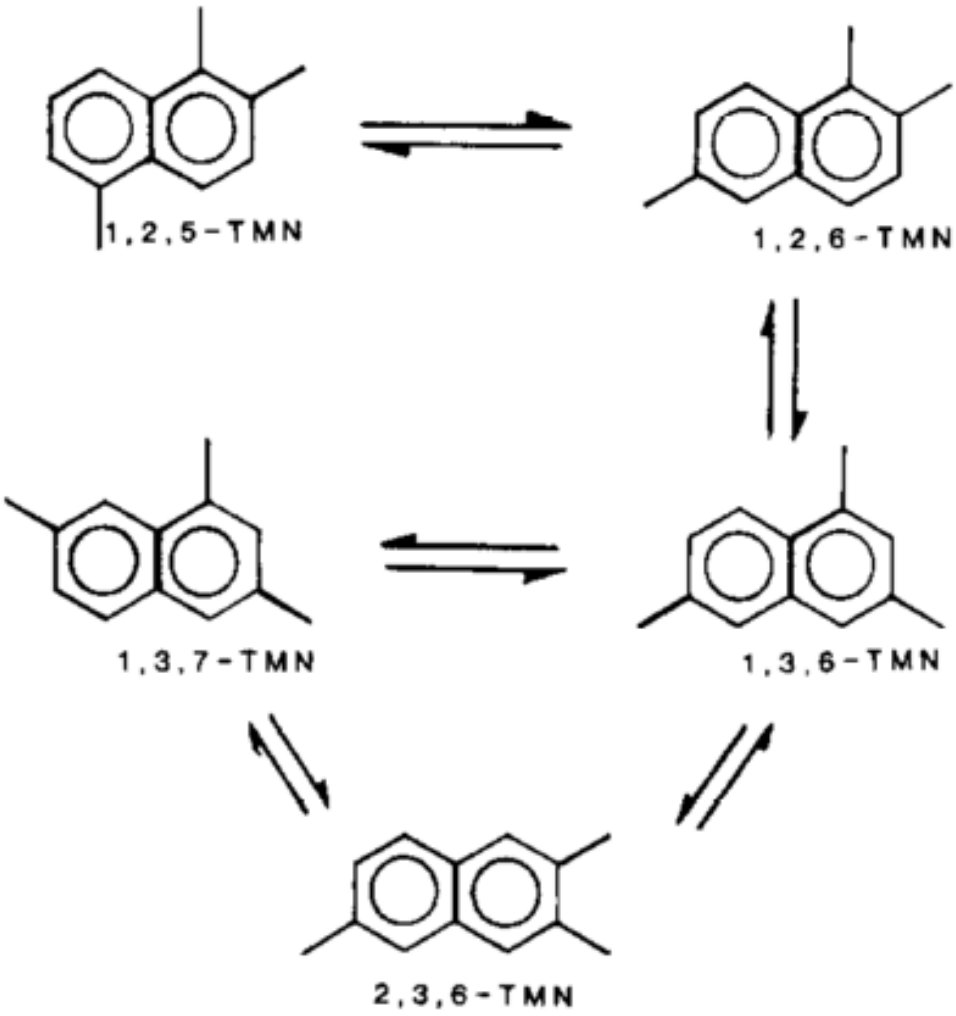


***Figure 12.*** *Schematic from Strachan et al. (1988) showing pathways for thermal maturity-driven isomerization reactions that can alter the observed abundances of 1,2,5-trimehtylnaphthalene. As maturity increases 1,2,5- trimethylnaphthalene shifts to 1,2,6-trimethylnaphthalene, which is thermally unstable and thus shifts again to 1,3,6-trimethylnaphthalene. A similar reaction is expected for 1,2,7- trimethylnaphthalene as well, which Strachan et al. (1988) proposed begins with a 1,2 methyl shift at C-2 to form the 1,3,7-trimethylnaphthalene isomer.*

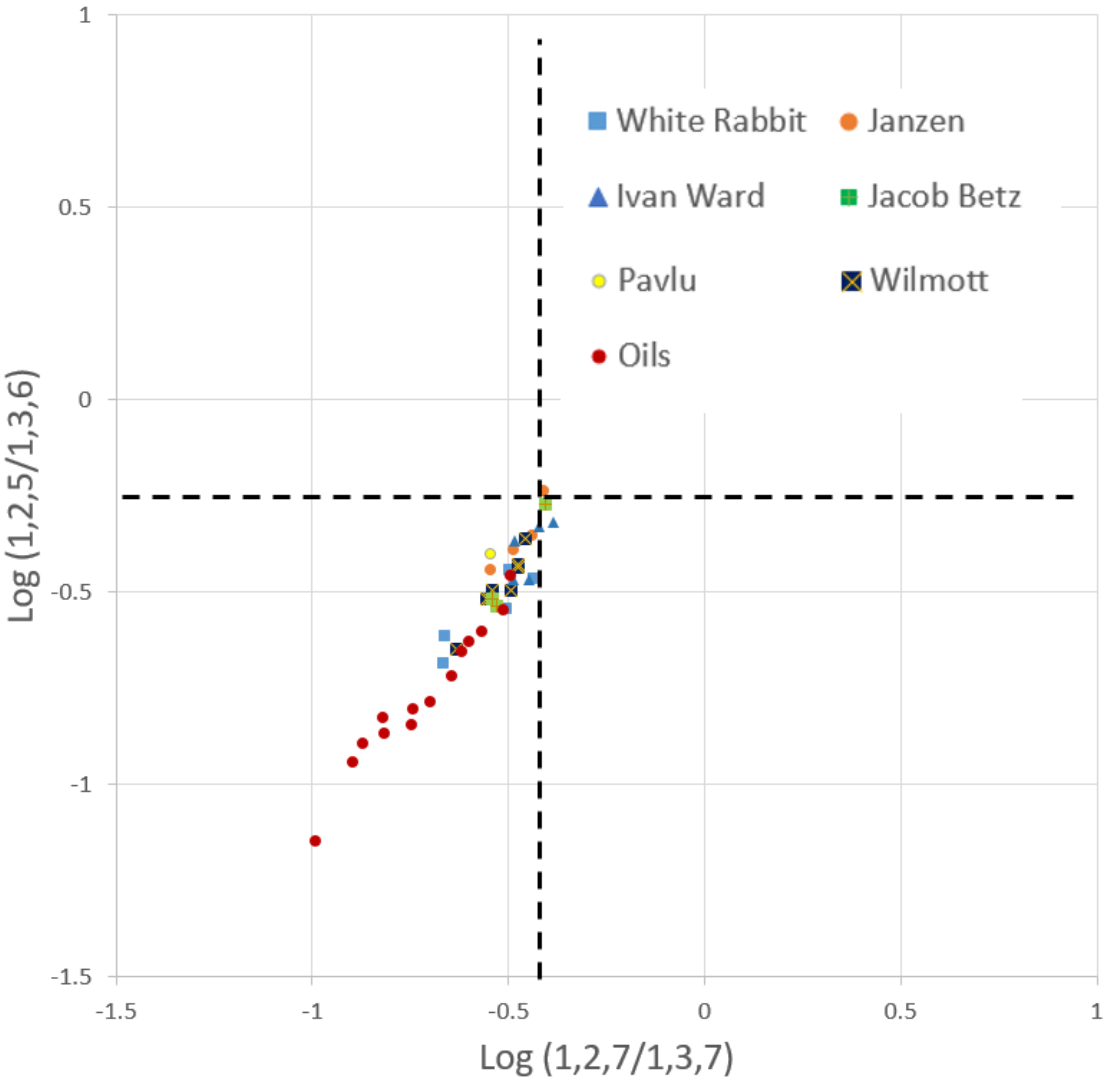


***Figure 13.*** *Cross plot after Strachan et al. (1988) displaying the relative abundance of the 1,2,5- and 1,2,7- trimethylnaphthalene isomers in the Mississippian samples from the Anadarko Basin. The plot is primarily a function of depositional environment with a secondary impact from thermal maturity. The samples from the Anadarko Basin plot in the lower left quadrant which indicates a low abundance of both the 1,2,5 and 1,2,7 isomers. The dashed lines are for comparison to Strachan et al. (1988) and Armstroff et al. (2006) and act as quadrant divisions for the discussion in these studies as well as the present study.*

#### *3.2.1.3. Lupane*

Lupane is a $C_{30}$ pentacyclic triterpene, related to 18α(H)-oleanane but whose distribution and timing of generation is less well understood than 18α(H)-oleanane. Lupane is known to be widespread among angiosperm plants and is likely dominantly, if not solely, produced by angiosperms (Nytoft et al., 2002). Lupane is structurally very similar to 18α(H)-oleanane (Figure 14). In fact, it has been shown that isomerization reactions of lup-20(29)-ene can produce oleanane-type compounds (Rullkötter et al., 1994). Lupane is known to co-elute with 18α(H)-oleanane on nonpolar GC columns which are typically used for routine biomarker analysis, and was used in the present study (Fowler et al., 1988; Rullkötter et al., 1994; George et al., 1998). When using a nonpolar column the presence of lupane can be identified by the presence of a *m/z* 369 ion fragment in the spectrum of the peak that is normally assigned to 18α(H)-oleanane. 18α(H)-Oleanane does not contain a *m/z* 369 fragment, whereas lupane does (Figure 14). The spectrum for the peak tentatively identified as 18α(H)-oleanane in this study does include a small 369 fragment, which indicates the possible presence of lupane in the samples. This does not mean that 18α(H)-oleanane is absent. In fact, samples containing lupane often also contain 18α(H)-oleanane. Gas chromatography/mass spectrometry/mass spectrometry analysis is required to confirm which proportion of the peak is derived from 18α(H)-oleanane relative to lupane (Moldowan et al., 1994; Alberdi and López, 2000; Nytoft et al., 2002) and will be undertaken in the future.

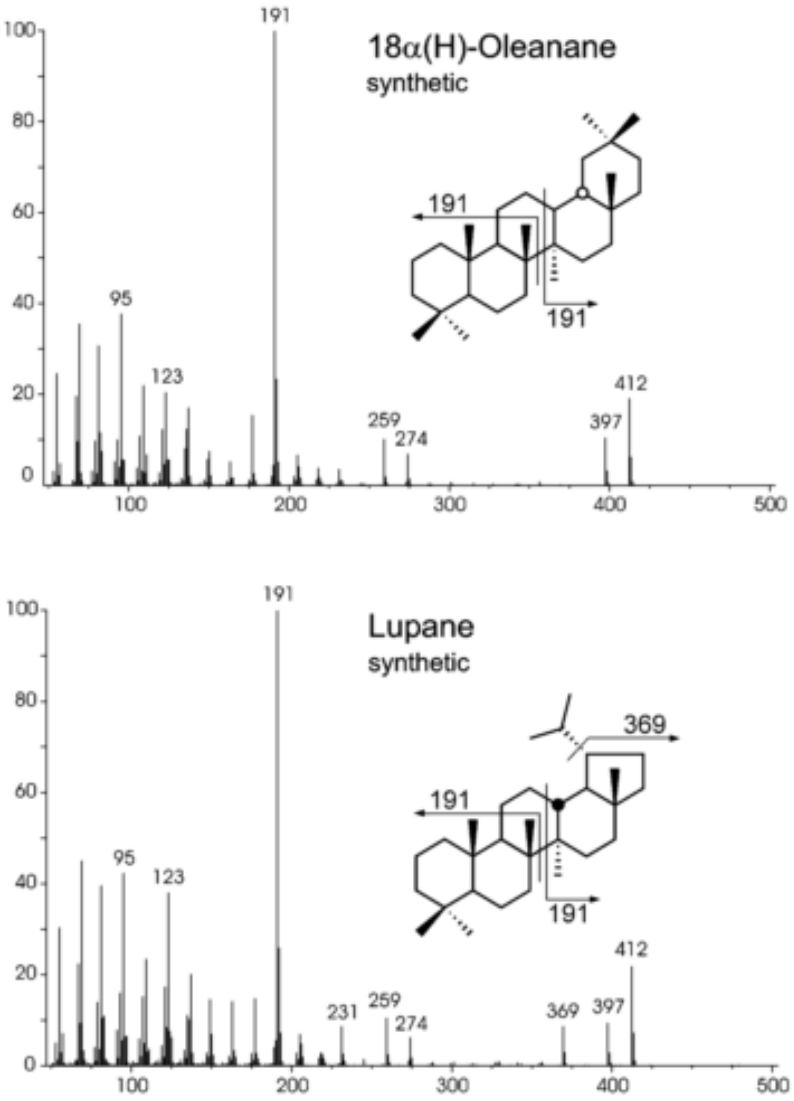


***Figure 14.*** *Illustration of the fragmentation patterns and structures of lupane and 18α(H)-oleanane isomer from Nytoft et al. (2002). Lupane and the oleananes have very similar structures and similar fragment patterns but can be differentiated by the presence of a m/z 369 fragment in lupane but not in 18α(H)-oleanane.*

### *3.2.2. Maturity Parameters*

#### *3.2.2.1. Methylphenanthrene Index*

The methylphenanthrene index (Figures 15 and 16) is a parameter based upon a maturity-driven shift in the distribution of the methylphenanthrene isomers and is more applicable than its predecessor, the methylphenanthrene ratio, because it incorporates the presumed parent compound for the methylphenanthrenes (phenanthrene). Incorporating phenanthrene into this index allows for compensation of facies-dependent variations impacting the degree of phenanthrene alkylation and results in a more accurate measurement of maturity (Radke et al., 1982; Radke, 1988). The methylphenanthrene index was one of the parameters used to estimate the maturity of the samples used in this study (Table 6). The methylphenanthrene index for the source rock samples ranged from 0.44 to 0.98 with an average of 0.59. This gives a calculated vitrinite reflectance of 0.68 to 0.98 with an average of 0.77 and places these samples in the early to mid-oil window (Radke and Welte, 1983). The methylphenanthrene index for oil samples ranged from 0.64 to 1.44 with an average of 0.89, corresponding to a calculated vitrinite reflectance of 0.79 to 1.23 with an average of 0.93 and placing these samples in the mid to late oil window. It is important to note that the methylphenanthrene index was originally developed for coals and Type III kerogen and may not work as well for Type II and Type I kerogens. Because the present study is in a marine carbonate setting (typically Type II kerogen) some error may occur in the application of this index (Radke and Welte, 1983).

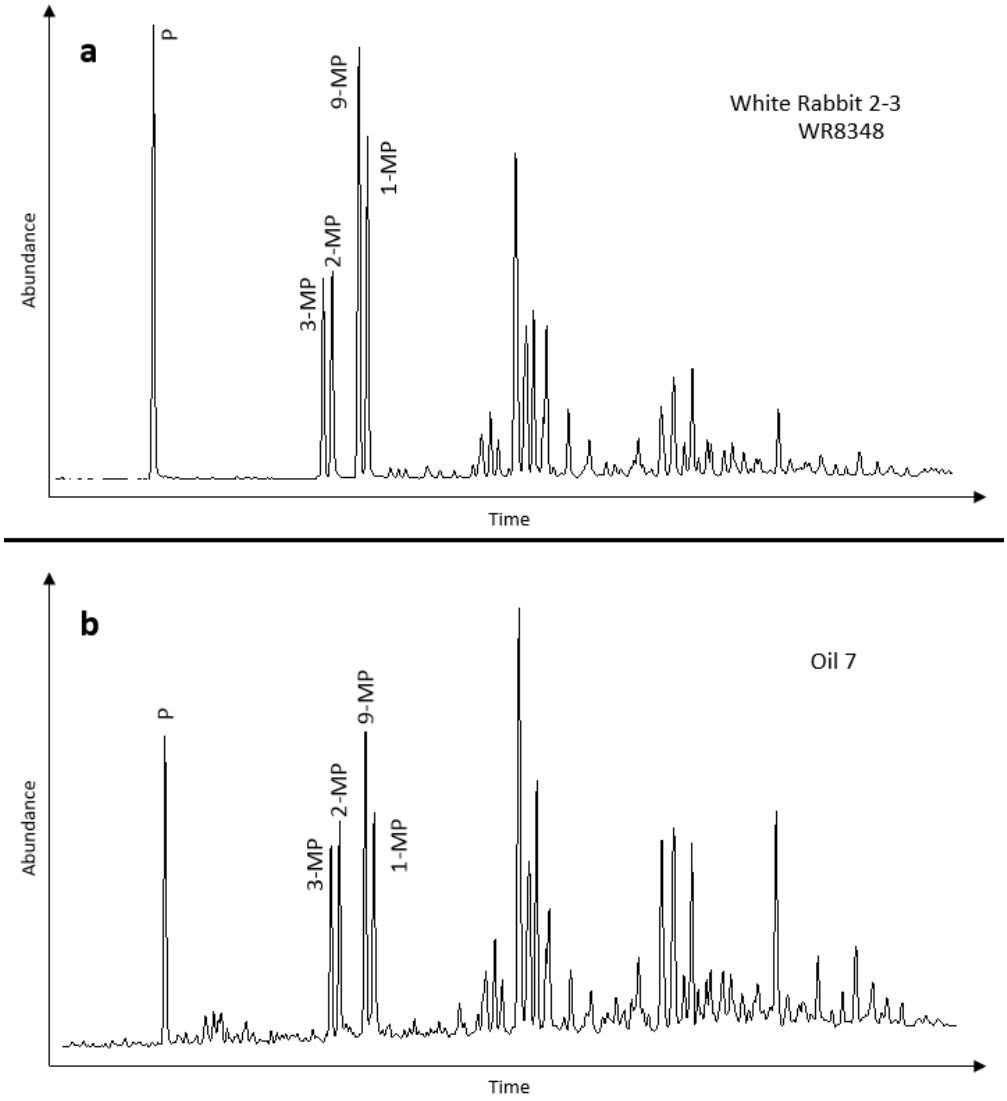


***Figure 15.*** *M/z 178 + 192 + 206 + 220 + 234 chromatogram showing the alkylphenanthrenes. Chromatograms are from the White Rabbit core and Oil 7. The peaks used for MPI 1 are labeled, P: phenanthrene MP: methylphenanthrene.*

$$\text{MPI 1} = \frac{1.5(\text{2-MP} + \text{3-MP})}{(\text{P} + \text{1-MP} + \text{9-MP})} \qquad \text{TAS} = \frac{\text{TA (I)}}{[\text{TA (I)} + \text{TA (II)}]}$$

$$\%Rc = 0.55\ (\text{MPI-1}) + 0.44$$

***Figure 16.*** *Equations used for maturity parameters.*

| Sample Name | Sample Type | MPI-1 | %Rc | TAS |
|---|---|---|---|---|
| **WR8318** | Core | 0.52 | 0.73 | 0.89 |
| **WR8322** | Core | 0.66 | 0.80 | 0.77 |
| **WR8342** | Core | 0.57 | 0.75 | 0.76 |
| **WR8348** | Core | 0.50 | 0.71 | 0.77 |
| **WR8364** | Core | 0.58 | 0.76 | 0.83 |
| **J7781** | Core | 0.66 | 0.80 | 0.63 |
| **J7788** | Core | 0.47 | 0.70 | 0.67 |
| **J7798** | Core | 0.51 | 0.72 | 0.76 |
| **J7816** | Core | 0.80 | 0.88 | 0.81 |
| **P7785** | Core | 0.99 | 0.98 | 0.65 |
| **W8147** | Core | 0.46 | 0.69 | 0.77 |
| **W8148** | Core | 0.46 | 0.69 | 0.78 |
| **W8150** | Core | 0.44 | 0.68 | 0.82 |
| **W8155** | Core | 0.62 | 0.78 | 0.89 |
| **W8156** | Core | 0.62 | 0.78 | 0.89 |
| **IW8317** | Core | 0.53 | 0.73 | 0.88 |
| **IW8320** | Core | 0.56 | 0.75 | 0.89 |
| **IW8330** | Core | 0.53 | 0.73 | 0.92 |
| **IW8334** | Core | 0.49 | 0.71 | 0.88 |
| **IW8335** | Core | 0.58 | 0.76 | 0.93 |
| **IW8339** | Core | 0.62 | 0.78 | 0.89 |
| **IW8365** | Core | 0.57 | 0.75 | 0.93 |
| **IW8406** | Core | 0.49 | 0.71 | 0.87 |
| **JB7868** | Core | 0.95 | 0.96 | 0.83 |
| **JB7889** | Core | 0.71 | 0.83 | 0.79 |
| **JB7912** | Core | 0.63 | 0.78 | 0.89 |
| **Oil 1** | Oil | 0.89 | 0.93 | 0.82 |
| **Oil 2** | Oil | 0.94 | 0.96 | 0.90 |
| **Oil 3** | Oil | 0.94 | 0.96 | 0.86 |
| **Oil 4** | Oil | 0.87 | 0.92 | 0.90 |
| **Oil 5** | Oil | 0.85 | 0.91 | 0.68 |
| **Oil 6** | Oil | 0.77 | 0.87 | 0.58 |
| **Oil 7** | Oil | 0.75 | 0.85 | 0.45 |
| **Oil 8** | Oil | 0.64 | 0.79 | 0.51 |
| **Oil 9** | Oil | 0.76 | 0.86 | 0.61 |
| **Oil 10** | Oil | 0.88 | 0.93 | 0.71 |
| **Oil 11** | Oil | 1.13 | 1.06 | 0.90 |
| **Oil 12** | Oil | 0.80 | 0.88 | 0.73 |
| **Oil 13** | Oil | 0.79 | 0.87 | 0.80 |
| **Oil 14** | Oil | 1.44 | 1.23 | 0.88 |

***Table 6.*** *Methylphenanthrene index (MPI-1) and triaromatic steroid hydrocarbon ratio (TAS) maturity parameters. The calculated vitrinite reflectance (%Rc) value is based on the MPI-1 value and places the samples used in this study in the mid-oil window. The TAS values are most effective when compared between samples rather than when associated with a vitrinite reflectance value.*

#### *3.2.2.2. Triaromatic Steroid Hydrocarbon Ratio*

The triaromatic steroid hydrocarbons (TAS) are likely derived from continued aromatization of the monoaromatic steroid hydrocarbons (MAS), and provide another useful maturity parameter (Mackenzie, 1984). Because continued aromatization occurs with increasing maturity the TAS are more sensitive at higher maturities than the same ratio of the MAS. However, due to polarity differences, which preferentially retain the TAS compounds in the bitumen during oil expulsion, caution should be used when applying TAS ratios to oils (Hoffmann et al., 1984).

There are two methods for calculating the TAS ratio. Both use the basic formula of TA(I)/(TA(I)+TA(II)) (Figures 16 and 17). The first method is from Mackenzie et al. (1981) and uses the $C_{28}$ triaromatic steroid (20R) as TA(II) and the $C_{20}$ triaromatic steroid as TA(I). The second method is from Peters et al. (2005) and uses the sum of $C_{26}$-$C_{28}$ (20S+20R) triaromatic steroids as TA(II) and the sum of $C_{20}$ and $C_{21}$ triaromatic steroids as TA(I). For this study the method proposed by Peters et al. (2005) was used (Table 6). Both methods measure the relative amount of TA(II) compounds that have shifted to TA(I) compounds, however, there are two proposed methods for this conversion. The first method for conversion of long-chain to short-chain TAS compounds is by side-chain cleavage. The second method is by preferential thermal degradation of the long-chain compounds over the short-chain compounds (Moldowan et al., 1986). Laboratory heating experiments by Beach et al. (1989) indicate that the dominant method for conversion of long-chain to short-chain TAS compounds is the preferential thermal degradation of the long-chain compounds. Because there are two methods for altering the TAS ratio, it is more reliable to use this maturity parameter for comparison between samples within the same basin.

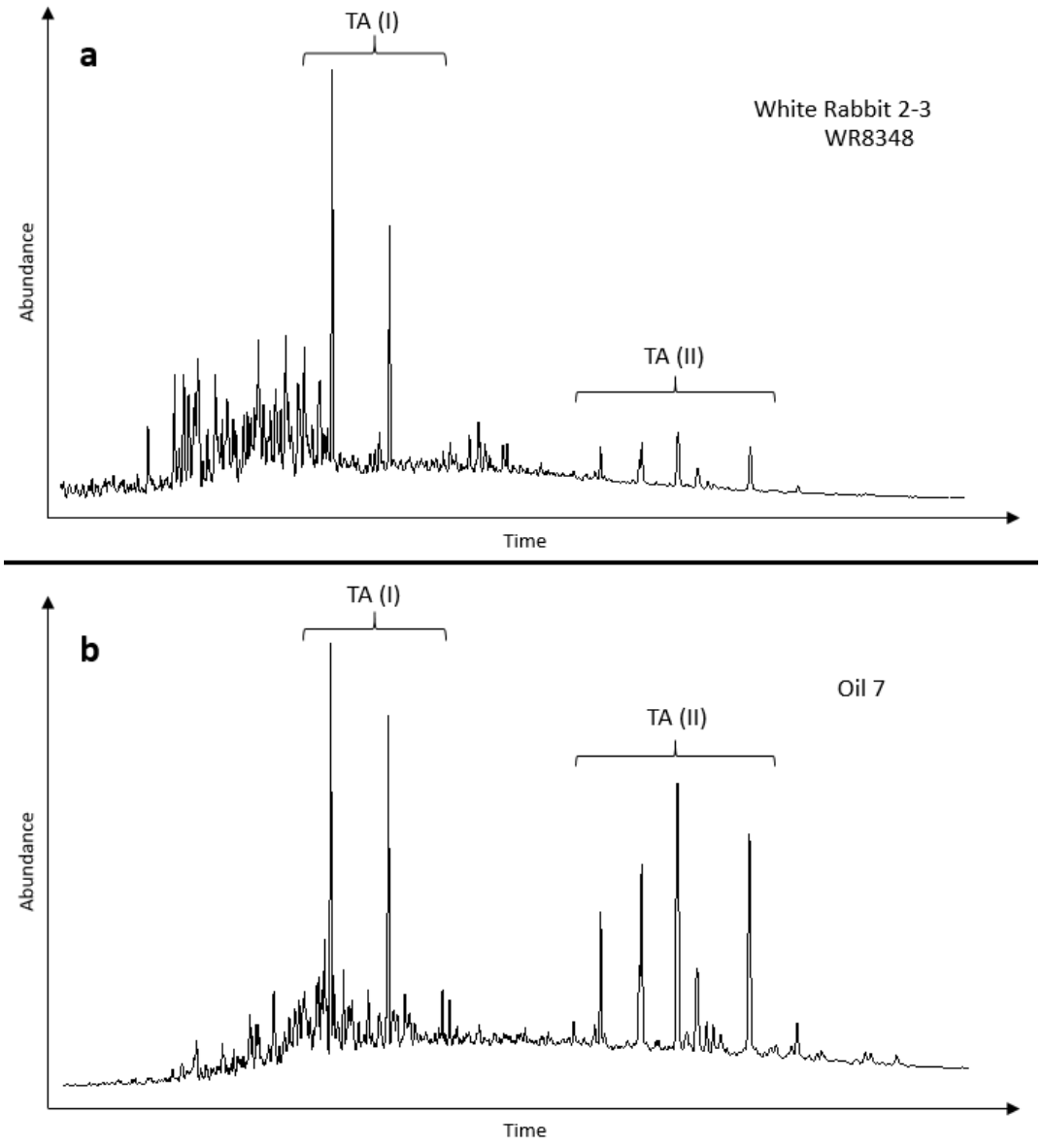


***Figure 17.*** *M/z 231 chromatograms from the White Rabbit core and Oil 7 showing peaks used for TAS ratio.*

### *3.2.3. n-Alkanes*

n-Alkanes can be used to indicate the thermal maturity, level of biodegradation of crude oils, and also provide some source information. However source information may be greatly impacted by thermal maturity (Bray and Evans, 1961) and biodegradation levels (McKirdy et al., 1983; Fritsche and Hofrichter, 2008). n-Alkanes are produced by direct input from plants, thermal cracking of kerogen, and short chain n-alkanes may also form from long chain n-alkanes. The thermal cracking of long chain n-alkanes may alter the source information contained in the distribution of these compounds. Biodegradation of n-alkanes preferentially removes the short-chain compounds (Fritsche and Hofrichter, 2008). Due to the n-alkanes being sensitive to both maturity and degradation the distribution of these compounds can be used as an indicator of the impact of these processes on a crude oil (Shanmugam, 1985; Wenger and Isaksen, 2002; Andersson and Meyers, 2012). n-Alkanes may also convey some depositional source information as shown by the abundance of short chain vs long chain compounds for lower maturity samples. The long-chain compounds ($C_{22}$ and higher) are uncommon in marine environments and are associated with terrestrial sources (Shanmugam, 1985). Marine environments are typically dominated by short-chain n-alkanes ($C_{15}$ to $C_{19}$; Ortiz et al., 2004).

The n-alkanes in the source rock samples generally showed similar results across the cores, with some notable exceptions. The n-alkanes in the White Rabbit core maximized at $C_{17}$ and were narrowly distributed around the $C_{17}$ and $C_{18}$ compounds (Figure 18a). The Janzen core has a similar distribution pattern in the middle samples (J7788 and J7798; Figure 18b). The uppermost sample for the Janzen core (J7781) shows a broad distribution from $C_{17}$ to $C_{23}$ maximizing at $C_{22}$. And the lowermost

sample (J7816) in the Janzen core shows a bimodal distribution with the primary maximum at $C_{18}$ and the secondary maximum at $C_{22}$. The Pavlu core sample shows a higher molecular weight n-alkane distribution with the abundance increasing at $C_{21}$ through $C_{30}$ and maximizing at $C_{23}$ (Figure 18c). With the exception of the lowermost sample (W8156) the Wilmott core samples show a bimodal distribution with the primary maximum at $C_{17}$ and the secondary maximum at $C_{22}$. The distribution around the maximum peaks is broad in these samples (Figure 18d). Sample W8156 is very similar to the distribution observed in the White Rabbit samples. The Ivan Ward core has more variation in its samples, with the uppermost samples maximizing at $C_{16}$ and $C_{17}$ and having a relatively narrow distribution (Figure 18e). The middle samples (IW8334 and IW8335) also maximize at $C_{17}$ but the n-alkane distribution is broader in these samples (Figure 18f). The lower samples are similar to the upper samples from this core. The Jacob Betz core is similar to the Ivan Ward core, with the upper samples maximizing at $C_{18}$ and having a narrow n-alkane distribution and the lower sample (JB7912) showing a heavier molecular weight distribution maximizing at $C_{22}$ and having a broader distribution than the upper portion of the core (Figure 18g). The oil samples were all very similar with respect to their n-alkane distributions, starting at $C_{11}$ or $C_{12}$ and continuing through $C_{35}$ at the end of the chromatogram and maximizing at $C_{15}$. They all have a broad distribution pattern that increases in abundance near the lighter molecular weights (Figure 18h).

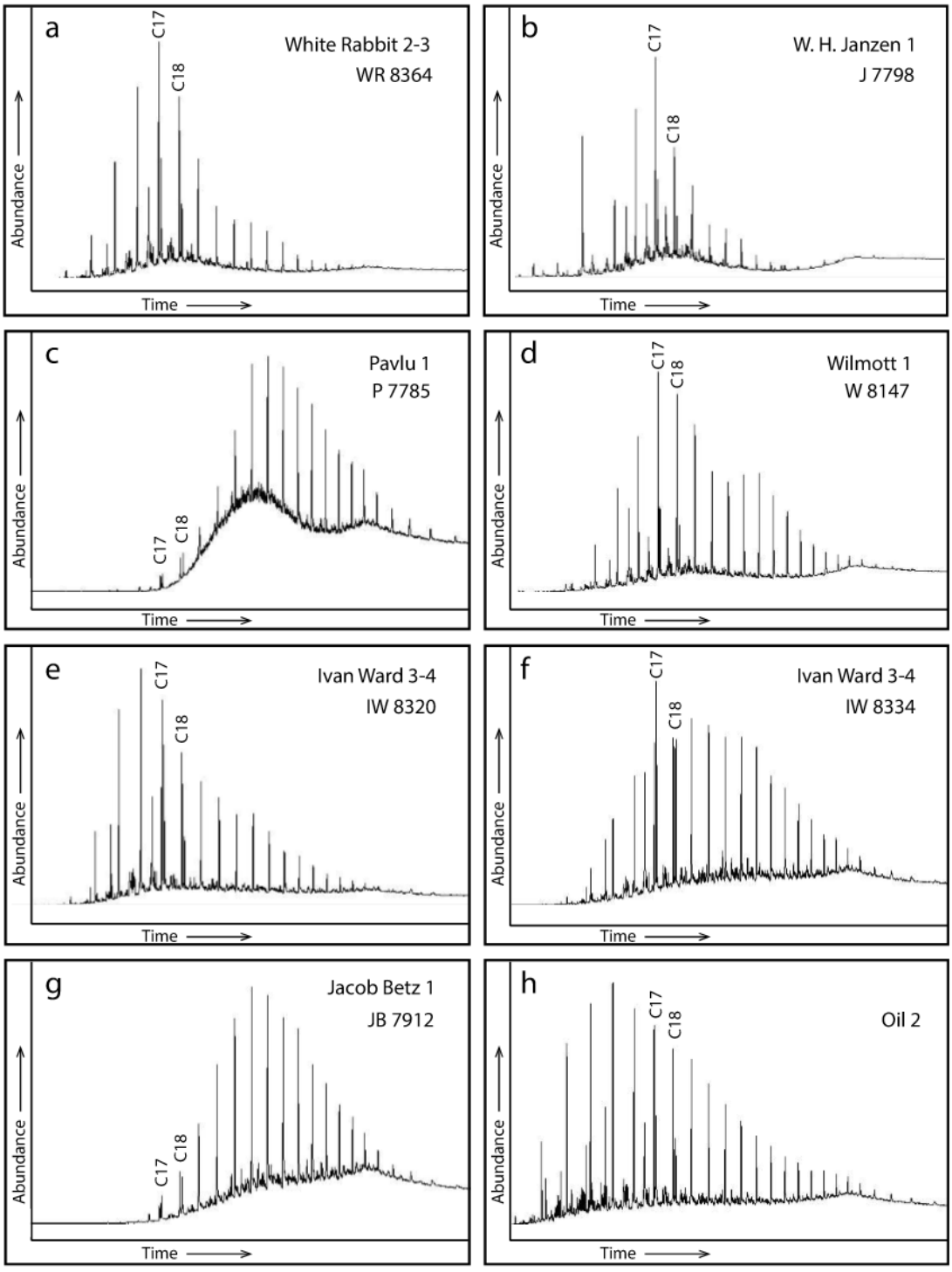


***Figure 18.*** *FID gas chromatograms showing examples of the n-alkane distributions for the Chesterian source rocks and one of the Mississippian oils. b and d are from whole extracts, the rest are from saturate fractions. See Appendix C for chromatograms of remaining samples.*

### *3.2.4. Isoprenoids*

The isoprenoids are a group of biomarkers that provide information on depositional environment conditions (Brassell et al., 1981; Petrov et al., 1990). The majority of the isoprenoids are composed of head-to-tail linkages in the isoprenoid chain. Some of the higher molecular weight isoprenoid compounds contain a single tail-to-tail linkage. Head-to-head linkages are less common, but do occur in organisms (Moldowan and Seifert, 1979; Petrov et al., 1990). Pristane and phytane contain the more common head-to-tail linkages, and can typically be observed by GC. Both pristane and phytane are primarily produced by diagenesis of chlorophyll and their formation is controlled by oxidation and reduction reactions, with oxidizing conditions favoring the formation of pristane and reducing conditions favoring the formation of phytane (Powell and McKirdy, 1975). Oxidation reactions are typical of terrestrial environments and reduction reactions are typical of some marine environments, thus the resulting pristane/phytane value may be used to indicate strong oxidizing or reducing environments. Isoprenoids are resistant to both thermal maturity and biodegradation effects making the pristane/phytane value useful across a wide range of maturities and degradation levels (Didyk et al., 1978). Pristane and phytane may also be combined with the n-alkanes (specifically $C_{17}$ and $C_{18}$ respectively) to provide additional insight into depositional conditions (Shanmugam, 1985).

The pristane/phytane value was calculated for both the source rock and the oil samples with the source rock samples ranging from 0.6 to 2.65 with an average of 1.59 (Table 7). The four values below 1.0 were samples from the Pavlu and Jacob Betz cores, which are the eastern most source rock samples. The highest pristane/phytane values are from the western cores, specifically the Ivan Ward, White Rabbit, and

| Sample Name | Pr/Ph | $Pr/C_{17}$ | $Ph/C_{18}$ |
|---|---|---|---|
| **WR8318** | 1.65 | 0.82 | 0.58 |
| **WR8322** | 1.94 | 0.74 | 0.57 |
| **WR8342** | 1.91 | 0.78 | 0.50 |
| **WR8348** | 1.49 | 0.76 | 0.57 |
| **WR8364** | 1.79 | 0.48 | 0.36 |
| **J7781** | 1.26 | 0.47 | 0.40 |
| **J7788** | 1.52 | 0.42 | 0.38 |
| **J7798** | 1.94 | 0.40 | 0.38 |
| **J7816** | 1.16 | 0.47 | 0.37 |
| **P7785** | 0.60 | 1.09 | 1.11 |
| **W8147** | 1.43 | 0.35 | 0.28 |
| **W8148** | 1.67 | 0.51 | 0.37 |
| **W8150** | 2.28 | 0.59 | 0.30 |
| **W8155** | 1.23 | 0.44 | 0.38 |
| **W8156** | 1.55 | 0.48 | 0.39 |
| **IW8317** | 2.32 | 0.49 | 0.41 |
| **IW8320** | 2.65 | 0.77 | 0.40 |
| **IW8330** | 2.37 | 0.45 | 0.28 |
| **IW8334** | 1.42 | 1.41 | 0.98 |
| **IW8335** | 1.55 | 0.96 | 0.72 |
| **IW8339** | 1.76 | 0.60 | 0.44 |
| **IW8365** | 1.48 | 0.94 | 0.65 |
| **IW8406** | 2.02 | 0.53 | 0.38 |
| **JB7868** | 0.82 | 0.78 | 0.48 |
| **JB7889** | 0.90 | 0.65 | 0.50 |
| **JB7912** | 0.66 | 1.58 | 0.85 |
| **Oil 1** | 1.20 | 0.40 | 0.40 |
| **Oil 2** | 1.25 | 0.50 | 0.46 |
| **Oil 3** | 1.28 | 0.48 | 0.43 |
| **Oil 4** | 1.50 | 0.35 | 0.30 |
| **Oil 5** | 1.44 | 0.57 | 0.48 |
| **Oil 6** | 1.41 | 0.33 | 0.29 |
| **Oil 7** | 1.38 | 0.67 | 0.56 |
| **Oil 8** | 1.31 | 0.51 | 0.44 |
| **Oil 9** | 1.40 | 0.52 | 0.44 |
| **Oil 10** | 0.98 | 0.35 | 0.37 |
| **Oil 11** | 1.39 | 0.44 | 0.39 |
| **Oil 12** | 1.29 | 0.56 | 0.50 |
| **Oil 13** | 0.95 | 0.28 | 0.31 |
| **Oil 14** | 1.48 | 0.36 | 0.31 |

***Table 7.*** *Pristane/phytane, pristane/$C_{17}$, and phytane/$C_{18}$ values for all source rock and oil samples. The pristane/$C_{17}$ and phytane/$C_{18}$ values are plotted in Figure 19.*

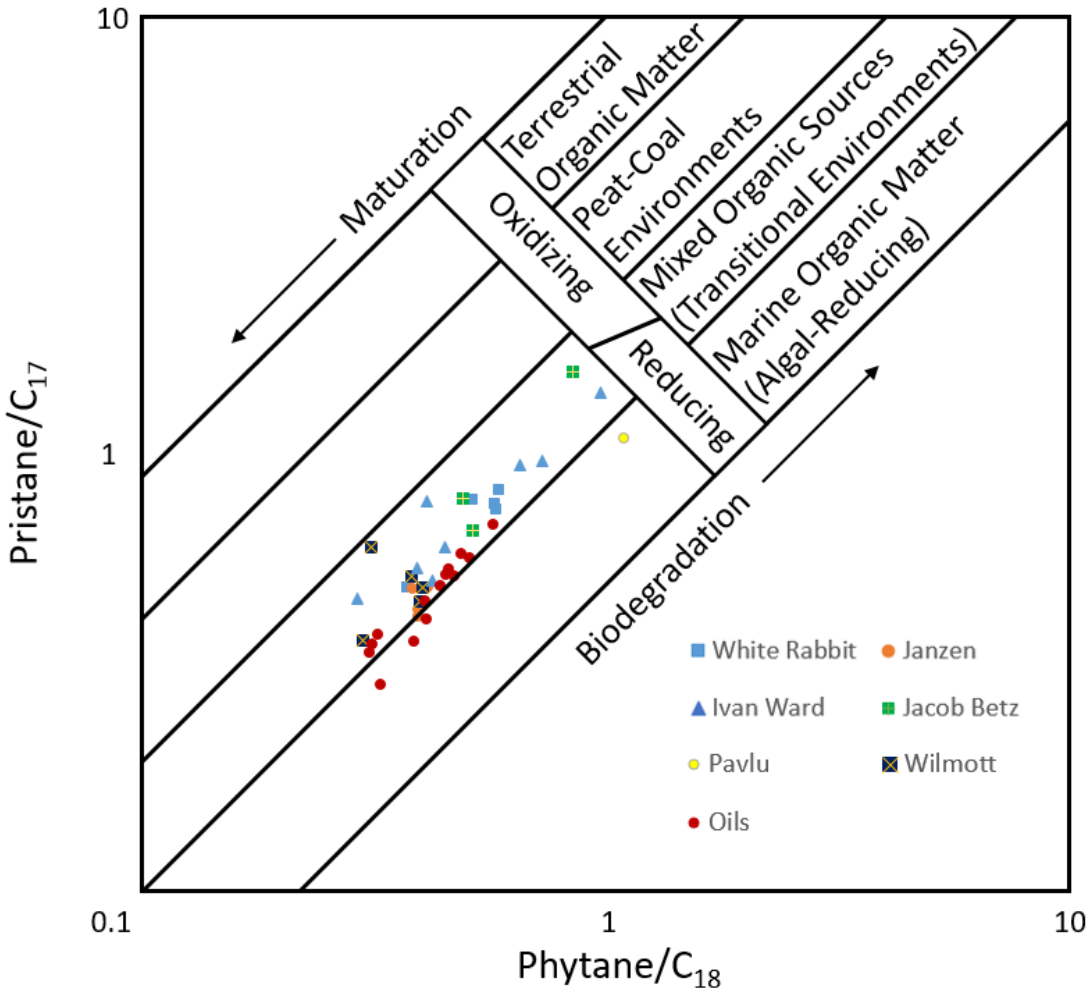


***Figure 19.*** *Plot after Shanmugam (1985) showing the type of organic material present in the samples. The majority of the samples contain mixed organic material, reflecting a transitional environment. Table 7 shows the pristane/$C_{17}$ and phytane/$C_{18}$ values used in this plot.*

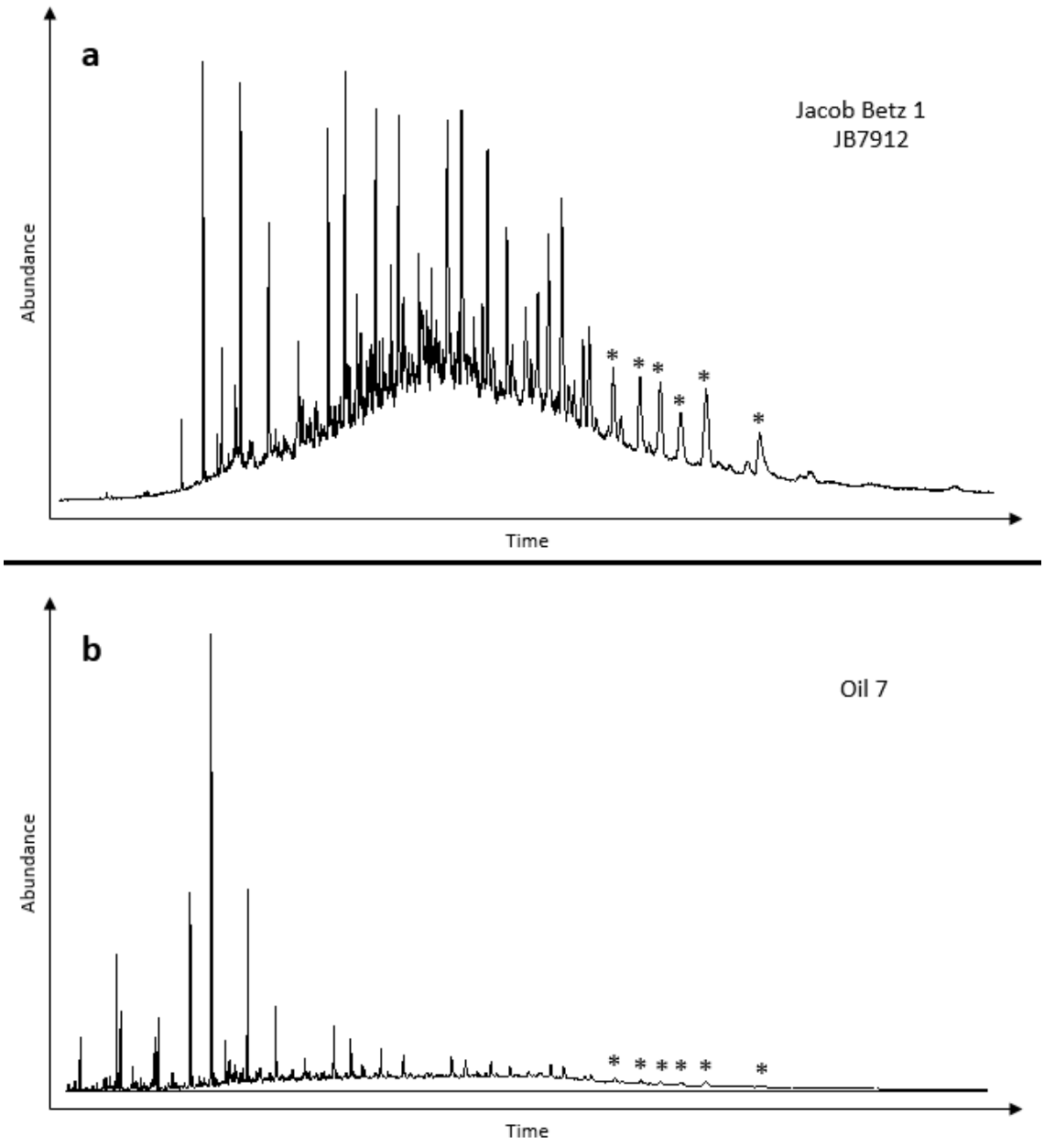


***Figure 20.*** *Representative m/z 183 chromatograms of the source rock and oil samples showing the head-to-head isoprenoids, which are marked by the * on the chromatograms. The n-alkanes were removed by molecular sieves.*

Wilmott cores (Figure 8). The oil samples ranged from 0.95 to 1.50 with an average of 1.30 (Table 7) but there were no obvious trends observed in the pristine/phytane values for the oil samples. The pristane/$C_{17}$ and phytane/$C_{18}$ values were calculated and plotted to obtain information about the depositional environment and redox conditions (Table 7; Figure 19). The resulting cross plot shows almost all samples (both source rocks and oils) as having a mixed organic source and being in the transitional region for the redox conditions (Shanmugam, 1985).

Interpretation of the *m/z* 183 chromatogram of the saturate fractions revealed the presence of head-to-head linkage isoprenoids (Figure 20). As mentioned previously, the head-to-head linkage isoprenoid compounds are less common than the typical head-to-tail linkages (Moldowan and Seifert, 1979). Like the other isoprenoids the head-to-head isoprenoids are also resistant to biodegradation and can be used for oil correlations. The head-to-head isoprenoids are formed from cell wall lipids of archaebacteria and their presence indicates a large bacterial contribution to an oil (Chappe et al., 1979; Petrov et al., 1990). Head-to-head isoprenoids are observed in all source rock and oil samples analyzed in the present study.

### *3.2.5. Tricyclic Terpanes*

Tricyclic terpanes extend from $C_{19}$ to at least $C_{54}$ (Connan et al., 1980; Aquino Neto et al., 1982; De Grande et al., 1993), with the extended tricyclic terpanes ($C_{25}$ and higher) having an isoprenoid-type side chain (Moldowan et al., 1983). The isoprenoid nature of the side chain (Figure 21) accounts for the observed low abundance in the $C_{22}$, $C_{27}$, $C_{32}$, $C_{37}$, and $C_{42}$ homologs as illustrated above using the Ivan Ward saturate fraction as an example (Figure 22 and Table 8; Kruge et al., 1990). There are four

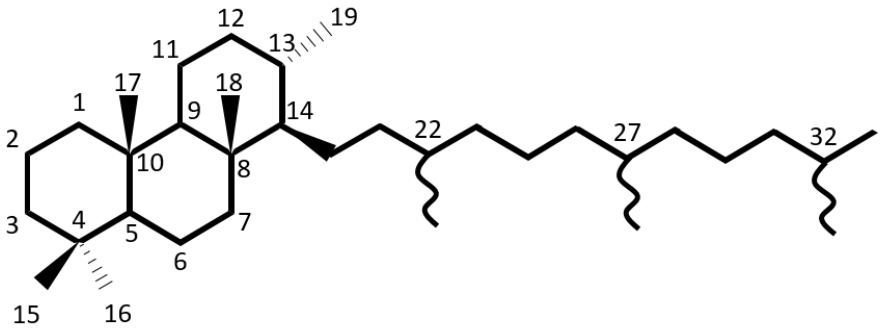


***Figure 21.*** *Structure of the 13β(H),14α(H)- tricyclic terpane isomers, also shows the isoprenoid side chain.*

possible isomers of the tricyclic terpanes at $C_{13}$ and $C_{14}$ (βα, αα, αβ, and ββ) all of which occur in immature rocks. Increasing maturity causes the βα isomer to become dominant (Chicarelli et al., 1988). The tricyclic terpanes observed in the present study are the βα isomer. Tricyclic terpanes are present, in at least low levels, in almost all oil and source rock samples that have been reported (Chicarelli et al., 1988; Philp et al., 1989; Azevedo et al., 1992; De Grande et al., 1993; Tao et al., 2015). Even with their common occurrence, the precursor for these compounds is still not completely understood and multiple possibilities are constantly debated (Dutta et al., 2006; Pearson, 2016).

The tricyclic terpanes in the White Rabbit core are present in relatively high abundance (relative abundance is compared with the regular hopanes for all samples in this section), but do not dominate the regular hopanes, and range from $C_{19}$ to at least $C_{31}$, with $C_{23}$ being the most abundant tricyclic terpane (Figure 23a). In the Janzen core the tricyclic terpanes increase in abundance with depth and overall are of medium to

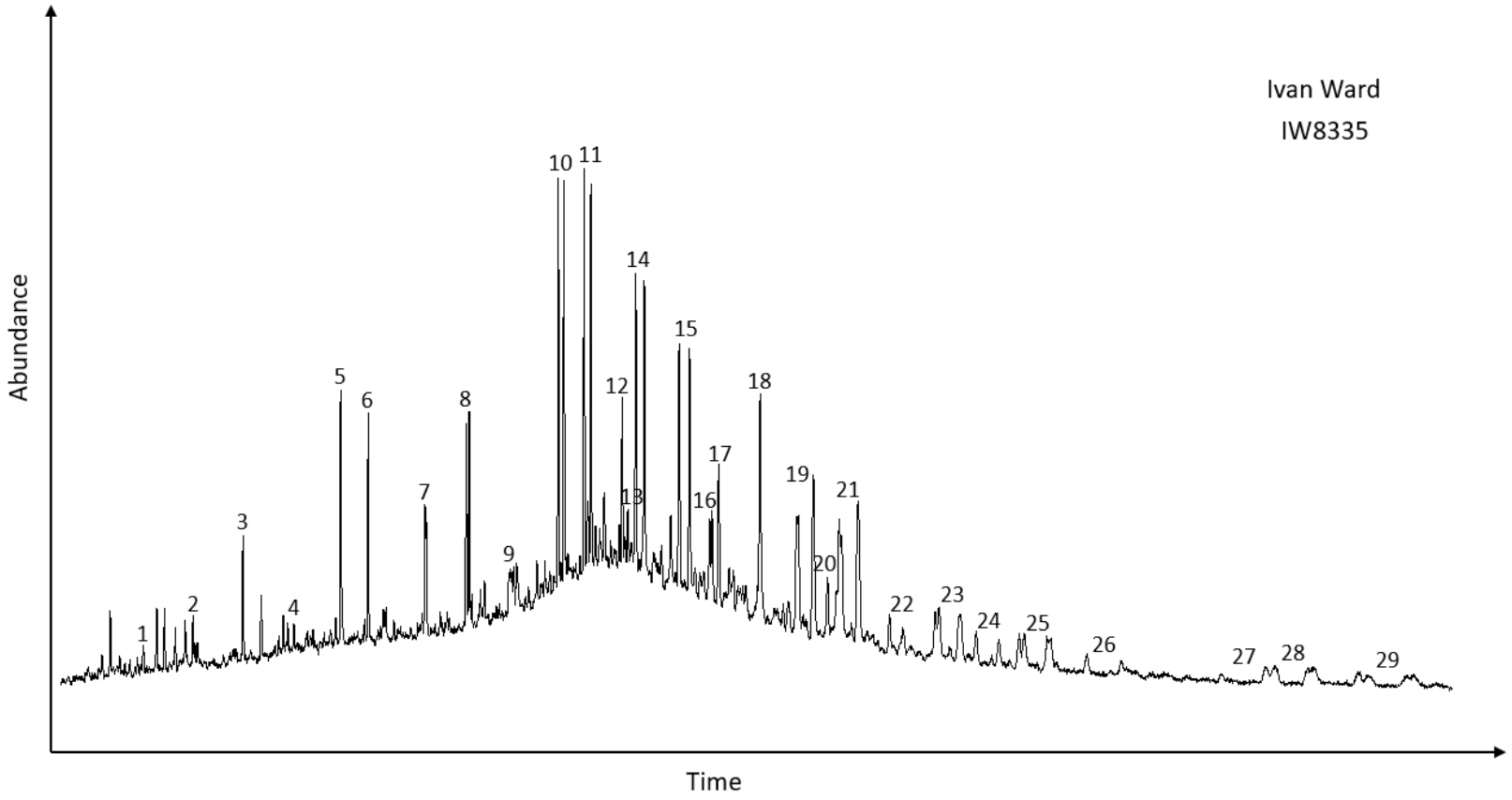


***Figure 22***. *M/z 191 chromatogram from the Ivan Ward core at 8335 ft. showing the distribution of tricyclic terpanes, hopanes, and rearranged hopanes. Compound names for numbered peaks are given in Table 8.*

| Peak Number | Compound Name |
|---|---|
| 1 | $C_{19}$ 13β(H),14α(H)-tricyclic terpane |
| 2 | $C_{20}$ 13β(H),14α(H)-tricyclic terpane |
| 3 | $C_{21}$ 13β(H),14α(H)-tricyclic terpane |
| 4 | $C_{22}$ 13β(H),14α(H)-tricyclic terpane |
| 5 | $C_{23}$ 13β(H),14α(H)-tricyclic terpane |
| 6 | $C_{24}$ 13β(H),14α(H)-tricyclic terpane |
| 7 | $C_{25}$ 13β(H),14α(H)-tricyclic terpane |
| 8 | $C_{26}$ 13β(H),14α(H)-tricyclic terpane |
| 9 | $C_{27}$ 13β(H),14α(H)-tricyclic terpane |
| 10 | $C_{28}$ 13β(H),14α(H)-tricyclic terpane |
| 11 | $C_{29}$ 13β(H),14α(H)-tricyclic terpane |
| 12 | 18α-22,29,30-trisnorneohopane |
| 13 | $C_{30}$ 9,15-dimethyl-25,27-bisnorhopane |
| 14 | $C_{30}$ 13β(H),14α(H)-tricyclic terpane |
| 15 | $C_{31}$ 13β(H),14α(H)-tricyclic terpane |
| 16 | $C_{29}$ 17α(H)-hopane |
| 17 | $C_{30}$ 17α(H)-diahopane |
| 18 | $C_{30}$ 17α(H)-hopane |
| 19 | $C_{33}$ 13β(H),14α(H)-tricyclic terpane |
| 20 | $C_{31}$ 17α(H)-hopane |
| 21 | $C_{34}$ 13β(H),14α(H)-tricyclic terpane |
| 22 | $C_{32}$ 17α(H)-hopane |
| 23 | $C_{35}$ 13β(H),14α(H)-tricyclic terpane |
| 24 | $C_{33}$ 17α(H)-hopane |
| 25 | $C_{36}$ 13β(H),14α(H)-tricyclic terpane |
| 26 | $C_{34}$ 17α(H)-hopane |
| 27 | $C_{35}$ 17α(H)-hopane |
| 28 | $C_{38}$ 13β(H),14α(H)-tricyclic terpane |
| 29 | $C_{39}$ 13β(H),14α(H)-tricyclic terpane |

***Table 8.*** *Peak identification for numbered peaks in Figure 22.*

low abundance relative to the regular hopanes. The tricyclic terpanes extend up to at least $C_{29}$ and $C_{23}$ is the most abundant (Figure 23b). The Pavlu core contains a high abundance of the tricyclic terpanes (Figure 23c), with $C_{23}$ being the most abundant and the extended tricyclics range up to at least $C_{39,}$ and possibly beyond. The $C_{39}$ component elutes near the end of the temperature program and appears to be at the analytical limit of the GC method used for this study. The Wilmott core has a high abundance of the regular tricyclic terpanes ($C_{19}$ to $C_{24}$) with $C_{23}$ being the most abundant. The extended tricyclic terpanes are in low abundance in this core and are observed from $C_{25}$ to $C_{29}$ (Figure 23d). The Ivan Ward core has more variability in the tricyclic terpane distribution with the uppermost samples showing the same distribution described in the Wilmott core (Figure 23e). The middle samples (IW8334 and IW8335) have a high abundance of the regular tricyclic terpanes and a very high abundance of the extended tricyclics with $C_{29}$ being the most abundant and ranging at least to $C_{39}$. In these samples the tricyclic terpanes dominate over the regular hopanes in abundance, though the regular hopanes are still present (Figure 23f). The extended tricyclic terpanes decrease in abundance with the next sample (IW8339) which shows a distribution similar to the upper portion of the Ivan Ward core. The lowermost samples (IW8365 and IW8406) have an intermediate distribution, with a high abundance of the regular tricyclic terpanes and a medium abundance of the extended tricyclics, which again range up to $C_{39}$ but do not dominate over the regular hopanes in theses samples (Figure 23g). The uppermost samples of the Jacob Betz core (JB7868 and JB7889) have a distribution very similar to the uppermost Ivan Ward and to the Wilmott cores. The distribution of the lowermost sample (JB7912) is similar to the middle of the Ivan Ward core, with a

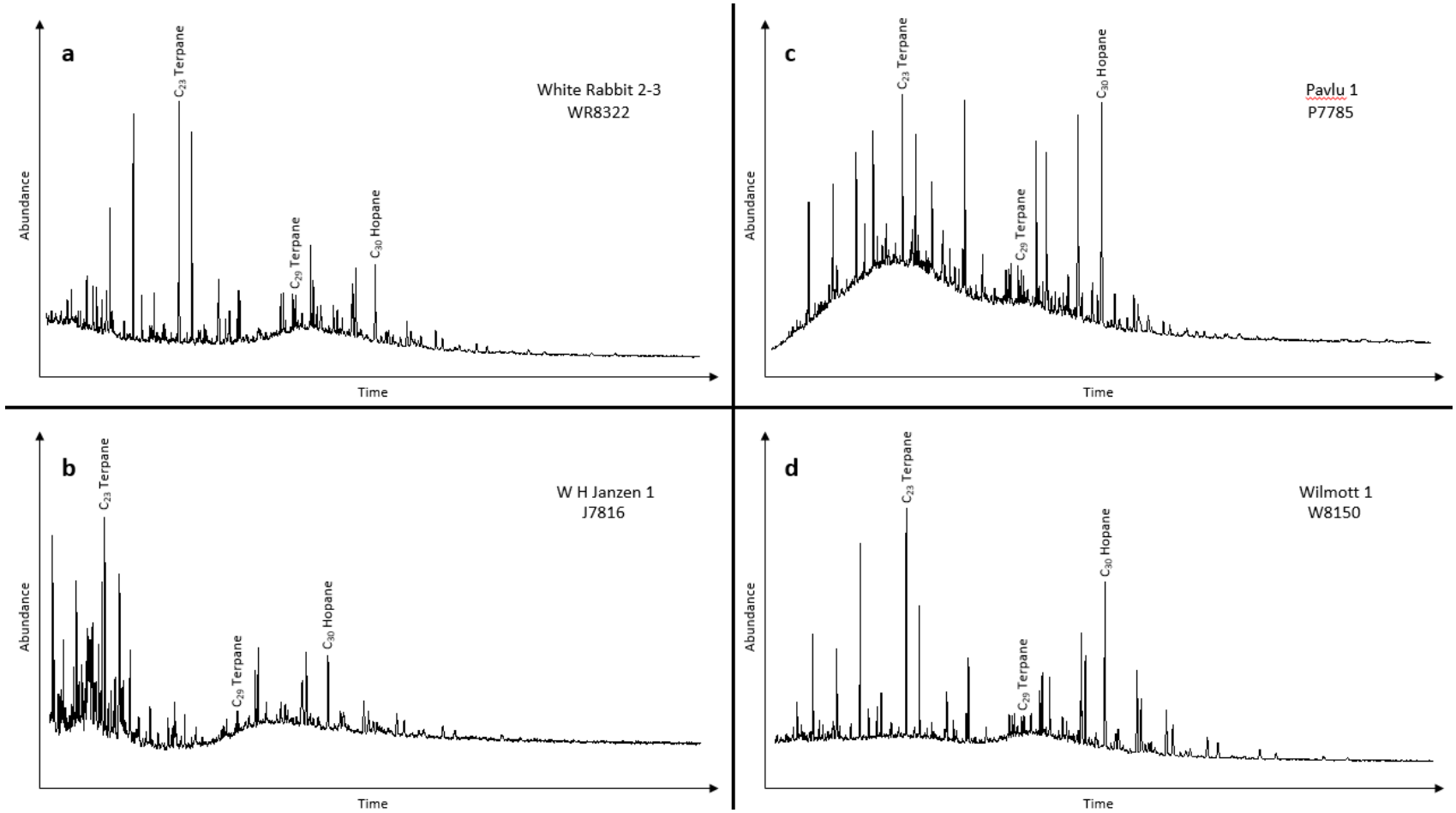


***Figure 23.*** *M/z 191 chromatograms showing tricyclic terpane distributions for select source rock samples in the study area. See Appendix A for the remaining chromatograms.*

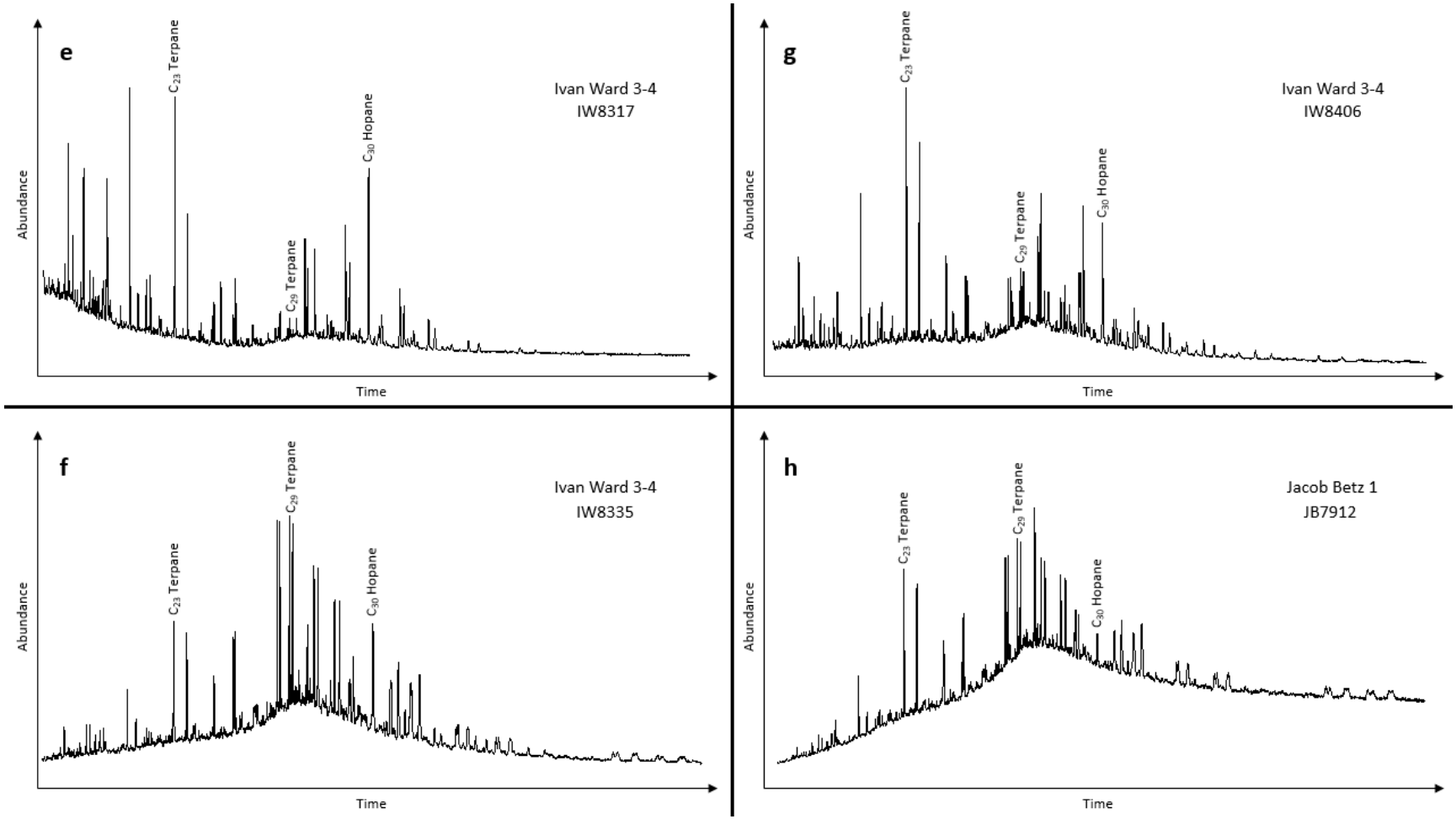


***Figure 23 continued.*** *M/z 191 chromatograms showing tricyclic terpane distributions for select source rock samples in the study area. See Appendix A for the remaining chromatograms.*

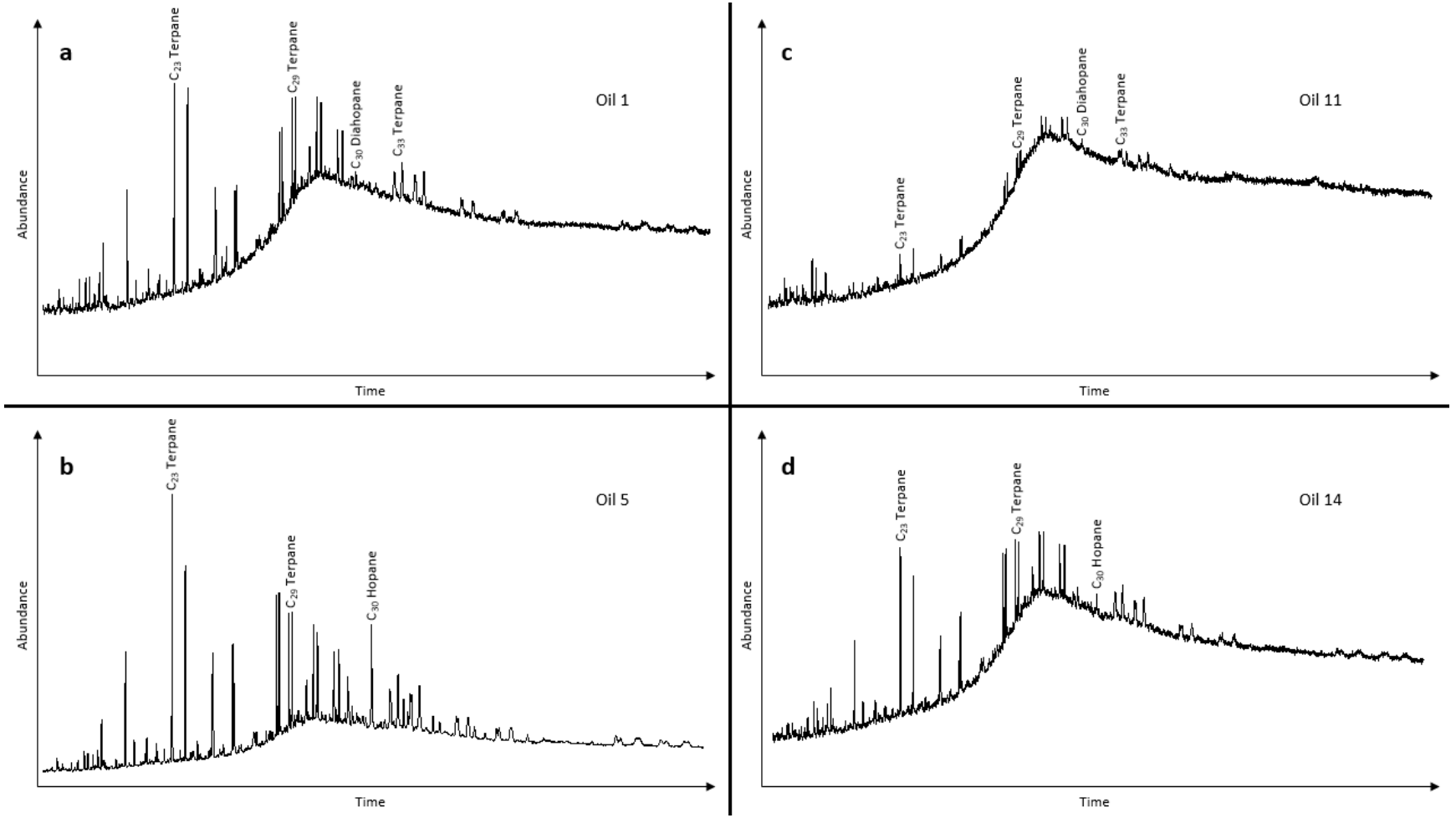


***Figure 24.*** *M/z 191 chromatograms showing the distribution of the tricyclic terpanes in select oils from the study area. See Appendix A for remaining chromatograms.*

high abundance of the extended tricyclic terpanes, ranging up to $C_{39}$ and dominating over the regular hopanes. The tricyclic terpanes are also in high abundance in this sample (Figure 23h).

The oil samples also have some variability in the distribution of the tricyclic terpanes. Oils 1 through 4 have no regular hopanes visible on the m/z 191 chromatogram from the GC/MS analysis and are completely dominated by the tricyclic terpanes, with $C_{23}$ being the most abundant and the extended tricyclic terpanes ranging up to $C_{39}$ (Figure 24a). The same temperature program was used for the oil samples as the source rocks, so this is also likely an analytical limit to the range, and not the actual limit of the compounds present. Oil 5 is still dominated by the tricyclic terpanes. Both the regular and extended tricyclics are in relatively high abundance and range up to $C_{39}$. However, the regular hopanes are also observed in this sample (Figure 24b). Oils 6 through 10 have the same distribution as Oil 5. Oil 11 is dominated by the tricyclic terpanes, which range up to at least the $C_{36}$ compound (Figure 24c). Oils 12, 13, and 14 have similar distributions to Oil 5 (Figure 24d).

### *3.2.6. Diahopanes*

The diahopanes are rearranged hopanes which are formed by catalytic rearrangement of hopenes during early diagenesis. The rearrangement occurs under oxic to suboxic conditions and requires clay minerals to mediate the reaction (Moldowan et al., 1991). These conditions are often associated with significant terrestrial input in the depositional environment (Volkman et al., 1983; Philp and Gilbert, 1986). The diahopanes are highly resistant to biodegradation (Seifert et al., 1984; Wenger and Isaken, 2002) and thermally more stable than the regular hopanes and other rearranged

hopane series (Moldowan et al., 1991). Thus, increasing thermal maturity will cause an increase in the abundance of the diahopanes relative to the regular hopanes.

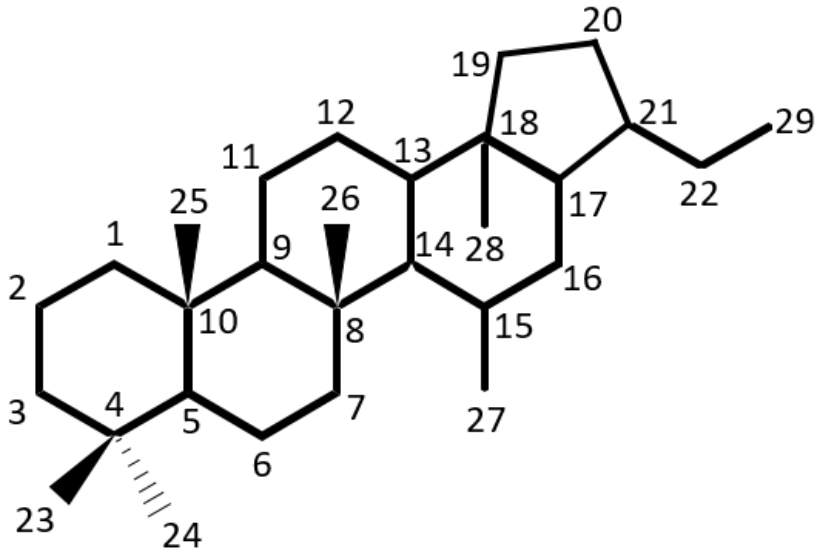


***Figure 25.*** *Structure for the diahopanes.*

17α(H)-Diahopane has been identified in high abundance relative to the 17α(H) hopane in the present study (Figure 25). Yang et al. (2016) conducted a study on the significance of the diahopanes in samples from the Ordos Basin in China. Using the samples from the Ordos Basin Yang et al. (2016) constructed a classification scheme that reflected the relative abundance of diahopane throughout the Ordos Basin. In comparing the samples from the Anadarko Basin with the samples from the Ordos Basin it is clear that the majority of the samples used in the present study are similar to the mid-range diahopane distribution observed in the Ordos Basin, which includes the carbonaceous mudstone and mudstone W56 (Figure 26) described by Yang et al. (2016). Samples J7788, J7798, P7785, and IW8365 compare with the silty mudstone

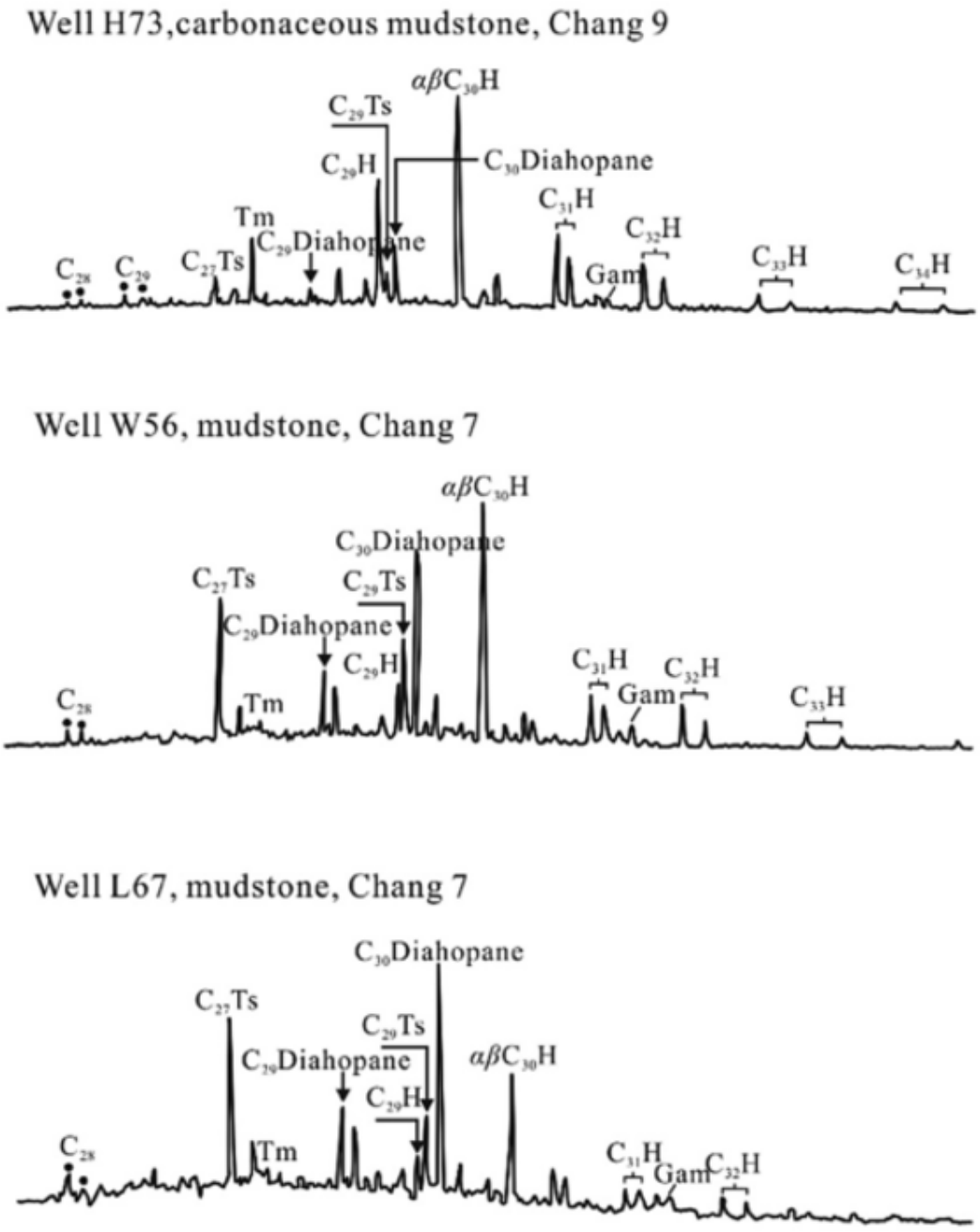


***Figure 26.*** *M/z 191 chromatograms from Yang et al. (2016) showing relative abundances of the $C_{29}$ and $C_{30}$ diahopanes relative to $C_{30}$ hopane in the Ordos Basin, China. The majority of the samples from the Anadarko Basin are similar to Yang et al.'s (2016) carbonaceous mudstone and mudstone W56, with some samples being similar to L67 mudstone.*

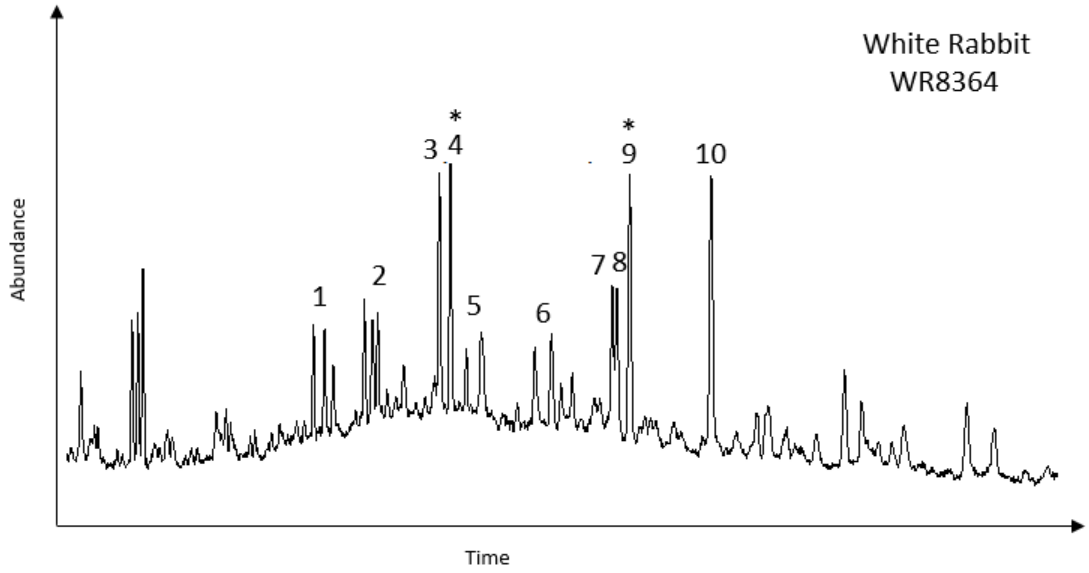


***Figure 27.*** *M/z 191 chromatogram from White Rabbit sample at 8364 ft. Peak 4 is 9,15-dimethyl-25,27-bisnorhopane. Peak 9 is the 17α(H)-diahopane. There is a high abundance of both compounds and these compounds are observed to co-vary throughout the source rocks in the study area. Table 9 has peak identifications.*

| Peak Number | Compound Name |
|---|---|
| 1 | $C_{28}$ 13β(H),14α(H)-tricyclic terpane |
| 2 | $C_{29}$ 13β(H),14α(H)-tricyclic terpane |
| 3 | 18α-22,29,30-trisnorneohopane |
| 4 | $C_{30}$ 9,15-dimethyl-25,27-bisnorhopane |
| 5 | $C_{30}$ 13β(H),14α(H)-tricyclic terpane |
| 6 | $C_{31}$ 13β(H),14α(H)-tricyclic terpane |
| 7 | $C_{29}$ 17α(H)-hopane |
| 8 | 18α-30-trisnorneohopane |
| 9 | 17α(H)-diahopane |
| 10 | 17α(H)-hopane |

***Table 9.*** *Peak identification for Figures 27 and 30.*

classification, which contained a low abundance of 17α(H)-diahopane. Samples J7816, W8156, IW8334, IW8335, IW8339, IW8406, and JB7912 compare with their mudstone L67 which contained 17α(H)-diahopane in higher abundances than the 17α(H)-hopane (Figure 26). Comparing the samples from the Anadarko Basin to the samples from the Ordos Basin revealed that the Anadarko Basin does not show as much variation in its diahopane abundance. When the regular hopanes were available for comparison to the Ordos Basin samples the Anadarko Basin oil samples compared with the carbonaceous mudstone classification, which displayed mid-range abundance of diahopanes. It was also observed that in the Anadarko Basin diahopanes increase in abundance with increasing depth/maturity in all of the cores sampled. This trend could not be confirmed in the Pavlu core as only one sample was taken from this core. The Anadarko Basin and the Ordos Basin are of similar thermal maturity, 0.68 to 1.23 %Rc for the Anadarko Basin and 0.77 to 1.12 %Rc for the Ordos Basin (Yang et al., 2016).

### *3.2.7. 9,15-Dimethyl-25,27-Bisnorhopanes*

An unusual peak was observed in the *m/z* 191 trace, occurring immediately after the 18α-22,29,30-trisnorneohopane ($C_{27}$ Ts) peak (Figure 27 and 30). Using GC/MS/MS analysis it was discovered that this peak is the $C_{30}$ compound of a series that matches the one identified as the unknown series in Telnæs et al. (1992) and as the early eluting rearranged hopane series in Farrimond and Telnæs (1996). This early eluting series was later identified by Nytoft et al. (2007) as the 9,15-dimethyl-25,27-bisnorhopane (Figure 28). The 9,15-dimethyl-25,27-bisnorhopane and associated homologues elute approximately two carbon numbers earlier than the regular hopanes

and range from $C_{27}$ to $C_{35}$ with the $C_{28}$ compound being absent (Farrimond and Telnæs, 1996; Figure 29).

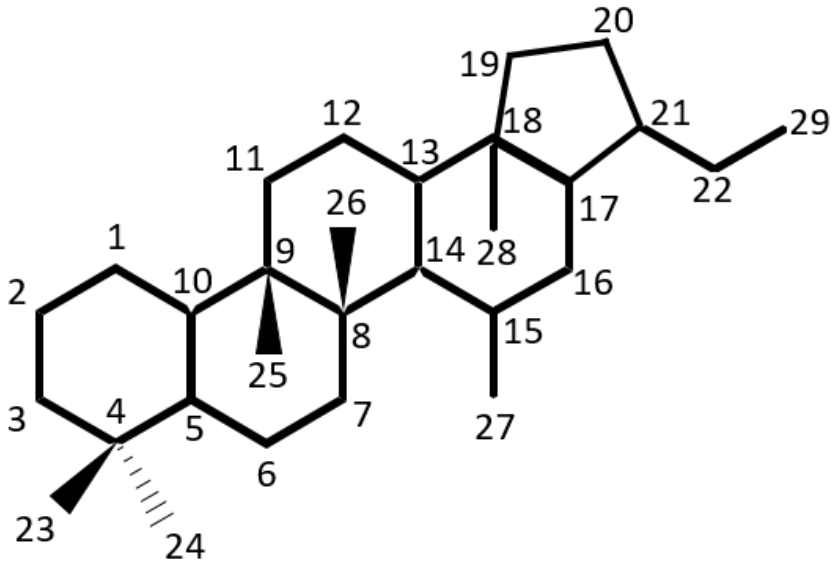


***Figure 28.*** *Structure of the 9,15-dimethyl-25,27-bisnorhopane as defined by Nytoft et al. (2007).*

The abundance of the $C_{30}$ 9,15-dimethyl-25,27-bisnorhopane closely co-varies with the abundance of 17α(H)-diahopane in the study area. An exception to this trend is found in samples IW8334, IW8335, and JB7912. In these samples the $C_{30}$ 17α(H)-diahopane peak is in high abundance and the $C_{30}$ 9,15-dimethyl-25,27-bisnorhopanes peak is in relatively low abundance (Figure 30). It is significant to note that the same samples where this trend does not continue are the samples where the tricyclic terpanes are dominant in the source rock samples. The 9,15-dimethyl-25,27-bisnorhopane series was were not observed on the GC/MS analysis for any of the oil samples used in this study.

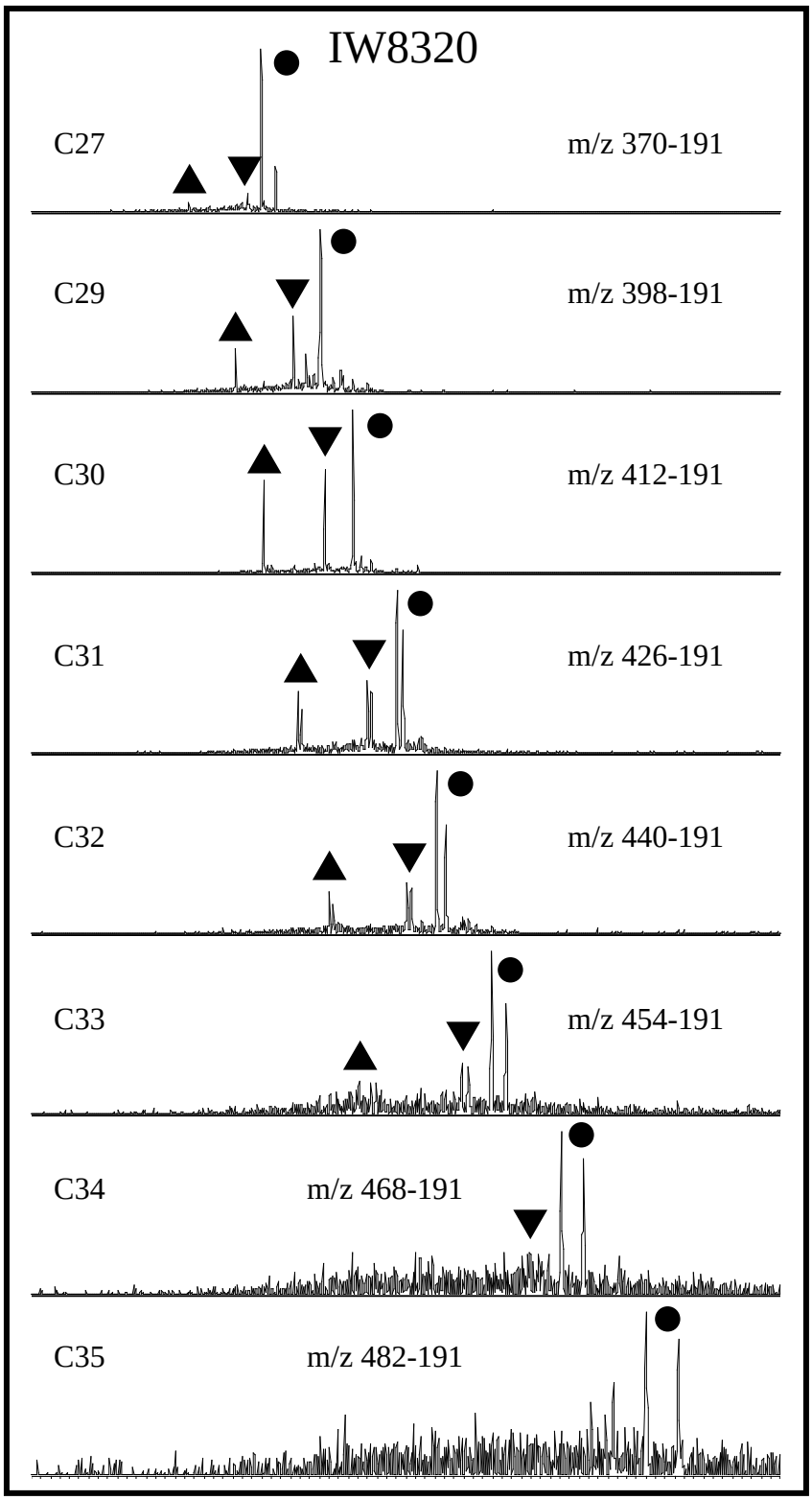


***Figure 29.*** *GC/MS/MS chromatograms showing the $C_{27}$ – $C_{35}$ (except the $C_{28}$ compounds) compounds of the 9,15-dimethyl-25,27-bisnorhopanes (marked by ▲), the 17α(H)-diahopanes (marked by ▼), and the 17α(H)-hopanes (marked by ●). This matches the series of early eluting rearranged hopanes reported by Farrimond and Telnæs (1996).*

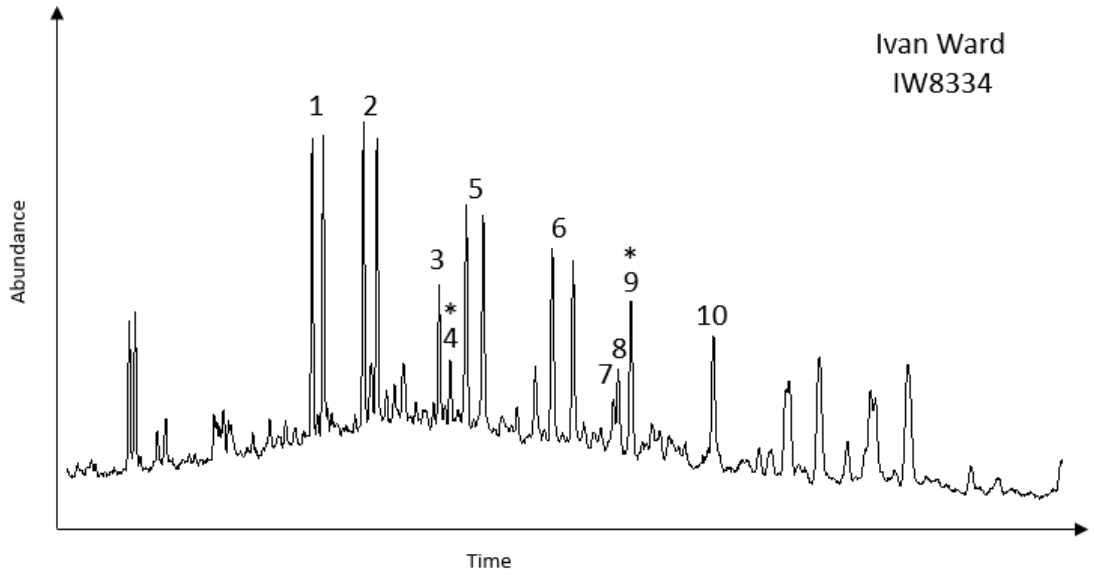


***Figure 30.*** *M/z 191 chromatogram of a rock extract dominated by the tricyclic terpanes from the Ivan Ward core at 8334 ft. The peak labeled 4 is $C_{30}$ 9,15-dimethyl-25,27-bisnorhopane. The peak labeled 9 is the $C_{30}$ 17α(H)-diahopane series. The samples that are dominated by the tricyclic terpanes are the only source rock samples where these two series do not co-vary in abundance in the study area. Peak labels are given in Table 9.*

### *3.2.8. Dibenzothiophene*

Dibenzothiophene is a sulfur containing aromatic compound (Figure 31; Williams et al., 1986 and Connan et al., 1992). Along with phenanthrene, dibenzothiophene is produced during diagenesis, catagenesis, and metagenesis. Since both dibenzothiophene and phenanthrene are produced during these stages and not from the biomass itself these compounds can be used as indicators of the depositional environment conditions (Hughes et al., 1995). By combining the value of dibenzothiophene/phenanthrene with the pristane/phytane value (Table 10), a cross plot indicating source rock lithology can be generated (Figure 32). Because both the dibenzothiophene/phenanthrene and pristane/phytane values are resistant to

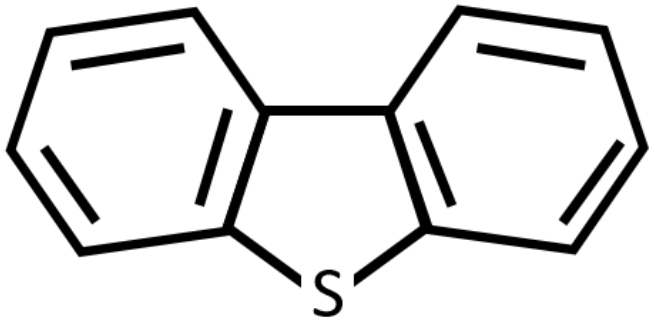


***Figure 31.*** *Structure of dibenzothiophene.*

biodegradation and thermal alteration they are useful parameters for determining environmental conditions for oils. These ratios indicate that the samples used for this study fall into two categories, lacustrine for the samples in zone 2 and marine for the samples in zone 3 (Hughes et al., 1995). It is interesting to note that the source rock samples that are in zone 2 are the samples from the Pavlu and Jacob Betz cores. These are the same cores where 18α(H)-oleanane was identified in the saturate *m/z* 191 chromatogram. It is important to realize that the divisions displayed in Figure 32 are not cast in stone and some variation is expected.

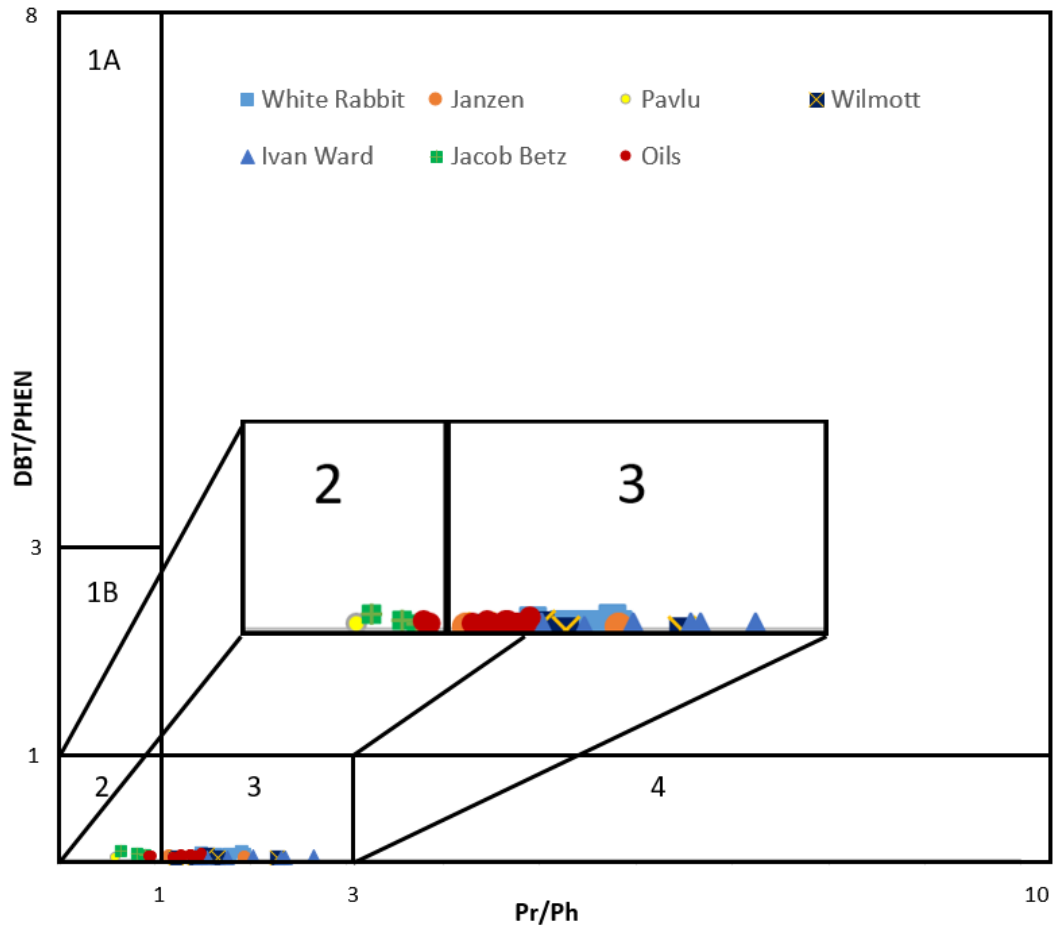


***Figure 32.*** *Cross plot after Hughes et al. (1995) showing depositional environment conditions based on the dibenzothiophene/phenanthrene (DBT/PHEN) and pristane/phytane (Pr/Ph) values. Zone 1A represents a marine carbonate environment. Zone 1B represents a mixed marine/lacustrine (sulfate-rich) environment. Zone 2 represents a lacustrine (sulfate-poor) type environment. Zone 3 represents a marine and lacustrine shale environment. Zone 4 represents a fluvio/deltaic environment with carbonaceous shale and coal. Values for the ratios are found in Table 10.*

| Sample Name | DBT/PHEN | Pr/Ph |
|---|---|---|
| **WR8318** | 0.029 | 1.65 |
| **WR8322** | 0.036 | 1.94 |
| **WR8342** | 0.065 | 1.91 |
| **WR8348** | 0.043 | 1.49 |
| **WR8364** | 0.029 | 1.79 |
| **J7781** | 0.014 | 1.26 |
| **J7788** | 0.014 | 1.52 |
| **J7798** | 0.014 | 1.94 |
| **J7816** | 0.022 | 1.16 |
| **P7785** | 0.014 | 0.60 |
| **W8147** | 0.014 | 1.43 |
| **W8148** | 0.007 | 1.67 |
| **W8150** | 0.007 | 2.28 |
| **W8155** | 0.014 | 1.23 |
| **W8156** | 0.036 | 1.55 |
| **IW8317** | 0.014 | 2.32 |
| **IW8320** | 0.021 | 2.65 |
| **IW8330** | 0.014 | 2.37 |
| **IW8334** | 0.022 | 1.42 |
| **IW8335** | 0.014 | 1.55 |
| **IW8339** | 0.007 | 1.76 |
| **IW8365** | 0.007 | 1.48 |
| **IW8406** | 0.022 | 2.02 |
| **JB7868** | 0.051 | 0.82 |
| **JB7889** | 0.029 | 0.90 |
| **JB7912** | 0.079 | 0.66 |
| **Oil 1** | 0.015 | 1.20 |
| **Oil 2** | 0.014 | 1.25 |
| **Oil 3** | 0.037 | 1.28 |
| **Oil 4** | 0.053 | 1.50 |
| **Oil 5** | 0.022 | 1.44 |
| **Oil 6** | 0.022 | 1.41 |
| **Oil 7** | 0.029 | 1.38 |
| **Oil 8** | 0.023 | 1.31 |
| **Oil 9** | 0.022 | 1.40 |
| **Oil 10** | 0.022 | 0.98 |
| **Oil 11** | 0.029 | 1.39 |
| **Oil 12** | 0.022 | 1.29 |
| **Oil 13** | 0.025 | 0.95 |
| **Oil 14** | 0.022 | 1.48 |

***Table 10.*** *Dibenzothiophene/phenanthrene and pristane/phytane values for all source rock and oil samples.*

### *3.2.9. Unusual Unknown Aromatic Compound*

An unknown compound was observed in the chromatograms of the aromatic fractions from the source rock extracts. The unknown compound elutes between the methylphenanthrene isomers, closer to the first pair than the second pair of isomers (Figure 33). This compound was not identified during this study but its presence in the sample set and spectrum are presented (Figure 34). The compound was present in the western most three cores, White Rabbit, Wilmott, and Ivan Ward and was not observed in the eastern most cores, Janzen, Pavlu, and Jacob Betz. In the Wilmott core the unknown compound was only observed in samples W8150 and W8156. It is significant to note that the other three samples from the Wilmott core where this compound was not observed did not produce enough extract to fractionate into saturate, aromatic, and polar fractions and were thus analyzed as whole extracts. This compound was not observed in the chromatograms of any sample that was left as a whole extract. This may be due to low relative abundance levels of this compound when not fractionated into an aromatic fraction. The unknown compound was observed in all of the White Rabbit core samples. However, it was in very low relative abundance (relative to the methylphenanthrenes) in the uppermost three samples (WR8318, WR8322, and WR8342) and increased significantly in the lower two samples (WR8348 and WR 8364). This compound was also observed in all samples from the Ivan Ward core. In this case it decreased in abundance in the middle of the core in samples IW8334 and IW8335 and increases again with the next sample (IW8339). The unknown compound was not observed in the oil samples.

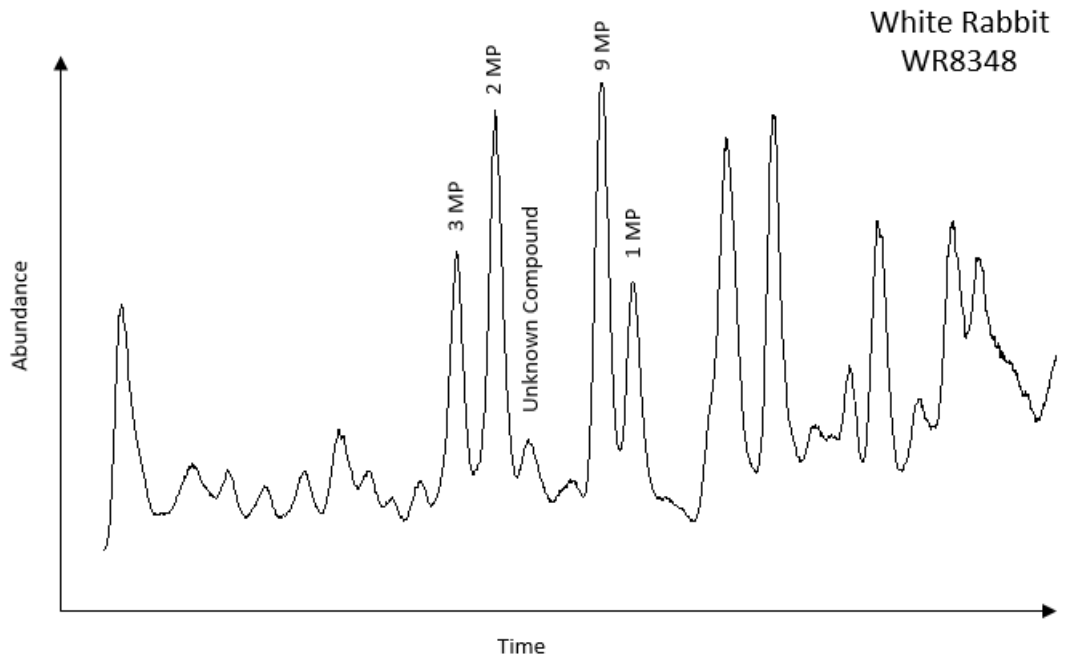


***Figure 33.*** *FID gas chromatogram of an aromatic fraction of a source rock extract from the White Rabbit core showing the presence of an unknown, unusual compound eluting between the methylphenanthrene isomer pairs.*

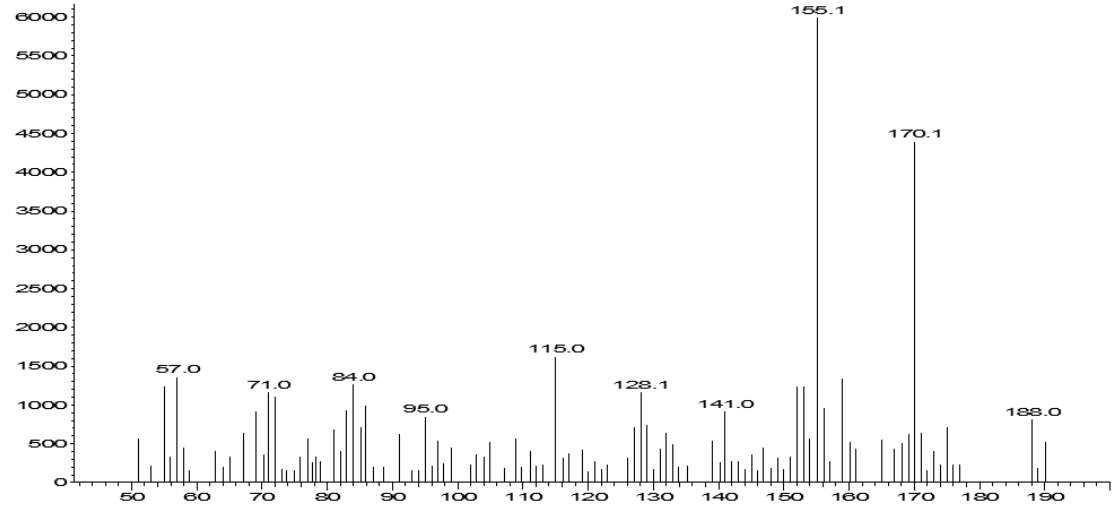


***Figure 34.*** *GC/MS full scan spectrum of the unknown compound eluting between the methylphenanthrene isomer pairs in the aromatic fractions. The spectrum was taken from sample WR8364 from the White Rabbit core.*

# 4. Discussion

## 4.1. Distribution of 18α(H)-Oleanane in the Chesterian Limestone

This study tentatively confirms the presence of 18α(H)-oleanane in three source rock samples from two cores in the Chesterian Limestone in the Anadarko Basin. Combining these samples with those from Kim and Philp (1999) gives a total of six source rock samples within the Chesterian Limestone from three cores (Pavlu, Jacob Betz, and Flint) where 18α(H)-oleanane has been tentatively identified. 18α(H)-Oleanane has also been tentatively identified in multiple samples from the overlying Pennsylvanian Morrow Formation in the Anadarko Basin in a presently ongoing study by Sumer Gorenekli, (2017). Identifying 18α(H)-oleanane in pre-Cretaceous source rocks is unusual but the Anadarko Basin is not the only case where such an occurrence has been reported. Peters et al. (1999) identified oleanane in the Jurassic aged Brora Coal near Scotland. Another rare occurrence of pre-Cretaceous 18α(H)-oleanane was identified by Moldowan et al. (1994) in a Middle Jurassic siltstone from West Siberia, Russia as well as in a Pennsylvanian coal ball from Illinois, USA (Moldowan at el., 1994). In each case 18α(H)-oleanane was present in low abundance relative to 17α(H)-hopane, but the presence of 18α(H)-oleanane in these samples clearly shows that the presence of 18α(H)-oleanane is not unequivocal proof of a Cretaceous or younger source (Peters et al., 1999).

In addition to the studies where pre-Cretaceous oleanane has been identified, a study by Taylor et al. (2005) points out that molecular phylogenetic and molecular clock data indicate a pre-Mesozoic age for when angiosperms diverged from other seed plants. Taylor et al. (2005) used zeolites to preferentially reduce hopanes that may co-

elute with the oleananes to provide more confident identification of very low amounts of oleanane. The samples used by Taylor et al. (2005) included two non-angiosperm seed plants that were found to contain 18α(H)-oleanane. The seed plants were the Cretaceous Bennettitales and the Permian Gigantopteridales. Both of these plants have significant similarities to angiosperm plants and may even be from a sister group to the angiosperms. The authors concluded that if oleanane originated in non-angiosperm seed plants, as is suggested by the presence of oleanane in the above mentioned specimens, then the angiosperm lineage would have separated from other seed plants by the Late Paleozoic (Taylor et al., 2005). If the angiosperm lineage did separate from other seed plants by the Late Paleozoic then the pre-Cretaceous occurrences of oleanane identified in the present study, as well as in the previously mentioned studies (Moldowan et al., 1994; Peters et al., 1999) may have been produced from angiosperm plant material present in the environment at the time of deposition.

The possibility of early angiosperms being the source of oleanane identified in pre-Cretaceous sources is further supported by calculations using DNA nucleotide sequences to determine the timing of when slow-evolving enzymes would be expected to develop. Martin et al. (1989) determined the rate of diversification of the slowly evolving glycolytic enzyme glyceraldehyde-3-phosphate dehydrogenase in nucleotide sequences from modern animals and angiosperm plants. After determining the enzyme's rate of diversification the authors applied this rate to calculating the timing of when this enzyme would have been initially synthesized to have reached its present day diversification. The method used by Martin et al. (1989) places the diversification of angiosperm plants as early as over 300 million years ago (Figure 35). This estimation

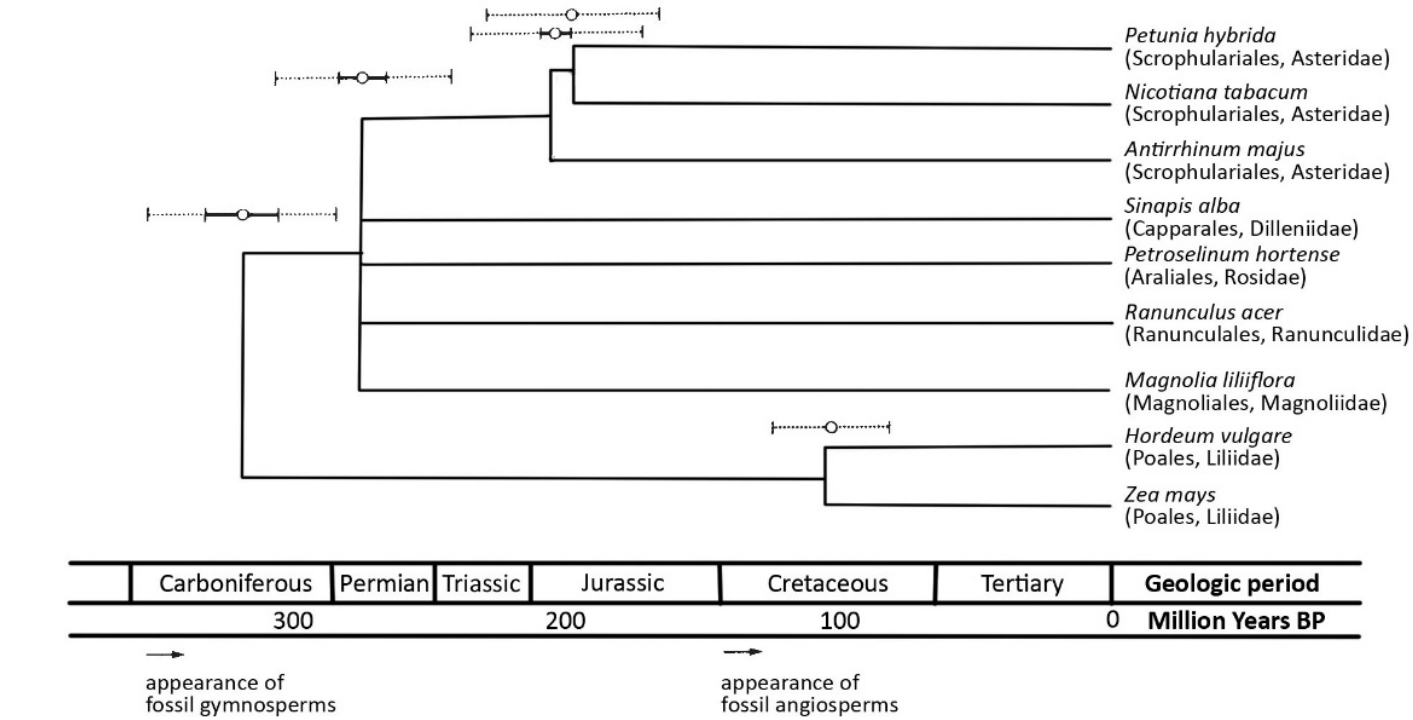


***Figure 35.*** *DNA nucleotide calculations using slow-evolving enzymes to determine the timing of the original diversification of angiosperm plants from Martin et al. (1989). These projections place the evolution of angiosperms early enough that angiosperms may have been the source of the 18α(H)-oleanane observed in the Chesterian Limestone.*

places the divergence of angiosperms from other seed plants in the Carboniferous. Combining this time estimation with the non-angiosperm seed plants found to contain oleanane (Taylor et al., 2005) provides supporting evidence that the oleanane identified in the Chesterian samples used in the present study may be from the earliest angiosperm plants (indicated by the DNA nucleotide sequences from Martin et al., 1989) or from closely related plants of non-angiosperm type, such as the samples from Taylor et al. (2005). Another possibility for the presence of oleanane in this, and other pre-Cretaceous occurrences, is that there may have been other, un-related, plant types available with the rarely expressed ability to synthesize oleanane-type compounds. While this explanation is certainly possible there is not any evidence indicating which plant group may have had such an ability, nor does this possibility diminish the validity of the explanations provided by Martin et al. (1989) and Taylor et al. (2005).

### 4.2. Distribution of 1,2,7-Trimethylnaphthalene in the Chesterian Limestone

The presence of 1,2,7-trimethylnaphthalene in the Chesterian Limestone of the Anadarko Basin was also confirmed in this study. 1,2,7-Trimethylnaphthalene was much more widely distributed than 18α(H)-oleanane in the samples used in this study, and samples previously studied by Kim and Philp (1999). Other studies that have identified 1,2,7- trimethylnaphthalene in pre-Cretaceous samples include Strachan et al. (1988) who identified this compound in Triassic aged samples, and Armstroff et al. (2006) who identified it in a wide range of samples from the Permian, Upper and Lower Carboniferous, and one Devonian sample. In both of these studies 1,2,7-trimethylnaphthalene was present in more samples than the oleananes and in fact Armstroff et al. (2006) reported no oleanane in any of their samples but 1,2,7-

trimethylnaphthalene present in all of them. Strachan et al. (1988) reported the presence of both compounds but oleanane was only identified in samples of Cretaceous or younger age, whereas 1,2,7-trimethylnaphthalene was also identified in samples of pre-Cretaceous age. There was a significant increase in the abundance of 1,2,7-trimethylnaphthalene in the samples that were Cretaceous or younger. Because of the wide spread distribution of 1,2,7-trimethylnaphthalene in pre-Cretaceous samples along with the total lack of oleanane and other saturated oleanane-type compounds Armstroff et al. (2006) concluded that the validity of using 1,2,7-trimethylnaphthalene as a marker for angiosperm plants is questionable at best and that another, currently unknown, precursor may be responsible for the presence of 1,2,7-trimethylnaphthalene in samples of pre-Cretaceous age.

The absence of oleanane and related saturated oleanane-type compounds in the samples studied by Armstroff et al. (2006) may be partially due to depositional conditions. Armstroff et al. (2006) plotted their samples on a cross plot using the values of pristane/$C_{17}$ verses phytane/$C_{18}$ which showed the majority of these samples to be terrestrial type III organic matter with some mixed type II/III and only a few containing marine type II organic matter. In terrestrial environments the diagenesis of β-amyrin is dominated by the aromatic pathways which results in higher abundance of the aromatic oleanoid compounds and potentially no preservation of the saturated oleanane-type compounds (Murray et al., 1997). Similarly, the cross plot of pristane/$C_{17}$ verses phytane/$C_{18}$ indicates that the majority of the samples used in the present study on the Anadarko Basin have a mixed or transitional organic matter origin (Figure 19). In addition to the mixed nature of the organic material, the high abundance of rearranged

hopanes relative to the hopanes indicates significant clay content in the depositional environment, and is often associated with terrestrial input (Volkman et al., 1983; Philp and Gilbert, 1986). This high terrestrial input may have caused conditions to favor aromatization of β-amyrin, thus resulting in low to no formation and preservation of 18α(H)-oleanane and instead forming 1,2,7-trimethylnaphthalene.

It is still entirely possible that 1,2,7-trimethylnaphthalene has an additional, currently unknown precursor. However, the studies confirming the presence of pre-Cretaceous oleanane (Moldowan et al., 1994; Peters et al., 1999) along with the studies supporting the possible early diversification of angiosperm (Martin et al., 1989) and closely related plants (Taylor et al., 2005) support 1,2,7- trimethylnaphthalene still being a valid marker for angiosperm plants, along with 18α(H)-oleanane. The presence of both 1,2,7- trimethylnaphthalene and 18α(H)-oleanane in the Chesterian Limestone of the Anadarko Basin further supports these compounds being related.

### 4.3. Distribution of Rearranged Hopanes in the Chesterian Limestone

17α(H)-Diahopane is observed in high abundance relative to 17α(H)-hopane throughout the samples used in this study on the Anadarko Basin. There has been some dispute over the origin of diahopanes but it is generally agreed that the diahopanes are formed from bacterial hopanoids that undergo rearrangement of their methyl side chains by clay-mediated acid catalysis which occurs during maturation (Philp and Gilbert 1986; Moldowan et al., 1991; Wang et al., 2000; Zhao and Zhang 2001; Zhu et al., 2007; Yang et al., 2016). Because the formation of diahopanes requires clay minerals to drive the rearrangement of the methyl side chain, the presence of diahopanes indicates that the depositional environment contained enough clay to allow for the rearrangement

of the bacterial hopanoids. Carbonate rocks typically contain low amounts of clay. This is because carbonate deposition functions best in clear water (Yancey, 1989). Thus, because clay is required to produce rearranged hopanes it is unusual to observe high levels of rearranged hopanes in carbonate rocks (Palacas, 1984). The Chesterian Limestone is described as a shallow marine carbonate platform with interbedded grey shales (Peace and Forgotson, 1991). Furthermore, when the values of pristane/$C_{17}$ and phytane/$C_{18}$ were plotted against each other (Figure 19) they indicate that the majority of the source rock and oil samples were deposited as mixed organic material in a transitional environment. The interbedded setting of the lithology and the mixed nature of the organic material indicate that the Chesterian Limestone received significant input from both terrestrial and marine environments and that the terrestrial input was sufficient to allow for the clay catalysis necessary to produce rearranged hopanes, including diahopanes and 9,15-dimethyl-25,27-bisnorhopanes (which will be discussed later).

Yang et al. (2016) concluded that high abundance of diahopanes is due to the depositional environment and the lithology of the source rock. High clay content and a suboxic environment within a shallow to semi-deep lacustrine facies were determined to be the optimal conditions for the rearrangement of bacterial hopanoids. While the Anadarko Basin is not a lacustrine setting the observed abundances of rearranged hopanes may indicate that the study area was under suboxic conditions during the Chesterian (Wang, 1993). Yang et al. (2016) also recognized that maturity typically plays a significant role in producing the observed abundances of diahopanes and other rearranged hopanes. However, in the case of the Ordos Basin, Yang et al. (2016)

observed that the diahopanes did not increase in abundance with depth or with increasing maturity. Yang et al. (2016) concluded that depositional conditions and lithology were the major factors in producing the high abundances of diahopane observed in the Ordos Basin. Unlike the Ordos Basin maturity does appear to play an important role in the observed abundances of rearranged hopanes, including the diahopanes, in the Anadarko Basin. However, both the Ordos and Anadarko Basins contain interbedded mudstone and carbonate sedimentary facies. Yang et al. (2016) concluded that the geochemical differences between the mudstones and carbonates of the Ordos Basin correlated very well with their observed high and low abundances in the diahopanes. The sampling method used for the present study on the Anadarko Basin does not allow for a similar detailed vertical observation of changes in the interbedded facies. However, the depositional conditions may also play a role in producing the rearranged hopanes, with the mudstone facies containing higher abundances than the carbonate facies, as was found in the Ordos Basin (Yang et al., 2016).

It has been clearly shown that diahopanes are thermally more stable than the regular hopanes and thus that the diahopanes will increase in abundance, relative to the hopanes, with increasing maturity (Kolaczkowska et al., 1990; Moldowan et al., 1991; Wang et al., 2000; Yang et al., 2016). Moldowan et al. (1991) suggested using the 17α(H)-diahopane/17α(H)-hopane value as a method for observing the thermal maturity relationship between the diahopanes and the hopanes. The 17α(H)-diahopane/17α(H)-hopane value was calculated for the source rock and oil samples from the Anadarko Basin (Table 11). The source rock samples show an increase of the diahopane/hopane value with depth in five of the six cores sampled (Pavlu core being the sixth core only

| Sample Name | Diahopane/Hopane | TAS |
|---|---|---|
| **WR8318** | 0.10 | 0.89 |
| **WR8322** | 0.88 | 0.77 |
| **WR8342** | 0.75 | 0.76 |
| **WR8348** | 0.50 | 0.77 |
| **WR8364** | 0.97 | 0.83 |
| **J7781** | 0.18 | 0.63 |
| **J7788** | 0.08 | 0.67 |
| **J7798** | 0.08 | 0.76 |
| **J7816** | 1.00 | 0.81 |
| **P7785** | 0.13 | 0.65 |
| **W8147** | 0.52 | 0.77 |
| **W8148** | 0.31 | 0.78 |
| **W8150** | 0.53 | 0.82 |
| **W8155** | 0.60 | 0.89 |
| **W8156** | 1.67 | 0.89 |
| **IW8317** | 0.44 | 0.88 |
| **IW8320** | 0.57 | 0.89 |
| **IW8330** | 0.48 | 0.92 |
| **IW8334** | 1.18 | 0.88** |
| **IW8335** | 0.62 | 0.93** |
| **IW8339** | 1.08 | 0.89 |
| **IW8365** | 0.09 | 0.93 |
| **IW8406** | 1.11 | 0.87 |
| **JB7868** | 0.60 | 0.83 |
| **JB7889** | 0.15 | 0.79 |
| **JB7912** | 1.33 | 0.89** |
| **Oil 7** | 0.12 | 0.45 |
| **Oil 8** | 0.14 | 0.51 |
| **Oil 6** | 0.14 | 0.58 |
| **Oil 9** | 0.26 | 0.61 |
| **Oil 5** | 0.18 | 0.68 |
| **Oil 10** | 0.43 | 0.71 |
| **Oil 12** | 0.27 | 0.73 |
| **Oil 13** | 0.50 | 0.80 |
| **Oil 1** | * | 0.82** |
| **Oil 3** | * | 0.86** |
| **Oil 14** | 1.10 | 0.88** |
| **Oil 4** | * | 0.90** |
| **Oil 2** | * | 0.90** |
| **Oil 11** | * | 0.90** |

***Table 11.*** *Showing the values of 17α(H)-diahopane/17α(H)-hopane. The ratio increases with depth in the source rock samples and with increasing maturity. This is especially visible in the oil samples. To better show the trend with maturity the oil samples have been sorted by increasing TAS ratio (relative maturity). * indicates that the 17α(H)-hopane was not visible in the corresponding 191 chromatogram and this ratio could not be calculated. ** indicates samples where the* m/z *191 chromatogram is dominated by the tricyclic terpanes.*

has one sample) and this trend generally follows the increasing maturity in these samples as indicated by the triaromatic hydrocarbon steroid ratio (TAS). This trend is also observed in the oil samples with the 17α(H)-diahopane/17α(H)-hopane ratio increasing with increasing maturity (again indicated by the TAS ratio; Table 11).

The 9,15-dimethyl-25,27-bisnorhopanes have been reported in previous studies (labeled as the early eluting rearranged hopane series), including Killops and Howell (1991); Telnæs et al., (1992); Wang (1993) and Farrimond and Telnæs (1996). Farrimond and Telnæs (1996) reported that the 9,15-dimethyl-25,27-bisnorhopane series closely co-varied with the 17α-diahopane series, similar to the trend observed in samples from the Anadarko Basin. Farrimond and Telnæs (1996) concluded that the similarities in abundance between these two series indicated a similar structure and similar formation process, which was confirmed by Nytoft et al. (2007) when the structure of the 9,15-dimethyl-25,27-bisnorhopanes was identified (Figures 25 and 28). A significant difference observed in the current study between these two series is observed in the source rock samples dominated by the extended tricyclic terpanes (samples IW8334, IW8335, and JB7912). In these samples, instead of their respective abundances co-varying the abundance of 17α(H)-diahopane was high relative to 9,15-dimethyl-25,27-bisnorhopane (Figure 30). Except for the above mentioned three samples these compounds co-vary very closely in abundance in the source rock samples (the trend could not be confirmed in the oil samples, as the 9,15-dimethyl-25,27-bisnorhopanes were not observed in the oil samples). Reasons for the observed deviance from the trend of co-variance between these two series are potentially related to the conditions that resulted in the extended tricyclic terpanes being in greater abundance

than the regular hopanes in these samples. These may be related to thermal maturity reactions with the tricyclic terpanes (will be discussed later); or due to depositional environment conditions (Wang, 1993; Yang et al., 2016).

## 4.4. Tricyclic Terpanes and Thermal Maturity

Previous studies have reported an unusually high abundance of tricyclic terpanes in the Mississippian rocks of the Anadarko Basin, including the Chesterian Limestone (Wang, 1993; Kim and Philp, 1999) as well Lower Mississippian Limestones (Wang, 1993), the Springer Formation (Wang, 1993; Pearson, 2016) and the Morrow Formation (Wang, 1993). A similar occurrence of tricyclic terpanes in high enough abundance to dominate over the regular hopanes has been observed in three of the source rock samples and six of the oil samples used in the present study. Similar cases of tricyclic terpanes dominating the regular hopanes have been reported from other basins as well. Kruge et al. (1990) observed tricyclic terpanes that dominated the regular hopanes in lacustrine black shales in the Hartford Basin in Connecticut; Aquino Neto et al. (1992) observed similar distributions of tricyclic terpanes in Alaska, Brazil, and Tasmania; and Dutta et al. (2006) also observed this distribution in south-east Turkey. Volkman et al. (1989) and Aquino Neto et al. (1992) proposed Tasmanacae algae (tasmanities) as a possible precursor for the tricyclic terpanes and suggested that the high abundances of the tricyclic terpanes were due to an increased level of the algae in the depositional environment. However, in contrast to this proposal, Dutta et al. (2006) tested well preserved tasmanities from south-east Turkey and found that the tricyclic terpanes were not present in the tasmanities fossil, but that the compounds were present within the formation the tasmanities were preserved in. Dutta et al. (2006) concluded that the

tasmanities are at least not the sole precursor of the tricyclic terpanes. With respect to possible mechanisms for creating the observed dominance of the tricyclic terpanes in the *m/z* 191 chromatogram Kruge et al. (1990) concluded that the tricyclic terpanes may have been concentrated by high thermal maturity in the samples, by preferential depletion of the hopanes by migration, or as a result of an increased production of tricyclic terpane precursors in the depositional environment (Kruge et al., 1990). Wang (1993) discussed similar mechanisms for the observed distribution of tricyclic terpanes in the Anadarko Basin. However, Wang (1993) ruled out migration in the Anadarko Basin as samples from the Lower Mississippian Limestones were found to contain the high abundances of tricyclic terpanes, but the underlying formations (specifically the Woodford Shale) did not indicate a similar distribution of tricyclic terpanes and thus, likely were not the source of these compounds in the Mississippian Limestones. Wang (1993) also concluded that thermal maturity was an unlikely mechanism as the samples from the Anadarko Basin were not overly mature and determined that the distribution was likely due to conditions related to the depositional environment, with thermal maturity as a potential secondary driving force (Wang, 1993).

Regarding the present study on the Anadarko Basin, a strong correlation was observed between the samples where the tricyclic terpanes dominate over the regular hopanes and the corresponding triaromatic hydrocarbon steroid ratio (TAS). The samples with the high tricyclic terpanes also have a high TAS value (0.82 to 0.90; Table 11) with the trend being more readily observed in the oil samples than in the source rock samples (which may also indicate a migration effect). The correlation of relatively high abundance of tricyclic terpanes with higher relative maturity suggests that

increasing thermal maturity may play a role in the occurrence of the high abundance of tricyclic terpanes in the Chesterian Limestone. The location of the oils where the tricyclic terpanes dominate over the hopanes also suggests that thermal maturity is involved in the occurrence of the observed pattern. Overlaying the study area with a vitrinite reflectance map of the underlying Woodford Formation by Cardott (2012) shows that thermal maturity increases to the southwest in the study area (Figure 36). The thermal maturity trend shown by Figure 36 confirms that the oil samples where the hopanes are absent and the tricyclic terpanes dominate the *m/*z 191 chromatogram are produced from more mature portions of the study area than the oil samples that retain the regular hopanes. It is recognized that the actual vitrinite values on the map from Cardott (2012) are from the Woodford Shale and do not directly indicate the thermal maturity in the overlying Mississippian rocks. However, based on the relatively conformable nature between the Mississippian Limestones and the Woodford Shale (Figure 6; Johnson, 1989), the trends are likely similar and still indicate that the thermal maturity is increasing as the tricyclic terpanes increase in abundance relative to the regular hopanes. This also agrees with Peters et al. (1990) and Farrimond et al., (1999) reporting that tricyclic terpanes are thermally more stable than the regular hopanes. However, because the tricyclic terpanes are not observed to dominate the hopanes in the underlying Woodford Shale (Connock, 2015; Villalba, 2016) it is unlikely that thermal maturity is the only factor involved in causing the distribution of tricyclic terpanes in the Chesterian Limestone. As was suggested by Wang (1993) there is likely a depositional environment component as well that is enhanced by increased thermal maturity.

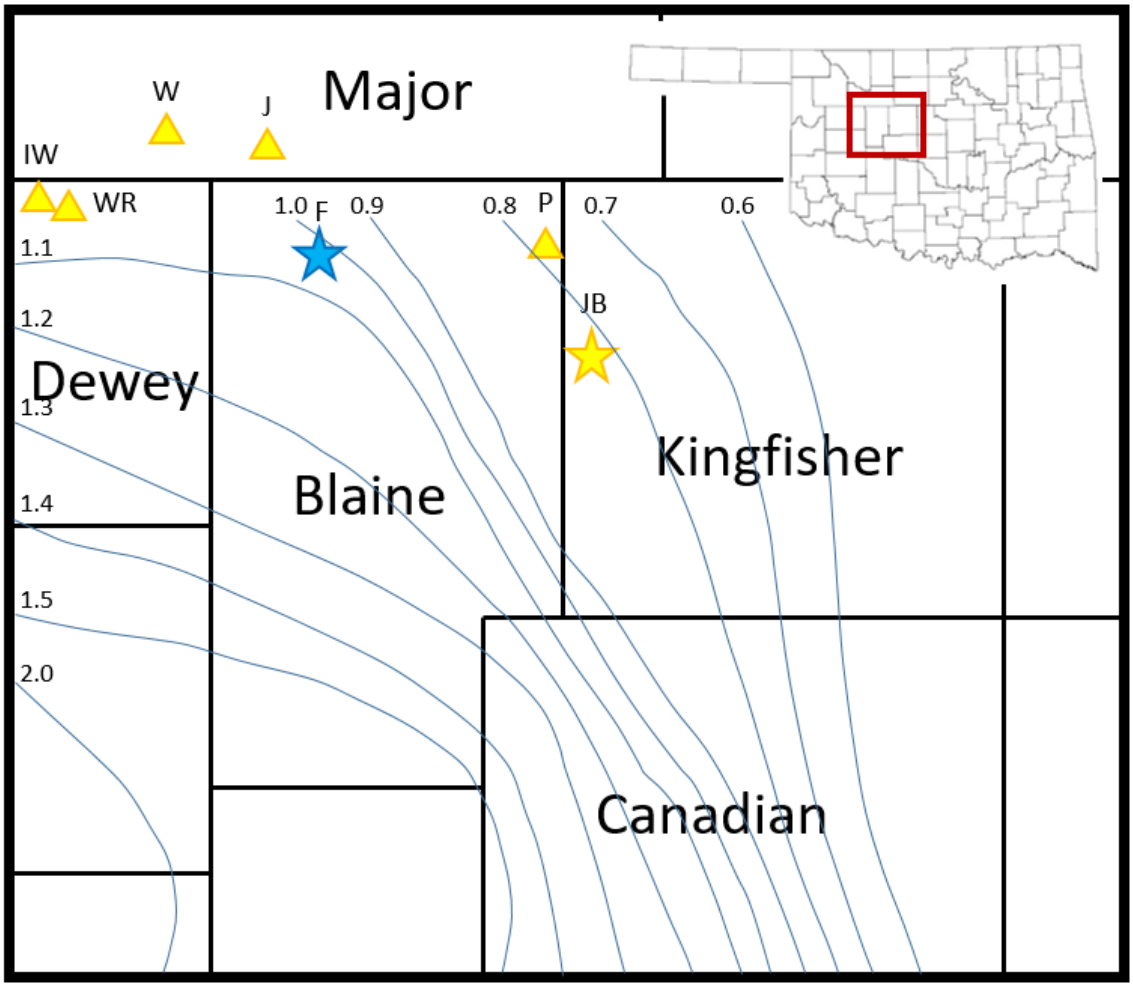


***Figure 36.*** *Map of the study area with vitrinite reflectance contours from the underlying Woodford Formation overlain. The vitrinite contours indicate that thermal maturity increase to the southwest in the study area. The thermal maturity trend shows that the oil samples that are dominated by the tricyclic terpanes are in more mature portions of the study area. This suggests that thermal maturity may be a factor in what causes the tricyclic terpanes to dominate the m/z 191 chromatograms. The vitrinite reflectance contours are from Cardott (2012). The locations of the oil samples are not included because of proprietary reasons.*

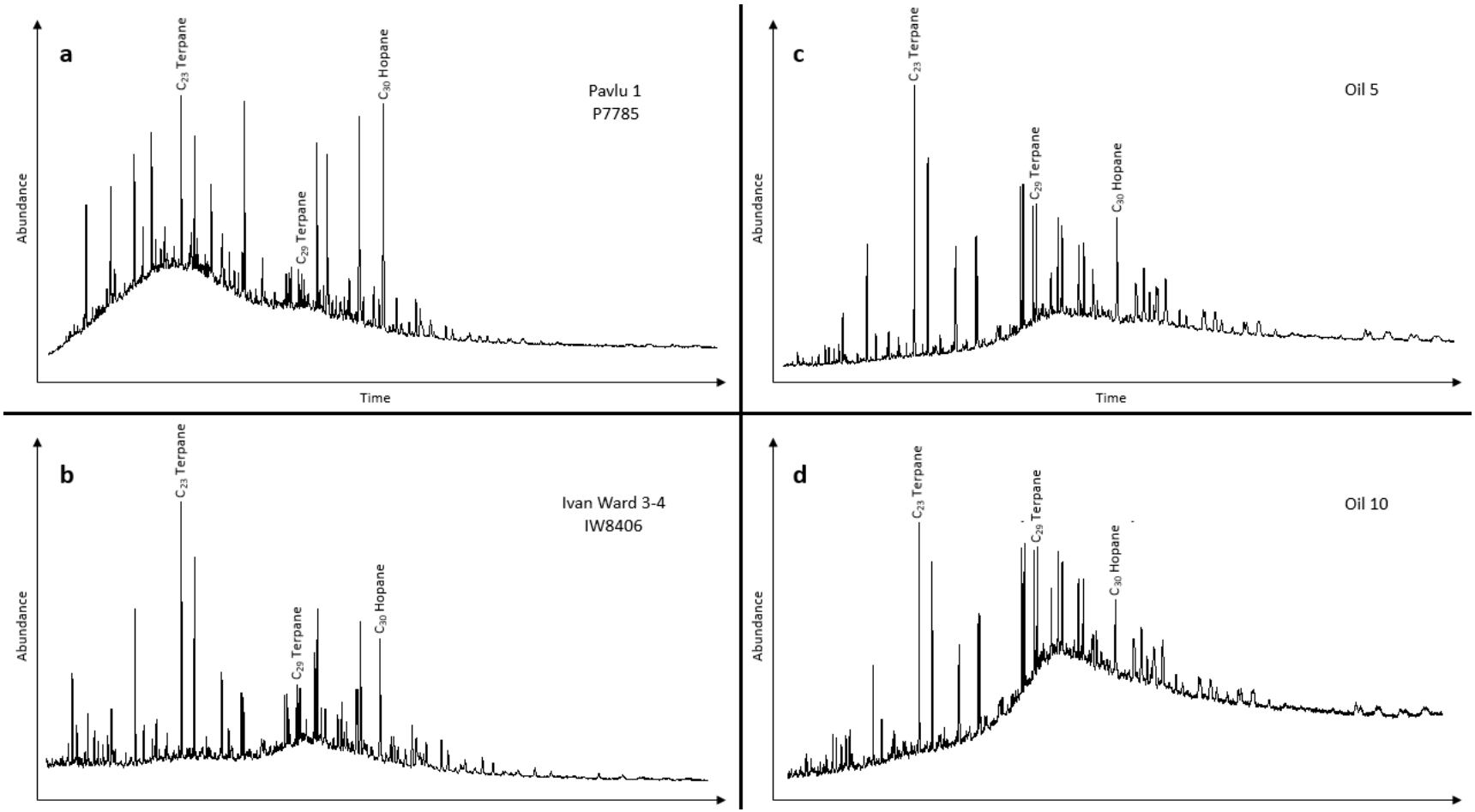


***Figure 37.*** *M/z 191 chromatograms showing source rock and oil samples containing high tricyclic terpane distributions while also containing similar abundances of hopanes. See Appendix A for chromatograms from remaining samples.*

In comparing the tricyclic terpane distribution from the samples used in the present study with the published distributions mentioned previously (Kruge et al., 1990; Aquino Neto et al., 1992; Dutta et al., 2006) a difference was noticed between the tricyclic terpane distributions from the Mississippian Limestones and the other formations. With the exception of the three source rock samples where the tricyclic terpanes actually dominate the hopanes (Figure 23f and 23h) the source rock samples containing high tricyclic terpane levels also have comparable abundances of hopanes (Figure 37a-d and Appendix A). The other published cases (Kruge et al., 1990; Aquino Neto et al., 1992; Dutta et al., 2006) show the tricyclic terpanes dominating the hopanes, but not examples of the tricyclic terpanes and the hopanes in similar abundances. As previously discussed, both thermal maturity and depositional environment conditions likely play significant roles in causing the tricyclic terpanes to eventually dominate the hopanes in the *m/z* 191 chromatogram. The distributions illustrated in Figure 37(a-d) are potentially in an intermediate stage in the process of the tricyclic terpanes coming to dominate the hopanes. These samples may also reflect slightly different depositional conditions that have resulted in the observed abundances.

## 4.5. Mississippian Limestones as a Hydrocarbon Source in the Anadarko Basin

The Anadarko Basin contains numerous hydrocarbon producing intervals, particularly in the STACK region (Johnson, 1989). Of the producing intervals the Woodford Shale is by far the most well-known and widely targeted in the STACK (Slatt et al., 2011). While the other intervals, including the Mississippian Limestones, are also productive and have been active exploration targets, it is generally thought that these intervals received their hydrocarbon charge from the Woodford Shale. Biomarker

analysis conducted in the STACK region (including the current study) indicate that the Woodford Shale does not appear to be responsible for the hydrocarbons in the Mississippian Limestones (Wang, 1993; Pearson, 2016; Sumer Gorenekli, 2017). The tricyclic terpane distribution observed in the Chesterian Limestone as well as in the Lower Mississippian Limestones (Wang, 1993), Springer Group (Wang, 1993; Pearson, 2016), and the Morrow Formation (Wang, 1993; Sumer Gorenekli, 2017) of the Anadarko Basin is not observed in the underlying Woodford Shale (Connock, 2015; Villalba, 2016). In addition, the high abundance of the diahopanes and 9,15-dimethyl-25,27-bisnorhopanes relative to 17α(H)-hopane has only been observed in the Chesterian Limestone, Springer Group, and Morrow Formation (Wang, 1993) and is not observed in the Woodford Shale or even in the Lower Mississippian Limestones (Wang, 1993; Connock, 2015; Villalba, 2016). A third group of biomarkers that supports the hydrocarbons in the Mississippian Limestones having a source other than the Woodford Shale are the head-to-head isoprenoids. These isoprenoid structures are much less common than the typical head-to-tail isoprenoids and the high-molecular weight isoprenoids containing a tail-to-tail linkage (Moldowan and Seifert, 1979). The head-to-head isoprenoids are present in the Mississippian Limestones in the Anadarko Basin (Figure 20), but not in the Woodford Shale (Philp, 2017). The relatively unique distribution of the tricyclic terpanes, rearranged hopanes, and head-to-head isoprenoids observed in the Chesterian Limestone and other Mississippian and Pennsylvanian intervals of the Anadarko Basin indicate that the hydrocarbons present in these intervals is produced by a source other than the Woodford Shale. The source of these hydrocarbons is likely the Mississippian Limestones themselves which is further

indicated by the distribution of the diahopanes, and even more so by the 9,15-dimethyl-25,27-bisnorhopanes, which have not been observed below the Chesterian Limestone in the Anadarko Basin (Wang, 1993).

The rearranged hopane distributions also suggest that the oil samples used in the present study are sourced stratigraphically below the Chesterian Limestone. As mentioned previously, the 9,15-dimethyl-25,27-bisnorhopanes were not observed by GC/MS analysis in any of the oil samples and 17α(H)-diahopane was present in lower abundance relative to the 17α(H)-hopane in the oils than in the source rock samples. Wang (1993) concluded that the 9,15-dimethyl-25,27-bisnorhopanes (referred to as "another homologue of rearranged hopanes") are not observed below the Chesterian Limestone. Wang's (1993) conclusion that the 9,15-dimethyl-25,27-bisnorhopanes are not observed below the Chesterian Limestone suggests that because the oils used in the present study do not contain the high abundance of the 9,15-dimethyl-25,27-bisnorhopanes relative to the 17α(H)-hopane that is observed throughout the Chesterian source rock samples, then the oils are likely sourced below the Chesterian Limestone. Another possibility for the source of the oils is that they may be sourced from a portion of the Chesterian Limestone that for some reason does not contain the observed distribution of the rearranged hopanes. The TAS of the oil samples provides additional confirmation that they are either sourced below the Chesterian, or from a deeper portion of the Chesterian Limestone (southeast of the study area; Figure 6). As shown in Table 6 the oil samples have higher TAS ratios than the source rock samples do, which suggests a higher thermal maturity for the oils. The vitrinite reflectance values mapped by Cardott (2012) also place the source rock samples in the deeper portion of the basin

(Figure 36) than the oils. If the source rocks and the oils were sourced from the same hydrocarbon charge the source rock samples should have a higher thermal maturity. Since the source rocks do not have a higher thermal maturity it follows that the oils were either generated stratigraphically below the source rock samples or that they were generated in a deeper portion of the basin (to the southeast) and have since migrated to their present position, below the Chesterian Limestone in the study area.

## 5. Conclusions

18α(H)-Oleanane has been tentatively identified in six source rock samples in the Chesterian Limestone of the Anadarko Basin (three from the present study and three from reanalysis of samples from Kim and Philp (1999)). The presence of 18α(H)-oleanane in these and other pre-Cretaceous samples (Moldowan et al., 1994; Peters et al., 1999) suggests the presence of plant groups capable of synthesizing β-amyrin or other, closely related compounds capable of producing 18α(H)-oleanane and oleanane-type compounds during diagenesis. The DNA nucleotide sequence and molecular phylogenetic studies suggest that the pre-Cretaceous oleanane was synthesized by the earliest angiosperm plants (Martin et al., 1989; Taylor et al., 2005). Other non-angiosperm plants that are closely related to angiosperms and possibly from a sister group to the angiosperms (Taylor et al., 2005), may also have been the source of pre-Cretaceous 18α(H)-oleanane observed in the present study as well as in other studies.

1,2,7-Trimethylnaphthalene was identified in both the source rock and the oil samples used in this study. The presence of this aromatic compound supports the above conclusions regarding the presence of 18α(H)-oleanane in the study area. The presence of 1,2,7-trimethylnaphthalene along with the presence of 18α(H)-oleanane in the

Anadarko Basin supports the validity of 1,2,7-trimethylnaphthalene being considered an aromatic marker for angiosperm input.

The relatively high abundance of rearranged hopanes, including 17α(H)-diahopane and the 9,15-dimethyl-25,27-bisnorhopanes indicate the presence of clay minerals at the time of deposition and early diagenesis in the study area. This agrees with other parameters which indicate that this region was a mixed or transitional depositional environment. The Chesterian Limestone also contains interbedded grey shales (Peace and Forgotson, 1991) which also supports the geochemical signature of a mixed setting. The diahopanes and the 9,15-dimethyl-25,27-bisnorhopanes were observed to closely co-vary in abundance in the source rock samples, with the exception of the three samples that were dominated by the extended tricyclic terpanes.

The tricyclic terpanes are present in high enough abundance to dominate the regular hopanes in three of the source rock samples and in six of the oil samples. The triaromatic hydrocarbon steroid ratio suggests that the unusual abundance of the tricyclic terpanes in the Chesterian Limestone may be caused by thermal maturity, although the lack of this distribution in the more mature Woodford Shale also implies a depositional environment control on the observed distribution.

Combining multiple biomarker interpretations that display unusual distributions suggests that the hydrocarbons produced from the Mississippian Limestones in the Anadarko Basin were also sourced from the Mississippian Limestones. The tricyclic terpane and head-to-head isoprenoid distributions are not observed in the underlying Woodford Shale, which suggests that their origin is in the Mississippian Limestones themselves. Furthermore, the high abundance of rearranged hopanes (especially the

9,15-dimethyl-25,27-bisnorhopanes) is not observed below the Chesterian Limestone, but is observed in the Chesterian Limestone, Springer Group, and Morrow Formations. This suggests that the hydrocarbons containing these compounds are sourced from the Chesterian Limestone or stratigraphically higher intervals.

# 6. Future Work

## 6.1. Confirm the tentative identification of 18α(H)-oleanane

1. As demonstrated by Alberdi and López (2000) and Nytoft et al. (2002) GC/MS/MS analysis can indicate the presence or absence of compounds that co-elute with 18α(H)-oleanane. The transitions that are useful for this analysis are the 412 to 191 transition, which is used to confirm that 18α(H)-oleanane may be present, this transition also includes lupane and select $C_{30}$ norhopanes. The 412 to 369 transition, which identifies the presence of lupane and does not include 18α(H)-oleanane. The 412 to 397 transition, which includes both 18α(H)-oleanane and the hopanes, however, the hopanes show a poor signal and 18α(H)-oleanane shows a strong signal which can be used in comparison with the 412 to 191 transition response to determine between these compounds (Alberdi and López, 2000; Nytoft et al., 2002).
2. Comparison of the tentative 18α(H)-oleanane peak with a pure standard of 18α(H)-oleanane is also recommended. Such a comparison should be done using either the above mentioned GC/MS/MS analysis or by using two capillary columns of differing polarities. Riva et al. (1988) used a non-polar capillary column followed by a polar capillary column to separate compounds that co-elute with 18α(H)-oleanane. The resulting peak identities were confirmed by co-

injection with a pure standard. Eiserbeck et al. (2011) used a similar method of two dimensional gas chromatography to separate compounds that co-elute with 18α(H)-oleanane on non-polar columns.

## 6.2. Further sampling of the Chesterian Limestone in the study area

1. The observed distribution of 18α(H)-oleanane in the study area may be impacted by the sampling criteria. The sampling for the present study focused on a lateral distribution of samples and did not allow for a high resolution vertical sampling of the Chesterian Limestone in the Anadarko Basin. It is possible that the observed distribution of 18α(H)-oleanane is related to a specific facies or lithologic horizon. Such a horizon or facies may be identified with a high resolution vertical sampling method. If such a facies exists, identifying it would provide a better understanding of the distribution of 18α(H)-oleanane in the Chesterian Limestone.
2. Further sampling would also provide a better understanding of the rearranged hopane distributions in the study area. A high resolution vertical sampling of the Chesterian Limestone could indicate where the diahopane and 9,15-dimethyl-25,27-bisnorhopane rearranged hopane series co-vary and where they do not co-vary in abundance. Identifying how these two series behave in relation to each other may increase our understanding of both series, but in particular the 9,15-dimethyl-25,27-bisnorhopane series, which is currently only sparsely mentioned in the literature (Killops and Howell, 1991; Telnæs et al., 1992; Wang, 1993; Farrimond and Telnæs, 1996; Nytoft et al., 2007).

3. The tricyclic terpane distributions are also potentially controlled or at least impacted by facies variations within the study. The unusually high abundance of tricyclic terpanes relative to the regular hopanes observed in select samples in the present study was concluded to be at least partially derived from depositional environment conditions. The suggested high resolution vertical sampling method would help to confirm or deny the role that the depositional environment plays in the resulting tricyclic terpane distribution.

## References


Alberdi, M. and López, L. (2000). Biomarker 18α(H)-oleanane: a geochemical tool to assess Venezuelan petroleum systems. *Journal of South American Earth Sciences*, 13(8), 751–759.

Andersson, R. A. and Meyers, P. A. (2012). Effect of climate change on delivery and degradation of lipid biomarkers in a Holocene peat sequence in the Eastern European Russian Arctic. *Organic Geochemistry*, 53, 63–72.

Aquino Neto, F. R., Restle, A., Connan, J., Albrecht, P. and Ourisson, G. (1982). Novel tricyclic terpanes ($C_{19}$, $C_{20}$) in sediments and petroleums. *Tetrahedron Letters* 23, 2027-2030.

Aquino Neto, F. R., Trigüis, J., Azevedo, D. A., Rodriques, R. and Simoneit, B. R. T. (1992). Organic geochemistry of geographically unrelated tasmanites. *Organic Geochemistry*, 18(6), 791–803.

Armstroff, A., Wilkes, H., Schwarzbauer, J., Littke, R. and Horsfield, B. (2006). Aromatic hydrocarbon biomarkers in terrestrial organic matter of Devonian to Permian age. *Palaeogeography, Palaeoclimatology, Palaeoecology*, 240(1–2), 253–274.

Asif, M. and Fazeelat, T. (2012). Petroleum geochemistry of the Potwar Basin, Pakistan: II – Oil classification based on heterocyclic and polycyclic aromatic hydrocarbons. *Applied Geochemistry*, 27(8), 1655–1665.

Azevedo, D. A., Aquino Neto, F. R., Simoneit, B. R. T. and Pinto, A. C. (1992). Novel series of tricyclic aromatic terpanes characterized in Tasmanian tasmanite. *Organic Geochemistry*, 18(1), 9–16.

Brassell, S. C., Wardroper, A. M. K., Thompson, I. D., Maxwell, J. R. and Eglinton, G. (1981). Specific acyclic isoprenoids as biological markers of methanogenic bacteria in marine sediments. *Nature*, 290, 693-6.

Brooks, J. and Smith, J. (1967). The diagenesis of plant lipids during the formation of coal, petroleum and natural gas—I. Changes in the n-paraffin hydrocarbons. *Geochimica et Cosmochimica Acta*, 31(12), 2389–2397.

Beach, F., Peakman, T. M., Abbott, G. D., Sleeman, R. and Maxwell, J. R. (1989). Laboratory thermal alteration of triaromatic steroid hydrocarbons. *Organic Geochemistry*, 14(1), 109–111.

Bray, E. and Evans, E. (1961). Distribution of n-paraffins as a clue to recognition of source beds. *Geochimica et Cosmochimica Acta*, 22(1), 2–15.

Caccialanza P. G. and Riva A. (1987). Separation and identification of a new biological marker, 18β(H)-oleanane, in crude oils and ancient sediments, using high resolution gas chromatography-mass spectrometry. *Documents from the Eighth International Symposium on Capillary Chromatography*, Vol. II, 704-713.

Cardott, B. J. (2012). Thermal maturity of Woodford Shale gas and oil plays, Oklahoma, USA. *International Journal of Coal Geology*, 103, 109–119.

Cardott B. J. and Chaplin J. R. (1993). Guidebook for selected stops in the Western Arbuckle Mountains, southern Oklahoma. *Oklahoma Geological Survey Special Edition* 93-3, 55.

Carman, R.M. and Craig, W. (1971). Diterpenoids XXVII. The selenium dehydrogenation of manool. *Australian Journal of Chemistry* 24, 361–370.

Chappe, B., Michaelis W., Albrecht, P. and Ourisson, G. (1979). Fossil evidence for a novel series of archaebacterial lipids. *Naturwissenschaften* 66, 522-523.

Charpentier R. R. (2001). Cherokee Platform Province (060), *US Geological Survey*, 1995 National Oil and Gas Resource Assessment Team, circular 1118, 1–13.

Chattopadhyay, A. and Dutta, S. (2014). Higher plant biomarker signatures of Early Eocene sediments of North Eastern India. *Marine and Petroleum Geology*, 57, 51–67.

Chicarelli, M. I., Neto, F. R. A. and Albrecht, P. (1988). Occurrence of four stereoisomeric tricyclic terpane series in immature Brazilian shales. *Geochimica et Cosmochimica Acta*, 52(8), 1955–1959.

Connan, J., Restle, A. and Albrecht, P. (1980). Biodegradation of crude oil in the Aquitaine basin. *Physics and Chemistry of the Earth*, 12, 1–17.

Connan, J., Nissenbaum, A. and Dessort, D. (1992). Molecular archaeology: Export of Dead Sea asphalt to Canaan and Egypt in the Chalcolithic-Early Bronze Age (4th-3rd millennium BC). *Geochimica et Cosmochimica Acta*, 56(7), 2743–2759.

Connock, G. T. (2015). Paleoenvironmental Interpretation of the Woodford Shale, Wyche Farm Shale Pit, Pontotoc County, Arkoma Basin, Oklahoma with Primary Focus on Water Column Structure (M.S. thesis). The University of Oklahoma, Norman, OK, 197.

Dahl, B. and G. C. Speers. (1986). Geochemical characterization of a tar mat in the Oseberg Field Norwegian Sector, North Sea. *Org. Geochemistry.*, 10, 547-588.

De Grande, S. M. B., Aquino Neto, F. R. and Mello, M. R. (1993). Extended tricyclic terpanes in sediments and petroleums. *Organic Geochemistry*, 20(7), 1039–1047.

Didyk, B. M., Simoneit, B. R. T., Brassell, S. C. and Eglinton, G. (1978). Organic geochemical indicators of paleoenvironmental conditions of sedimentation. *Nature*, 272, 216-22.

Dutta, S., Greenwood, P. F., Brocke, R., Schaefer, R. G. and Mann, U. (2006). New insights into the relationship between Tasmanites and tricyclic terpenoids. *Organic Geochemistry*, 37(1), 117–127.

Eiserbeck, C., Nelson, R. K., Grice, K., Curiale, J., Reddy, C. M. and Raiteri, P. (2011). Separation of 18α(H)-, 18β(H)-oleanane and lupane by comprehensive two-dimensional gas chromatography. *Journal of Chromatography A* (Vol. 1218).

Ekweozor, C. and Udo, O. (1988). The oleananes: Origin, maturation and limits of occurrence in Southern Nigeria sedimentary basins. *Organic Geochemistry*, 13(1–3), 131–140.

Farrimond, P., Bevan, J. C. and Bishop, A. N. (1999). Tricyclic terpane maturity parameters: Response to heating by an igneous intrusion. *Organic Geochemistry*, 30(8 B), 1011–1019.

Farrimond, P. and Telnæs, N. (1996). Three series of rearranged hopanes in Toarcian sediments (northern Italy). *Organic Geochemistry*, 25(3–4), 165–177.

Fowler, M. G., Snowdon, L. R., Brooks, P. W. and Hamilton, T. S. (1988). Biomarker characterisation and hydrous pyrolysis of bitumens from Tertiary volcanics, Queen Charlotte Islands, British Columbia, Canada. *Organic Geochemistry*, 13(4–6), 715–725.

Fritsche, W. and Hofrichter, M. (2008). Aerobic degradation by microorganisms. In *Biotechnology*, Vol. 11b (second edition), John Wiley & Sons, New York, 144-167.

George, S. C., Eadington, P. J., Lisk, M. and Quezada, R. A. (1998). Geochemical comparison of oil trapped in fluid inclusions and reservoired oil in Blackback oilfield, Gippsland Basin, Australia. *Petroleum Exploration Society of Australia Journal*, 26(January 1998), 64–81.

Hendrickson, W.J., Smith, P. W., Woods, R. J., Hogan, J. V. and Willey, C. E. (2001). Example of a carbonate platform and slope system and its stratigraphically equivalent basinal clastic system: Springeran-Chesterian relationships in the Anadarko Basin and shelf of northwestern Oklahoma and Texas panhandle. *AAPG Search and Discovery Article #90921*.

Heppenheimer, H., Steffens, K., Püttman, W. and Kalkreuth, W. (1992). Comparison of resinite-related aromatic biomarker distributions in Cretaceous-Tertiary coals from Canada and Germany. *Organic Geochemistry*, 18(3), 273–287.

Hoffmann, C. F., Mackenzie, A. S., Lewis, C. A., Maxwell, J. R., Oudin, J. L., Durand, B. and Vandenbroucke, M. (1984). A biological marker study of coals, shales and oils from the Mahakam Delta, Kalimantan, Indonesia. *Chemical Geology*, 42(1–4), 1–23.

Hughes, W. B., Holba, A. G. and Dzou, L. I. P. (1995). The ratios of dibenzothiophene to phenanthrene and pristane to phytane as indicators of depositional environment and lithology of petroleum source rocks. *Geochimica et Cosmochimica Acta*, 59(17), 3581–3598.

Hunt, J. M. (1996). Petroleum Geochemistry and Geology. Second Edition. W. H. Freeman and Company, USA, 434-435.

Johnson K. S. (1989). Geologic evolution of the Anadarko Basin. *Oklahoma Geological Survey Circular* 90, 197.

Johnson, K. (2008). Geologic history of Oklahoma. *Oklahoma Geologic Survey, Educational Publication 9,* 1.

Killops, S. D. and Howell, V. J. (1991). Complex series of pentacyclic triterpanes in a lacustrine sourced oil from Korea Bay Basin. *Chemical Geology*, 91(1), 65–79.

Kim, D. and Philp, R. P. (1999). Extended Tricyclic Terpanes in Mississippian Rocks from the Anadarko Basin, Oklahoma. *Silurian, Devonian, and Mississippian Geology and Petroleum in the Southern Midcontinent, 1999 Symposium*, 109–128.

Kolaczkowska, E., Slougui, N.-E., Watt, D. S., Maruca, R. E., and Moldowan, J. M. (1990). Thermodynamic stability of various alkylated, dealkylated and rearranged 17α- and 17β-hopane isomers using molecular mechanics calculations. *Organic Geochemistry*, 16(4–6), 1033–1038.

Kruge, M. A., Hubert, J. F., Jay Akes, R. and Meriney, P. E. (1990). Biological markers in Lower Jurassic synrift lacustrine black shales, Hartford basin, Connecticut, U.S.A. *Organic Geochemistry*, 15(3), 281–289.

Mackenzie, A. S. (1984). Applications of Biological Markers in Petroleum Geochemistry. In *Advances in Petroleum Geochemistry*, 115–214.

Mackenzie, A., Hoffmann, C. and Maxwell, J. (1981). Molecular parameters of maturation in the Toarcian shales, Paris Basin, France—III. Changes in aromatic steroid hydrocarbons. *Geochimica et Cosmochimica Acta*, 45(8), 1345–1355.

Martin, W., Gierl, A. and Saedler, H. (1989). Molecular evidence for pre-Cretaceous angiosperm origins. *Nature*, 339, 46-8.

McKirdy, D. M., Aldridge, A. K. and Ypma, P. J. M. (1983). A geochemical comparison of some crude oils from pre-Ordovician carbonate rocks. In *Advances in Organic Geochemistry 1981*, Jon Wiley and Sons, New York, 99-107.

Moldowan, J. M. and Seifert, W. K. (1979). Head-to-head linked isoprenoid hydrocarbons in petroleum. *Science*, 204, 169–171.

Moldowan, J. M., Seifert, W. K. and Gallegos, E. J. (1983). Identification of an extended series of tricyclic terpanes in petroleum. *Geochimica et Cosmochimica Acta*, 47(8), 1531–1534.

Moldowan, J. M., Sundararaman, P. and Schoell, M. (1986). Sensitivity of biomarker properties to depositional environment and/or source input in the Lower Toarcian of SW-Germany. *Organic Geochemistry*, 10(4–6), 915–926.

Moldowan, J. M., Fago, F. J., Carlson, R. M. K., Young, D. C., an Duvne, G., Clardy, J. and Watt, D. S. (1991). Rearranged hopanes in sediments and petroleum. *Geochimica et Cosmochimica Acta*, 55(11), 3333–3353.

Moldowan, J. M., Dahl, J., Huizinga, B. J., Fago, F. J., Hickey, L. J., Peakman, T. M. and Taylor, D. W. (1994). The molecular fossil record of oleanane and its relation to angiosperms. *Science*, 265, 768–771.

Murray, A. P., Sosrowidjojo, I. B., Alexander, R., Kagi, R. I., Norgate, C. M. and Summons, R. E. (1997). Oleananes in oils and sediments: Evidence of marine influence during early diagenesis? *Geochimica et Cosmochimica Acta*, 61(6), 1261–1276.

Nytoft, H. P., Bojesen-Koefoed, J. A., Christiansen, F. G. and Fowler, M. G. (2002). Oleanane or lupane? Reappraisal of the presence of oleanane in Cretaceous–Tertiary oils and sediments. *Organic Geochemistry*, 33(11), 1225–1240.

Nytoft, H.P., Lund, K., Corleone Jorgensen, T.K., Thomsen, J.V., Wendel Sorensen, S., Lutnaes, B.-F., Kildahl-Andersen, G. and Johansen, J.E. (2007). Identification of an early-eluting rearranged hopane series. Synthesis from hop-17(21)-enes and detection of intermediates in sediments. In: The 23rd International Meeting on Organic Geochemistry (IMOG) 9th-14th September 2007, I.G.I. Ltd., Bideford.

Ortiz, J. E., Torres, T., Delgado, A., Julià, R., Lucini, M., Llamas, F. J. and Valle, M. (2004). The palaeoenvironmental and palaeohydrological evolution of Padul Peat Bog (Granada, Spain) over one million years, from elemental, isotopic and molecular organic geochemical proxies. *Organic Geochemistry*, 35(11–12), 1243–1260.

Palacas, J.G., Anders, D.E. and King, J.D. (1984). South Florida basin-a prime example of carbonate source rocks in petroleum. In: Palaces, J.G. (Ed.), Petroleum

Geochemistry and Source Rock Potential of Carbonate Rocks, *American Association of Petroleum Geologists*, Studies in Geology, 18, pp. 71-96.

Peace, H. W. and Forgotson, J. M. (1991). Mississippian facies relationships, eastern Anadarko basin, Oklahoma. *AAPG Bulletin* 75:8 @ 1999 AAPG Mid-Continent Section Meeting, Wichita, Kansas.

Pearson, C. (2016). Geochemical Characterization of the Upper Mississippian Goddard Formation, Springer Group, in the Anadarko Basin of Oklahoma (M. S. thesis). The University of Oklahoma, Norman, OK.

Peters, K. E., Clutson, M. J. and Robertson, G. (1999). Mixed marine and lacustrine input to an oil-cemented sandstone breccia from Brora, Scotland. *Organic Geochemistry*, 30(4), 237–248.

Peters, K. E., Walters, C.C. and Moldowan, J. M. (2005). The Biomarker Guide. Volume 2. Biomarkers and Isotopes in Petroleum Exploration and Earth History. Cambridge University Press, Cambridge, UK, 633-634.

Petrov, A. A., Vorobyova, N. S. and Zemskova, Z. K. (1990). Isoprenoid alkanes with irregular “head-to-head” linkages. *Organic Geochemistry*, 16(4–6), 1001–1005.

Philp, R. P. and Gilbert, T. D. (1986). Biomarker distributions in Australian oils predominantly derived from terrigenous source material. *Organic Geochemistry*, 10(1–3), 73–84.

Philp, R. P., Jinggui, L. and Lewis, C. A. (1989). An organic geochemical investigation of crude oils from Shanganning, Jianghan, Chaidamu and Zhungeer Basins, People’s Republic of China. *Organic Geochemistry*, 14(4), 447–460.

Philp, R. P. (2017). Geochemical characterization of potential source rocks in the Anadarko Basin, Oklahoma. Presented at American Association of Petroleum Geologists Annual Convention and Exhibition, Houston, TX.

Powell, T. G. and McKirdy D. M. (1975). Geologic factors controlling crude oil composition in Australia and Papua New Guinea. *AAPG Bulletin*, v. 59, 1176-1197.

Püttmann, W. and Villar, H. (1987). Occurrence and geochemical significance of 1,2,5,6-tetramethylnaphthalene. *Geochimica et Cosmochimica Acta*, 51(11), 3023–3029.

Radke, M. (1988). Application of aromatic compounds as maturity indicators in source rocks and crude oils. *Marine and Petroleum Geology*, 5(3), 224–236.

Radke, M., Welte, D. H. and Willsch, H. (1982). Geochemical study on a well in the Western Canada Basin: relation of the aromatic distribution pattern to maturity of organic matter. *Geochimica et Cosmochimica Acta*, 46(1), 1–10.

Radke, M. and Welte, D.H. (1983). The methylphenanthrene index (MPI). A maturity parameter based on aromatic hydrocarbons. In: *Advances in Organic Geochemistry 1981* (M. Bjorøy, C. Albrecht, C. Cornford, *et al.*, eds.), John Wiley and Sons, New York, 504-12.

Rascoe, B. Jr. and Adler, F. J. (1983). Permo-Carboniferous hydrocarbon accumulations, Mid-Continent, U.S.A. *AAPG Bulletin*, v. 67, 979-1001.

Riva, A., Caccialanza, P. G. and Quagliaroli, F. (1988). Recognition of 18β(H)-oleanane in several crudes and Tertiary-Upper Cretaceous sediments. Definition of a new maturity parameter. *Organic Geochemistry*, 13(4–6), 671–675.

Rose, K. K., Douds, A. S. B., Pancake, J. A., Pratt III, H. R. and Boswell, R. M. (2004). Assessing Subeconomic Natural gas resources in the Anadarko and Uinta Basins. *AAPG Search and Discovery Article #10069.*

Rullkötter, J., Peakman, T. M. and Lo Ten Haven, H. (1994). Early diagenesis of terrigenous triterpenoids and its implications for petroleum geochemistry. *Organic Geochemistry*, *21*(3–4), 215–233.

Seifert, W. K., Michael Moldowan, J. and Demaison, G. J. (1984). Source correlation of biodegraded oils. *Organic Geochemistry*, 6, 633–643.

Shanmugam, G. (1985). Significance of Coniferous Rain Forests and Related Organic Matter in Generating Commercial Quantities of Oil, Gippsland Basin, Australia. *American Association of Petroleum Geologists Bulletin*, 69(8), 1241–1254.

Slatt, R. M., Buckner, N., Abousleiman, Y., Sierra, R., Philp, P., Miceli-Romero, A. and Wawrzyniec, T. (2011). Outcrop-behind outcrop (quarry), multiscale characterization of the Woodford Gas Shales, Oklahoma. *American Association of Petroleum Geologists Memoir*, *97*, 1–22.

Strachan, M. G., Alexander, R. and Kagi, R. I. (1988). Trimethylnaphthalenes in crude oils and sediments: Effects of source and maturity. *Geochimica et Cosmochimica Acta*, *52*(5), 1255–1264.

Sumer Gorenekli, Y. (2017). Geochemical characterization of the Lower Pennsylvanian Morrow Formation in the Anadarko Basin of Oklahoma (M. S. thesis in preparation) The University of Oklahoma, Norman, OK.

Tao, S., Wang, C., Du, J., Liu, L. and Chen, Z. (2015). Geochemical application of tricyclic and tetracyclic terpanes biomarkers in crude oils of NW China. *Marine and Petroleum Geology*, 67, 460–467.

Taylor, D.W., Li, H., Dahl, J., Fago, F.J., Zinniker, D. and Moldowan, J.M. (2005). Biogeochemical evidence for late Paleozoic origin of angiosperms. *Paleobiology*, 32, 179-190.

Telnæs, N., Isaksen, G. H. and Farrimond, P. (1992). Unusual triterpane distributions in lacustrine oils. *Organic Geochemistry*, 18(6), 785–789.

Thomas, B. R. (1969). Kauri Resins—Modern and Fossil, Organic Geochemistry: Methods and Results. Springer Berlin Heidelberg, Germany, 599-618.

Villalba, D. M. (2016). Organic Geochemistry of the Woodford Shale, Cherokee Platform, OK and its Role in a Complex Petroleum System (M. S. thesis) The University of Oklahoma, Norman, OK, 47-51.

Volkman, J. K., Alexander, R., Kagi, R. I., Noble, R. A., and Woodhouse, C. W. (1983). A geochemical reconstruction of oil generation in the Barrow Sub-basin of Western Australia. *Geochimica et Cosmochimica Acta*, 47(12), 2091–2105.

Volkman, J. K., Banks, M. R., Denwer, K. and Aquino Neto, F. R. (1989). Biomarker composition and depositional setting of Tasmanite oil shale from northern Tasmania, Australia. Presented at the 14th International Meeting on Organic Geochemistry, September 18-22, 1989, Paris.

Wang, C.J., Fu, J.M., Sheng, G.Y., Xiao, Q.H., Li, J.Y., Zhang, Y.L. and Piao, M.Z. (2000). Geochemical characteristics and applications of 18α (H)-neohopanes and 17α(H)-diahopanes. *Chinese Science Bulletin*, 45, 1366-1372.

Wang, H. D. (1993). A geochemical study of potential source rocks and crude oils in the Anadarko Basin, Oklahoma (PhD dissertation). The University of Oklahoma, Norman, OK, 176-187.

Weaver, C. E. (1958). Geologic interpretation of argillaceous sediments: Part II. Clay petrology of Upper Mississippian-Lower Pennsylvanian sediments of Central United States. *American Association of Petroleum Geologists Bulletin*, 42(2), 272-309.

Wenger, L. M. and Isaksen, G. H. (2002). Control of hydrocarbon seepage intensity on level of biodegradation in sea bottom sediments. *Organic Geochemistry*, 33(12), 1277–1292.

Wilhelms, A. and S. R. Larter. (1994a). Origin of tar mats in petroleum reservoirs: Part I. Introduction and case studies. *Marine and Petroleum Geology*, 11(4), 418-441.

Wilhelms, A. and S. R. Larter. (1994b). Origin of tar mats in petroleum reservoirs: Part II. Formation mechanisms for tar mats. *Marine and Petroleum Geology,* 11(4), 442-456.

Williams, J. A., Bjorøy, M., Dolcater, D. L. and Winters, J. C. (1986). Biodegradation in South Texas Eocene oils — Effects on aromatics and biomarkers. *Organic Geochemistry*, 10(1–3), 451–461.

Yancey, T. E. (1989). Controls on carbonate deposition on a Pennsylvanian sloping shelf with mixed carbonate-siliciclastic sedimentation. *Kansas Geological Survey, Subsurface Geology,* 12, 77-78.

Yang, W., Liu, G. and Feng, Y. (2016). Geochemical significance of 17α(H)-diahopane and its application in oil-source correlation of Yanchang formation in Longdong area, Ordos basin, China. *Marine and Petroleum Geology*, *71*, 238–249.

Zhao, M.J. and Zhang, S.C. (2001). The special sedimentary facies indicated by 17α(H)-diahopane in Tarim basin. *Petroleum Exploration and Development*. 28, 36-38.

Zhu, Y.M., Zhong, R.C., Cai, X.Y. and Luo, Y. (2007). Composition and origin approach of rearranged hopanes in Jurassic oils of central Sichun basin. *Geochemica* 36, 253-260.

# Appendix A

*M/z* 191 chromatograms of the saturate fractions for all source rock and oil samples. The time ranges were selected to better display the tricyclic terpane distributions. The samples that show a group of high intensity peaks at the beginning of the chromatogram were not able to be fractionated and were analyzed as whole maltenes or as whole extracts. The group of high intensity peaks are from aromatic compounds that also contain a 191 fragment. The chromatograms containing these peaks have been normalized to the most abundant tricyclic terpane or hopane peak within the sample's distribution.

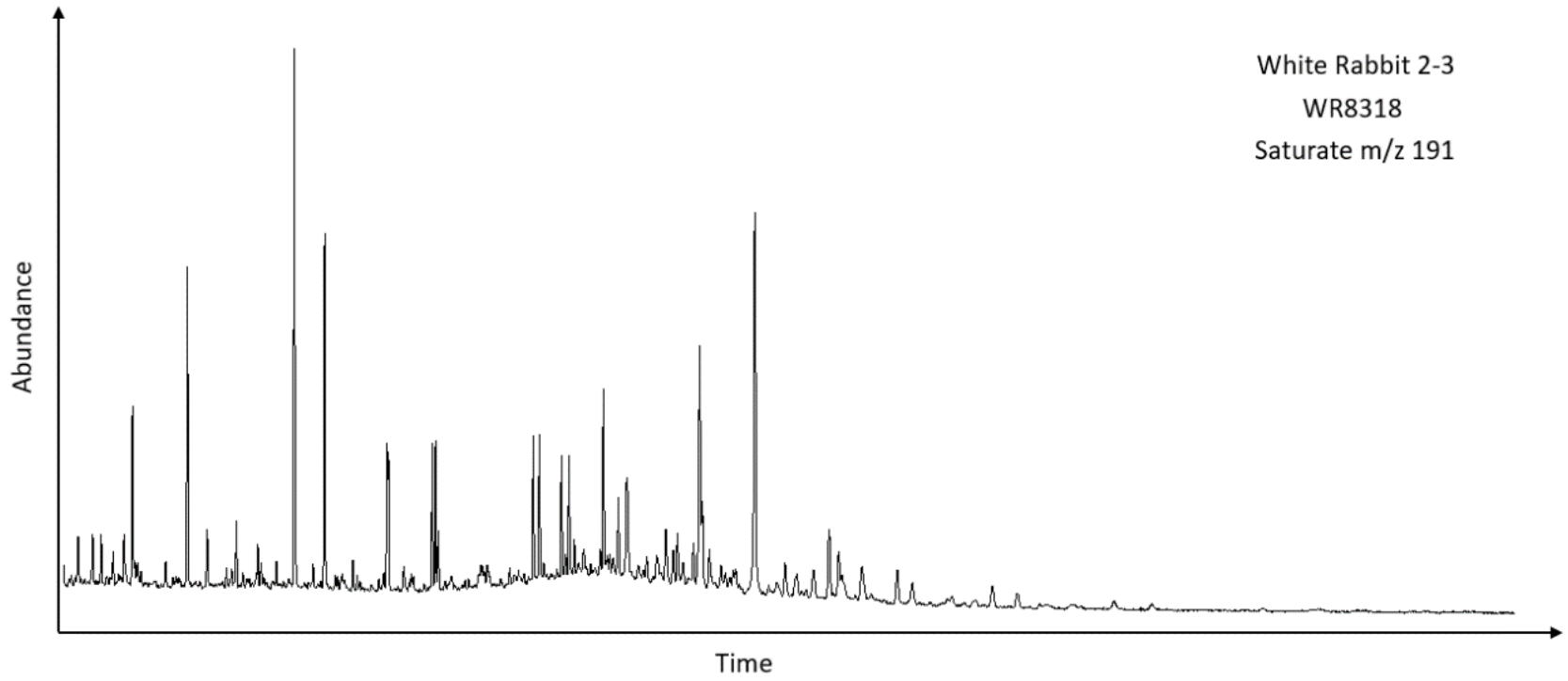
White Rabbit 2-3
WR8318
Saturate m/z 191
Abundance
Time

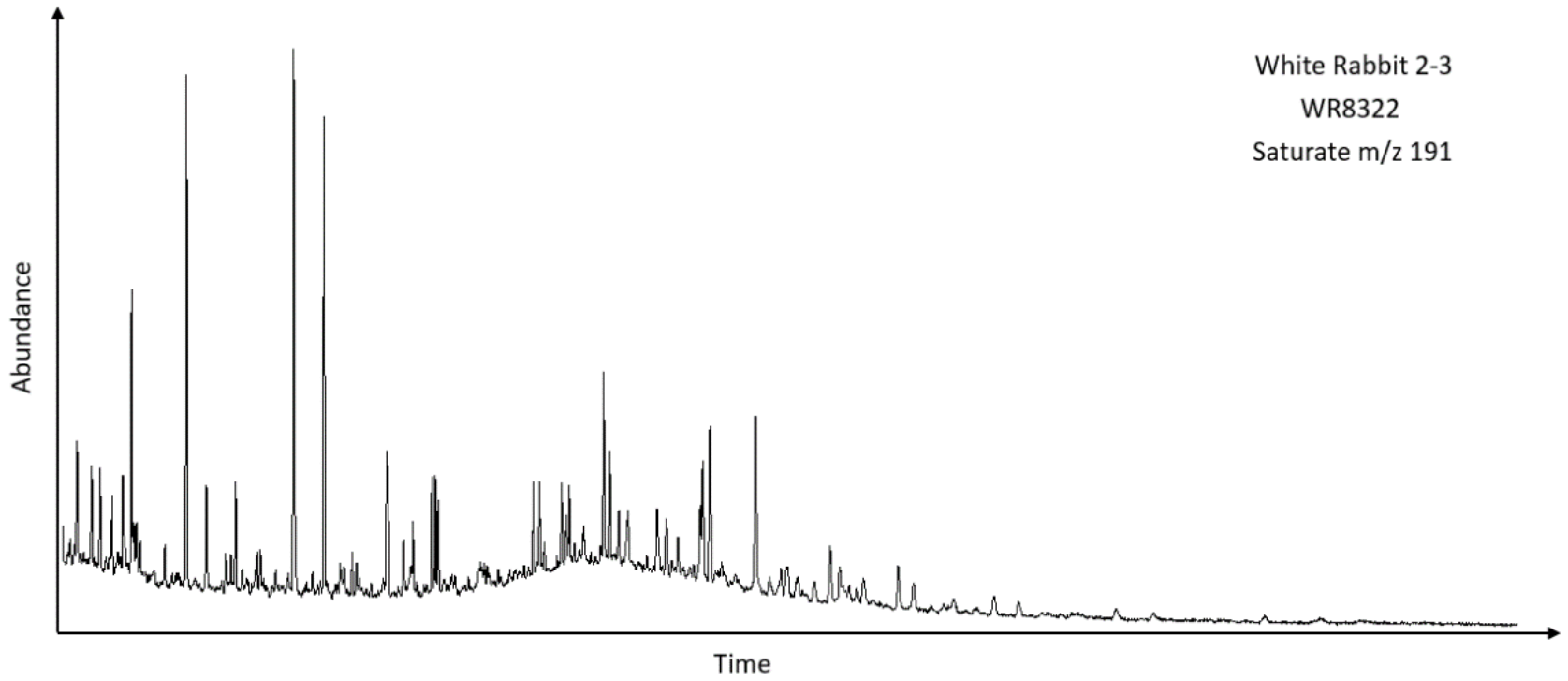
White Rabbit 2-3
WR8322
Saturate m/z 191
Abundance
Time

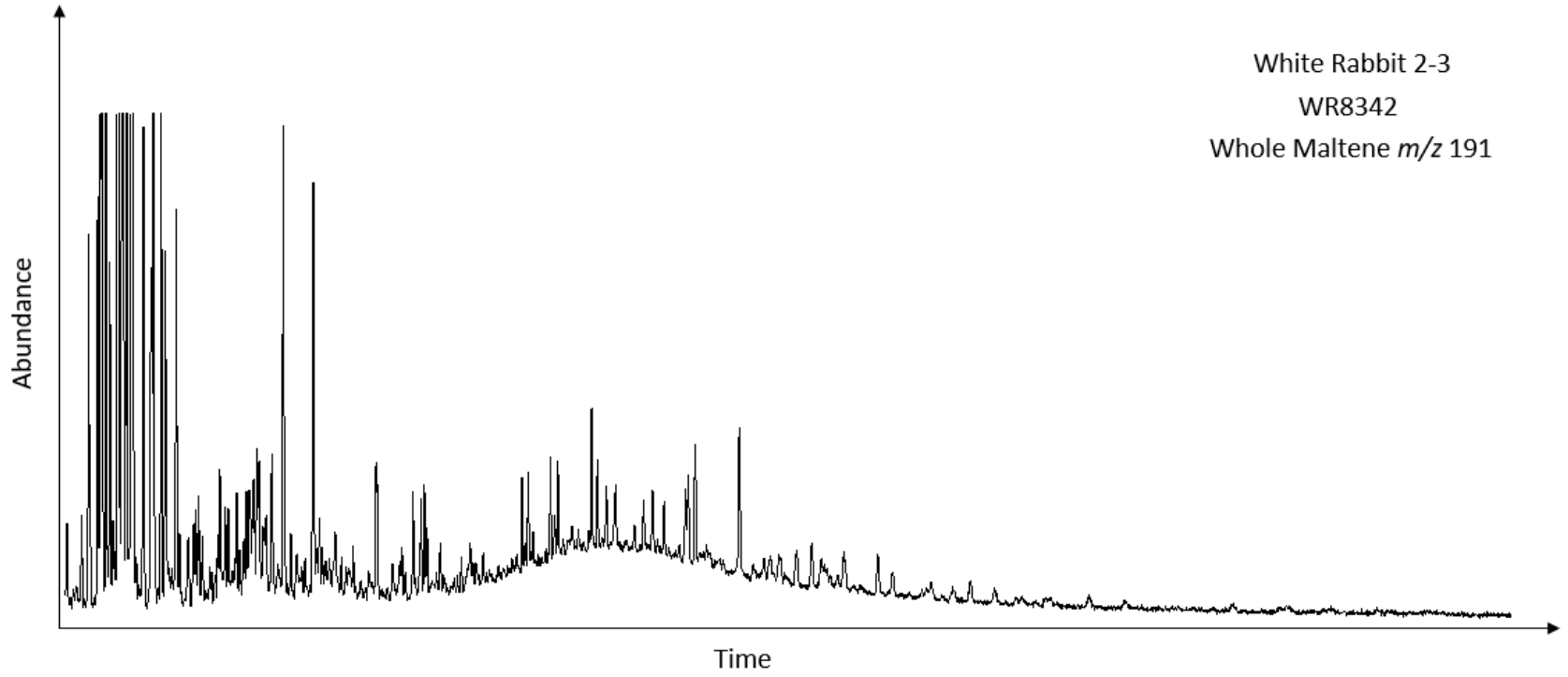
White Rabbit 2-3
WR8342
Whole Maltene m/z 191
Abundance
Time

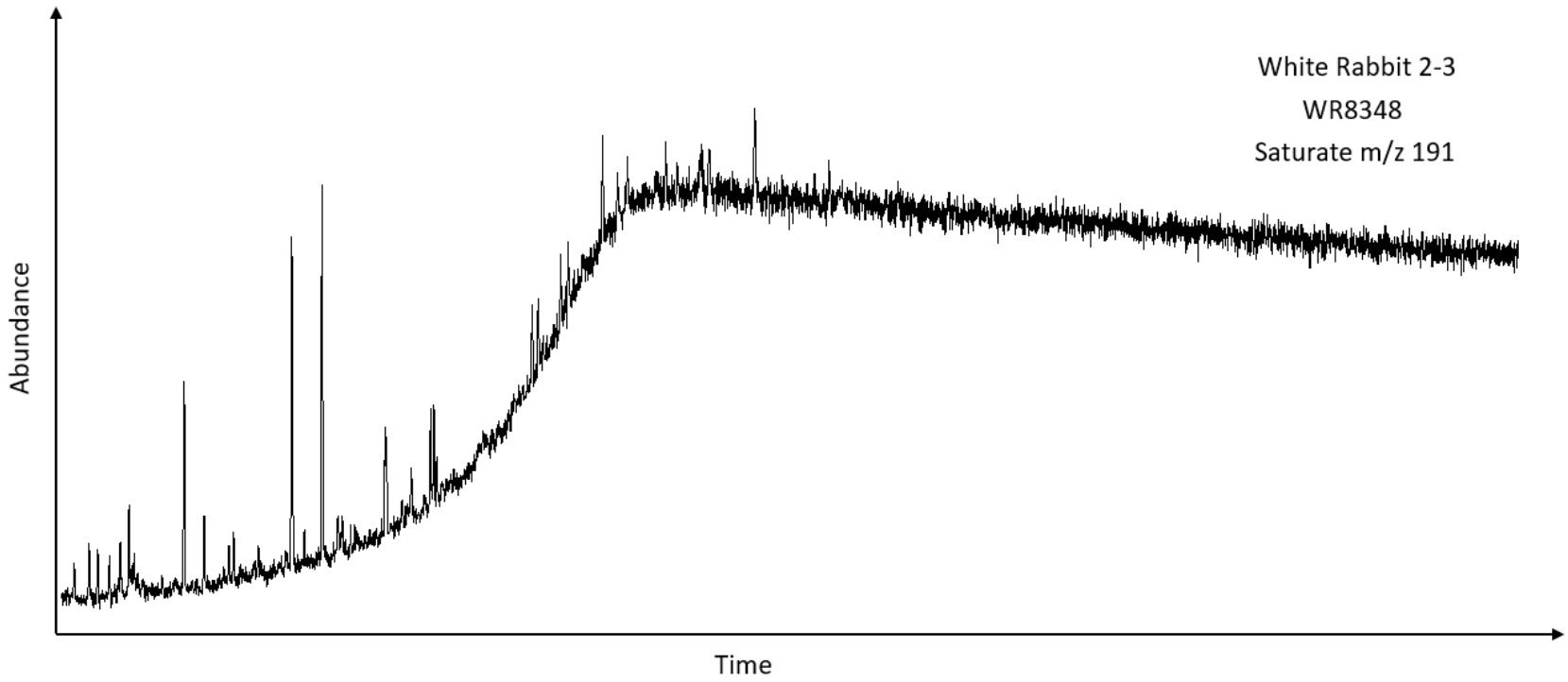
White Rabbit 2-3
WR8348
Saturate m/z 191
Abundance
Time

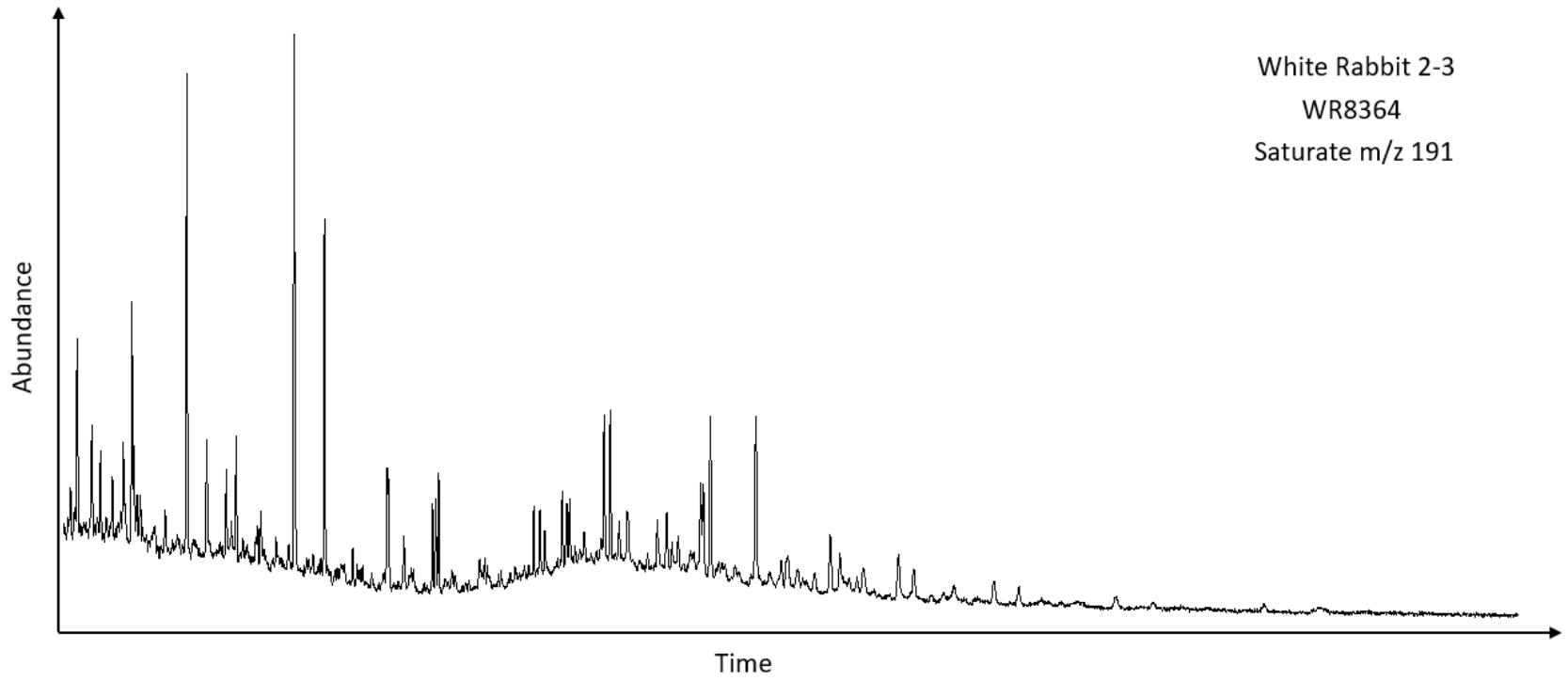
White Rabbit 2-3
WR8364
Saturate m/z 191
Abundance
Time

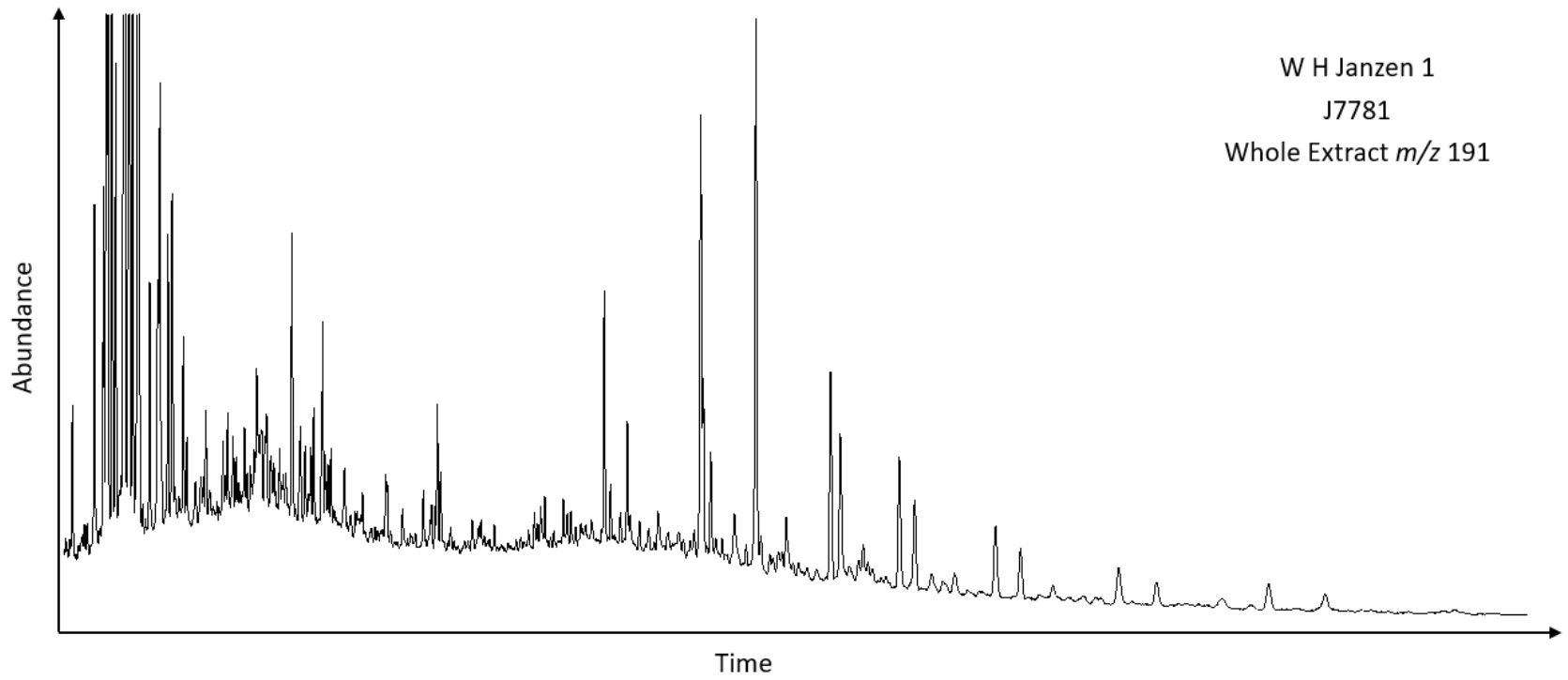
W H Janzen 1
J7781
Whole Extract m/z 191
Abundance
Time

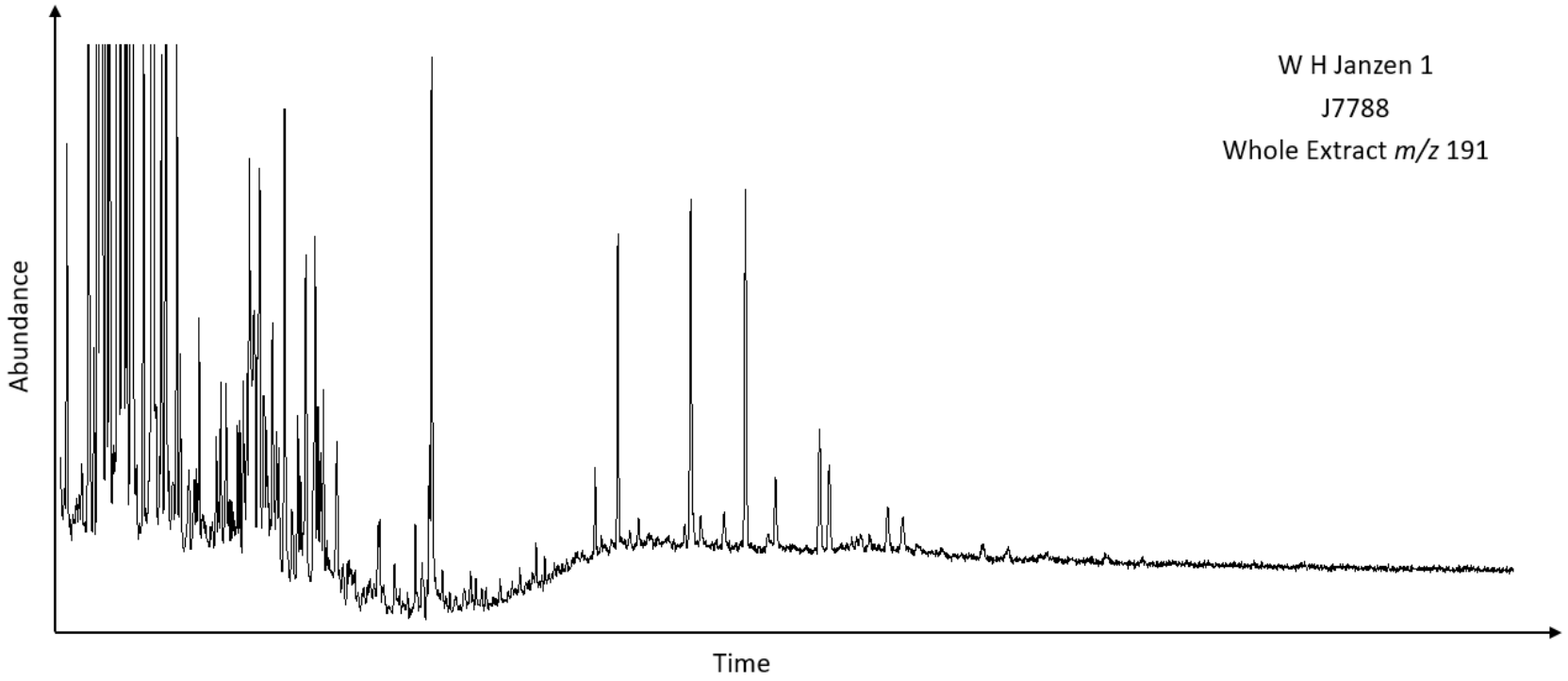
W H Janzen 1
J7788
Whole Extract m/z 191
Abundance
Time

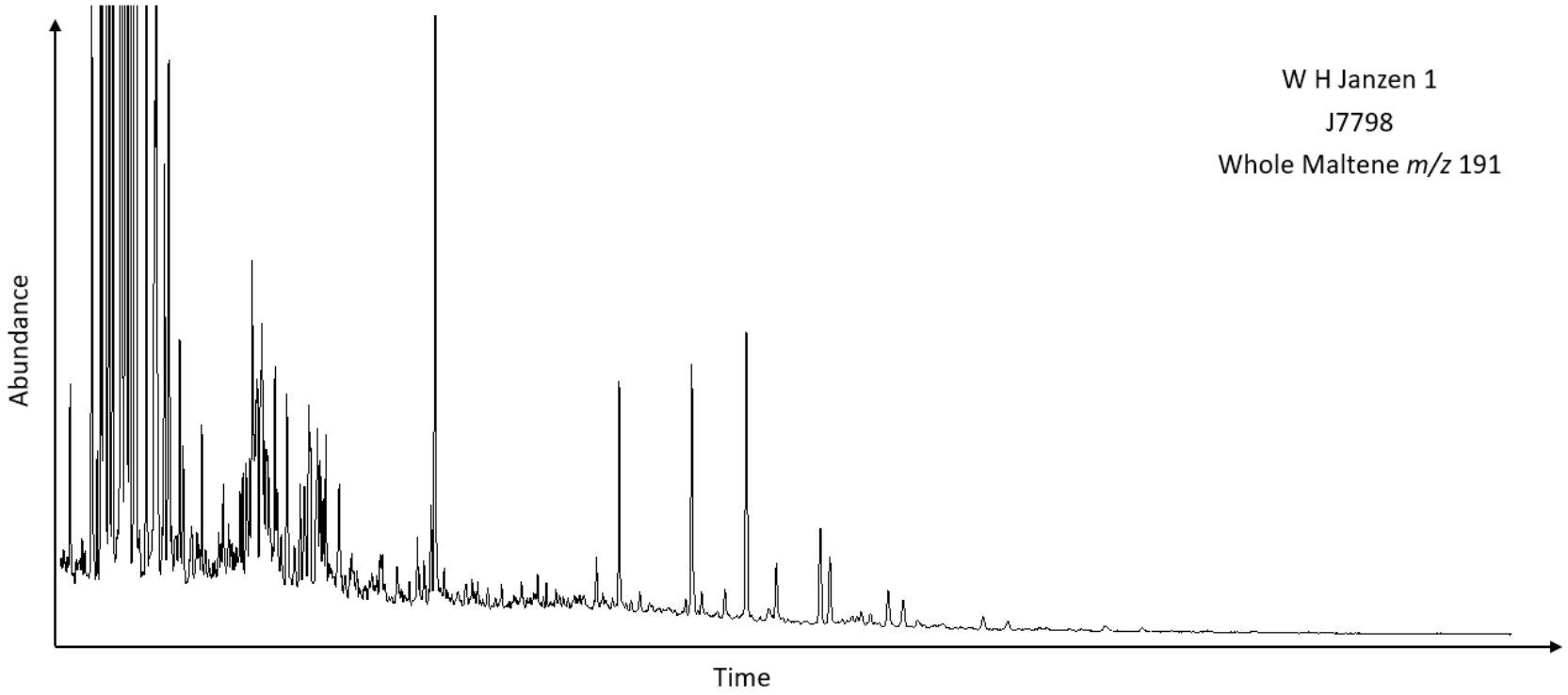
W H Janzen 1
J7798
Whole Maltene m/z 191
Abundance
Time

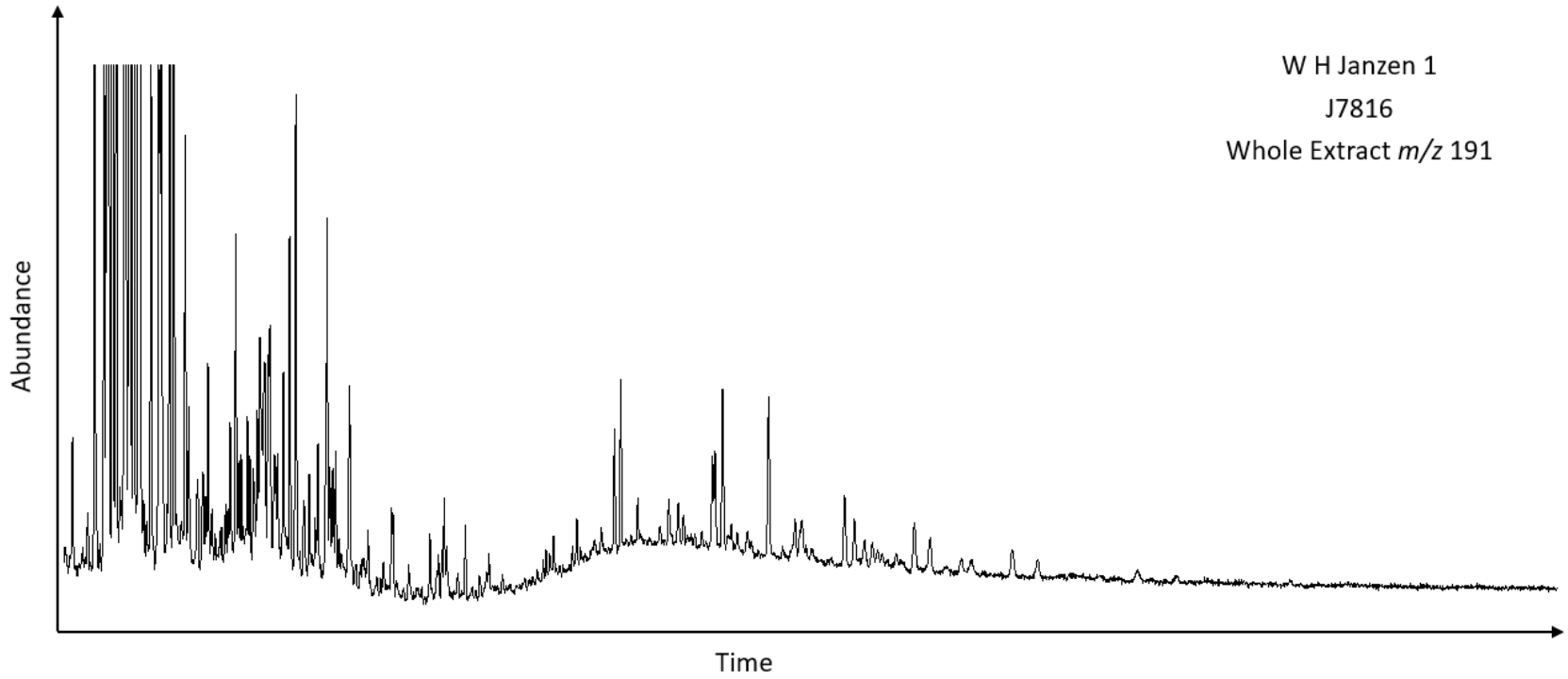
W H Janzen 1
J7816
Whole Extract m/z 191
Abundance
Time

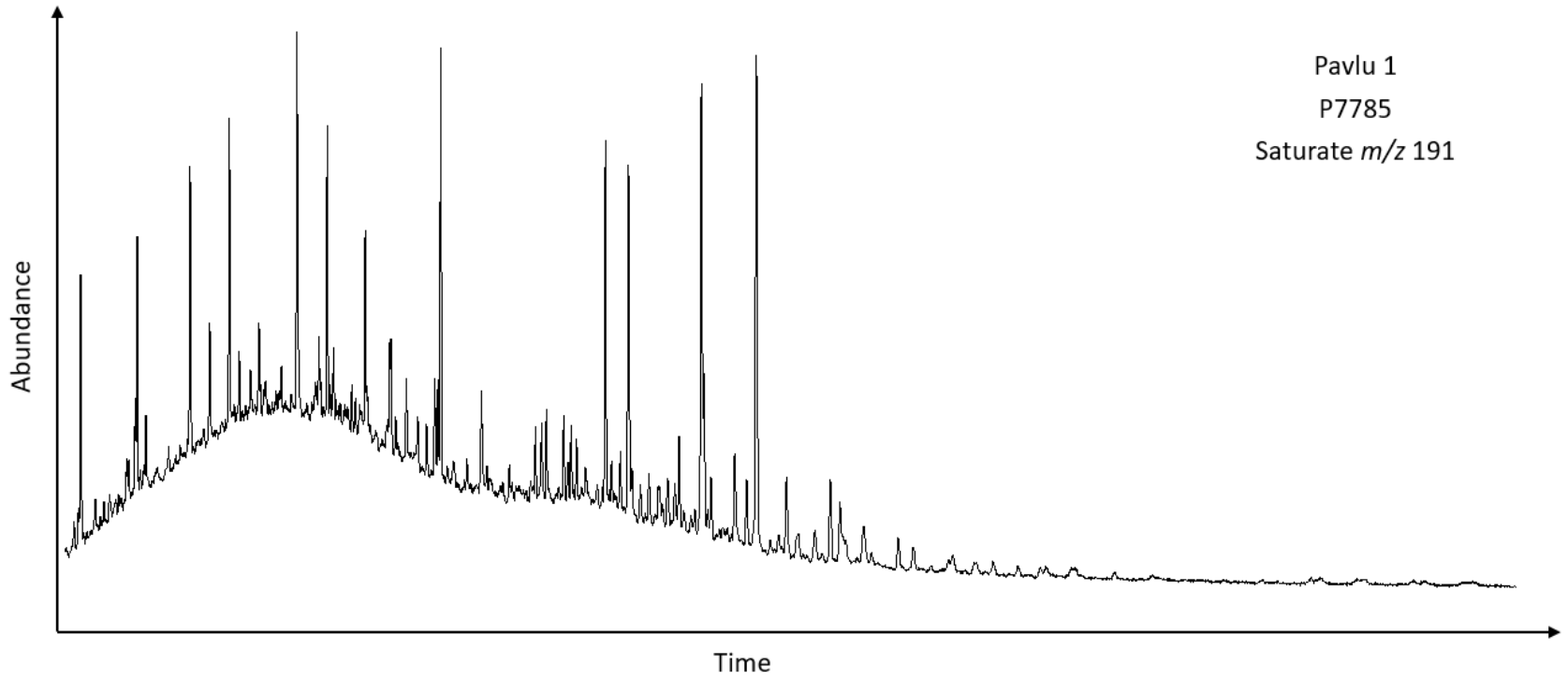
Abundance
Time
Pavlu 1
P7785
Saturate m/z 191

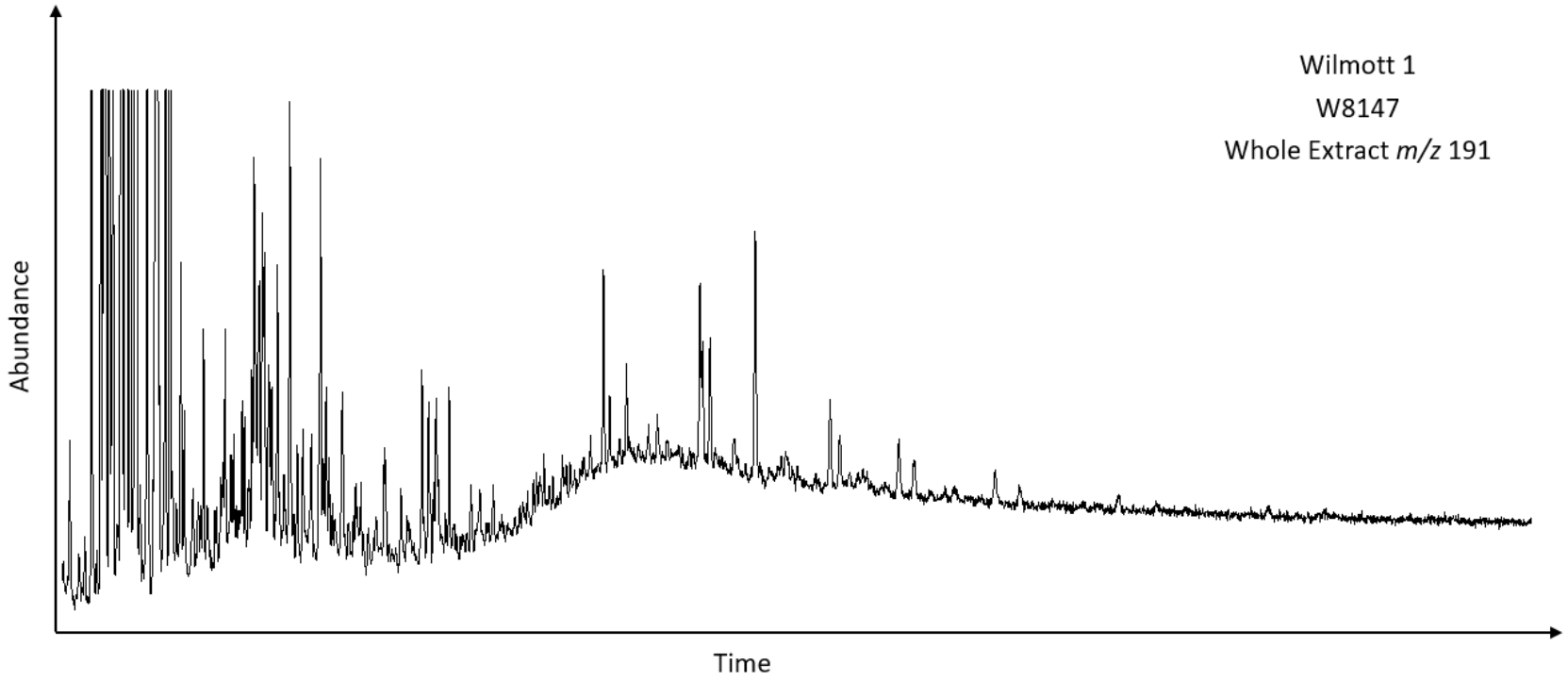
Wilmott 1
W8147
Whole Extract m/z 191
Abundance
Time

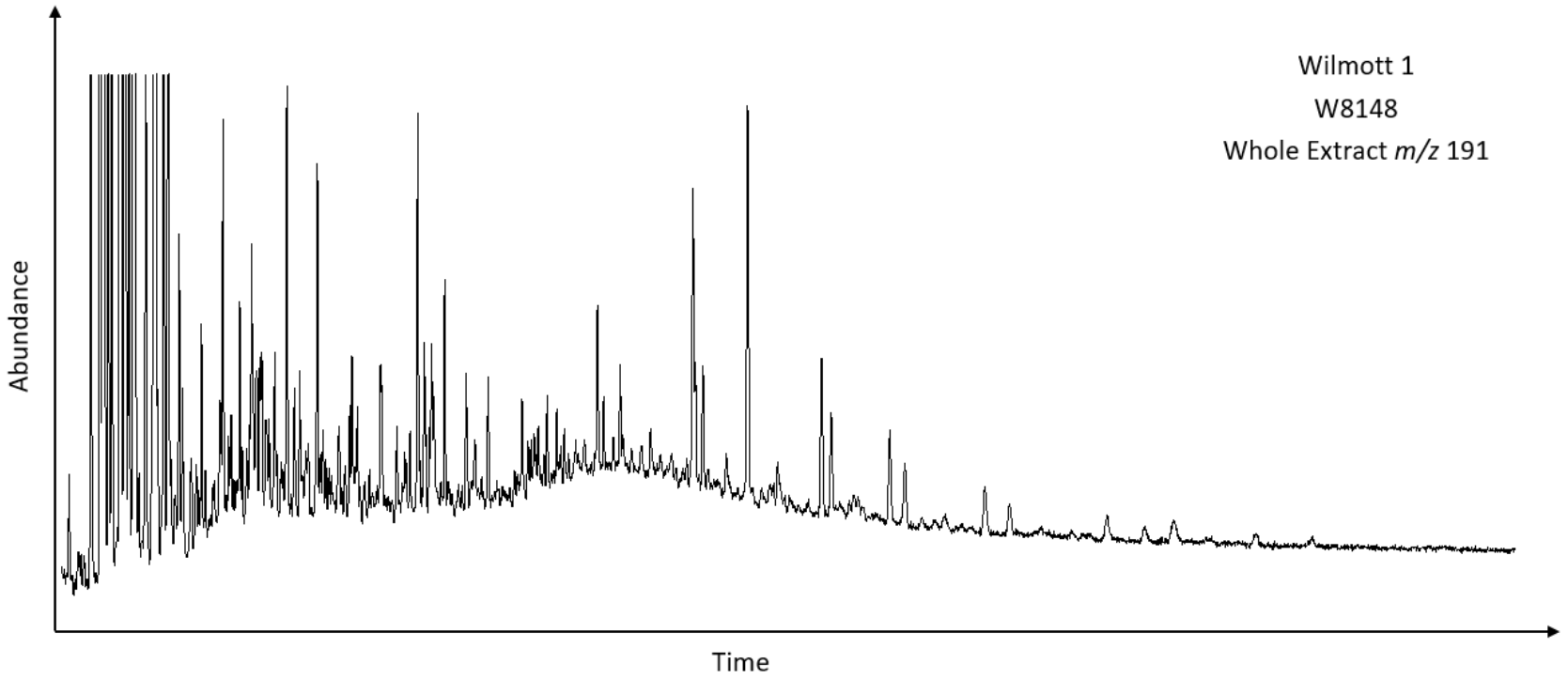
Wilmott 1
W8148
Whole Extract m/z 191
Abundance
Time

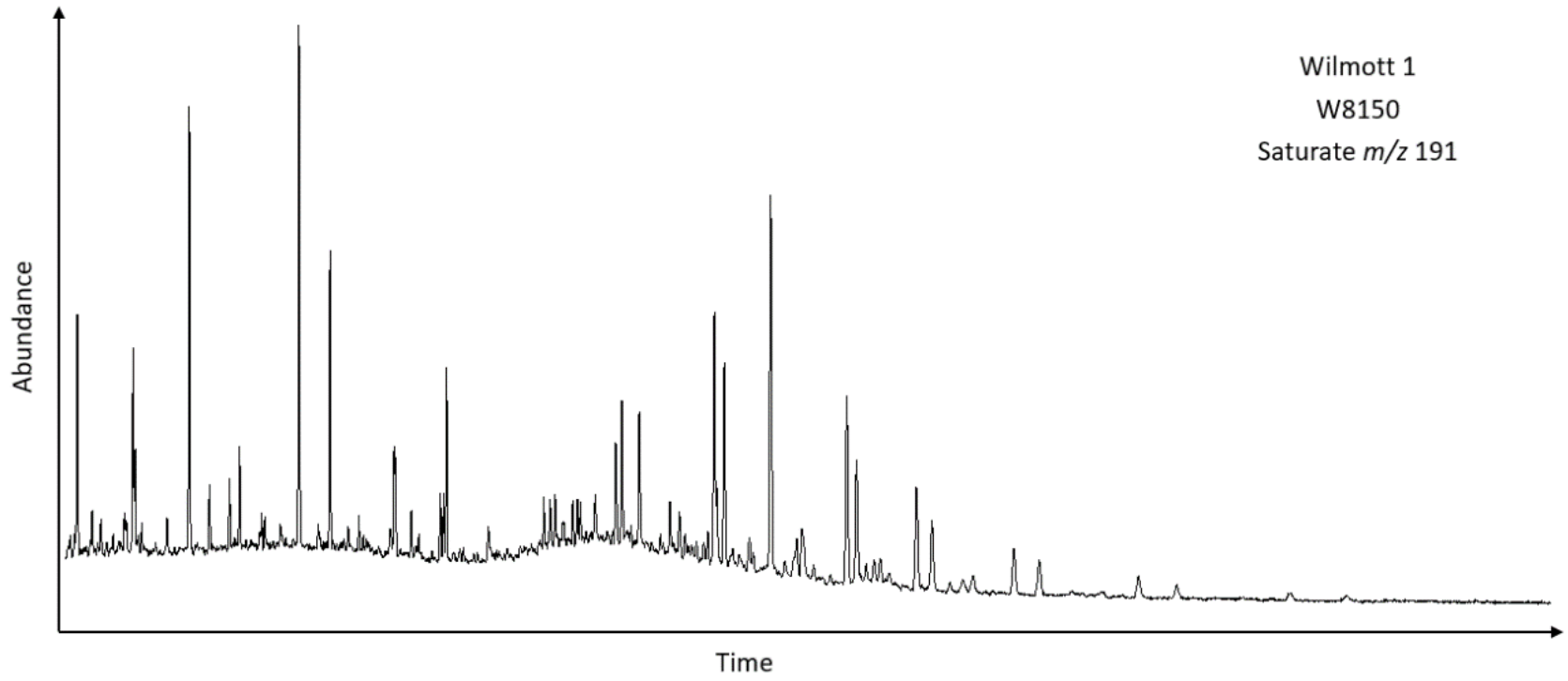
Wilmott 1
W8150
Saturate m/z 191
Abundance
Time

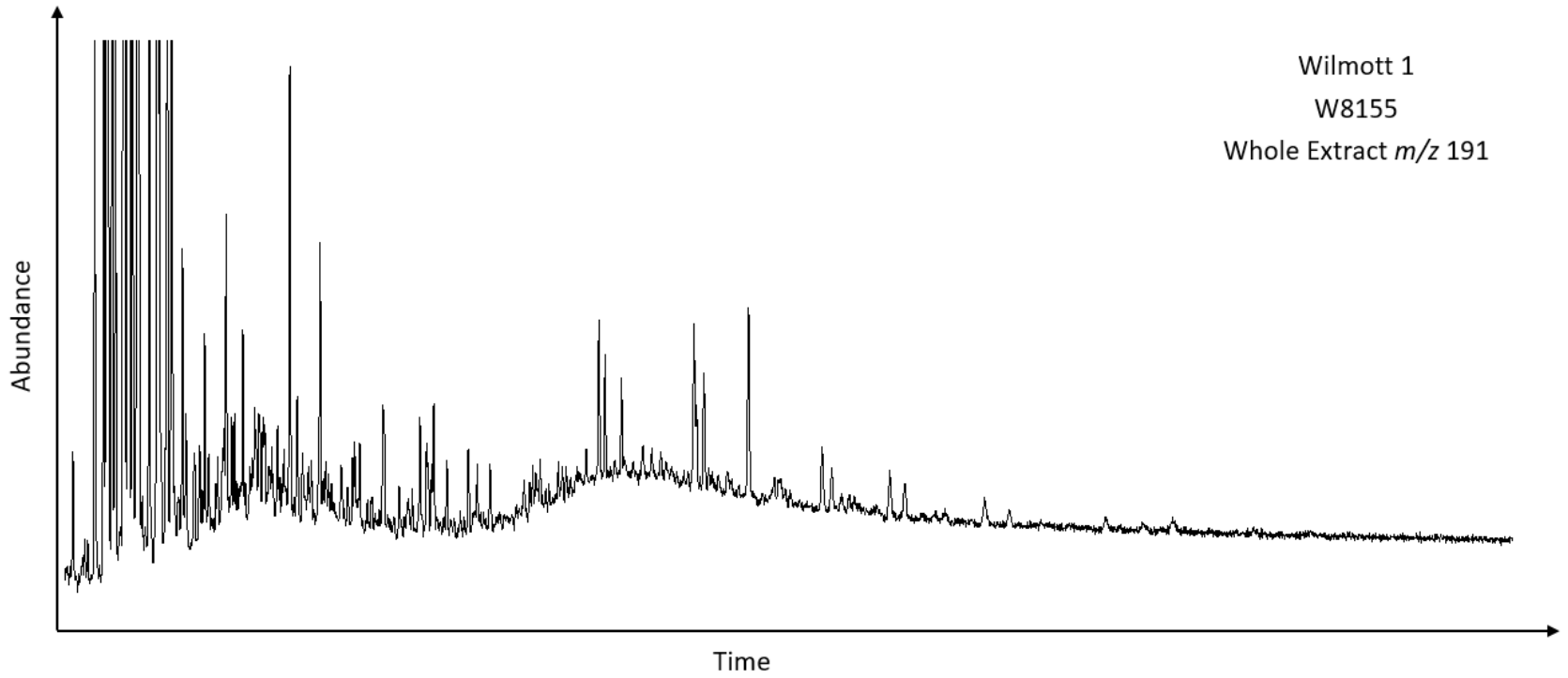
Wilmott 1
W8155
Whole Extract m/z 191
Abundance
Time

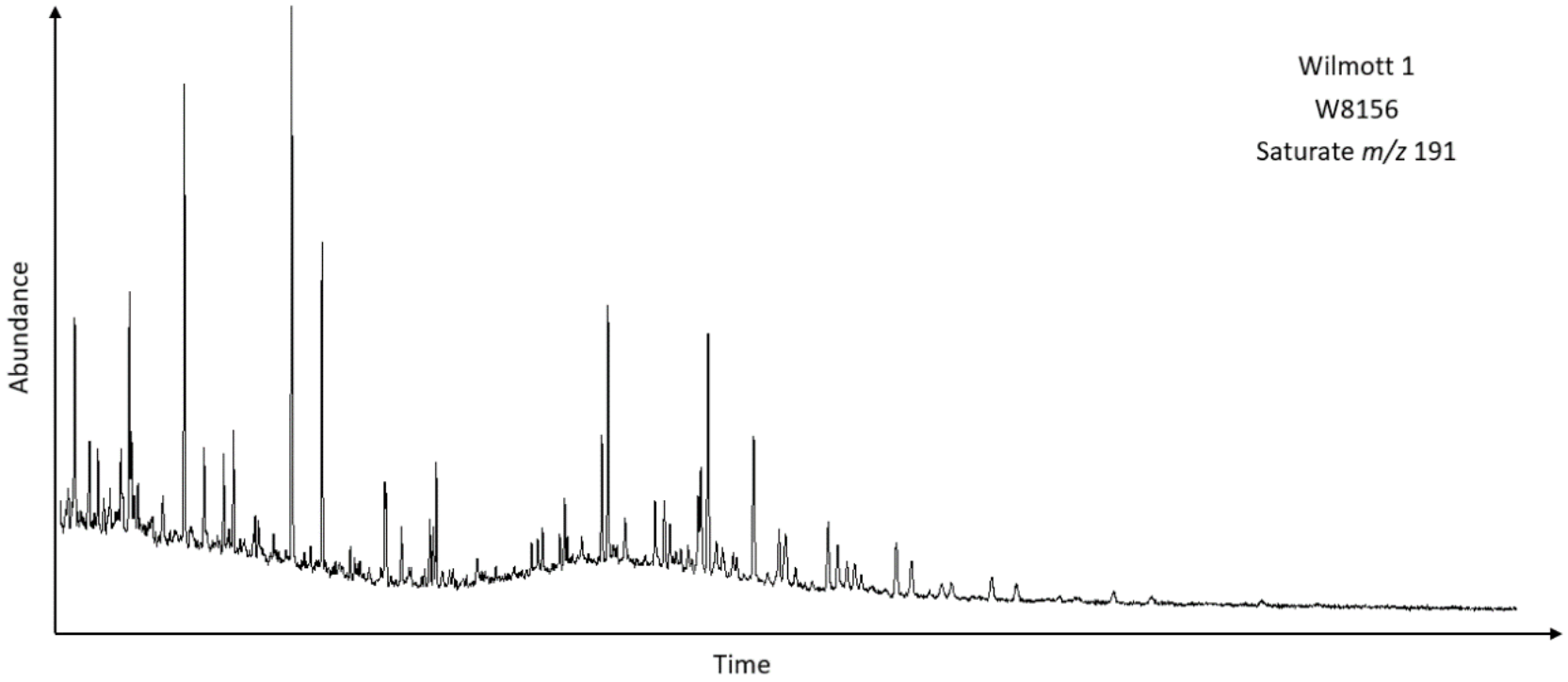
Wilmott 1
W8156
Saturate m/z 191
Abundance
Time

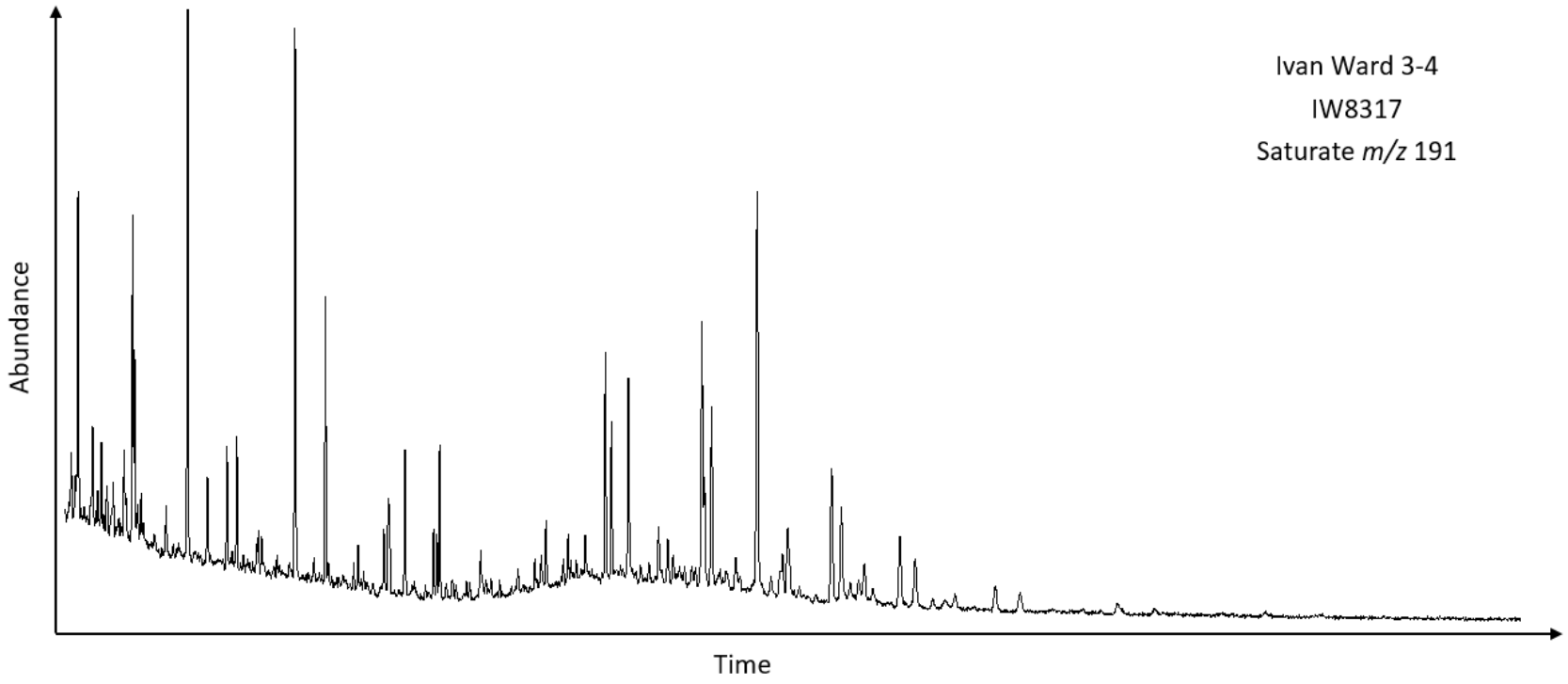
Ivan Ward 3-4
IW8317
Saturate m/z 191
Abundance
Time

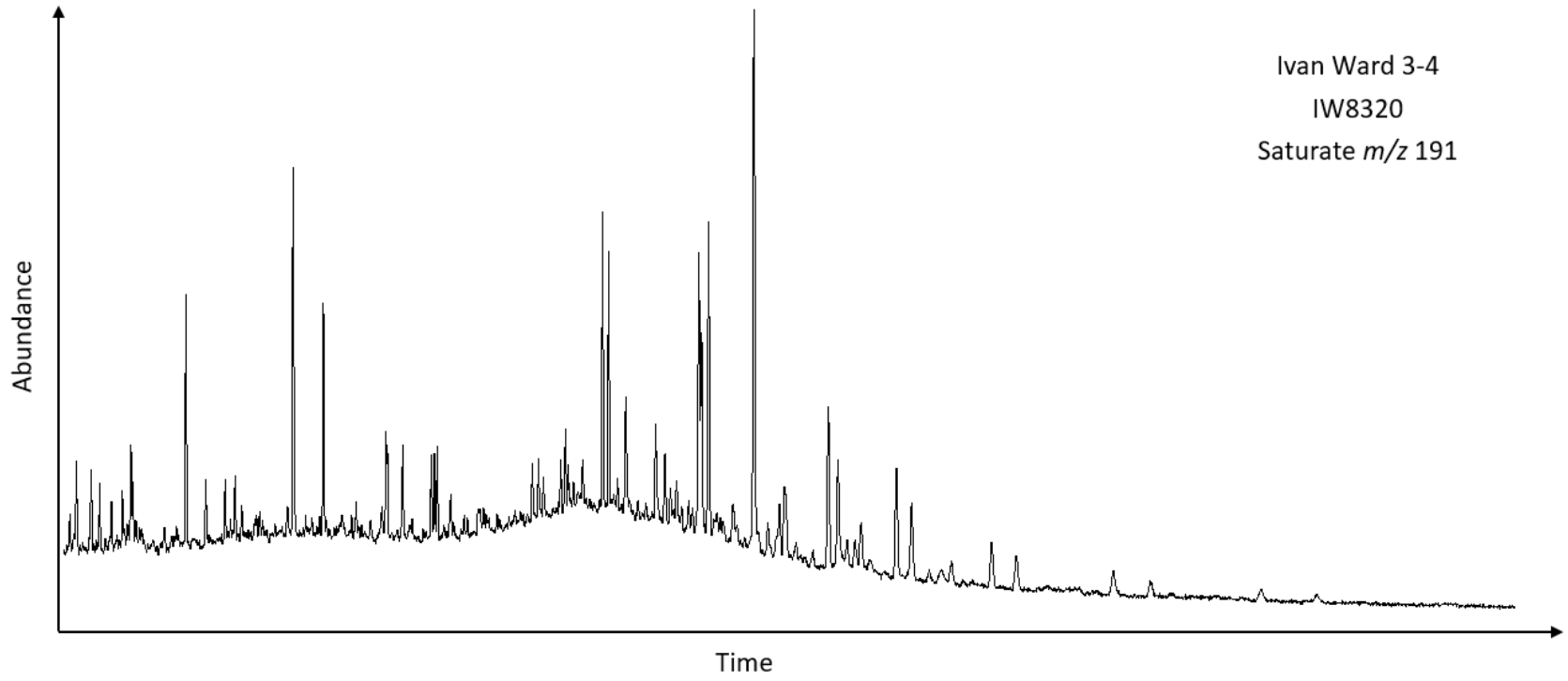
Ivan Ward 3-4
IW8320
Saturate m/z 191
Abundance
Time

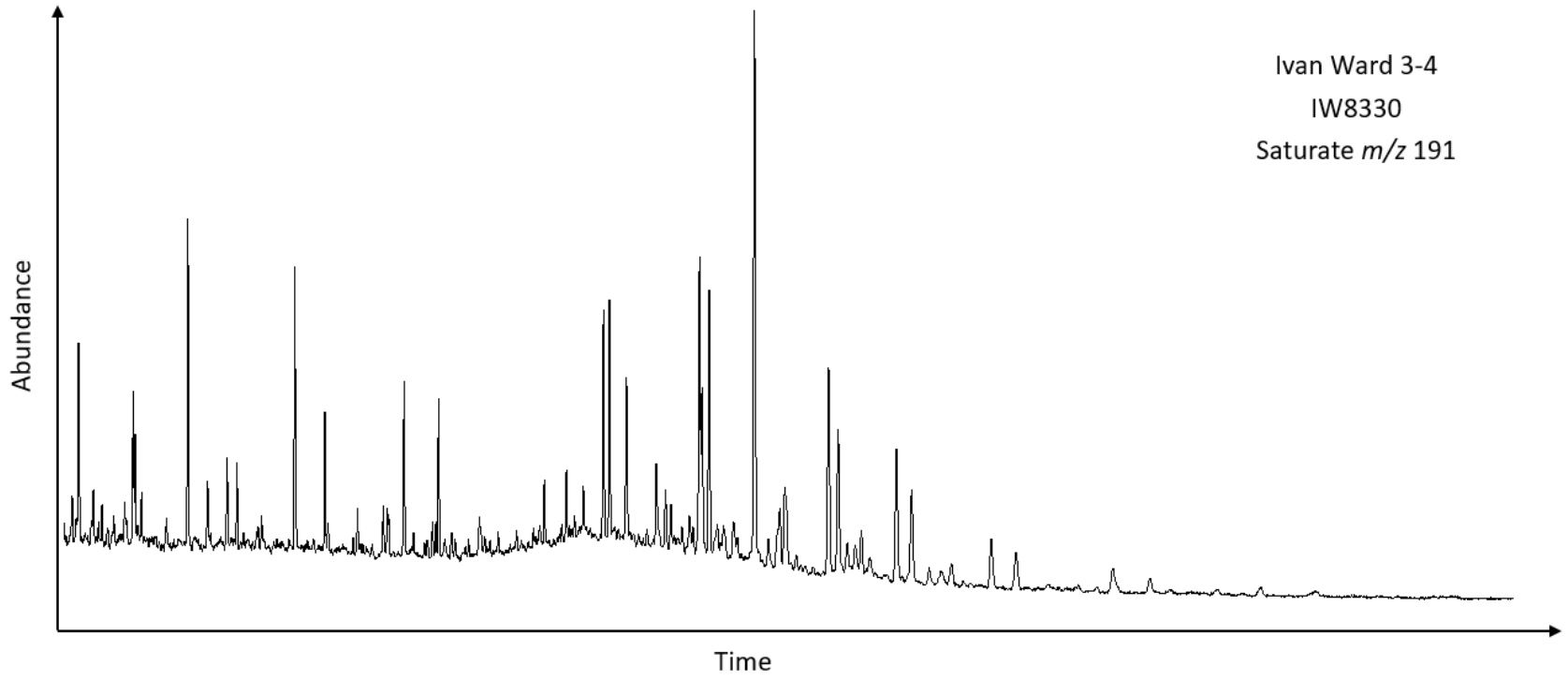
Ivan Ward 3-4
IW8330
Saturate m/z 191
Abundance
Time

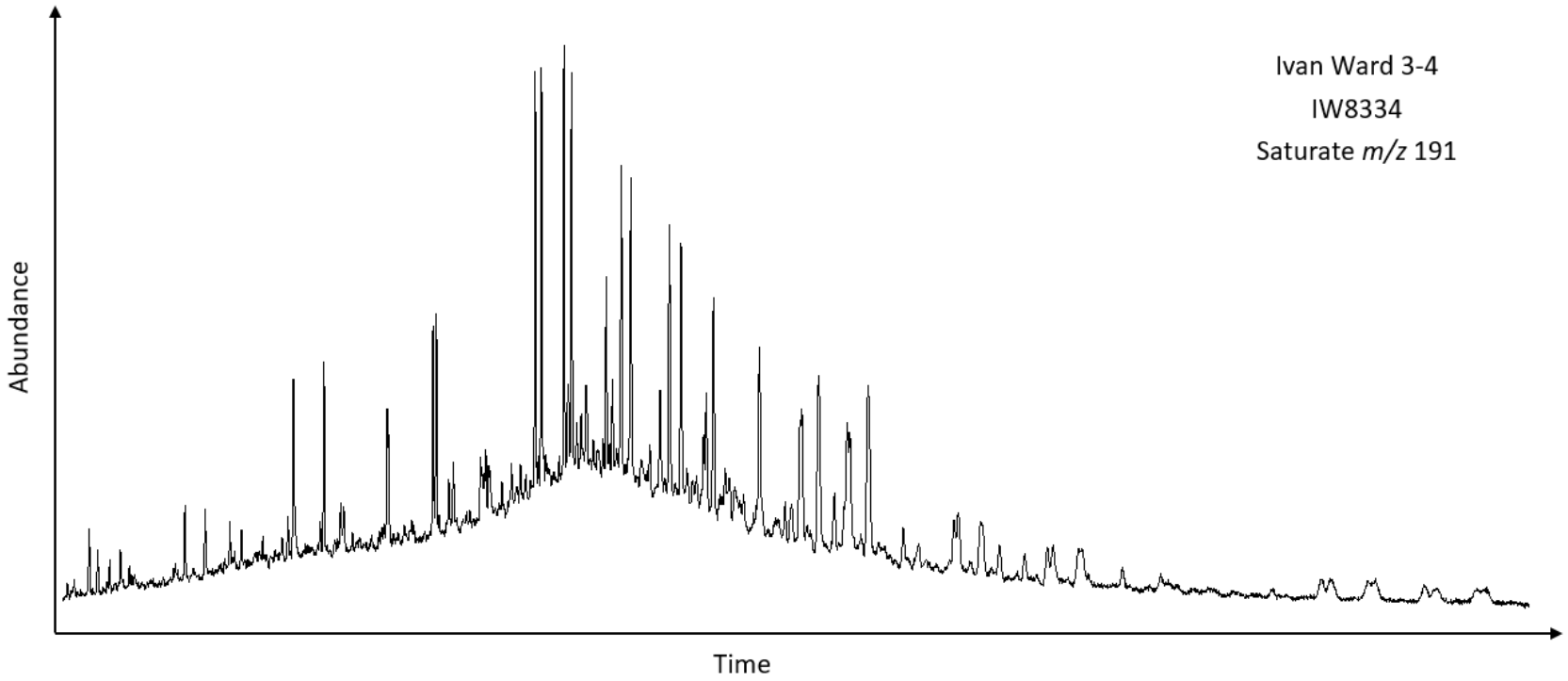
Ivan Ward 3-4
IW8334
Saturate m/z 191
Abundance
Time

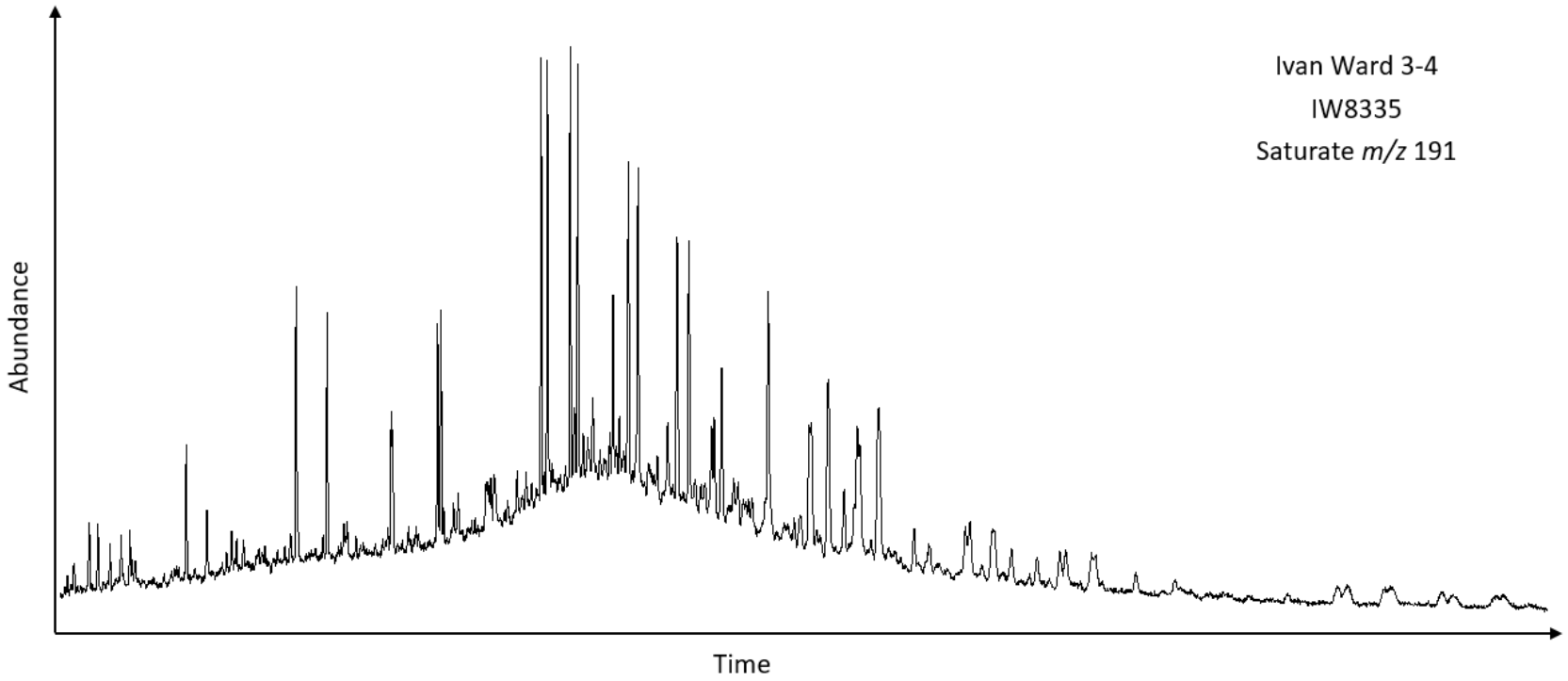
Ivan Ward 3-4
IW8335
Saturate m/z 191
Abundance
Time

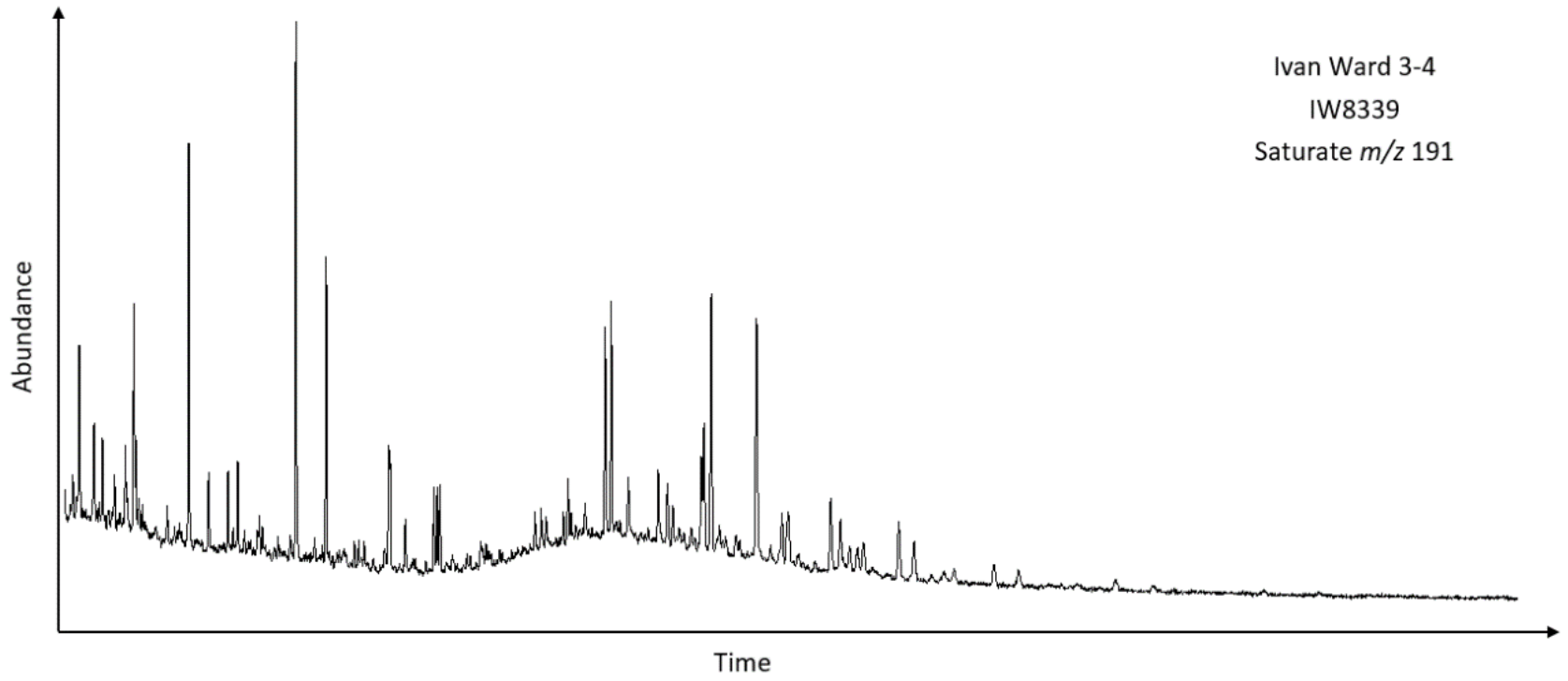
Ivan Ward 3-4
IW8339
Saturate m/z 191
Abundance
Time

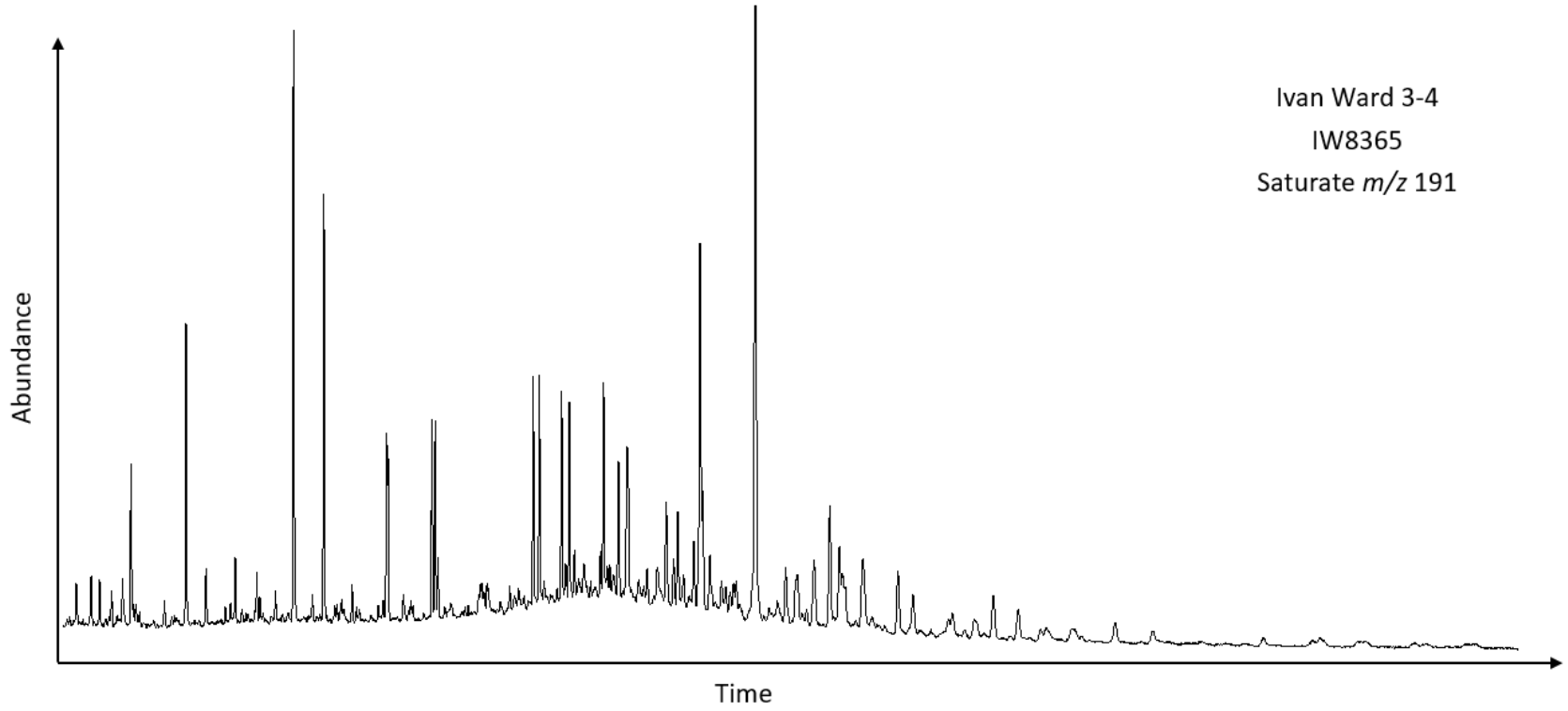
Ivan Ward 3-4
IW8365
Saturate m/z 191
Abundance
Time

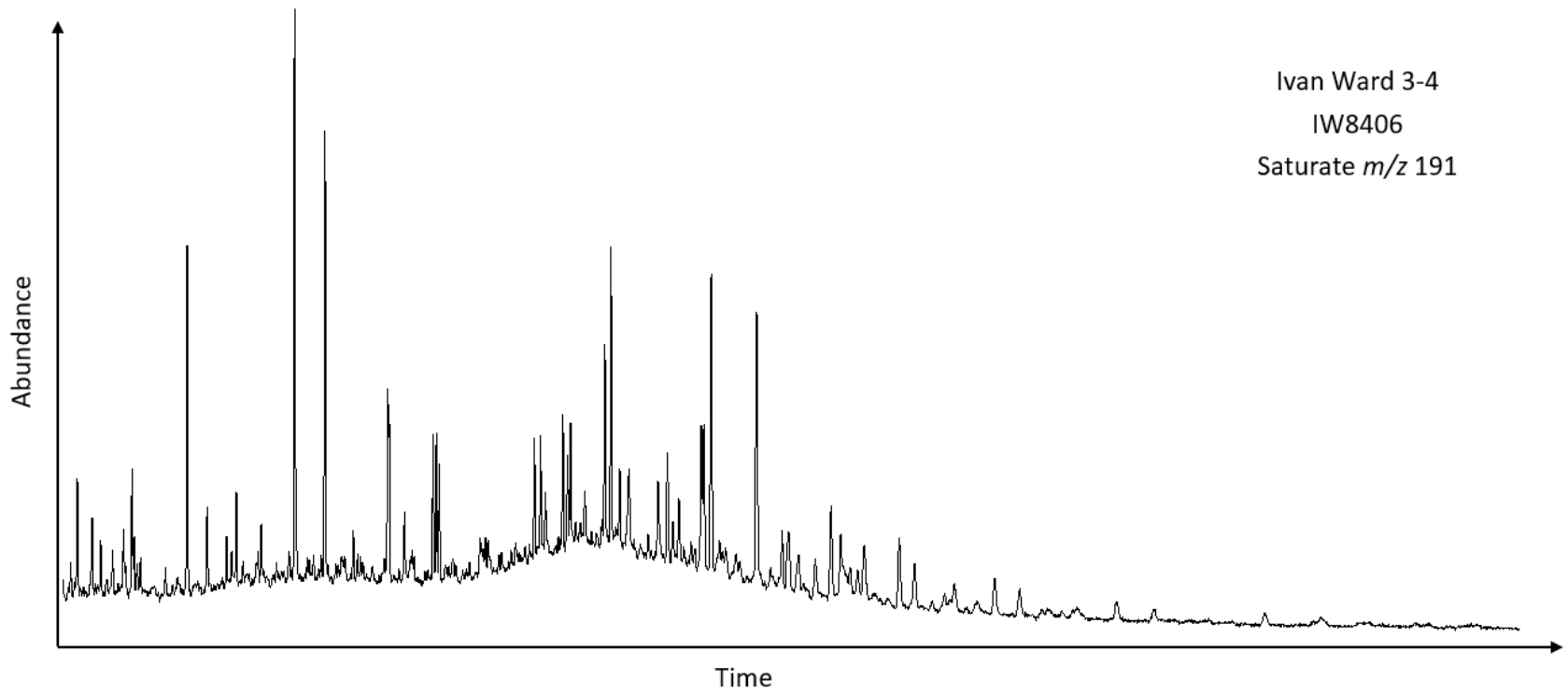
Ivan Ward 3-4
IW8406
Saturate m/z 191
Abundance
Time

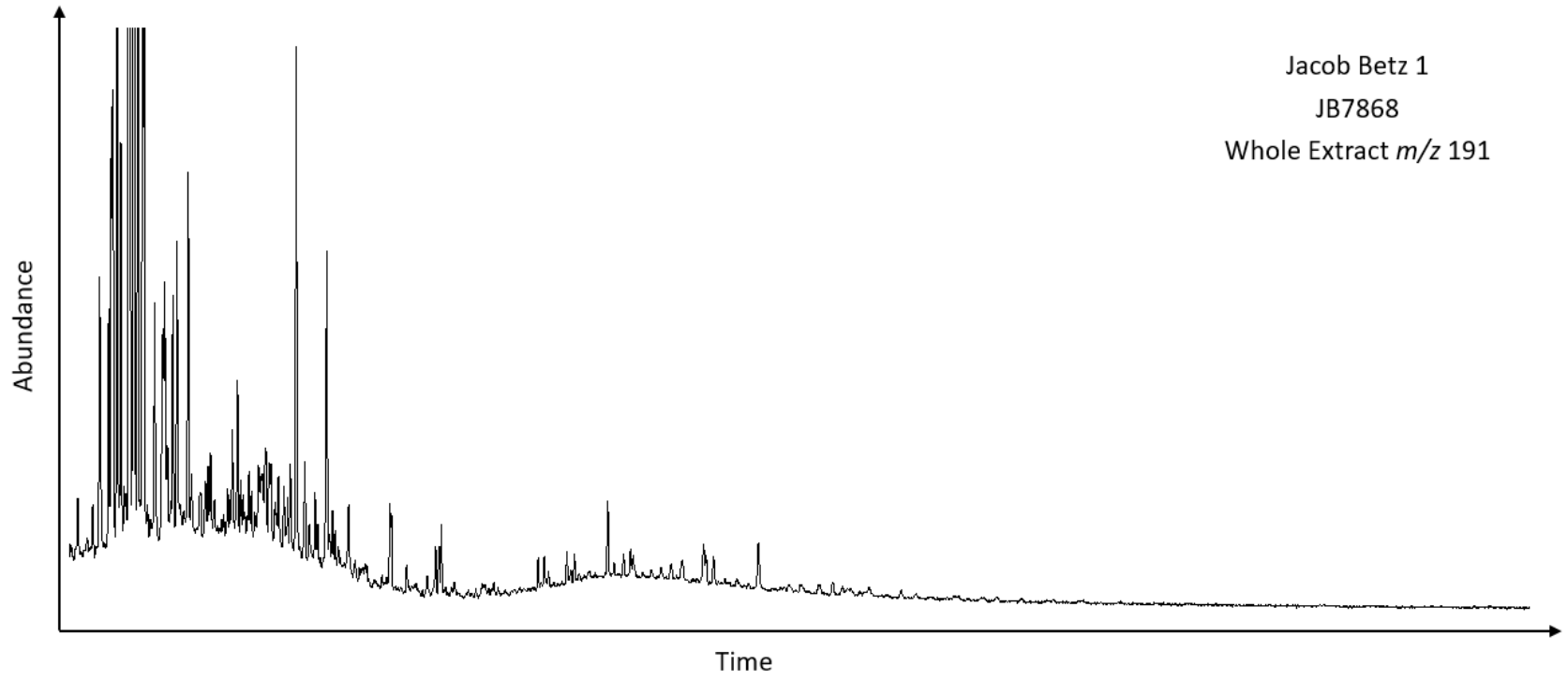
Jacob Betz 1
JB7868
Whole Extract m/z 191
Abundance
Time

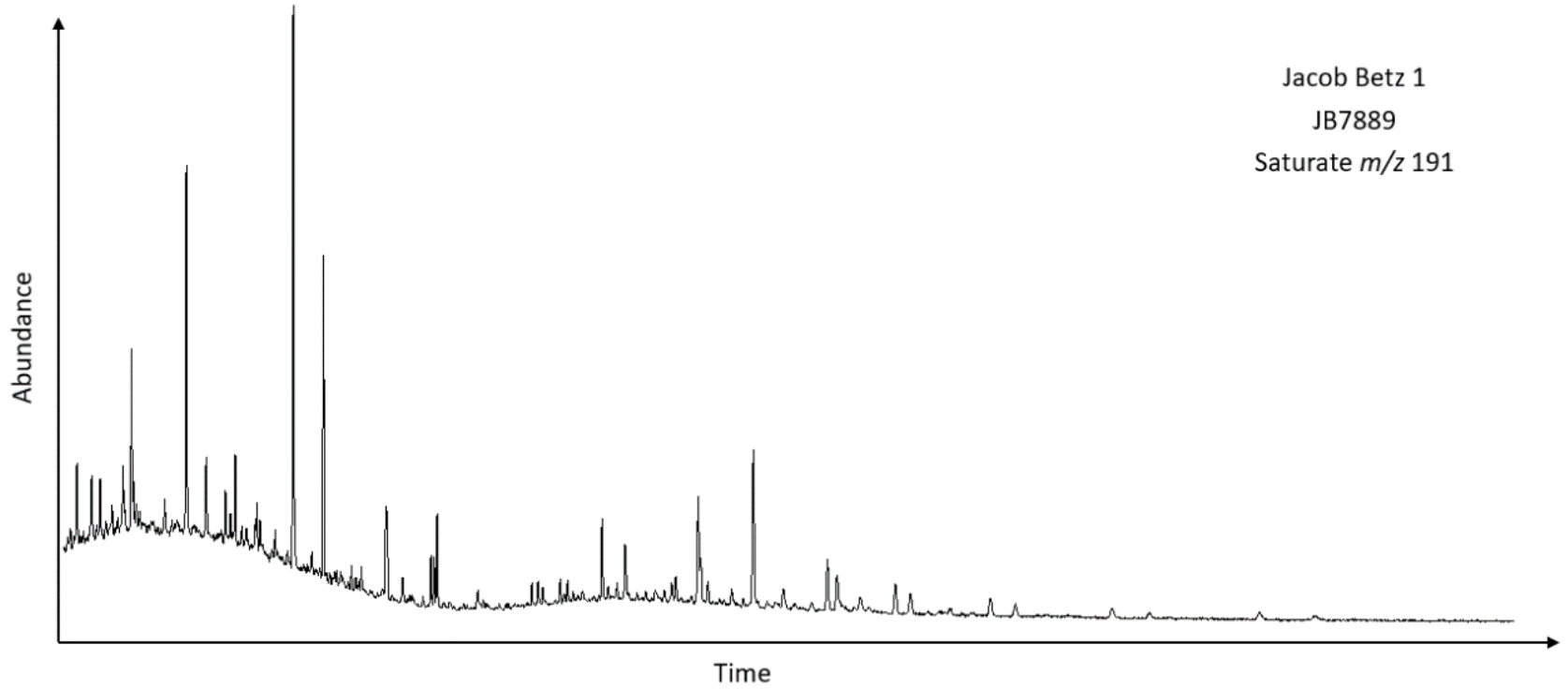
Jacob Betz 1
JB7889
Saturate m/z 191
Abundance
Time

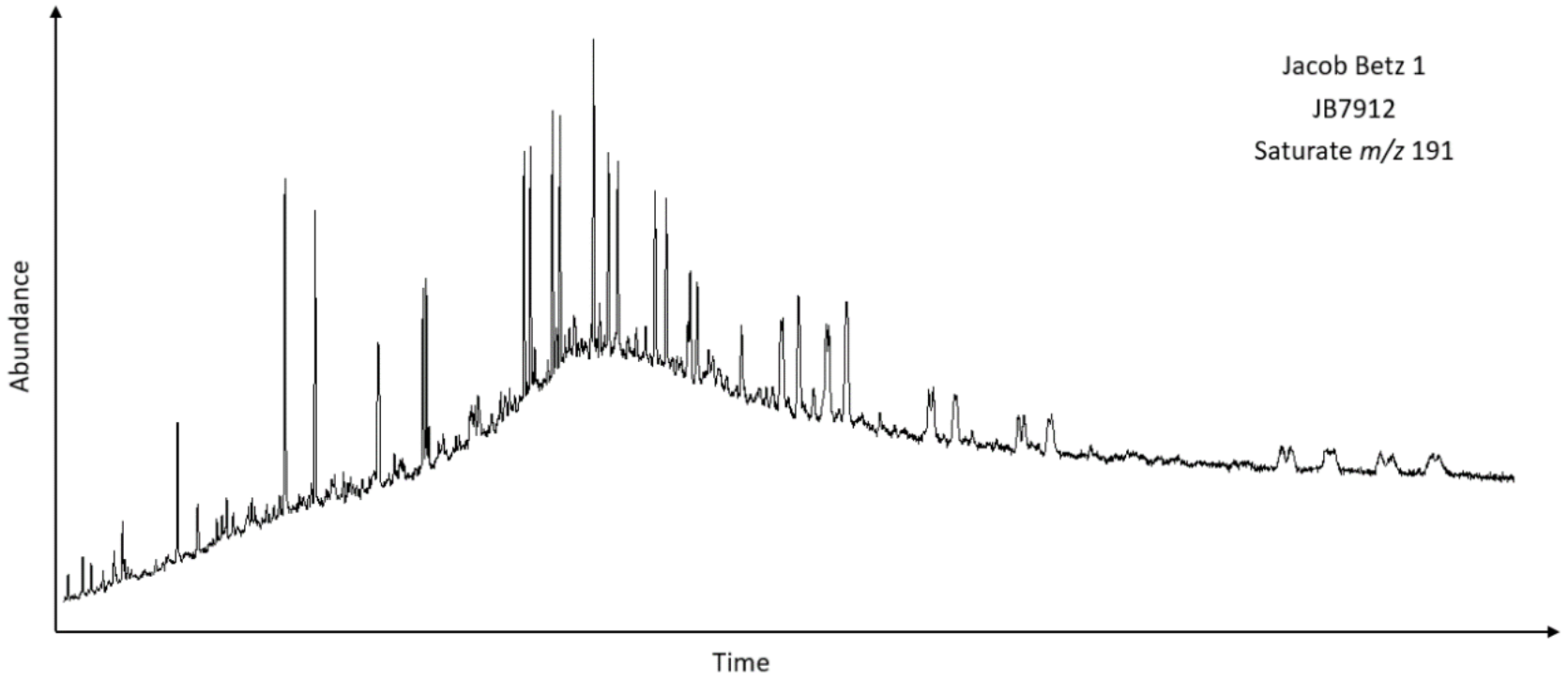
Jacob Betz 1
JB7912
Saturate m/z 191
Abundance
Time

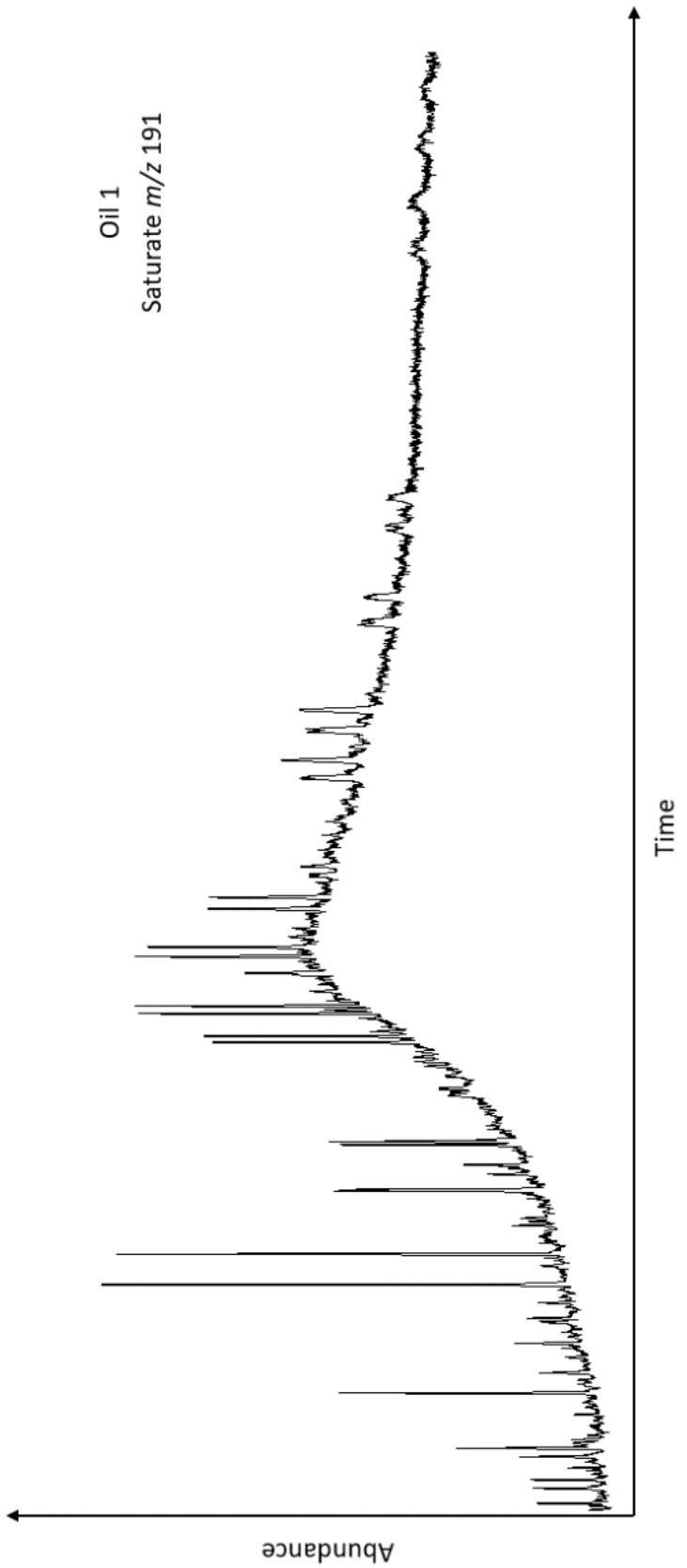
Oil 1
Saturate m/z 191
Abundance
Time

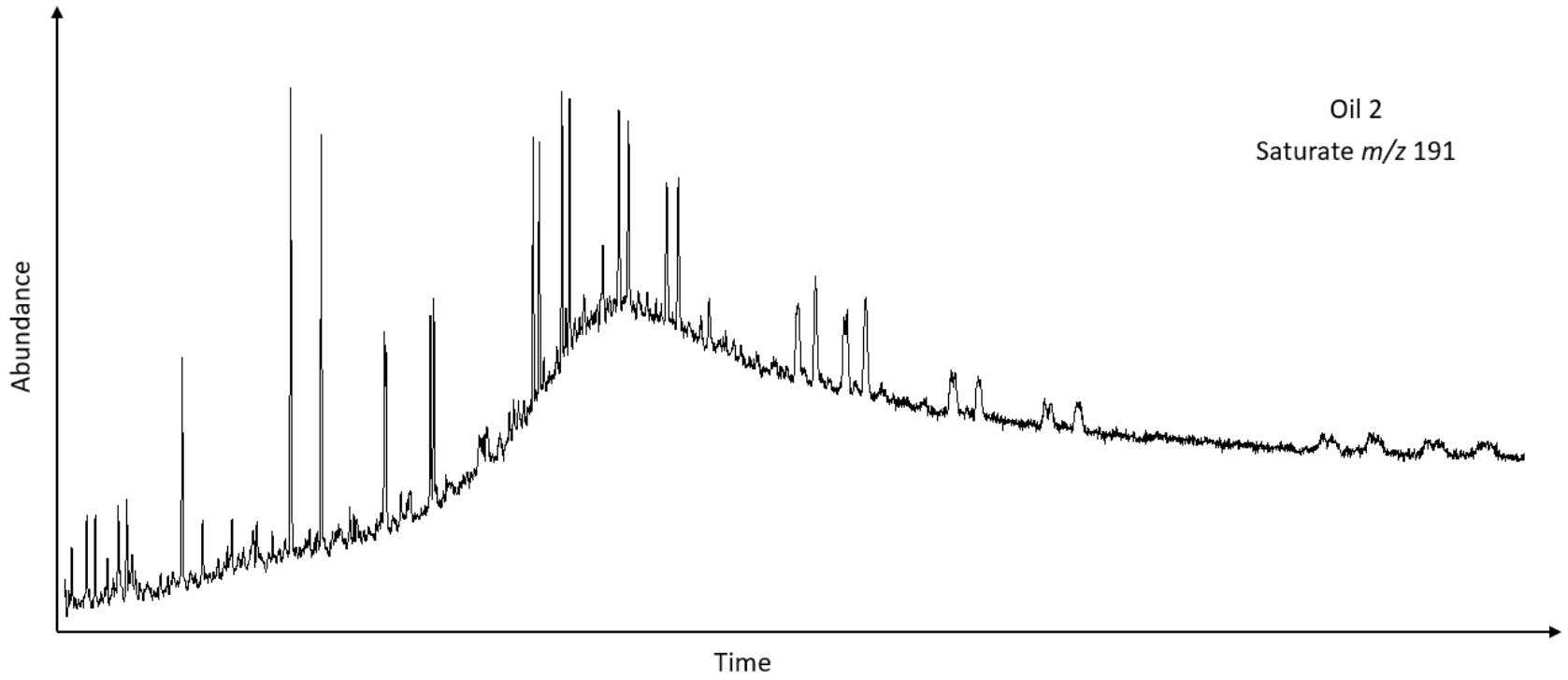
Oil 2
Saturate *m/z* 191
Abundance
Time

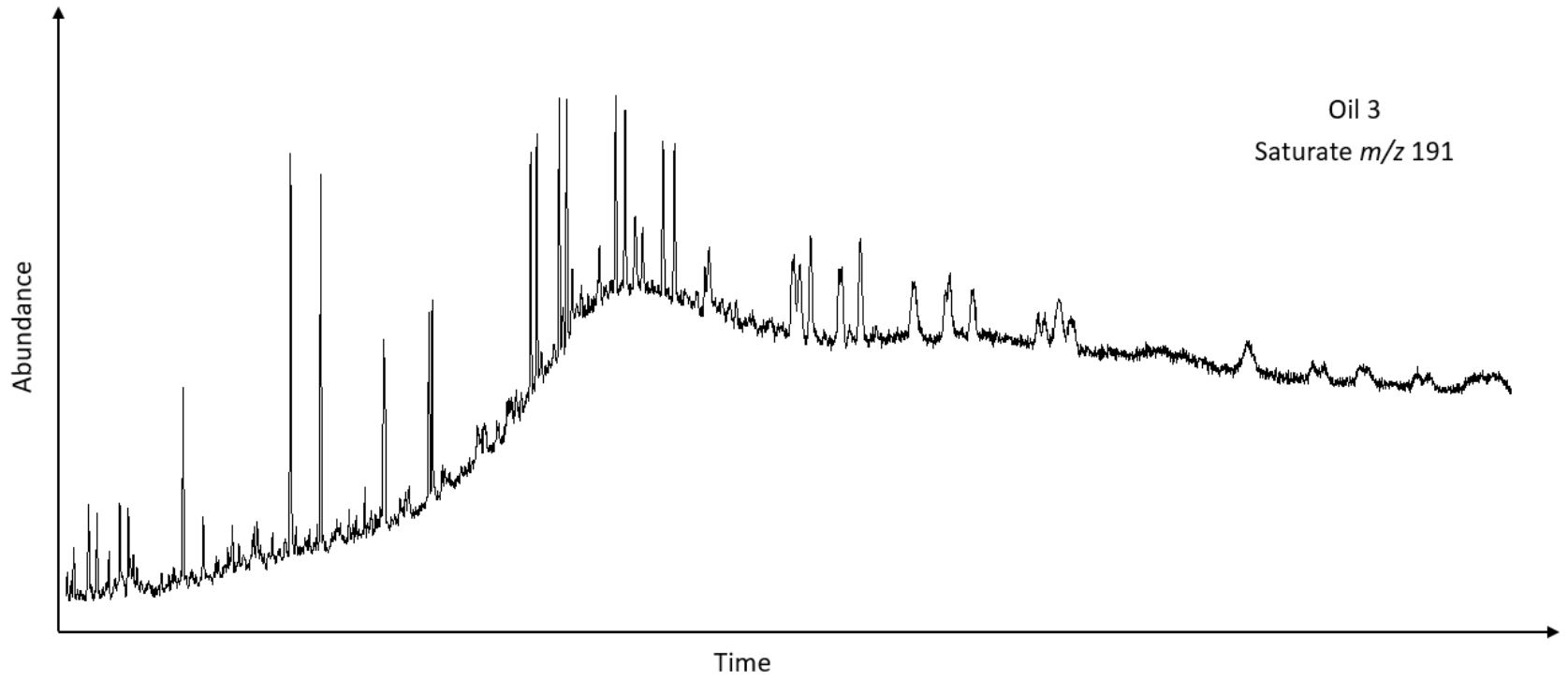
Oil 3
Saturate m/z 191
Abundance
Time

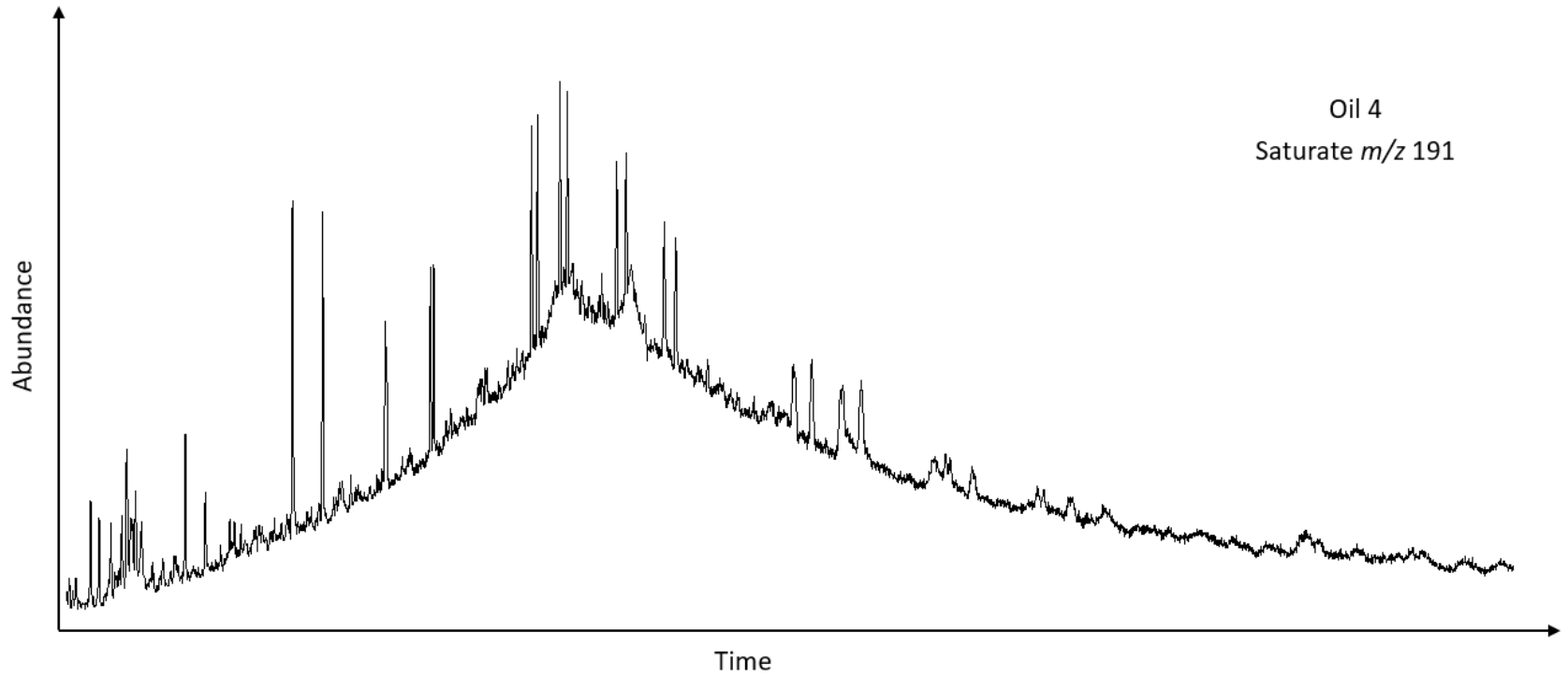
Oil 4
Saturate m/z 191
Abundance
Time

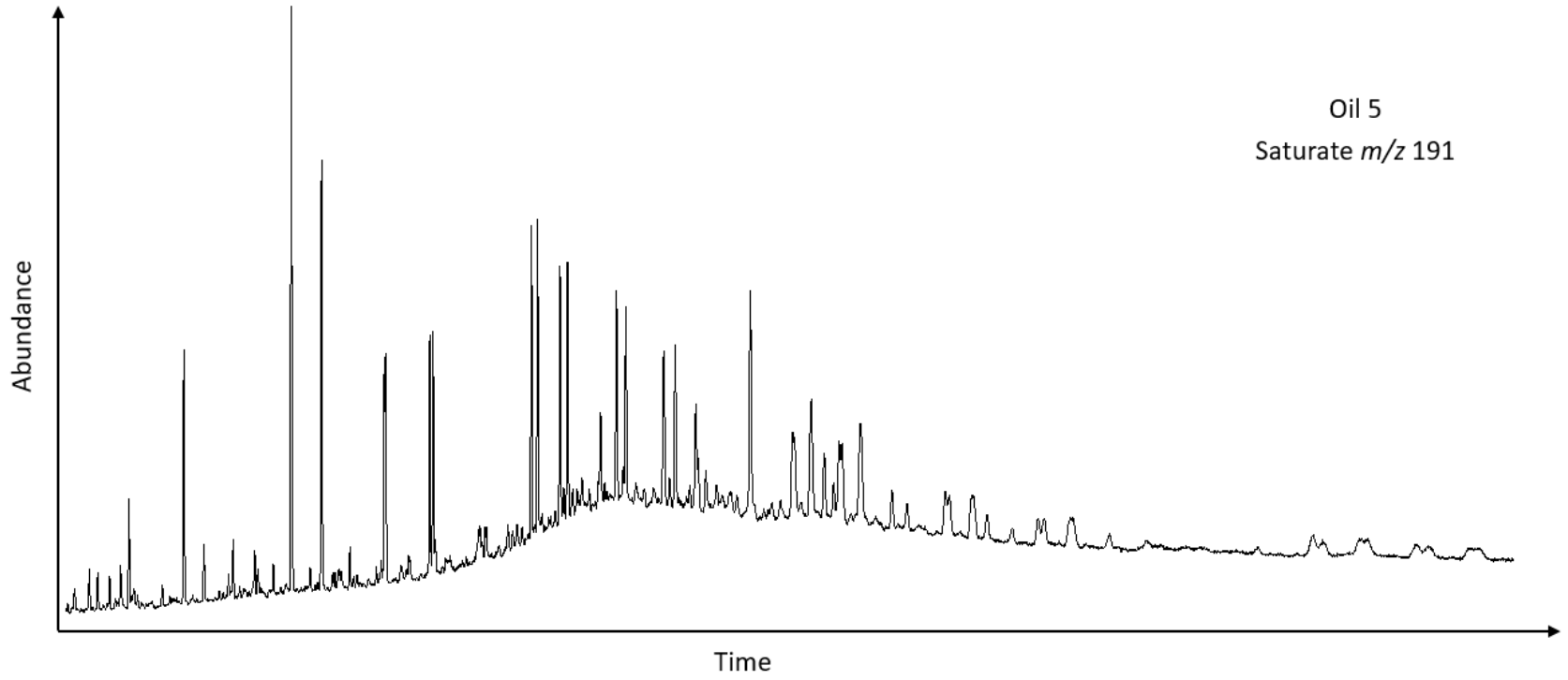
Oil 5
Saturate m/z 191
Abundance
Time

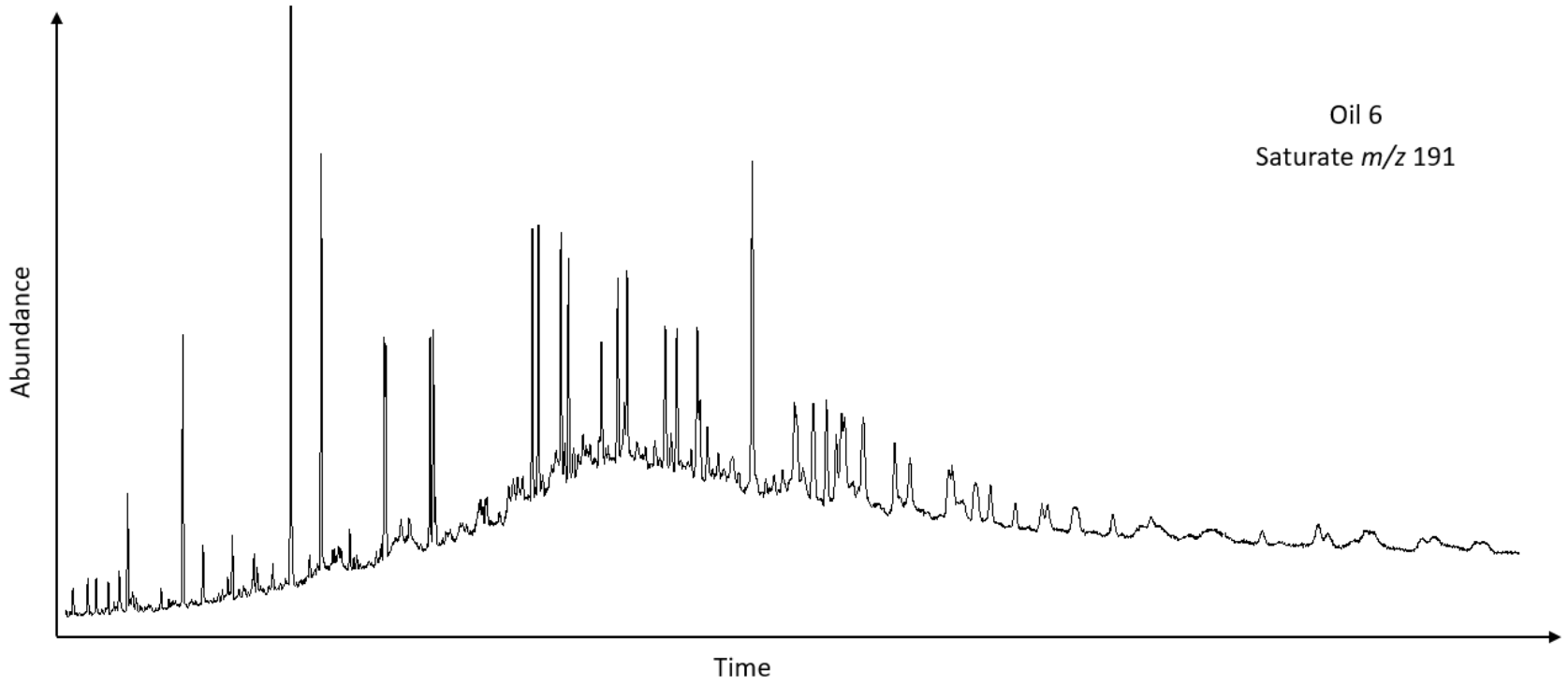
Oil 6
Saturate m/z 191
Abundance
Time

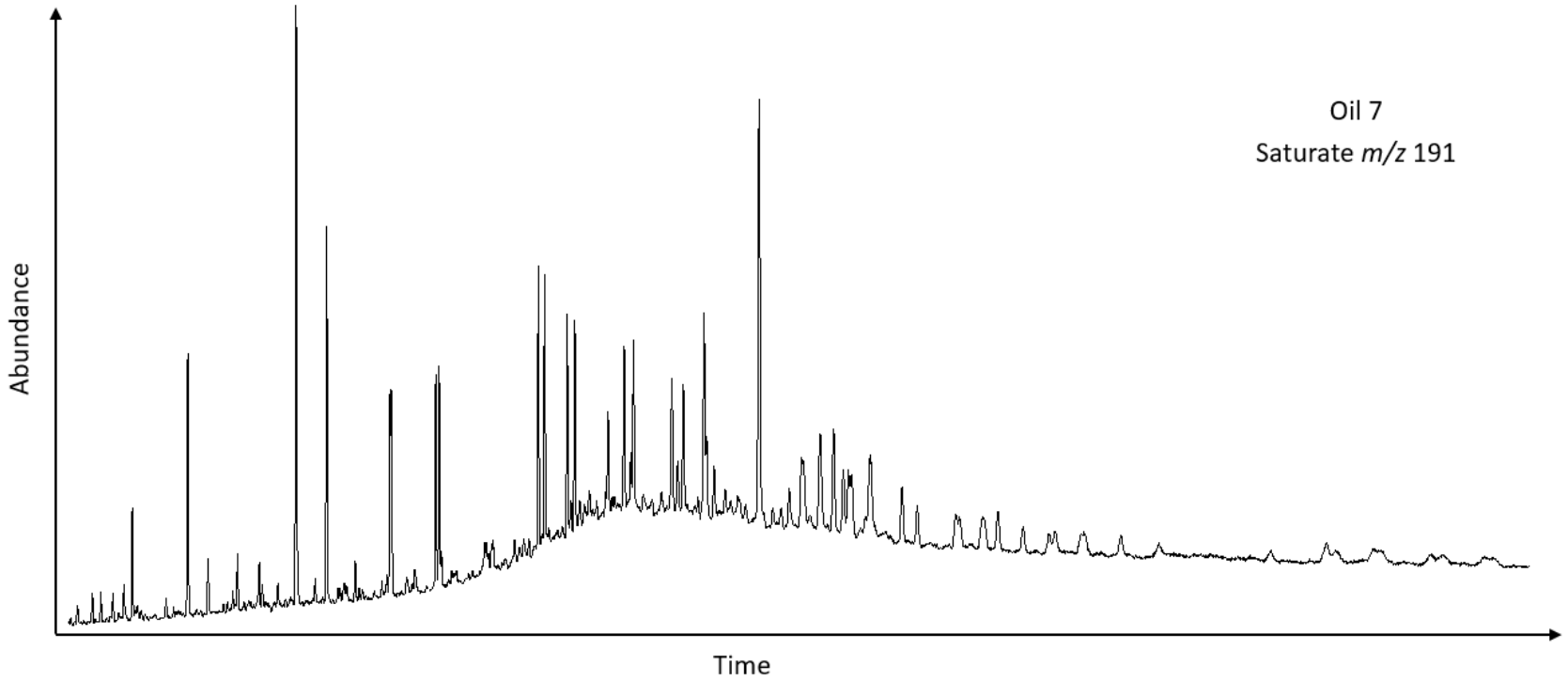
Oil 7
Saturate m/z 191
Abundance
Time

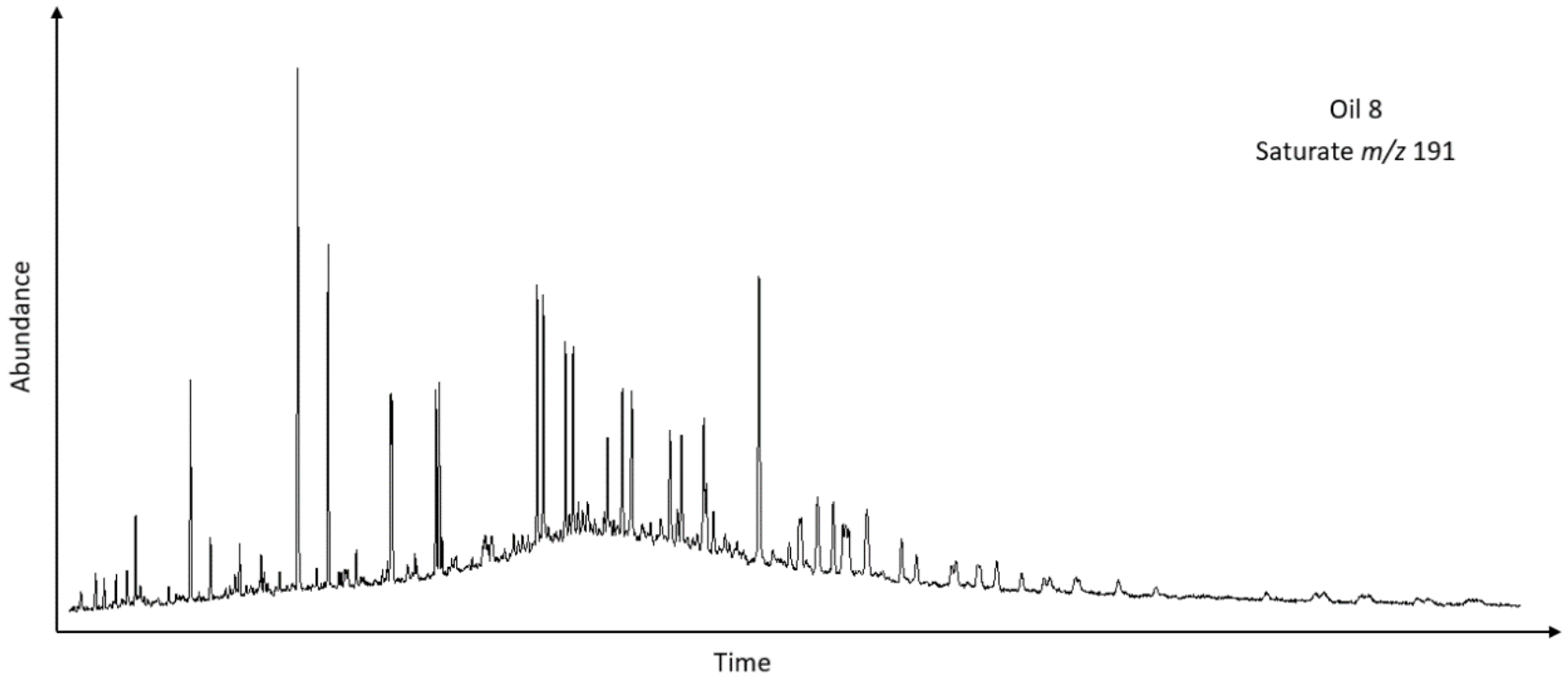
Oil 8
Saturate m/z 191
Abundance
Time

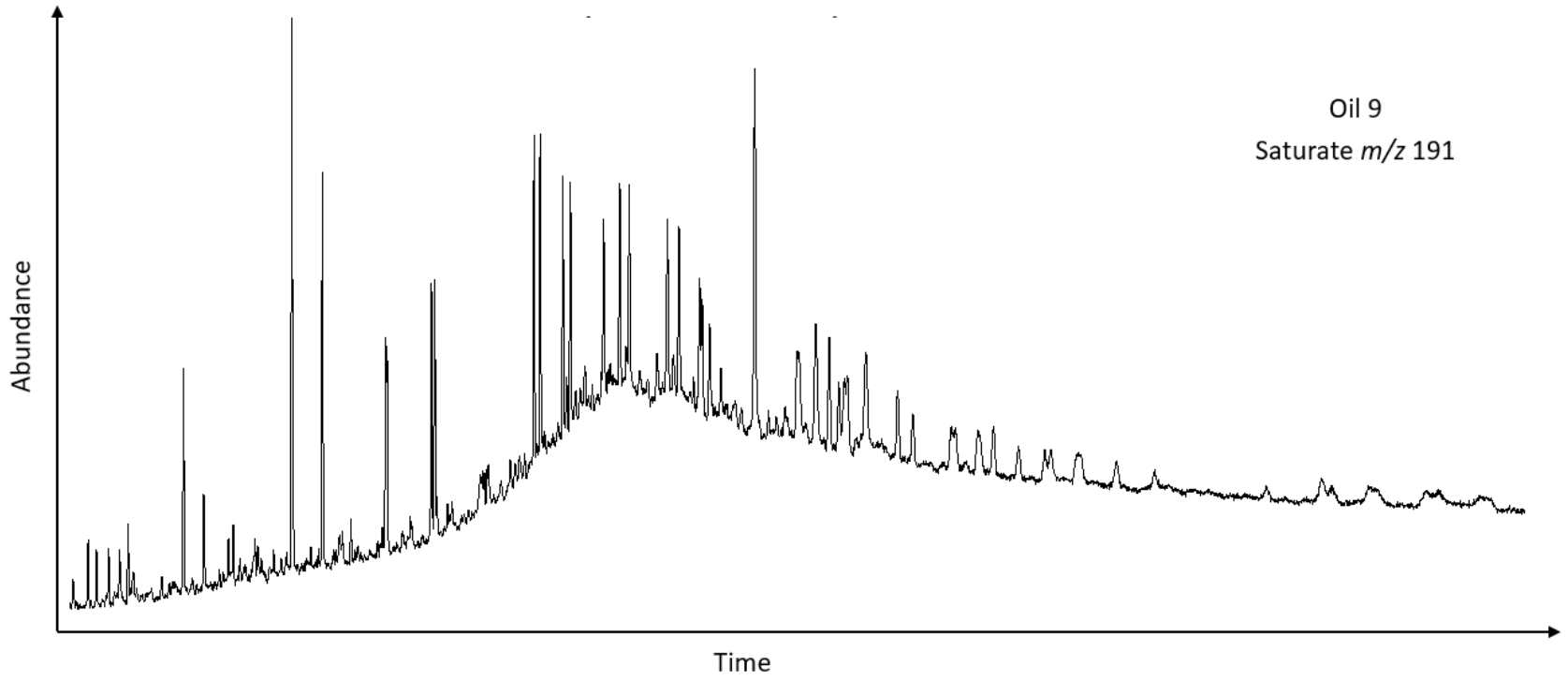
Oil 9
Saturate m/z 191
Abundance
Time

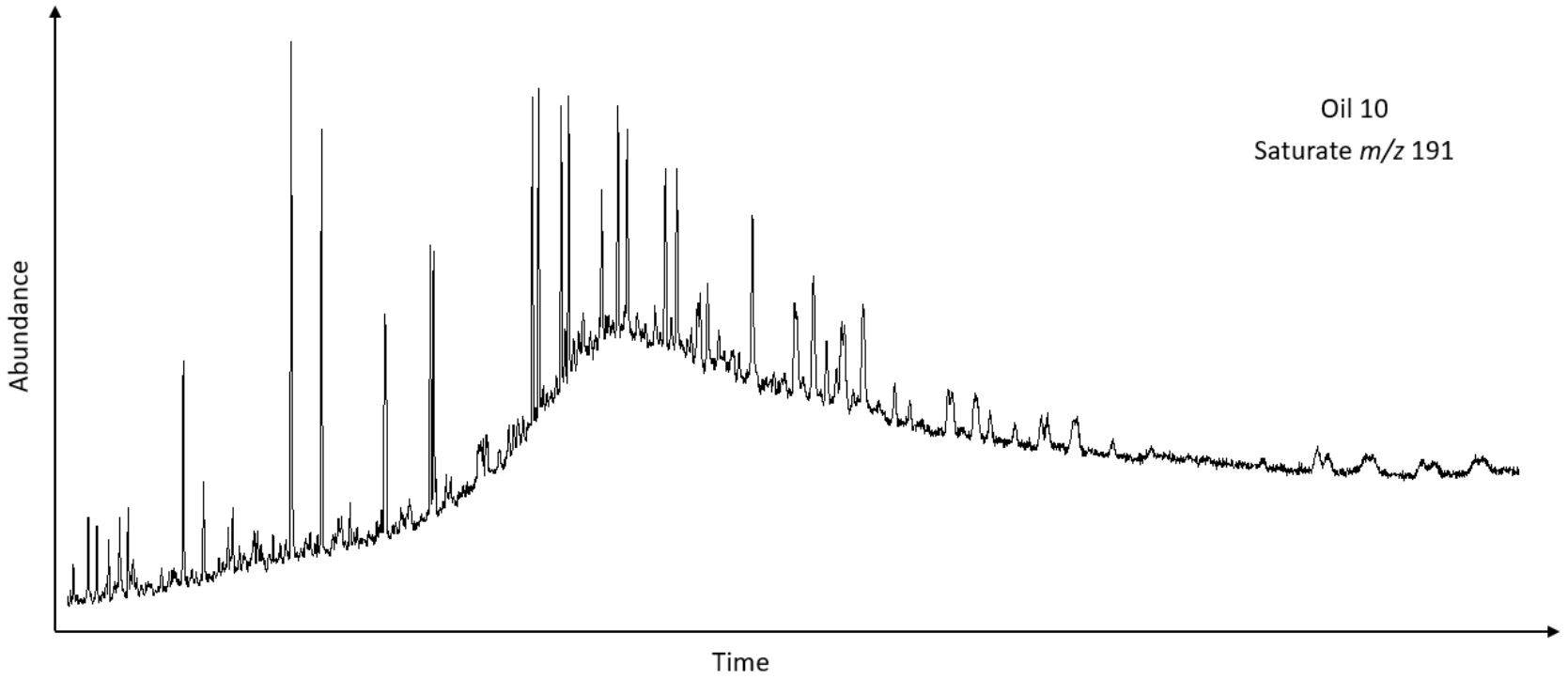
Oil 10
Saturate *m/z* 191
Abundance
Time

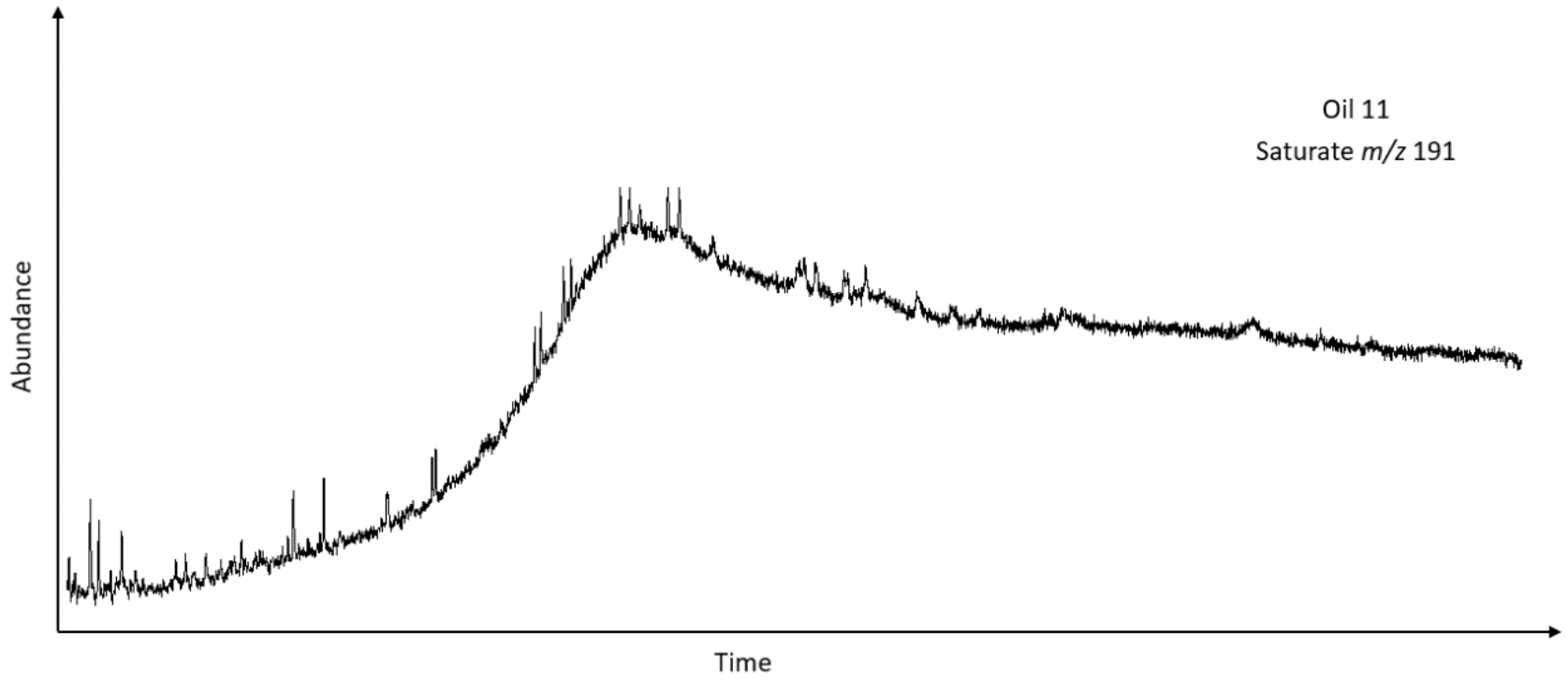
Oil 11
Saturate m/z 191
Abundance
Time

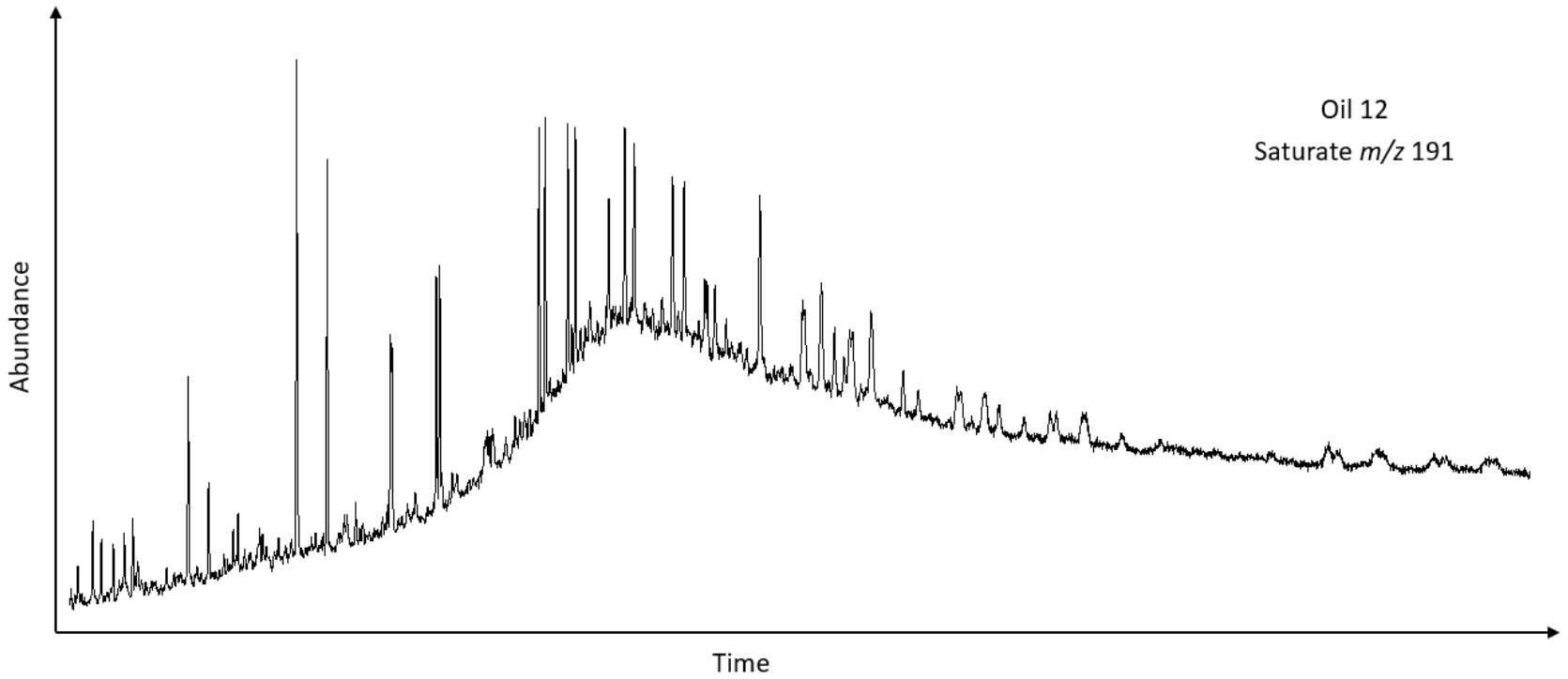
Oil 12
Saturate m/z 191
Abundance
Time

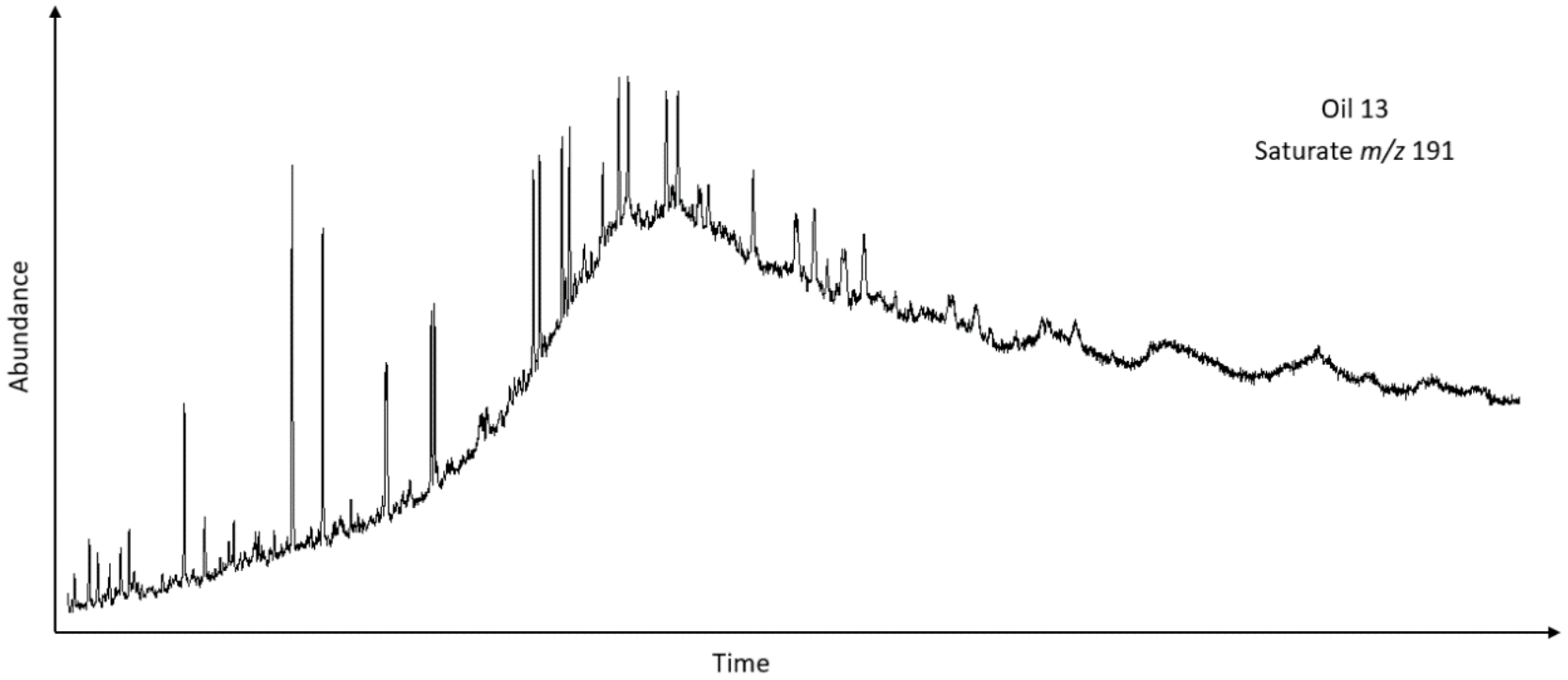
Oil 13
Saturate m/z 191
Abundance
Time

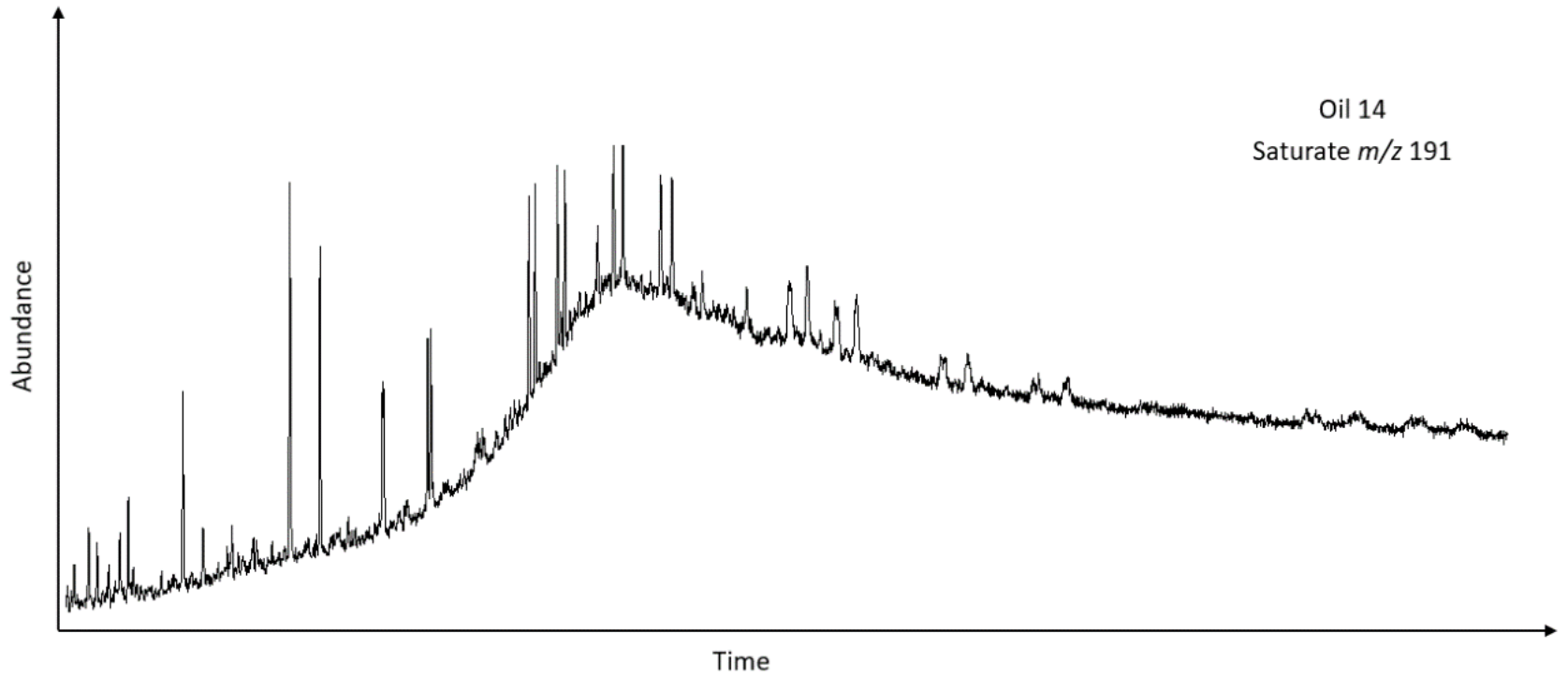
Oil 14
Saturate m/z 191
Abundance
Time

## Appendix B

*M/z* 170 chromatograms of the aromatic fractions for all source rock and oil samples, time ranges were selected to better display the trimethylnaphthalene distributions.

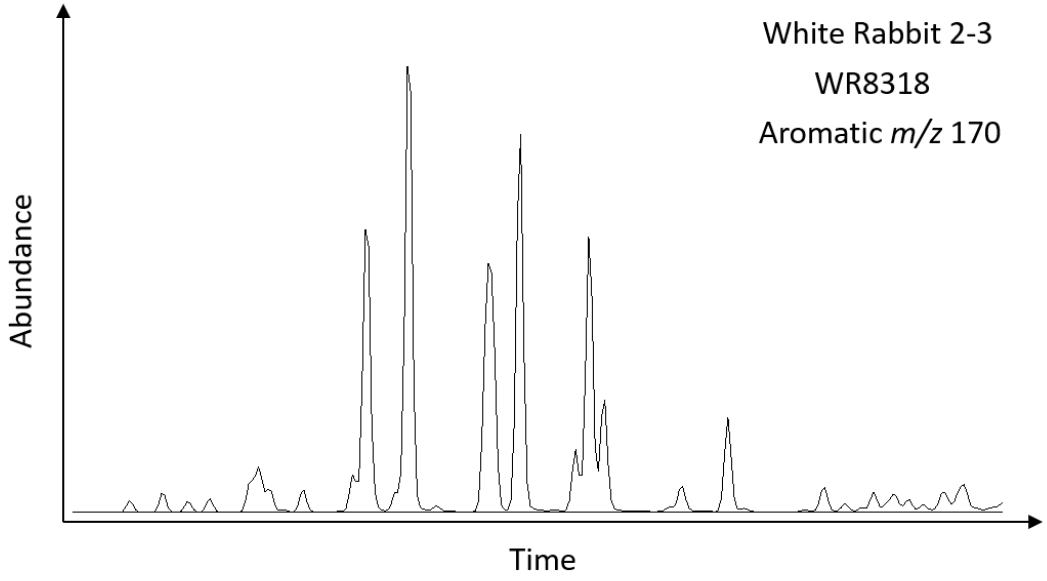

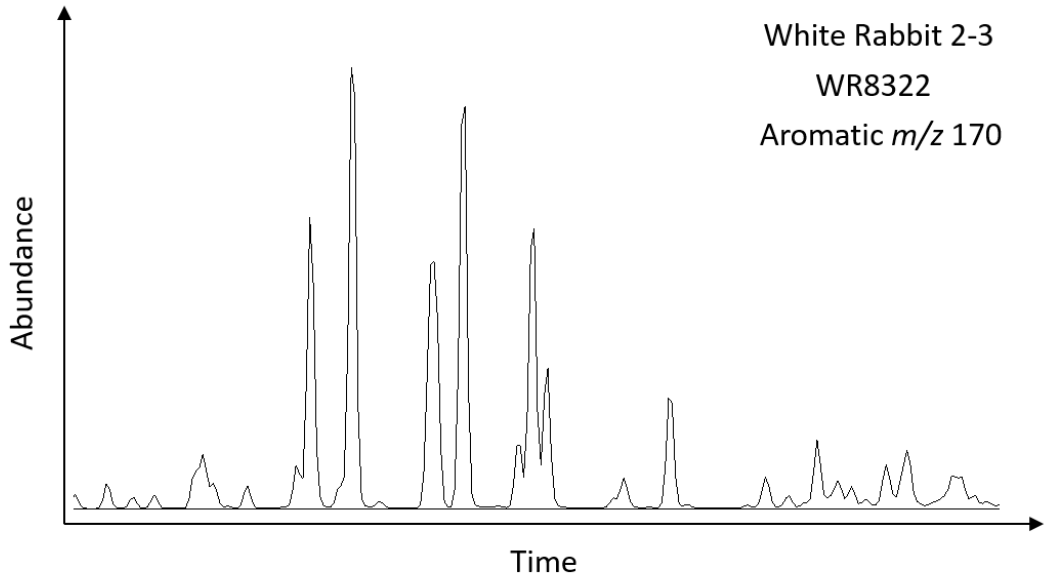
White Rabbit 2-3
WR8322
Aromatic *m/z* 170
Abundance
Time

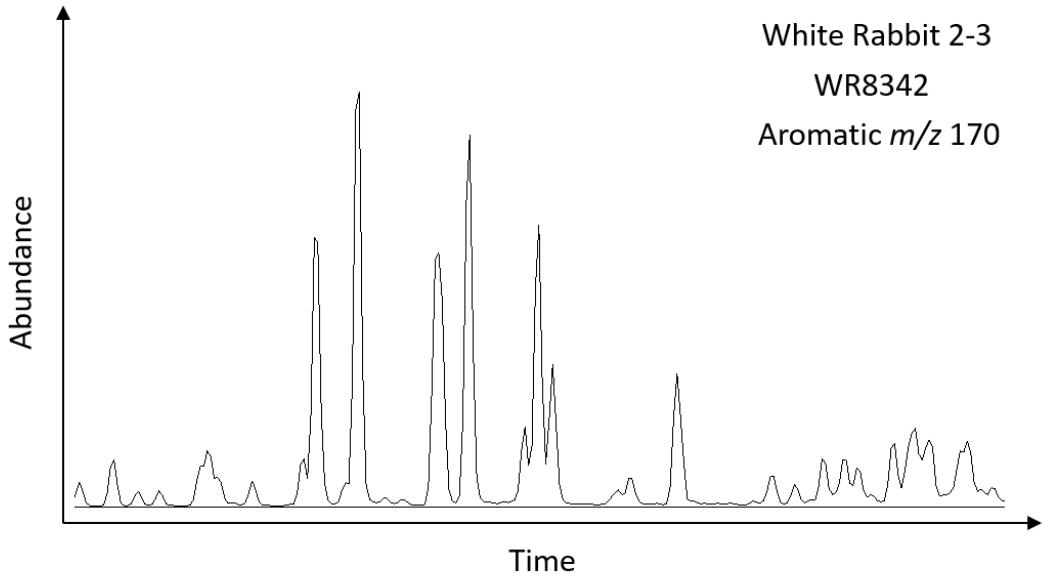
White Rabbit 2-3
WR8342
Aromatic *m/z* 170
Abundance
Time

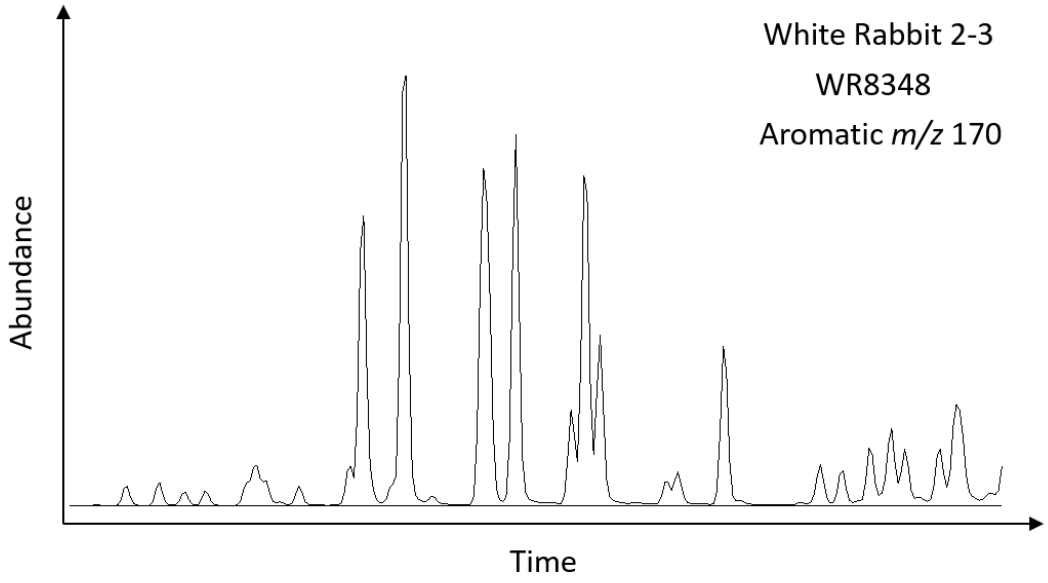
White Rabbit 2-3
WR8348
Aromatic *m/z* 170
Abundance
Time

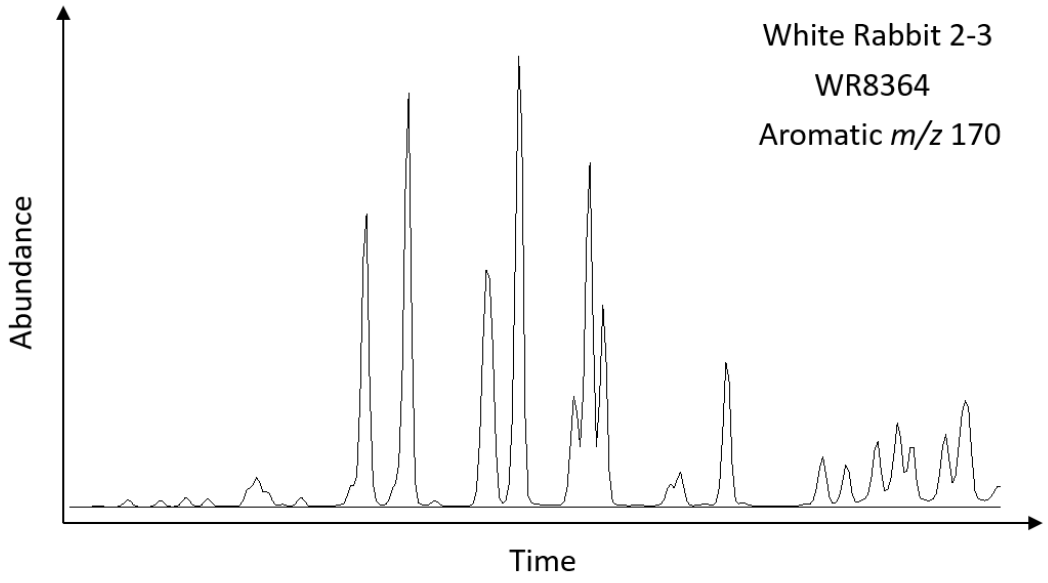
White Rabbit 2-3
WR8364
Aromatic *m/z* 170
Abundance
Time

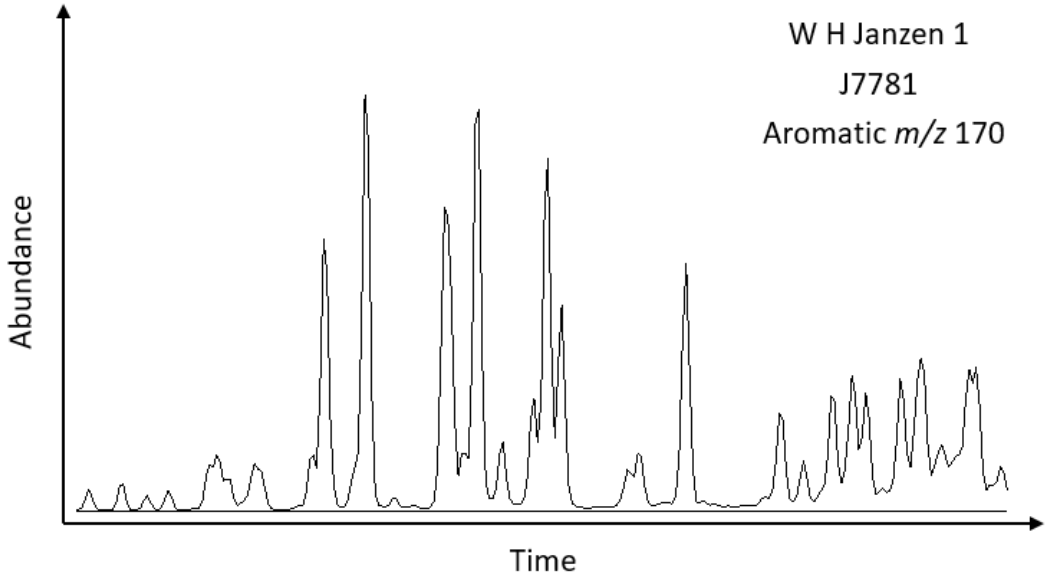
W H Janzen 1
J7781
Aromatic *m/z* 170
Abundance
Time

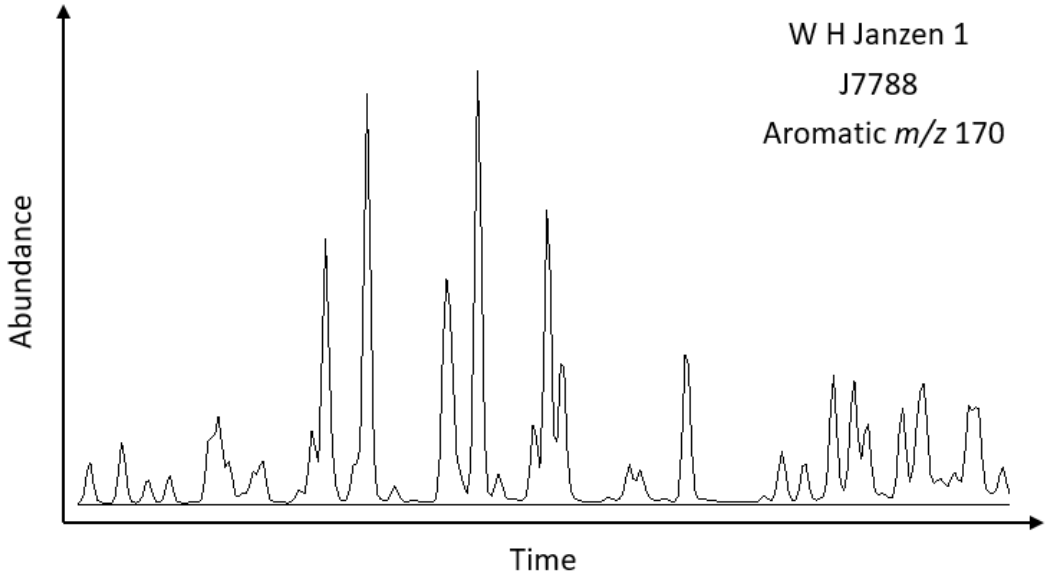
W H Janzen 1
J7788
Aromatic *m/z* 170
Abundance
Time

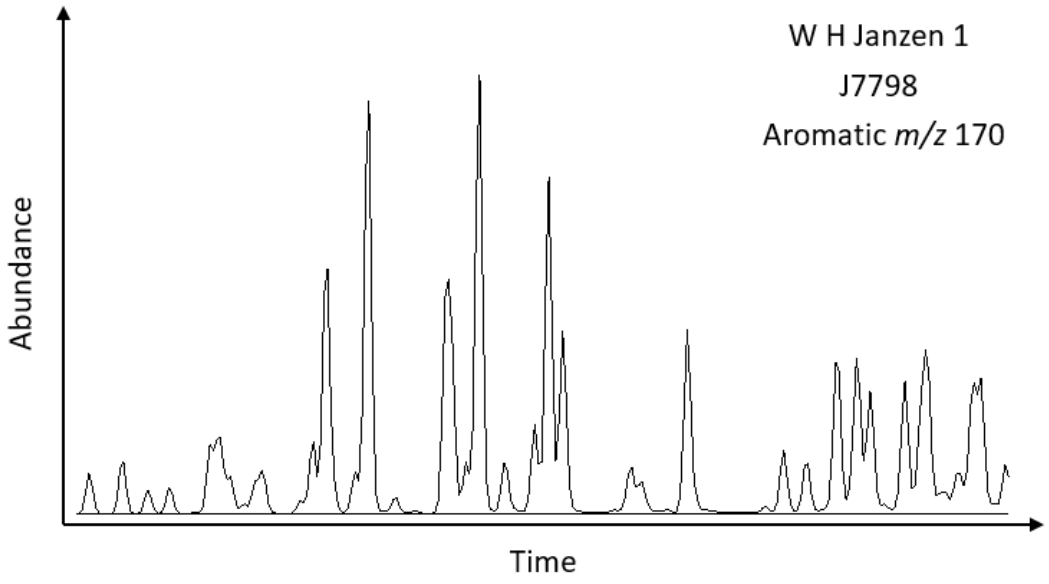
W H Janzen 1
J7798
Aromatic m/z 170
Abundance
Time

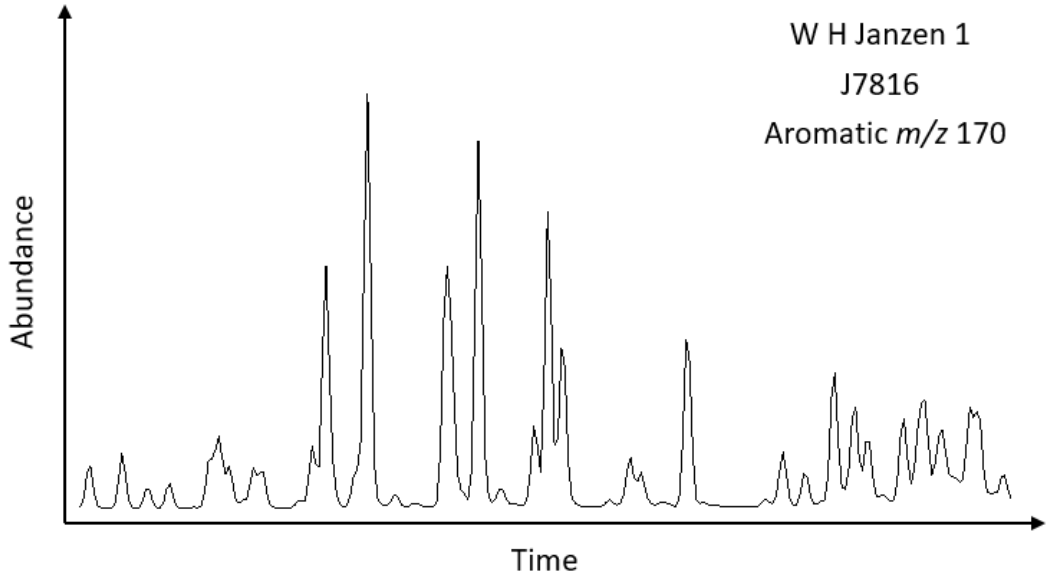
W H Janzen 1
J7816
Aromatic m/z 170
Abundance
Time

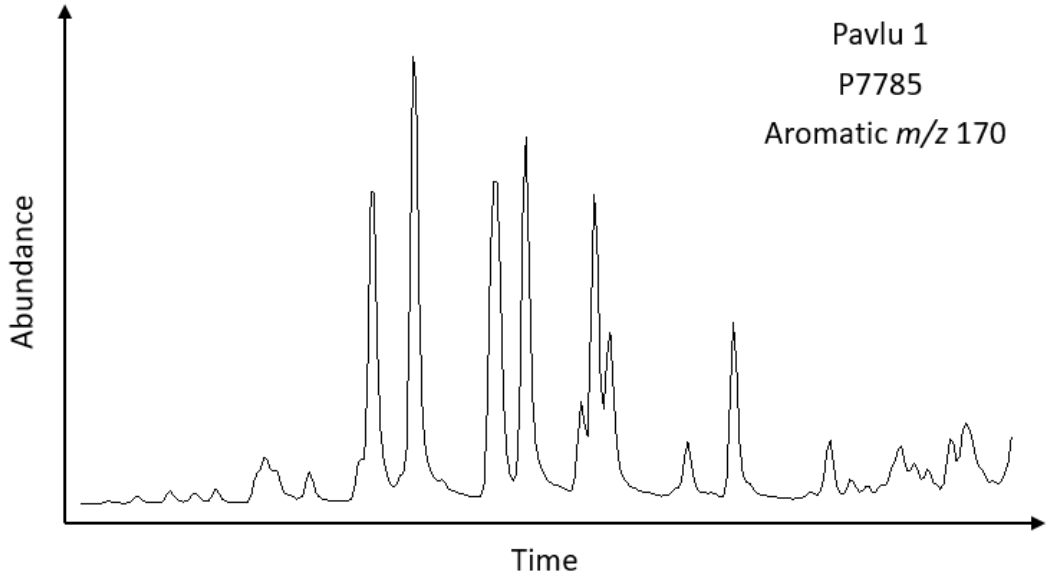
Pavlu 1
P7785
Aromatic *m/z* 170
Abundance
Time

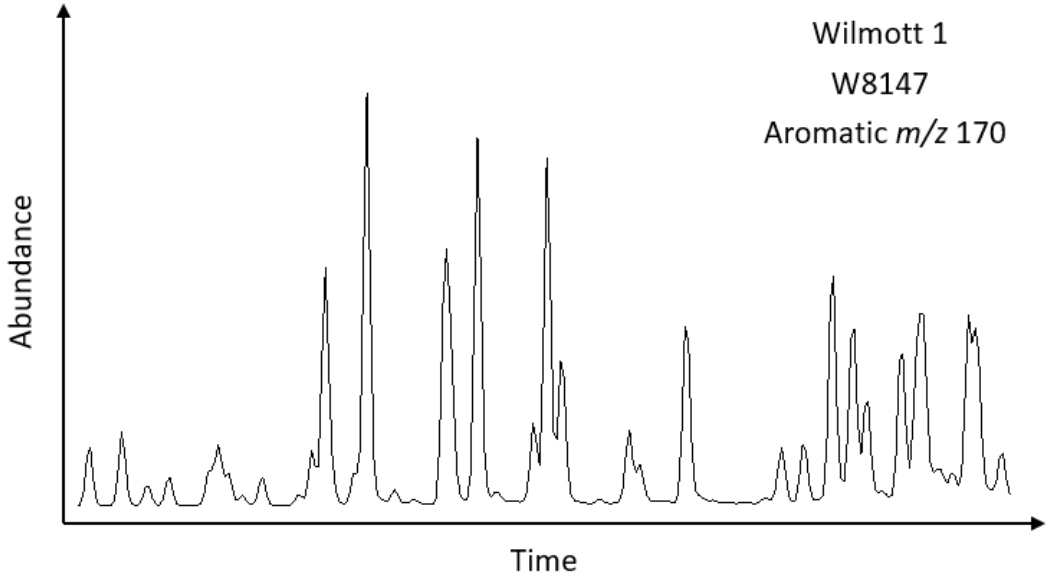
Wilmott 1
W8147
Aromatic *m/z* 170
Abundance
Time

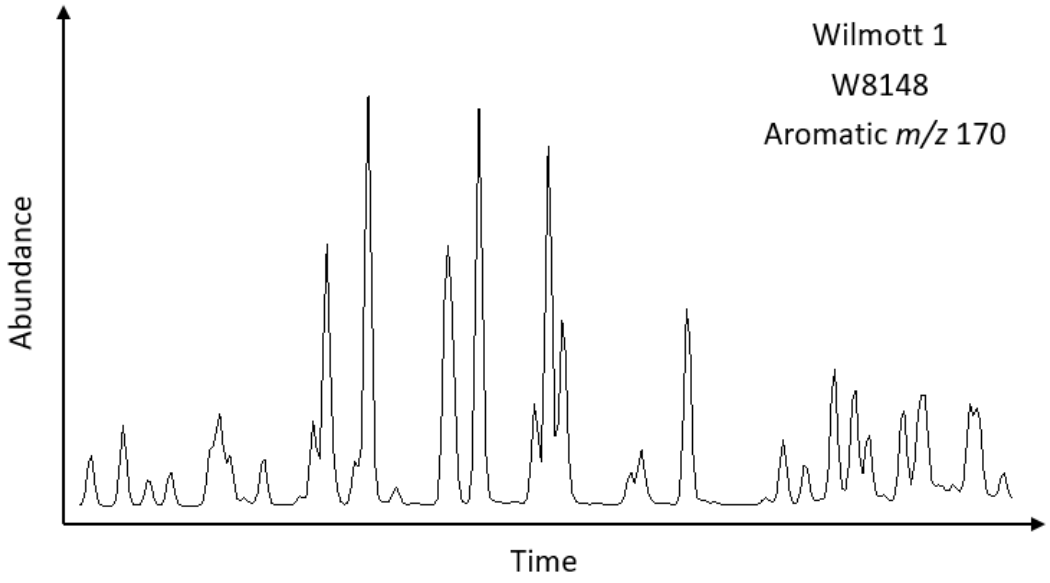
Wilmott 1
W8148
Aromatic m/z 170
Abundance
Time

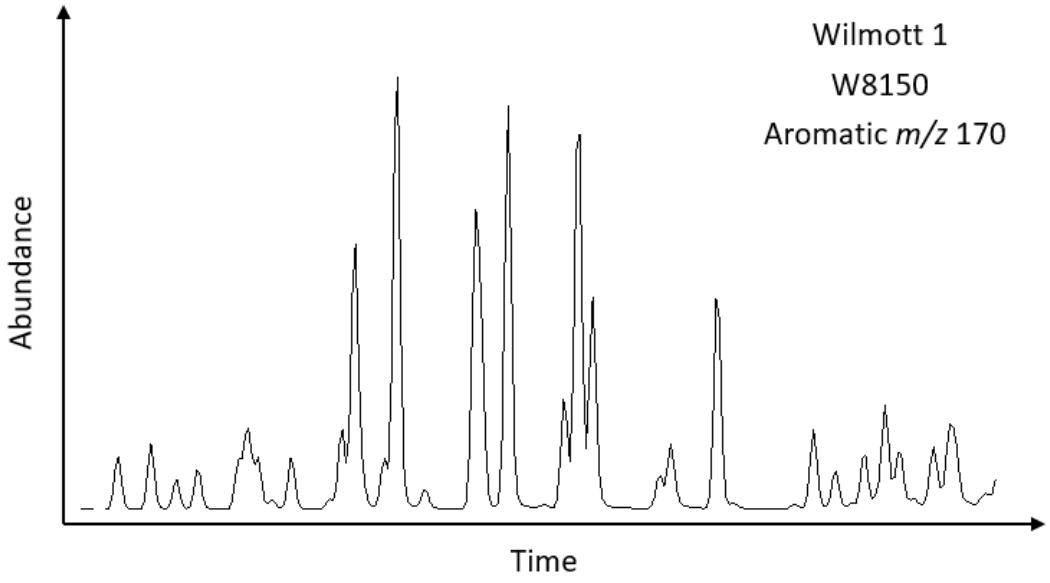
Wilmott 1
W8150
Aromatic m/z 170
Abundance
Time

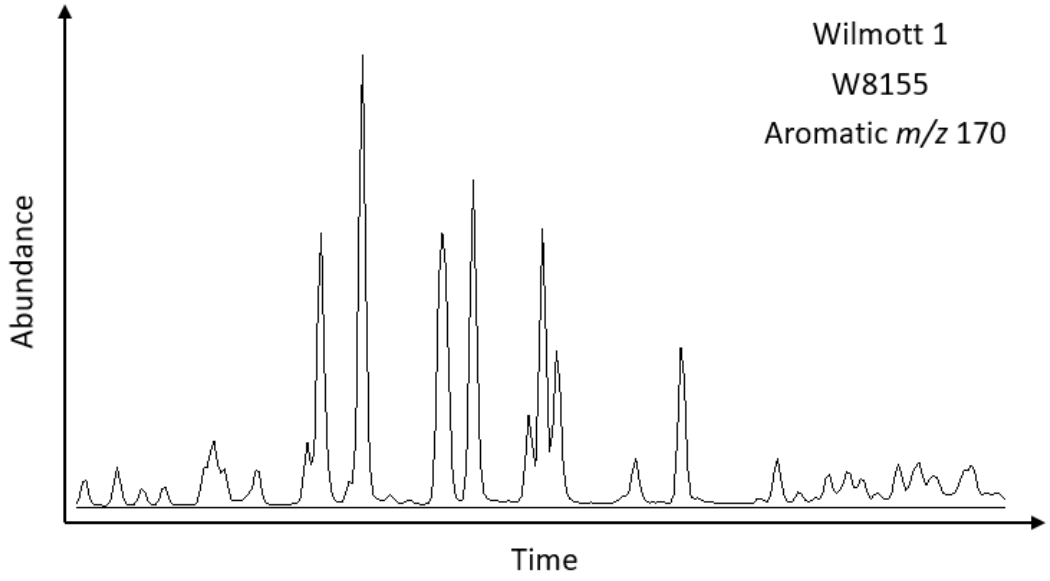
Wilmott 1
W8155
Aromatic m/z 170
Abundance
Time

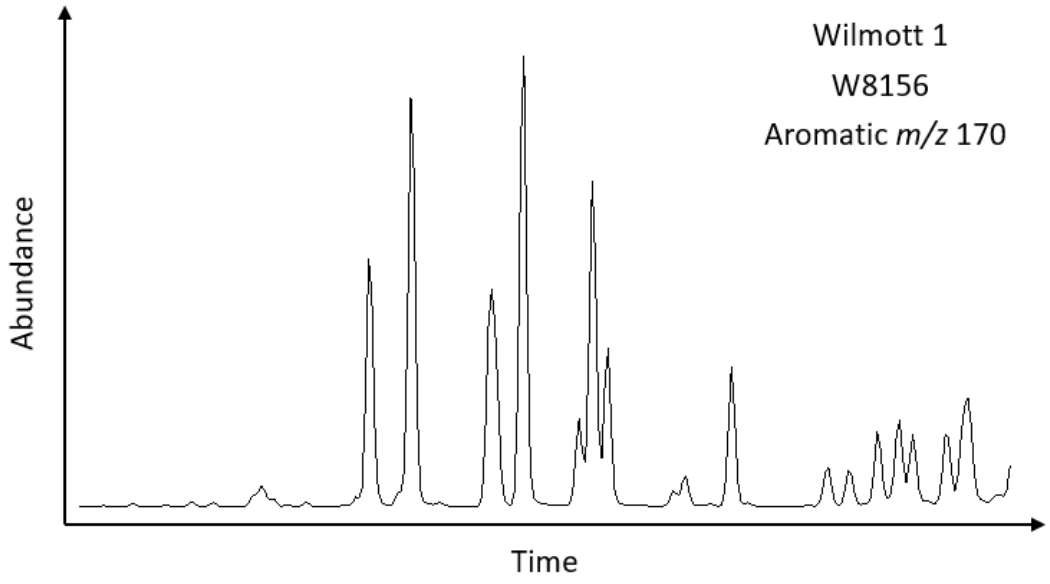
Wilmott 1
W8156
Aromatic m/z 170
Abundance
Time

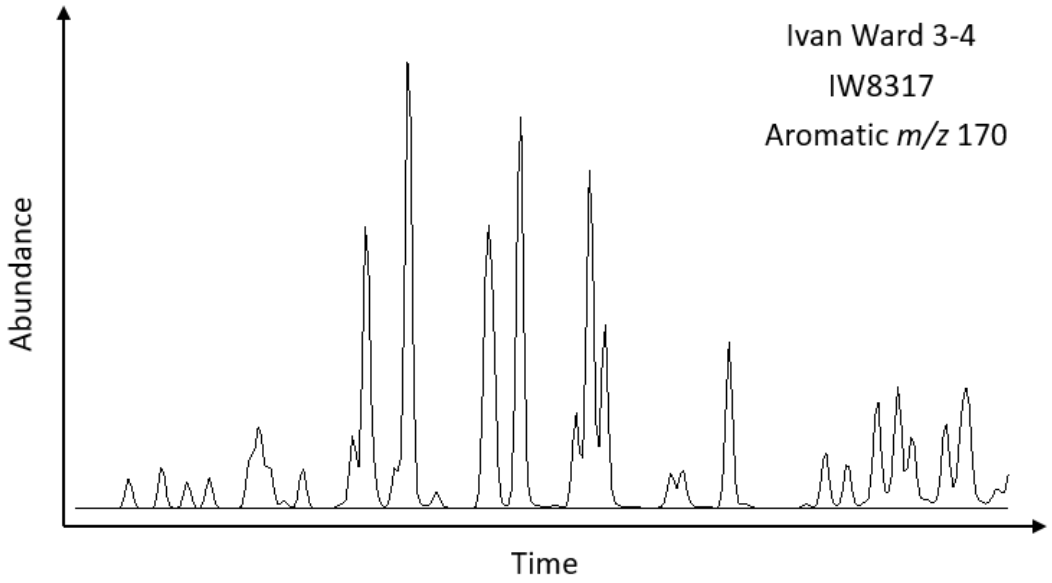
Ivan Ward 3-4
IW8317
Aromatic *m/z* 170
Abundance
Time

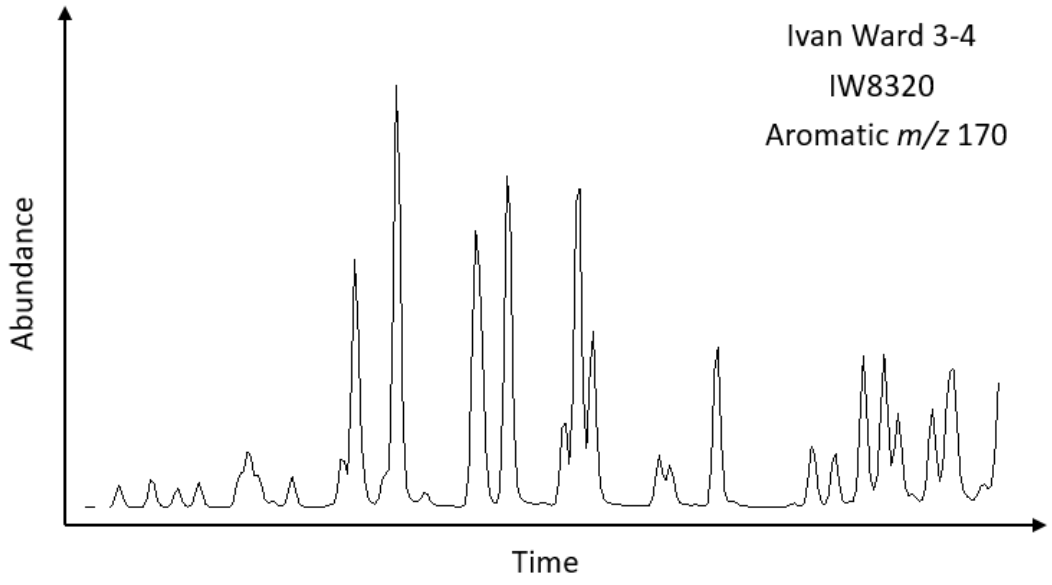
Ivan Ward 3-4
IW8320
Aromatic *m/z* 170
Abundance
Time

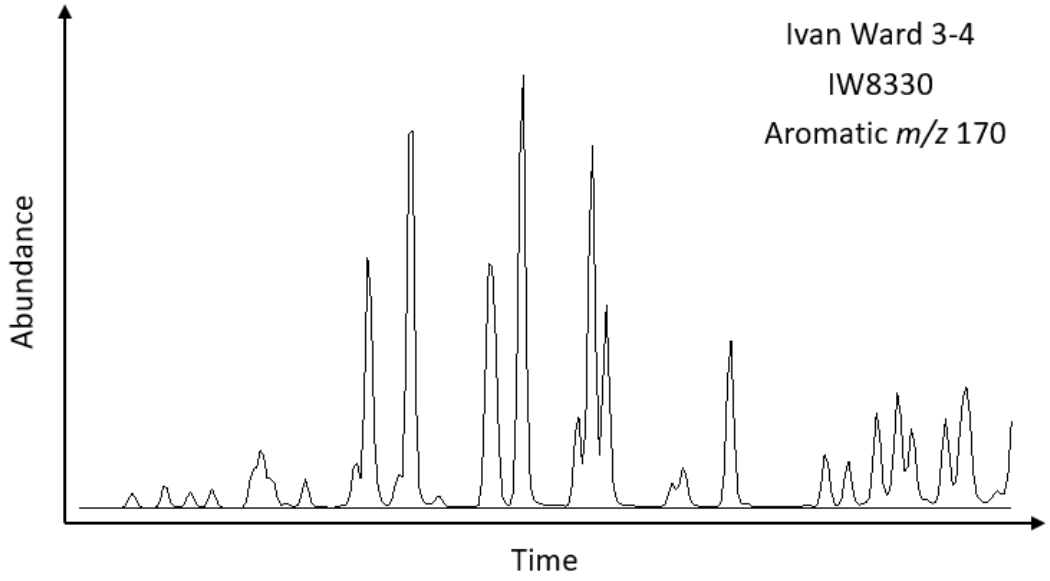
Ivan Ward 3-4
IW8330
Aromatic *m/z* 170
Abundance
Time

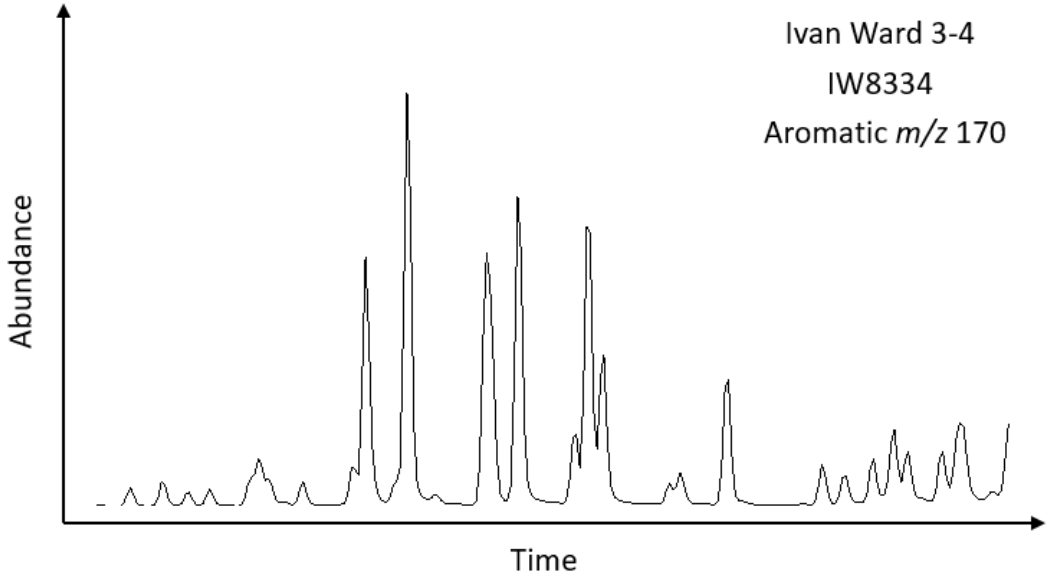
Ivan Ward 3-4
IW8334
Aromatic *m/z* 170
Abundance
Time

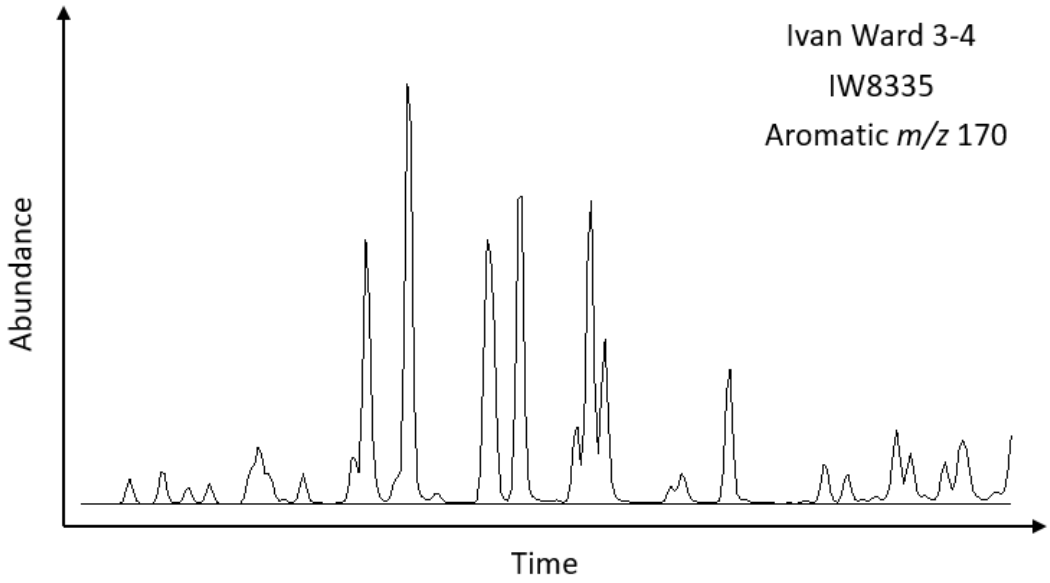
Ivan Ward 3-4
IW8335
Aromatic *m/z* 170
Abundance
Time

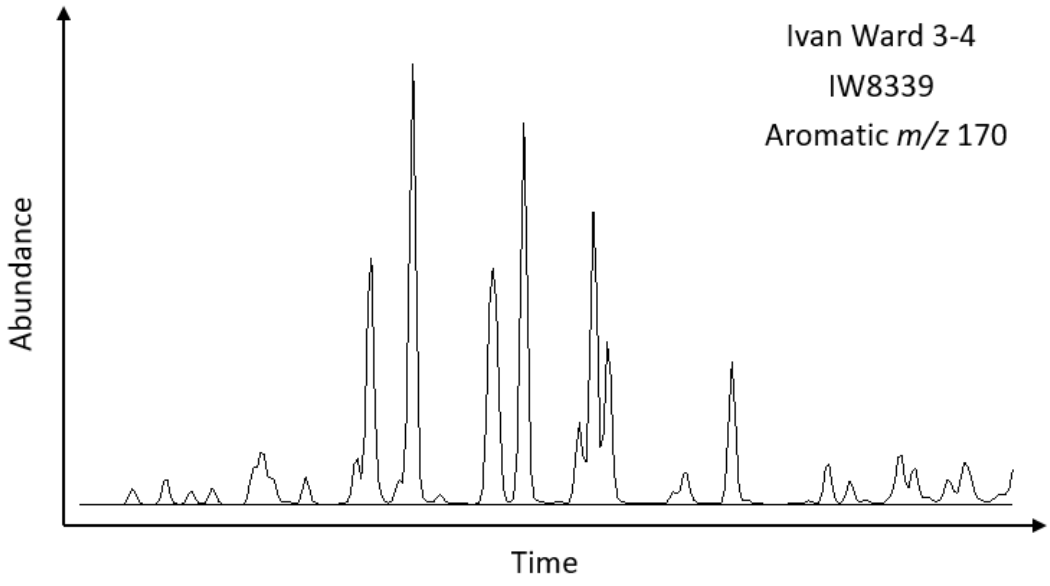
Ivan Ward 3-4
IW8339
Aromatic *m/z* 170
Abundance
Time

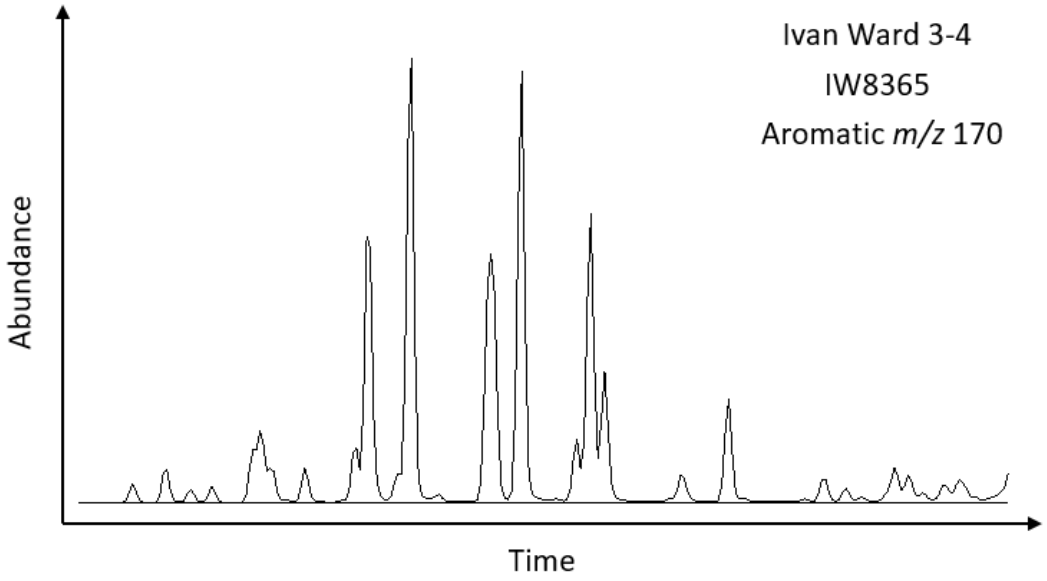
Ivan Ward 3-4
IW8365
Aromatic *m/z* 170
Abundance
Time

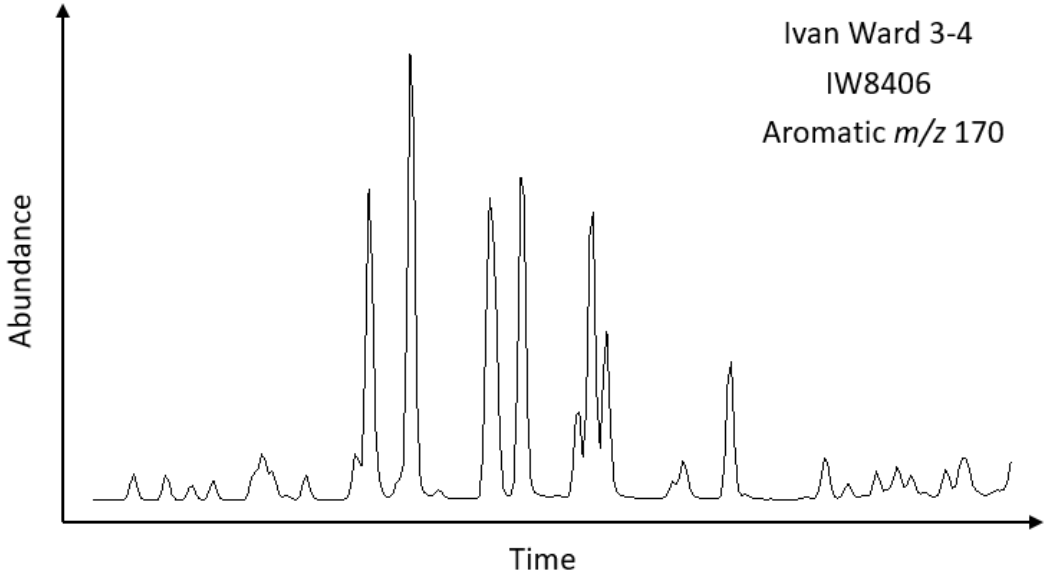
Ivan Ward 3-4
IW8406
Aromatic *m/z* 170
Abundance
Time

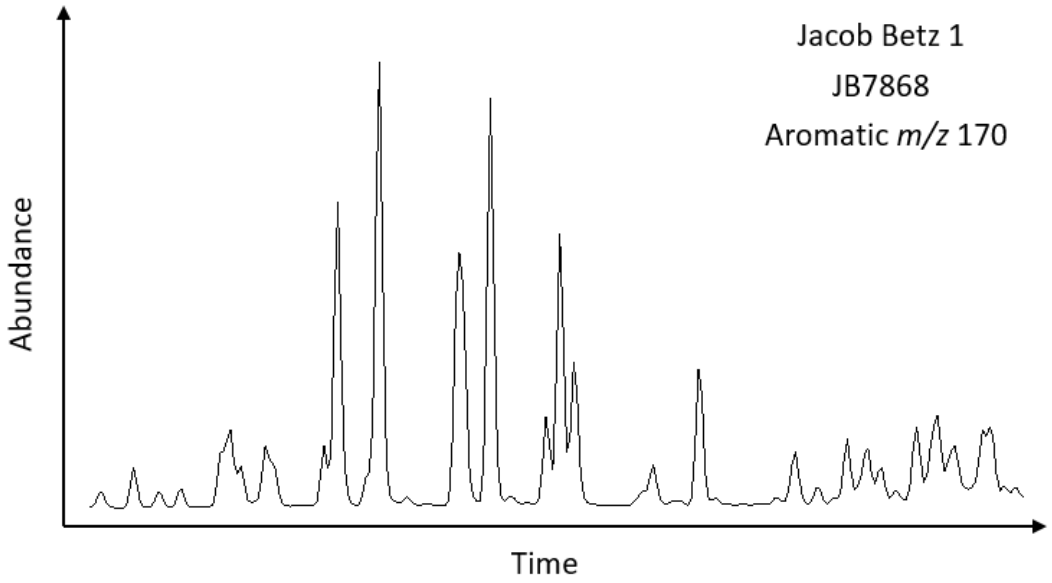
Jacob Betz 1
JB7868
Aromatic *m/z* 170
Abundance
Time

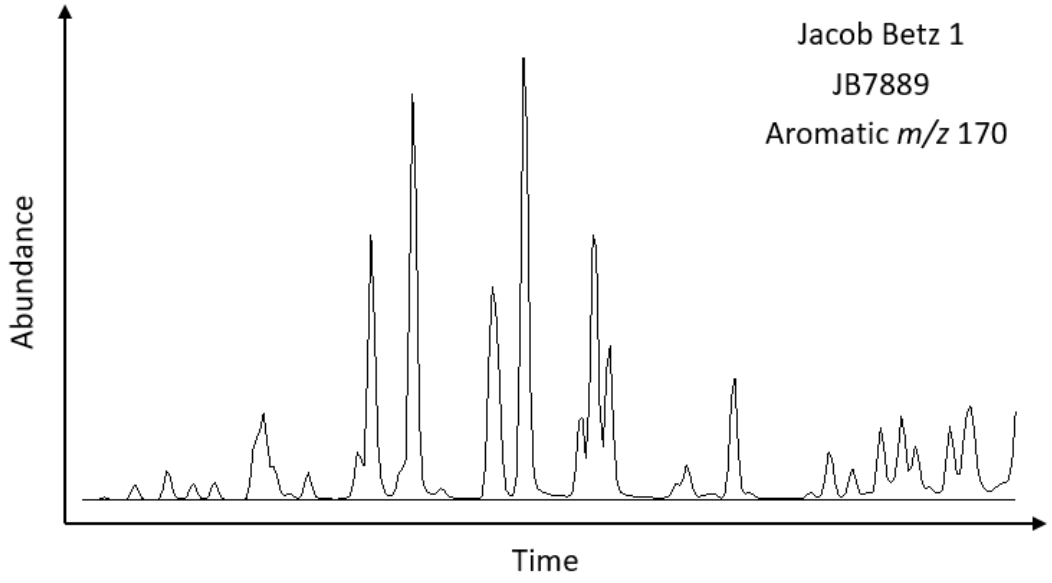
Jacob Betz 1
JB7889
Aromatic *m/z* 170
Abundance
Time

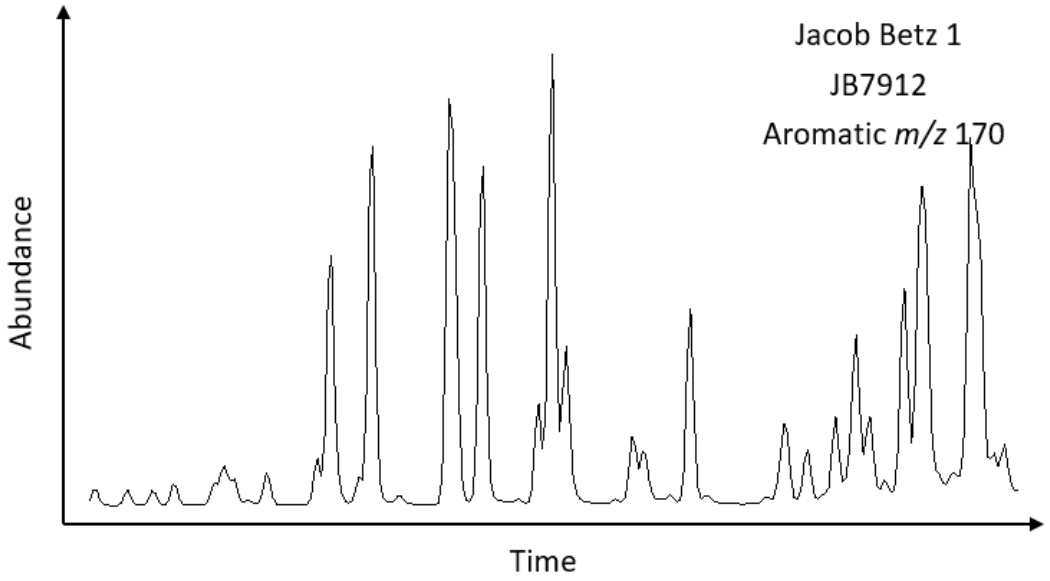
Jacob Betz 1
JB7912
Aromatic m/z 170
Abundance
Time

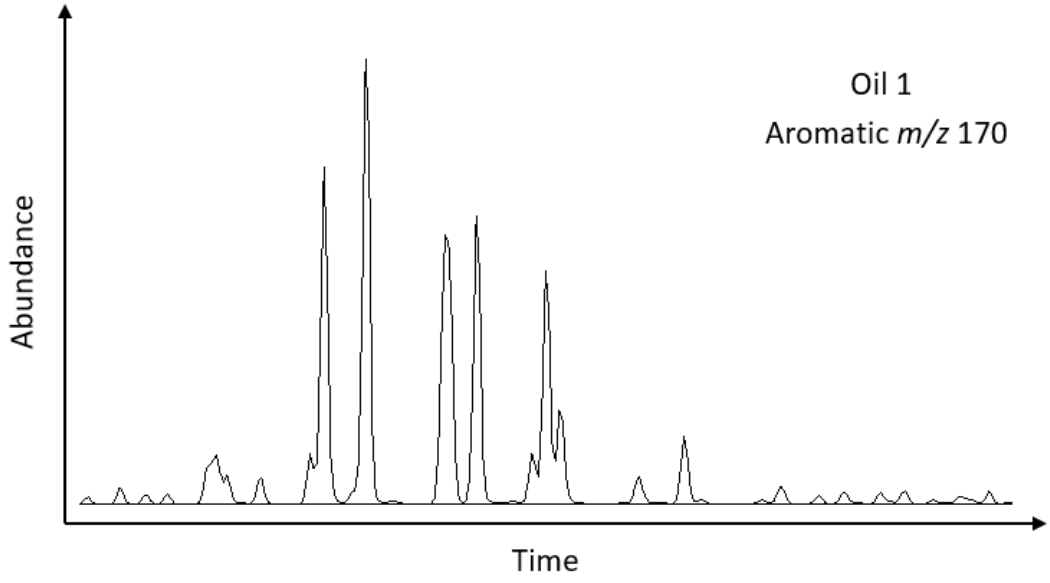
Oil 1
Aromatic m/z 170
Abundance
Time

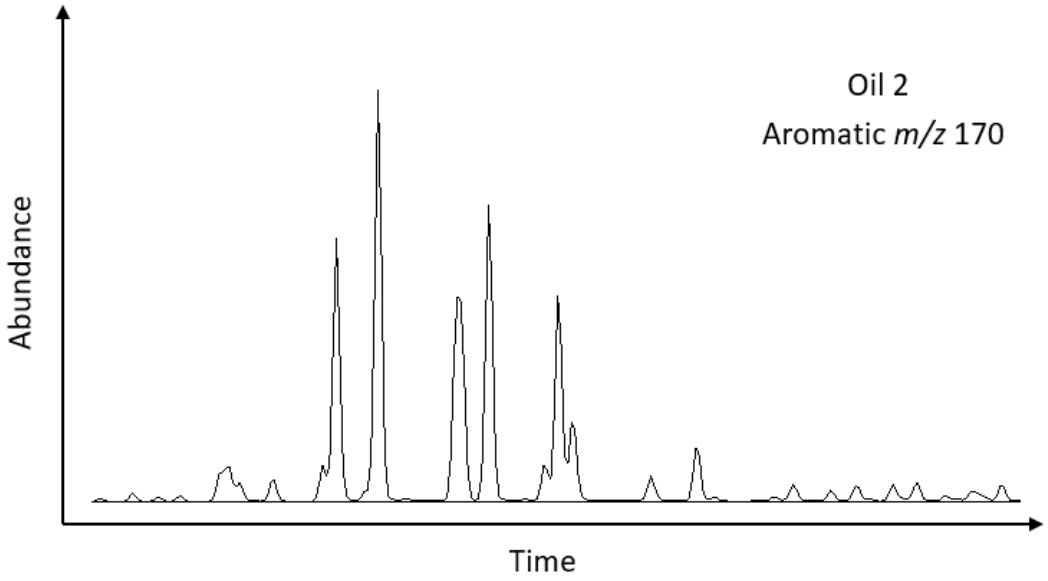
Oil 2
Aromatic m/z 170
Abundance
Time

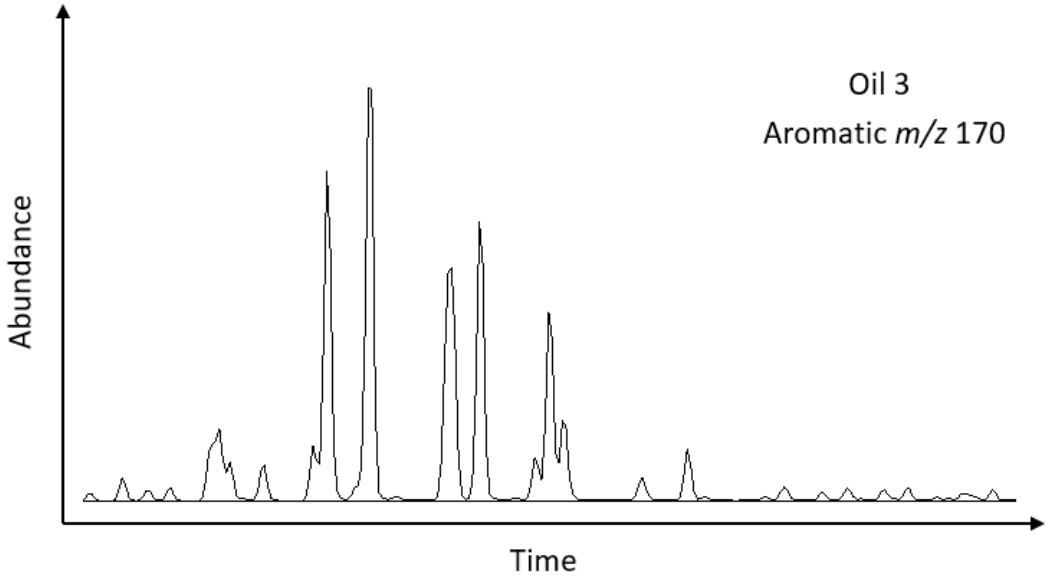
Oil 3
Aromatic m/z 170
Abundance
Time

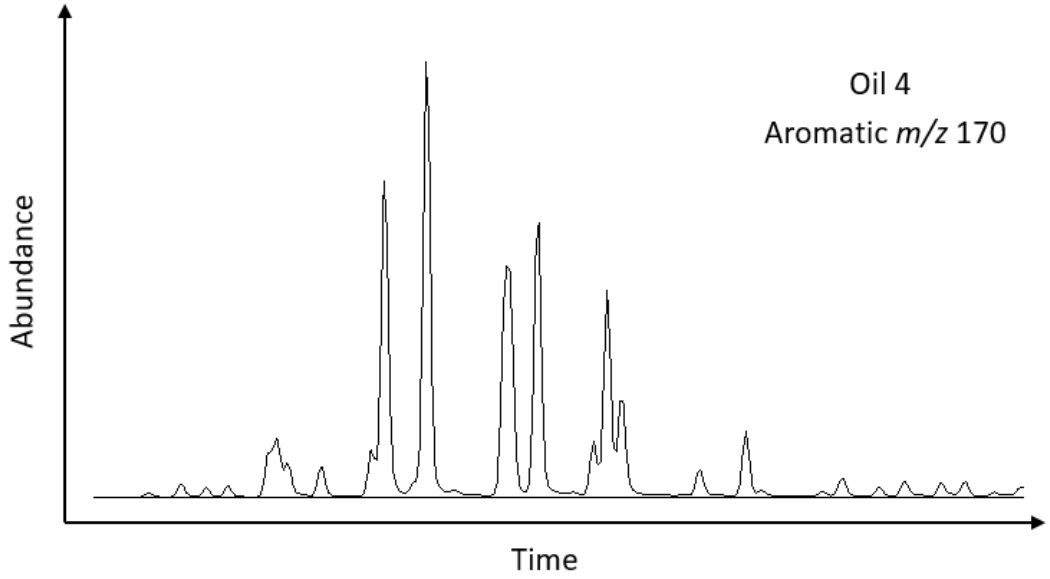
Oil 4
Aromatic m/z 170
Abundance
Time

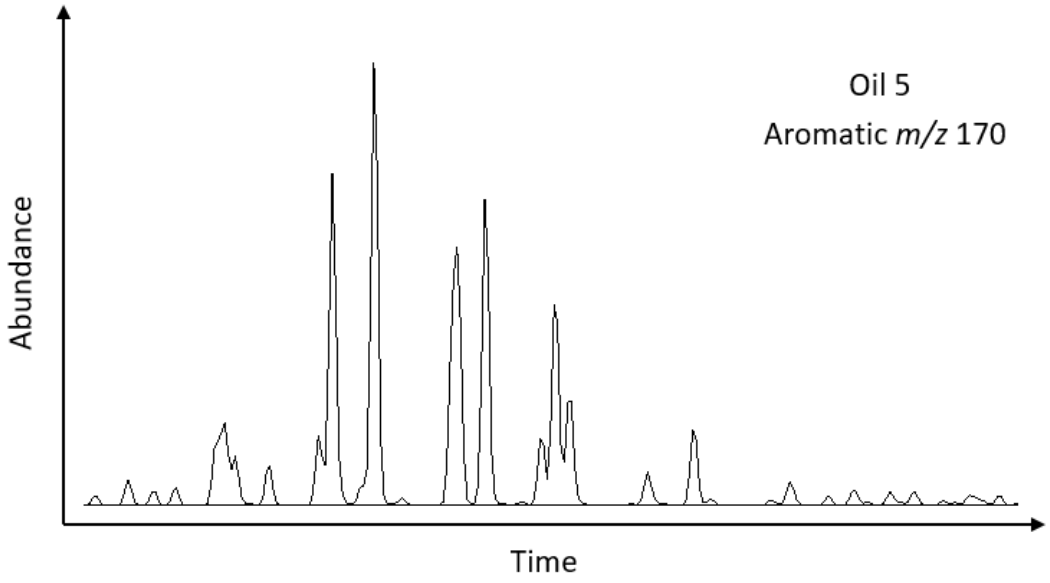
Oil 5
Aromatic m/z 170
Abundance
Time

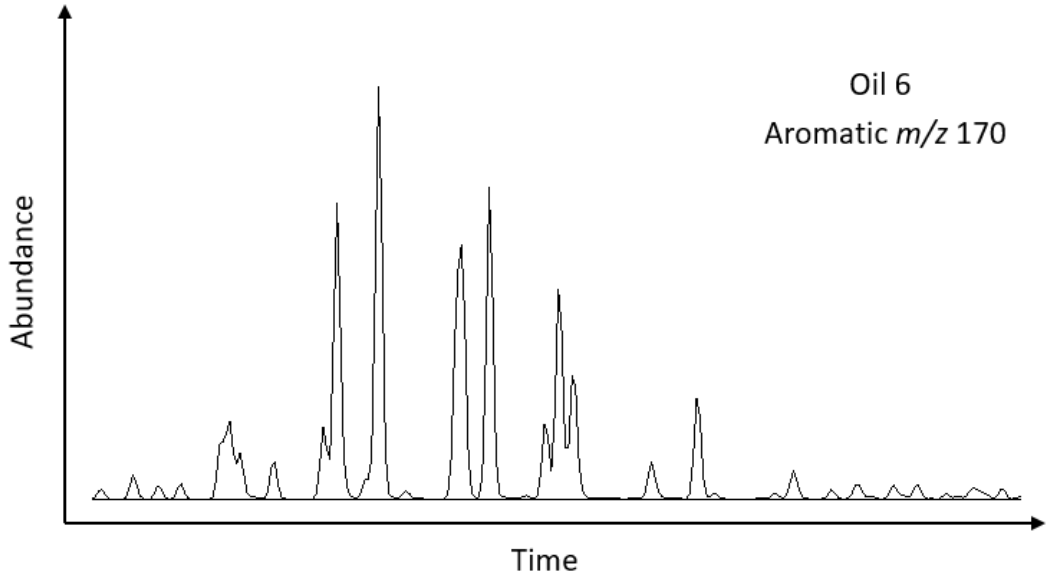
Oil 6
Aromatic m/z 170
Abundance
Time

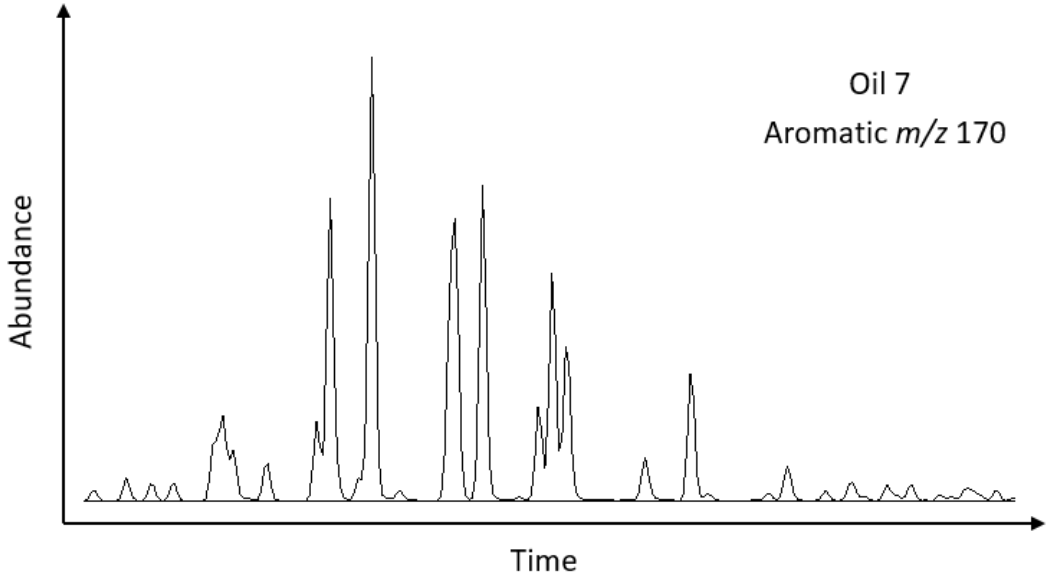
Oil 7
Aromatic m/z 170
Abundance
Time

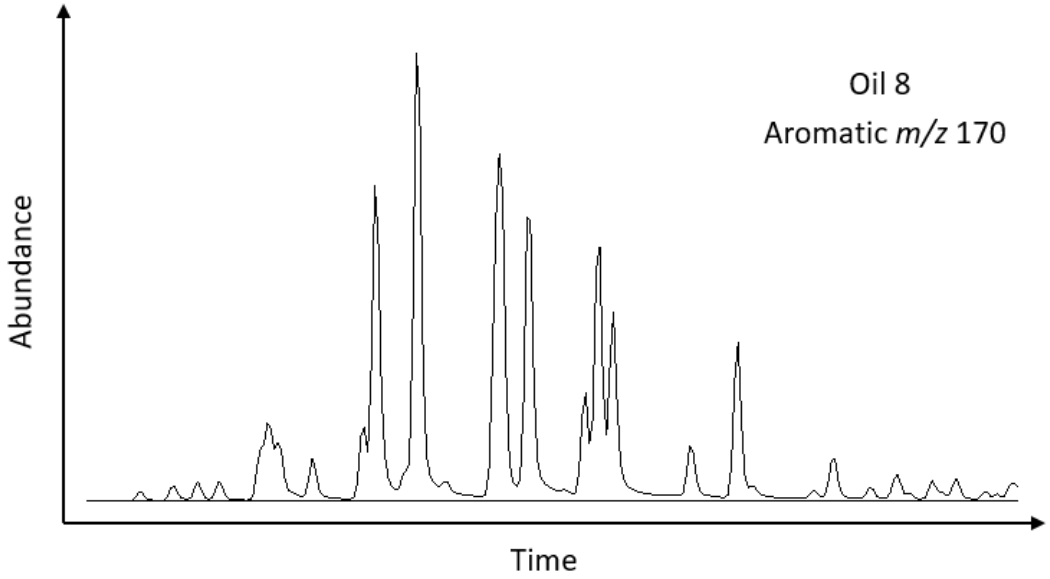
Oil 8
Aromatic m/z 170
Abundance
Time

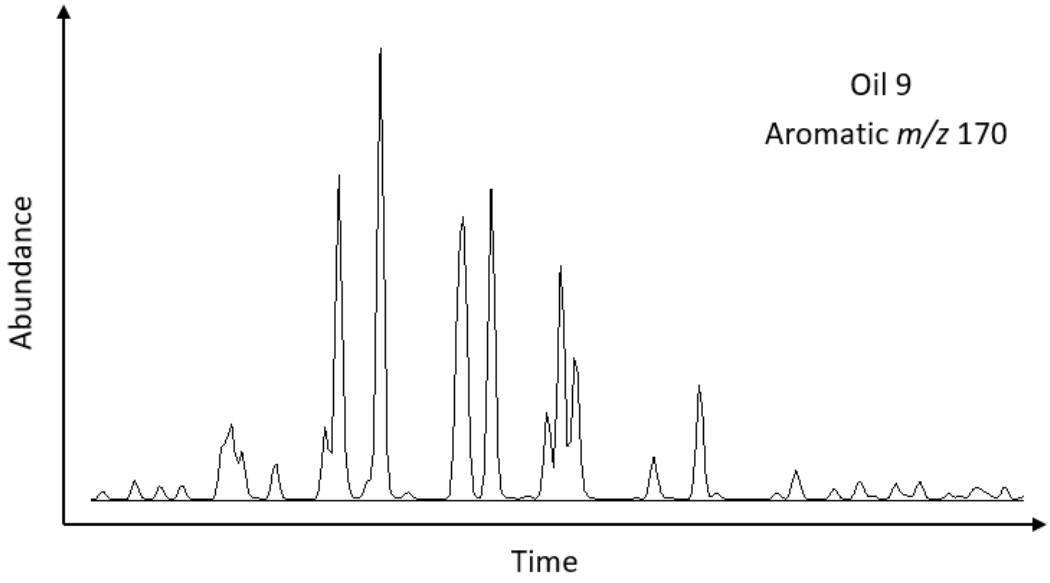
Oil 9
Aromatic m/z 170
Abundance
Time

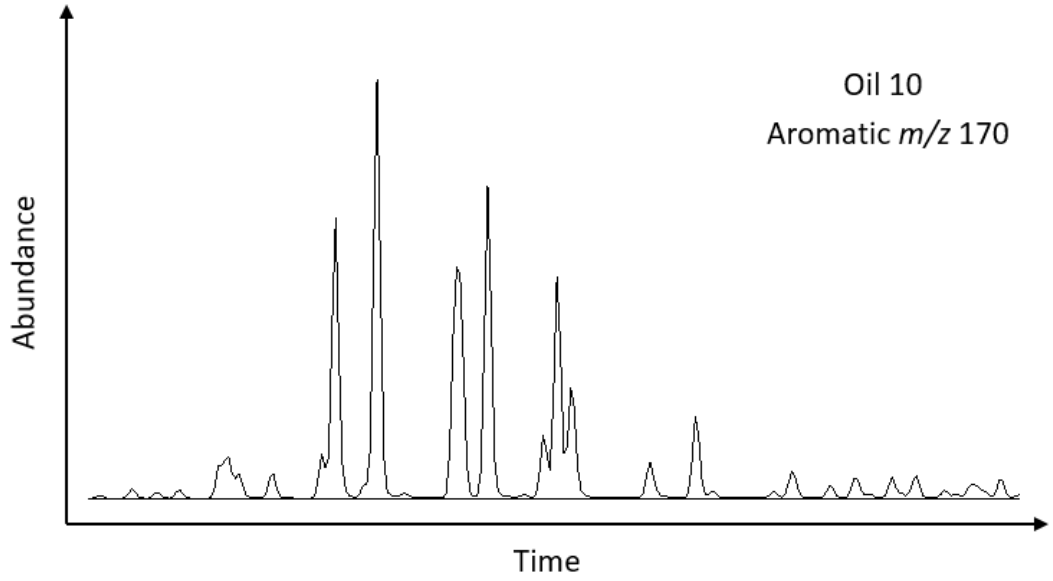
Oil 10
Aromatic m/z 170
Abundance
Time

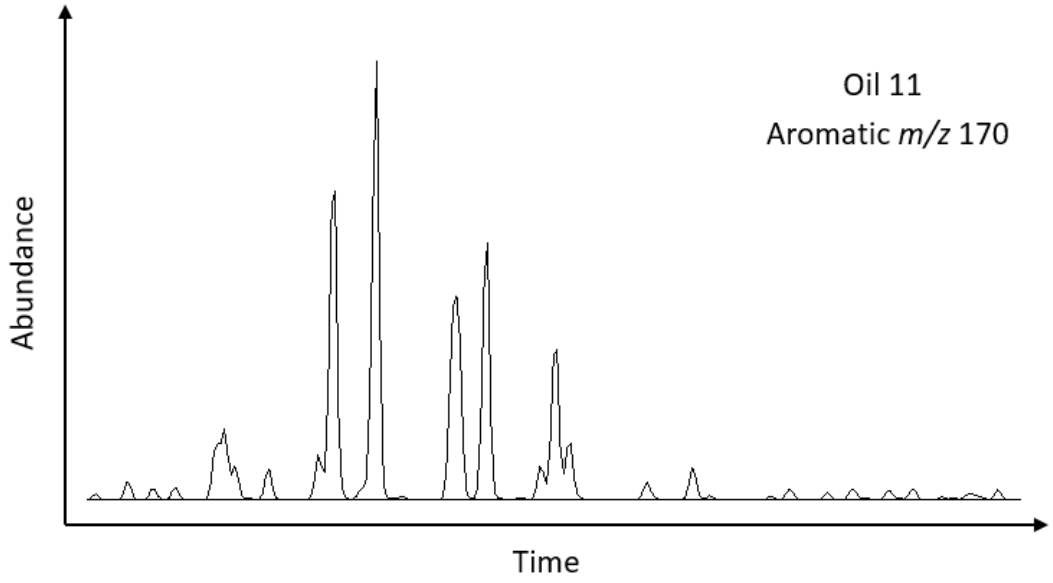
Oil 11
Aromatic m/z 170
Abundance
Time

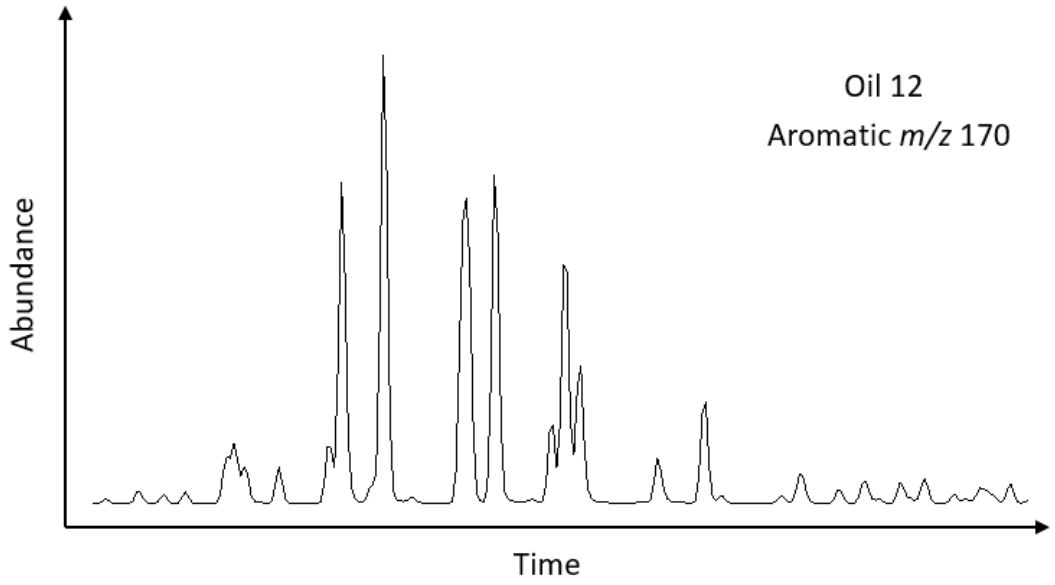
Oil 12
Aromatic m/z 170
Abundance
Time

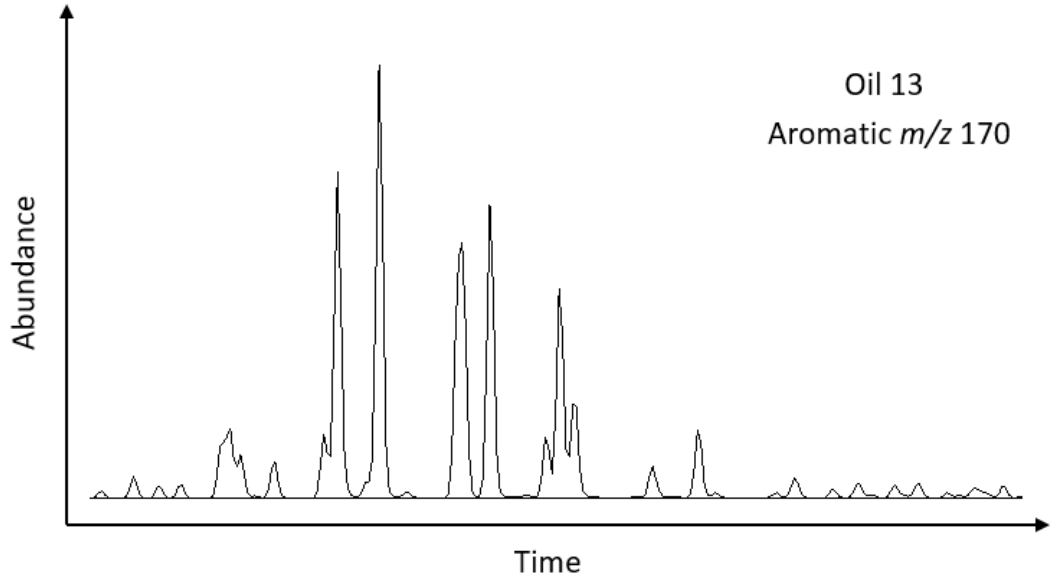
Oil 13
Aromatic m/z 170
Abundance
Time

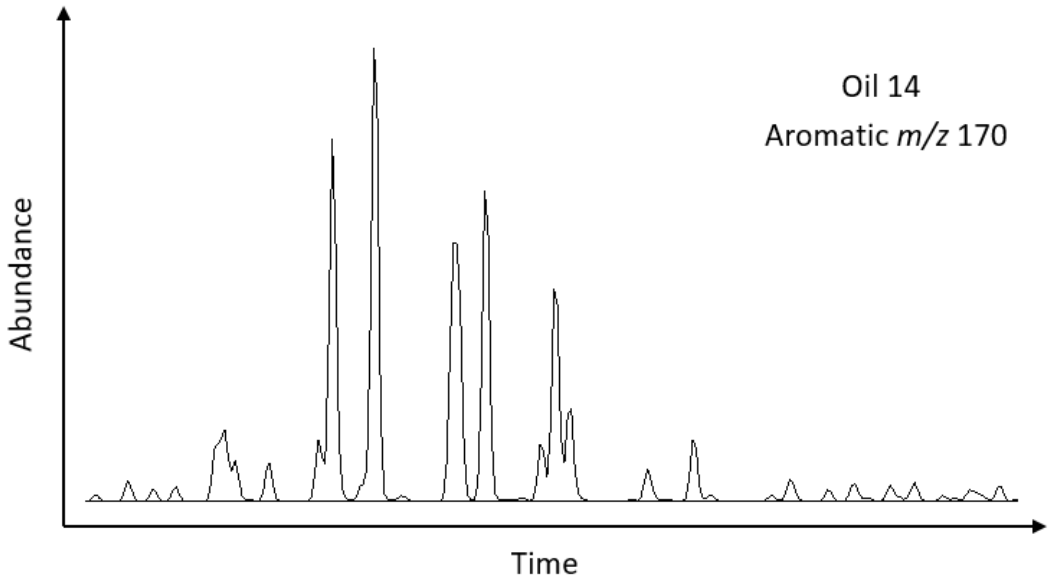
Oil 14
Aromatic *m/z* 170
Abundance
Time

## Appendix C

FID chromatograms of the saturate fractions for all source rock and oil samples.

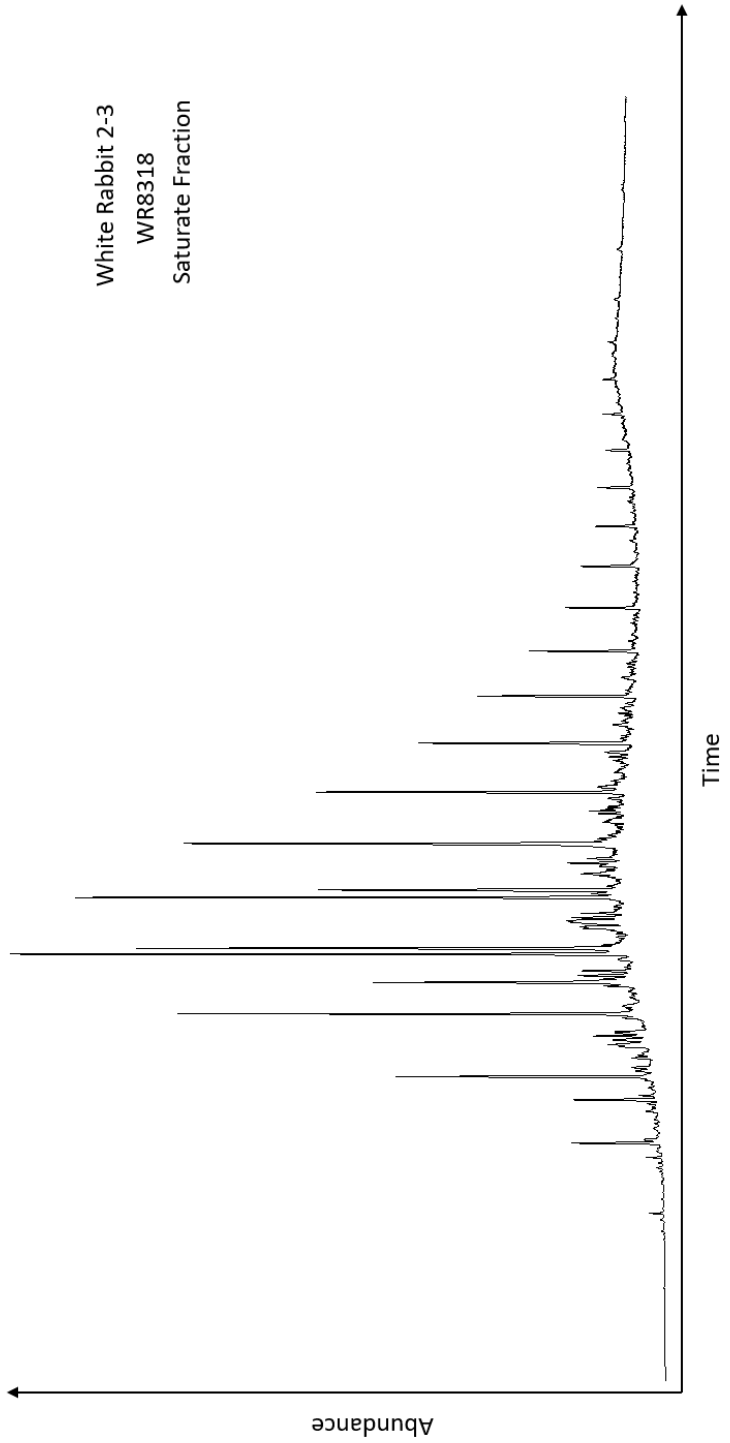

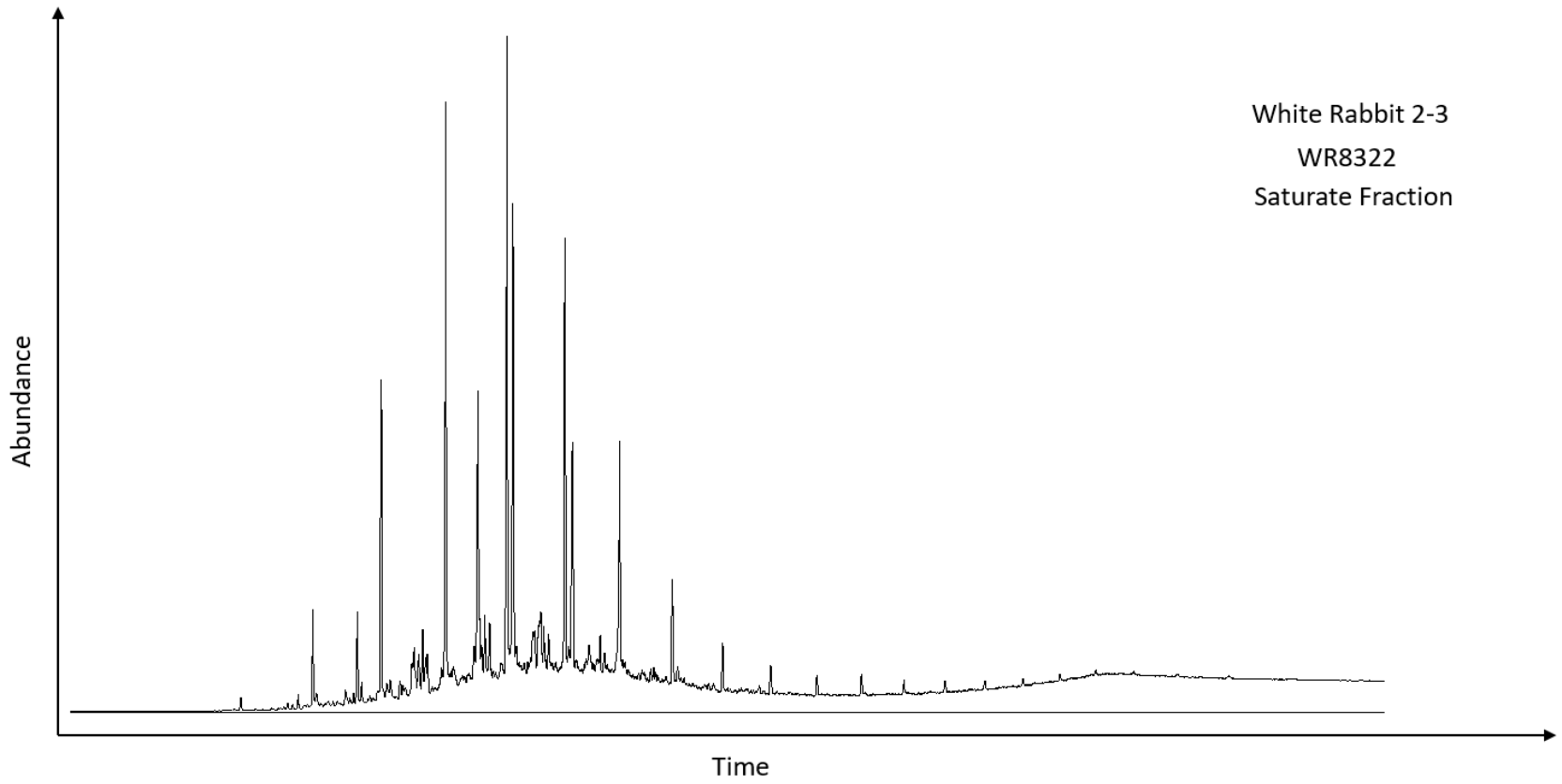
White Rabbit 2-3
WR8322
Saturate Fraction
Abundance
Time

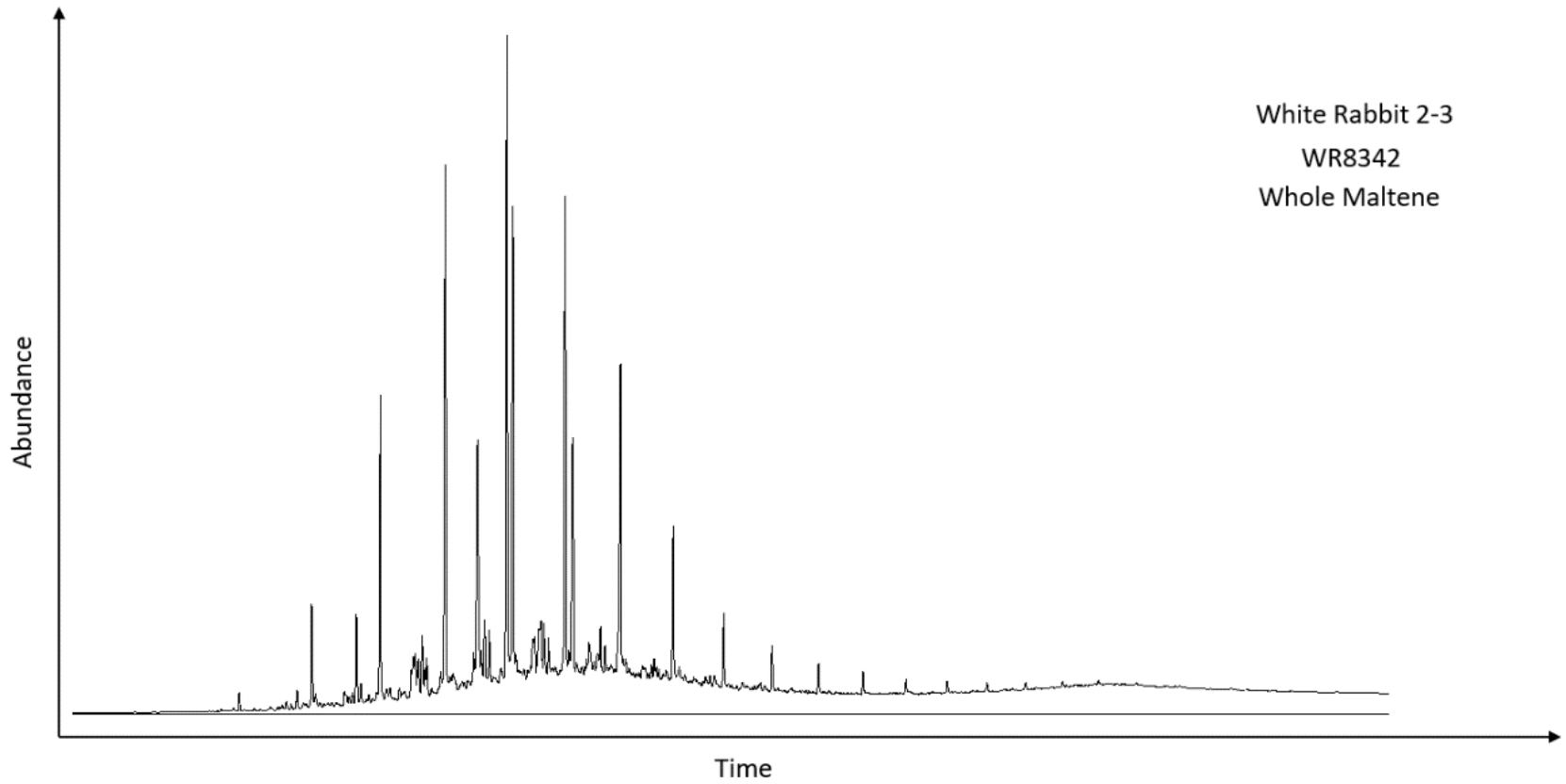
White Rabbit 2-3
WR8342
Whole Maltene
Abundance
Time

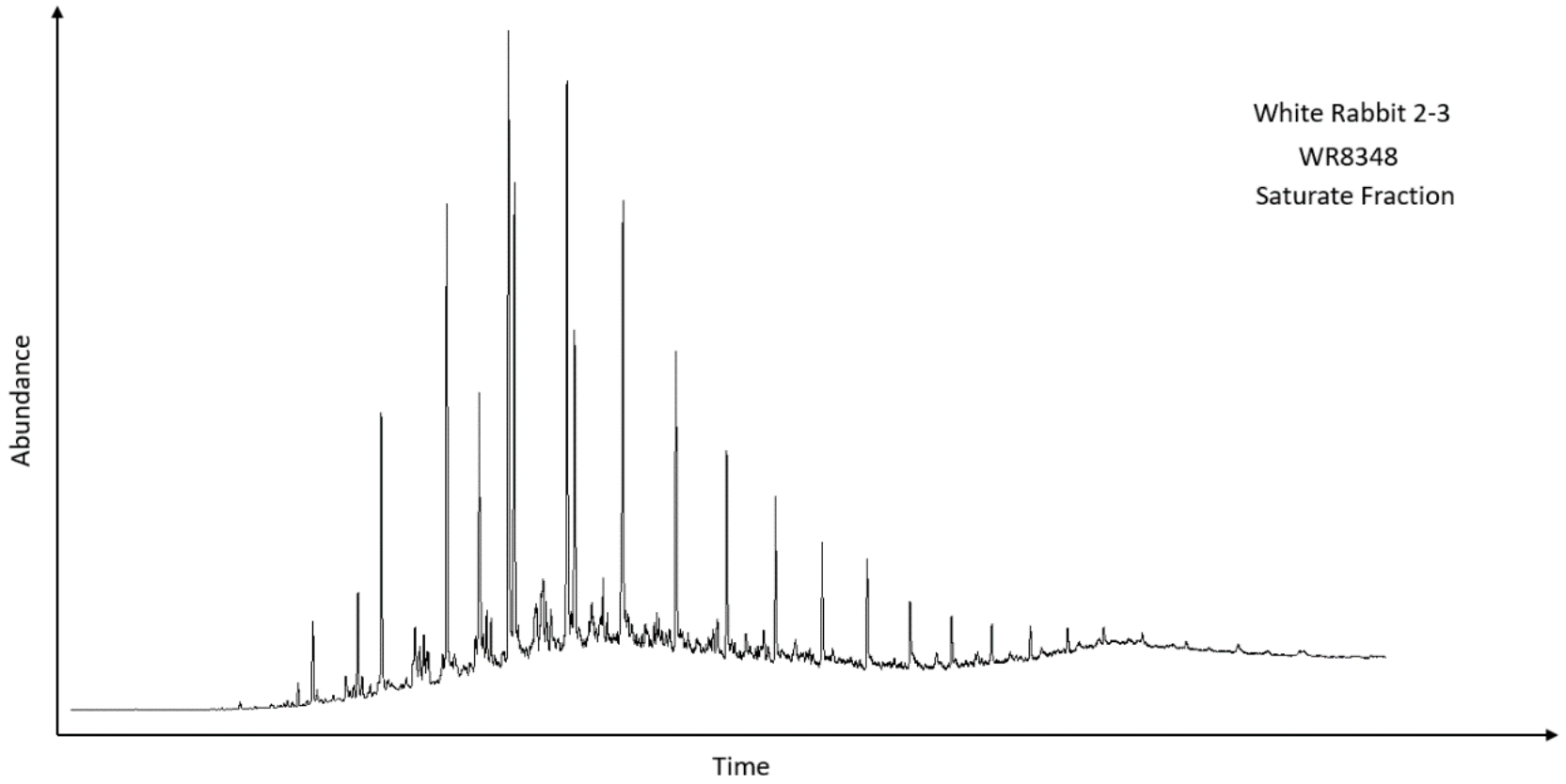
White Rabbit 2-3
WR8348
Saturate Fraction
Abundance
Time

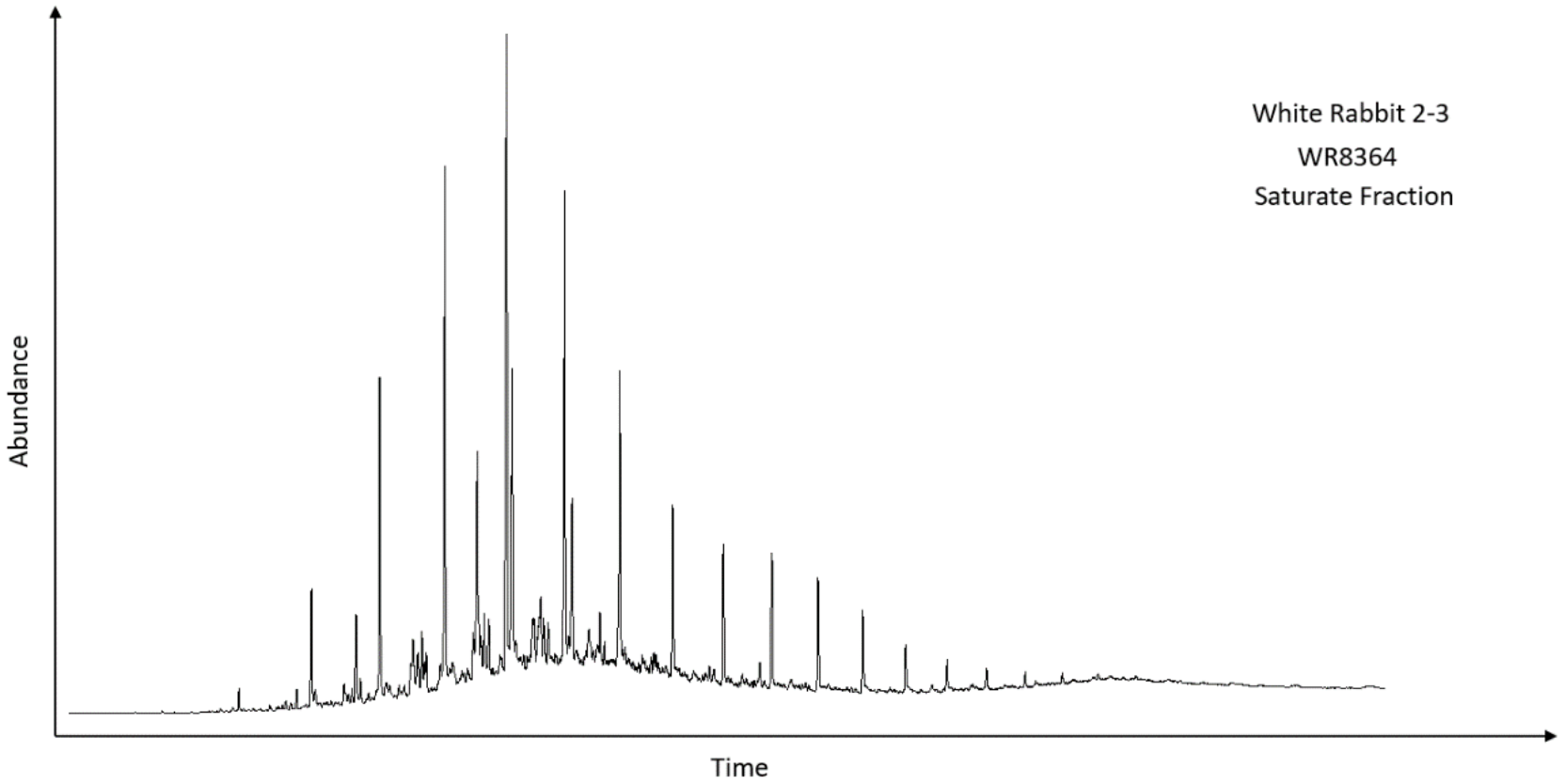
White Rabbit 2-3
WR8364
Saturate Fraction
Abundance
Time

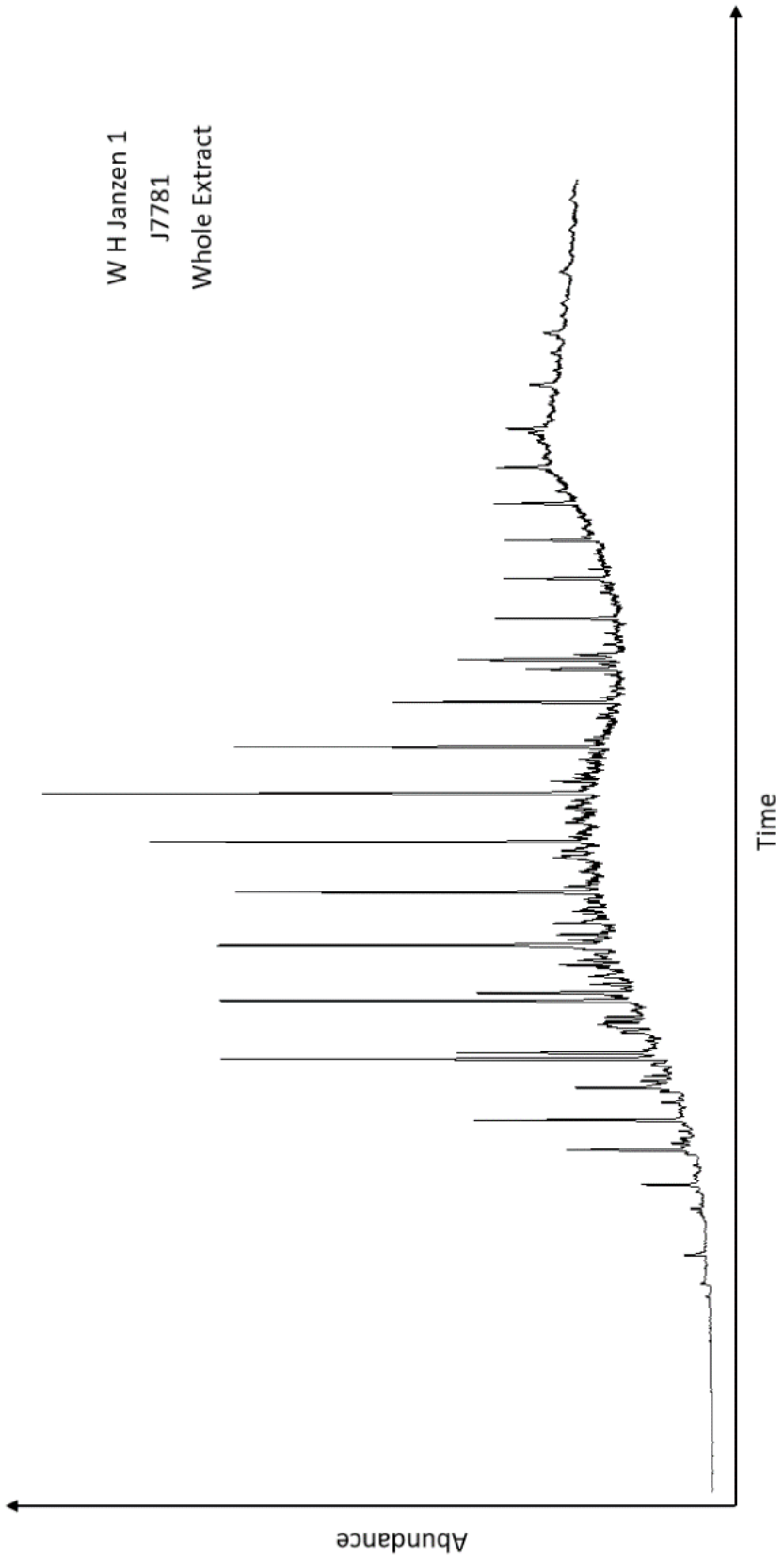
W H Janzen 1
J7781
Whole Extract
Abundance
Time

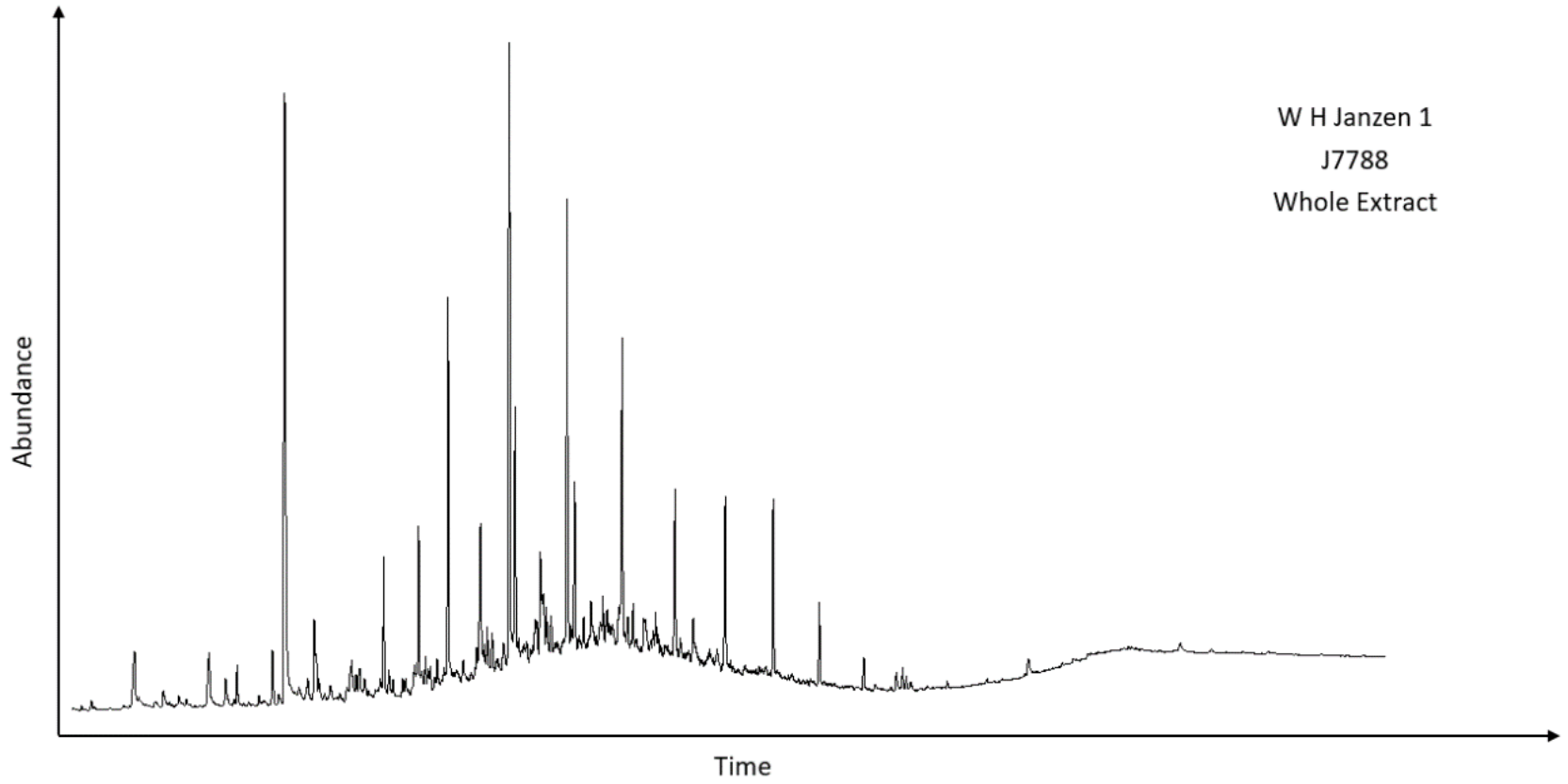
W H Janzen 1
J7788
Whole Extract
Abundance
Time

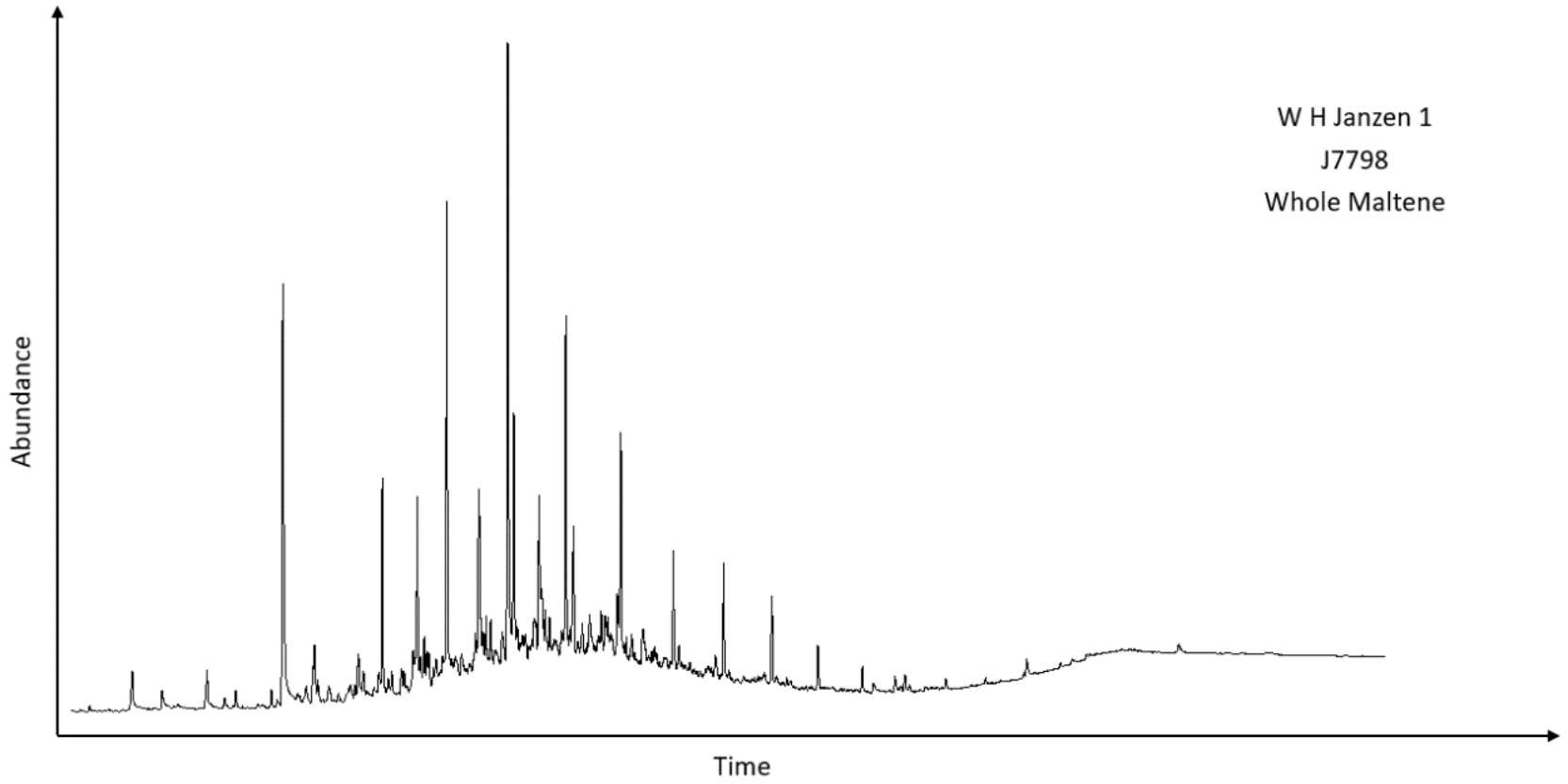
W H Janzen 1
J7798
Whole Maltene
Abundance
Time

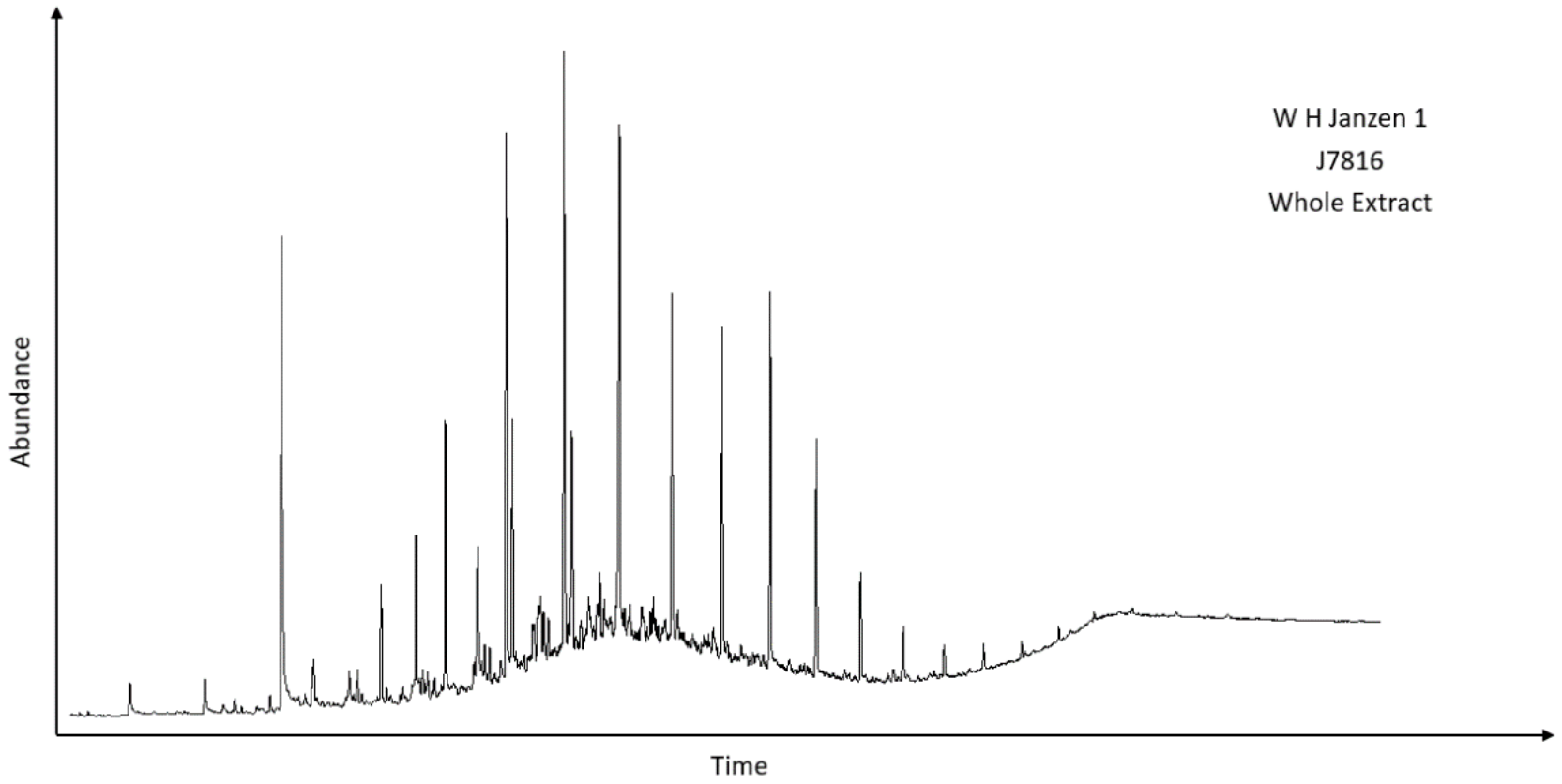
W H Janzen 1
J7816
Whole Extract
Abundance
Time

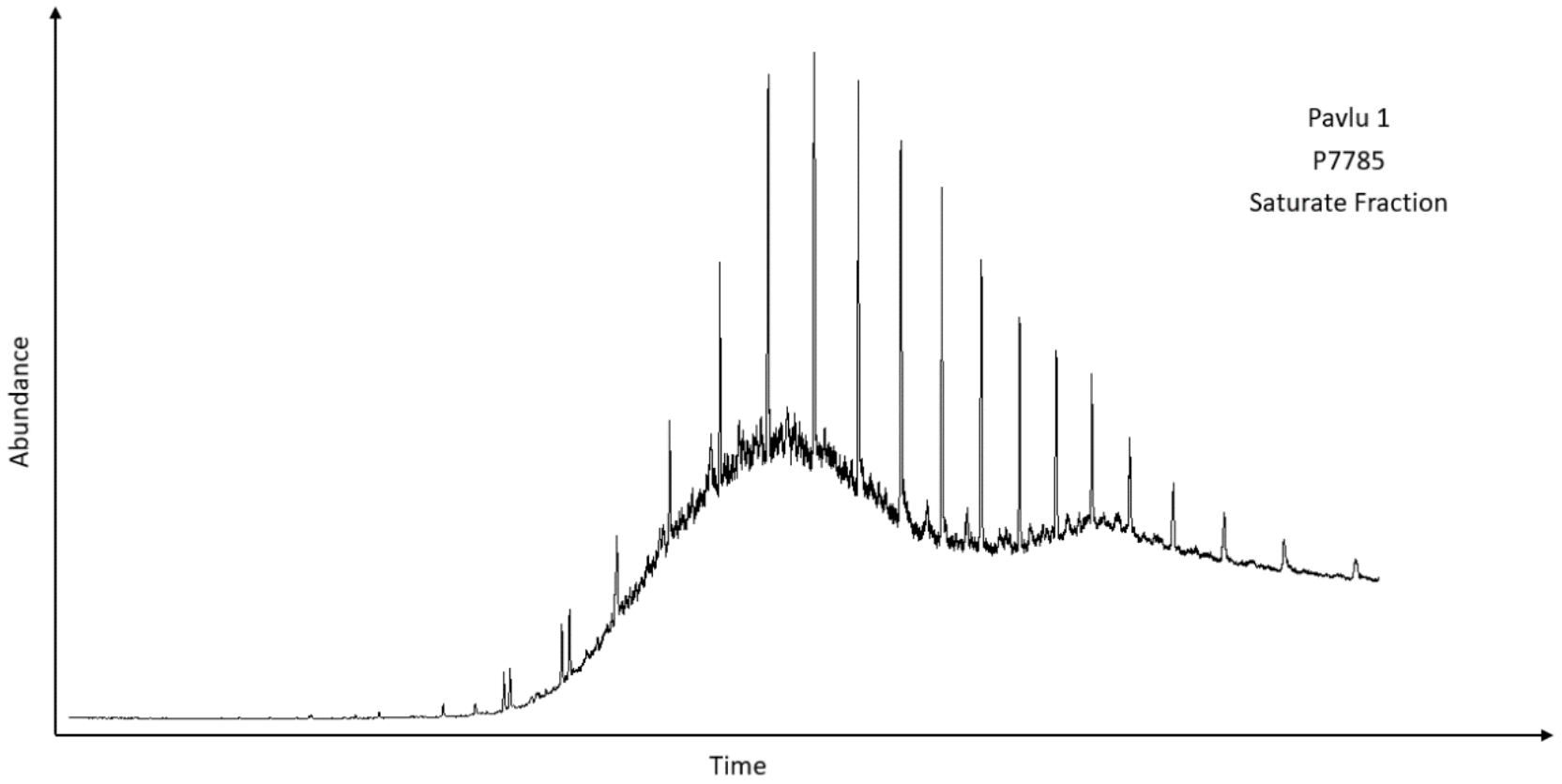
Pavlu 1
P7785
Saturate Fraction
Abundance
Time

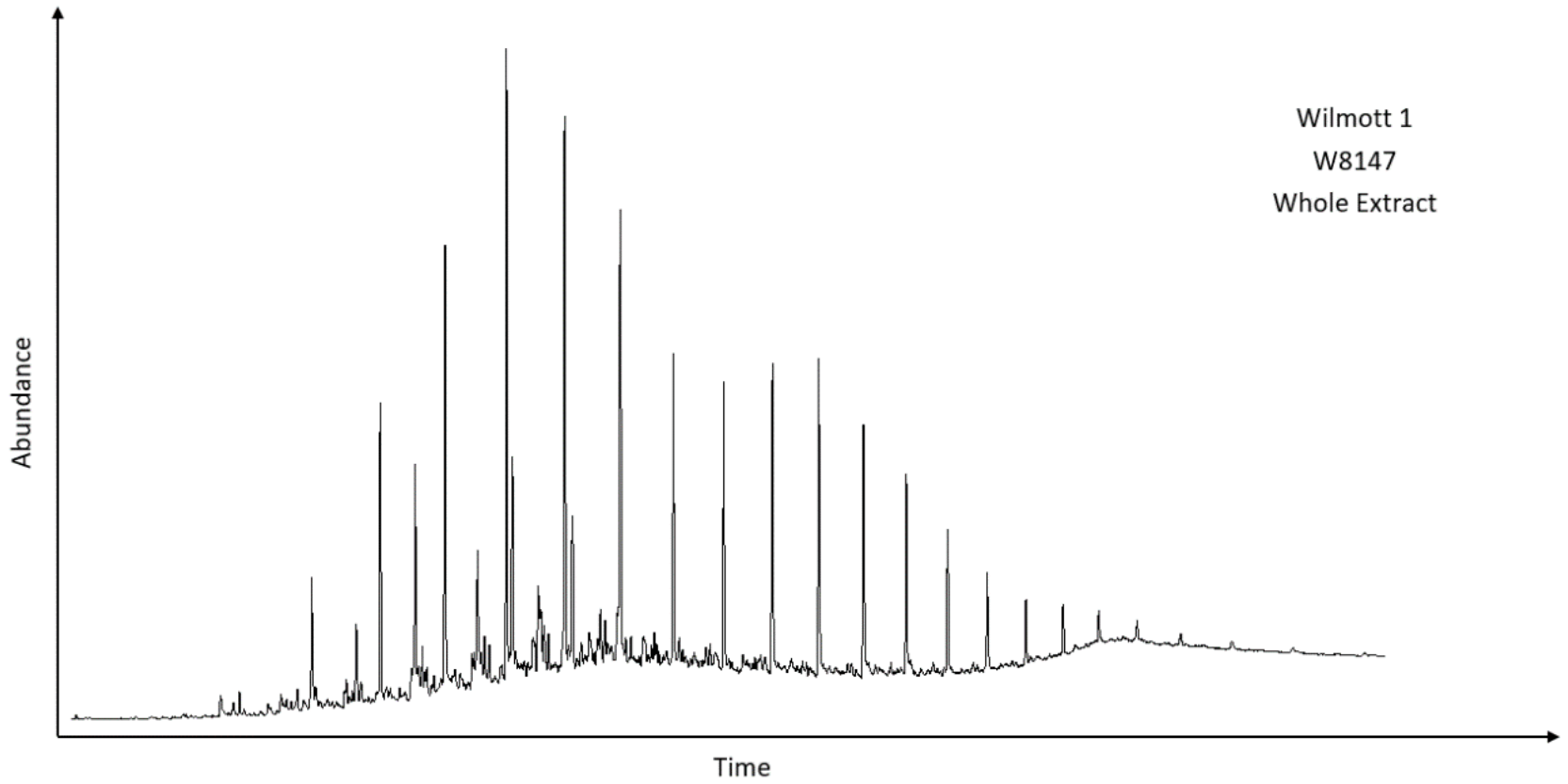
Wilmott 1
W8147
Whole Extract
Abundance
Time

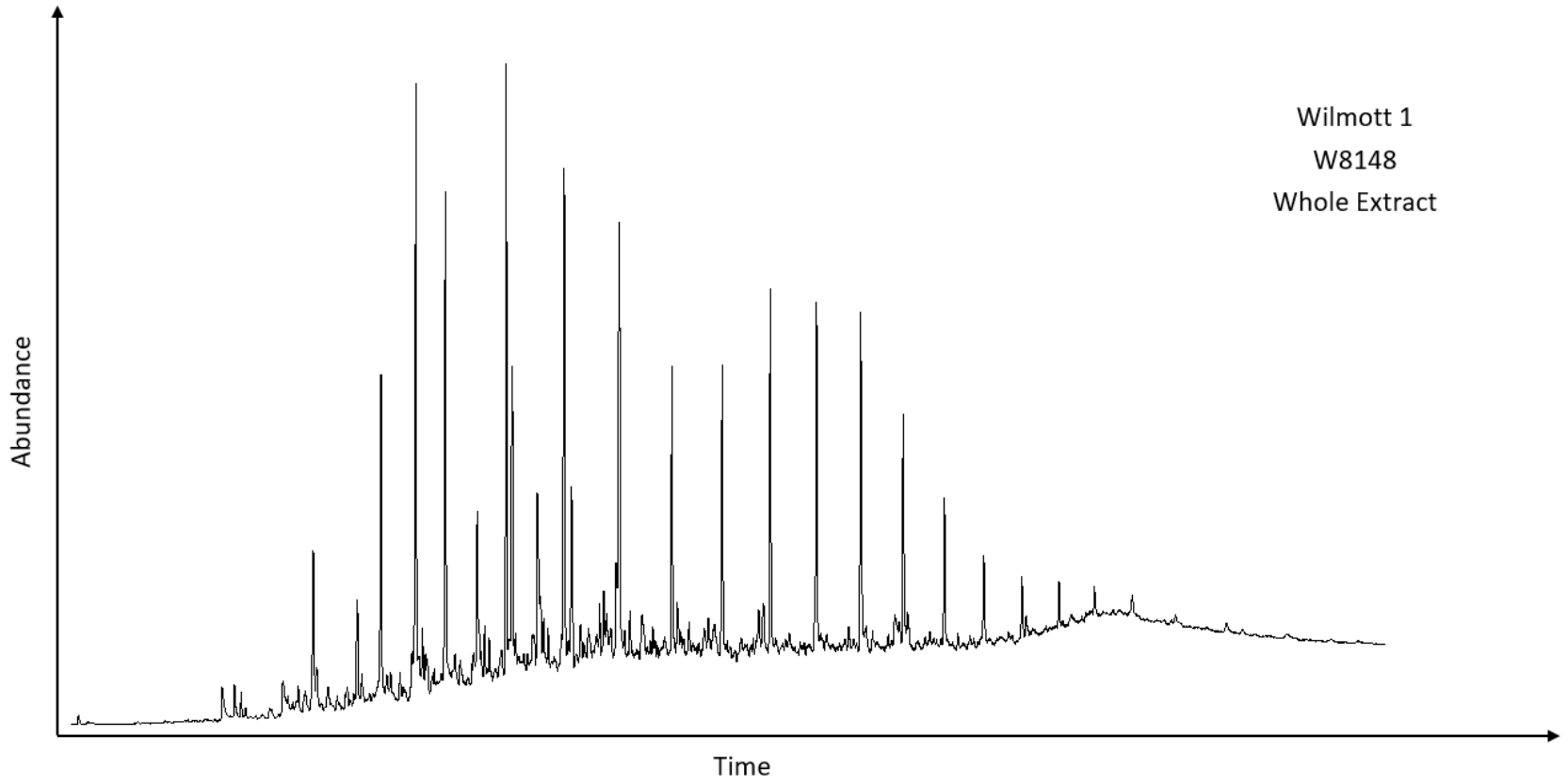
Wilmott 1
W8148
Whole Extract
Abundance
Time

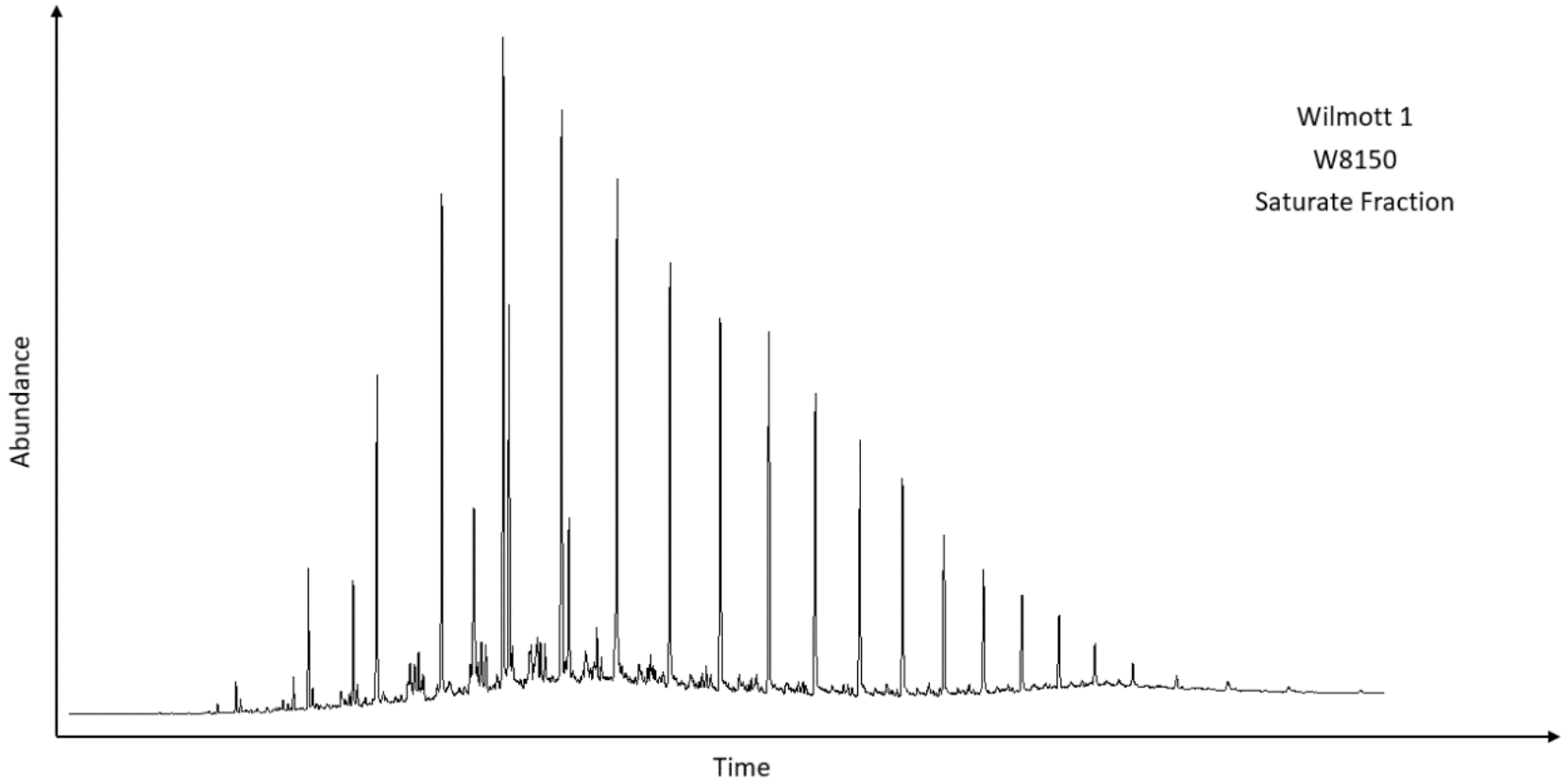
Wilmott 1
W8150
Saturate Fraction
Abundance
Time

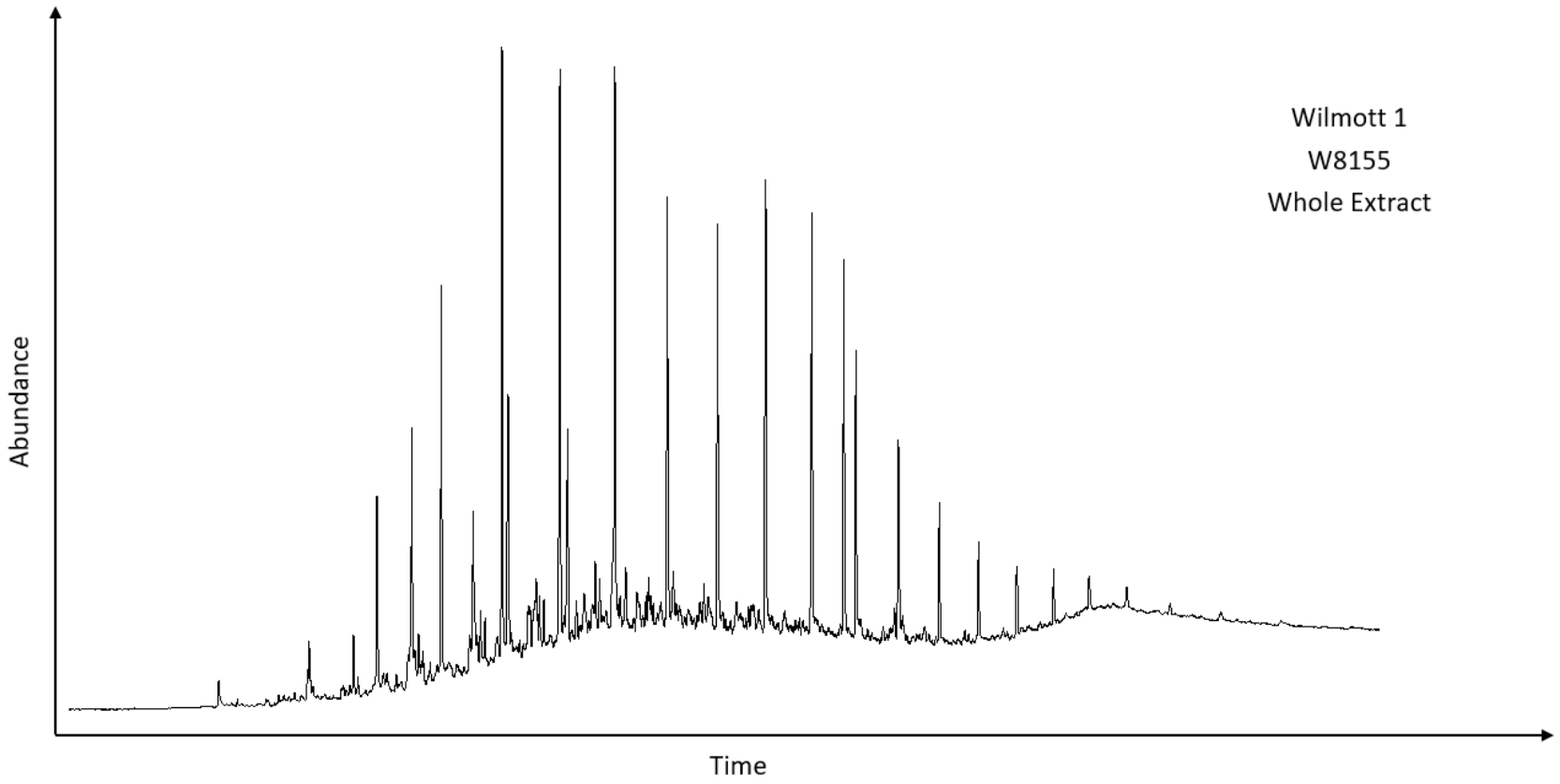
Wilmott 1
W8155
Whole Extract
Abundance
Time

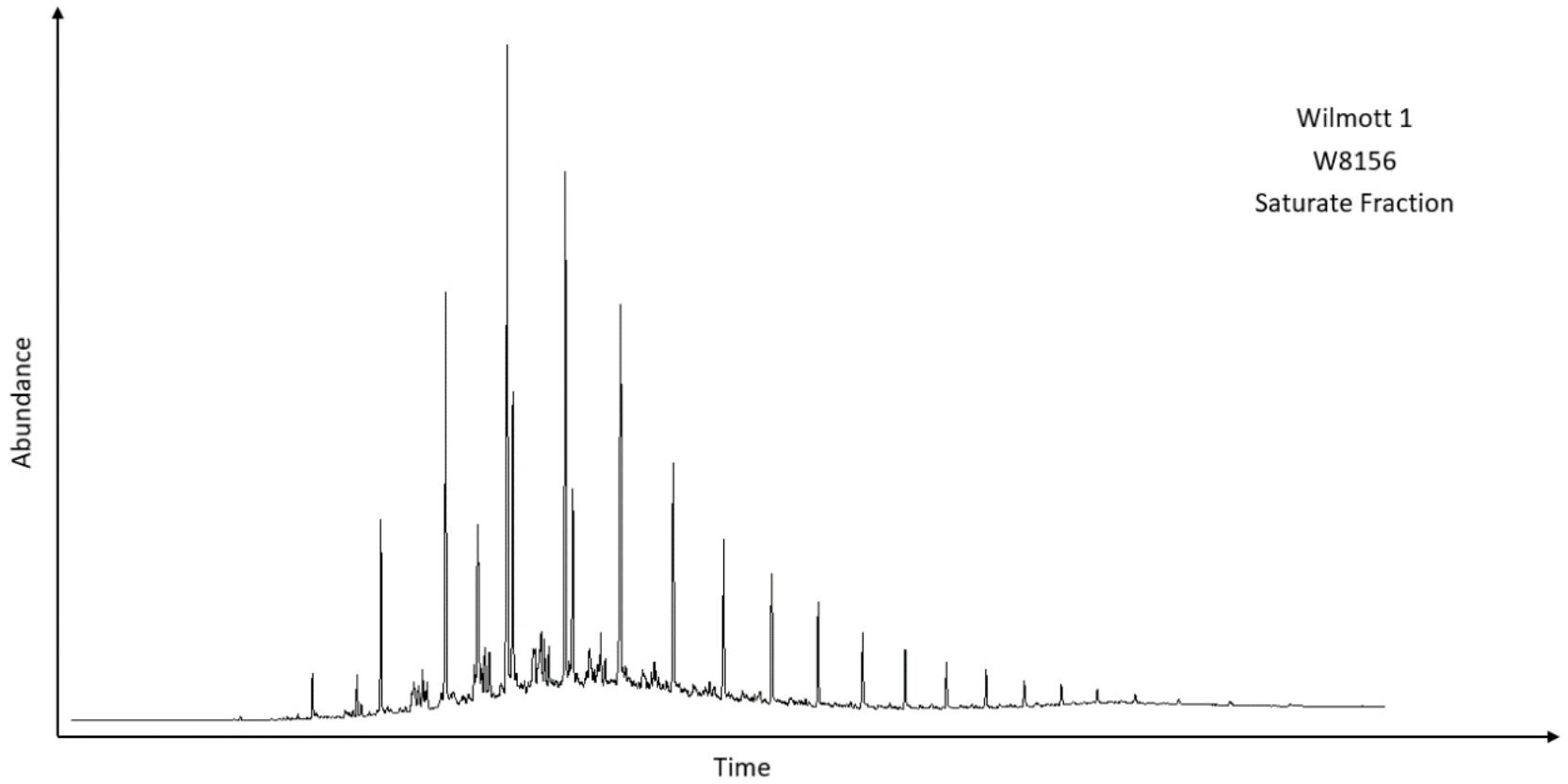
Wilmott 1
W8156
Saturate Fraction
Abundance
Time

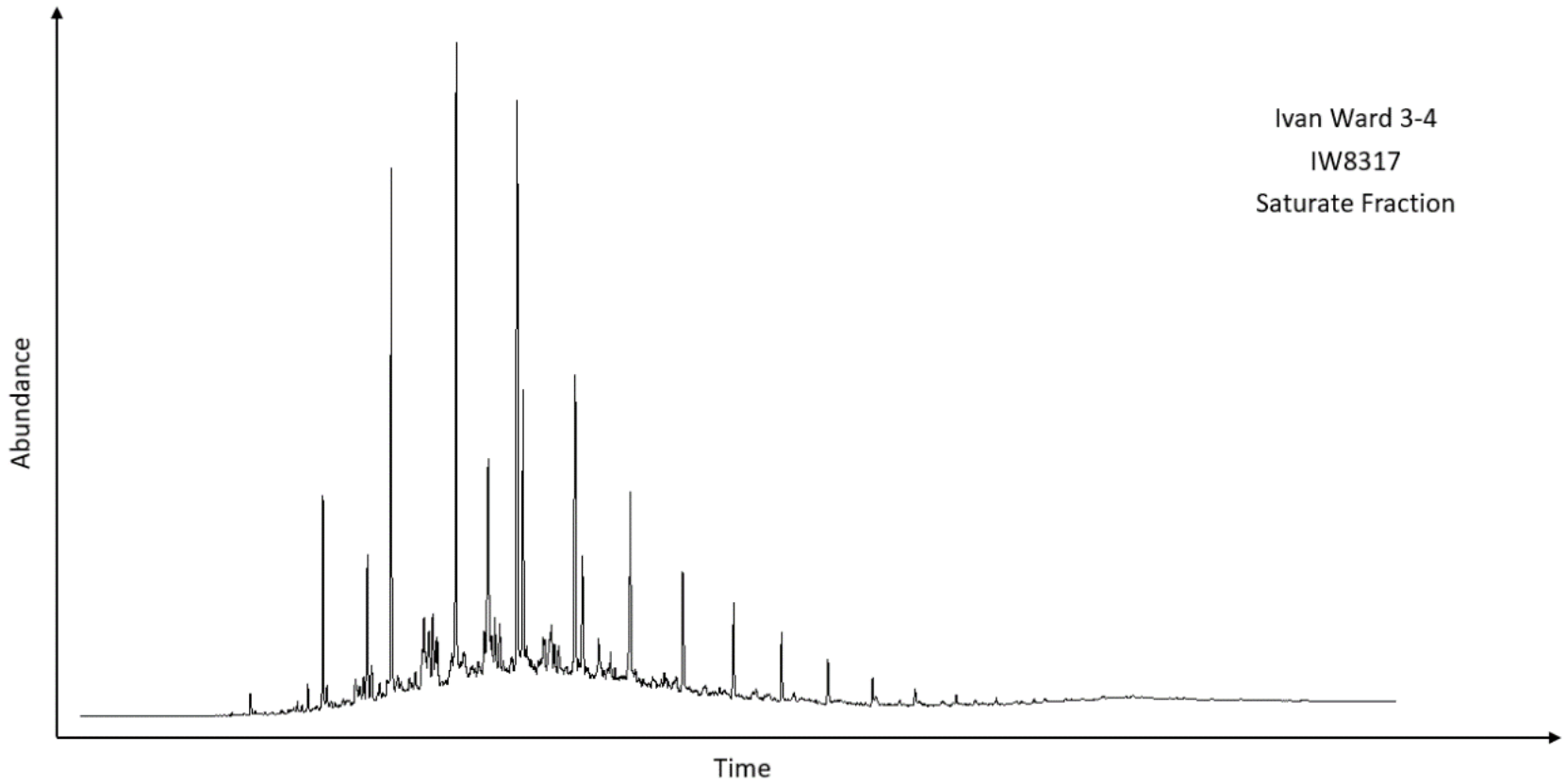
Ivan Ward 3-4
IW8317
Saturate Fraction
Abundance
Time

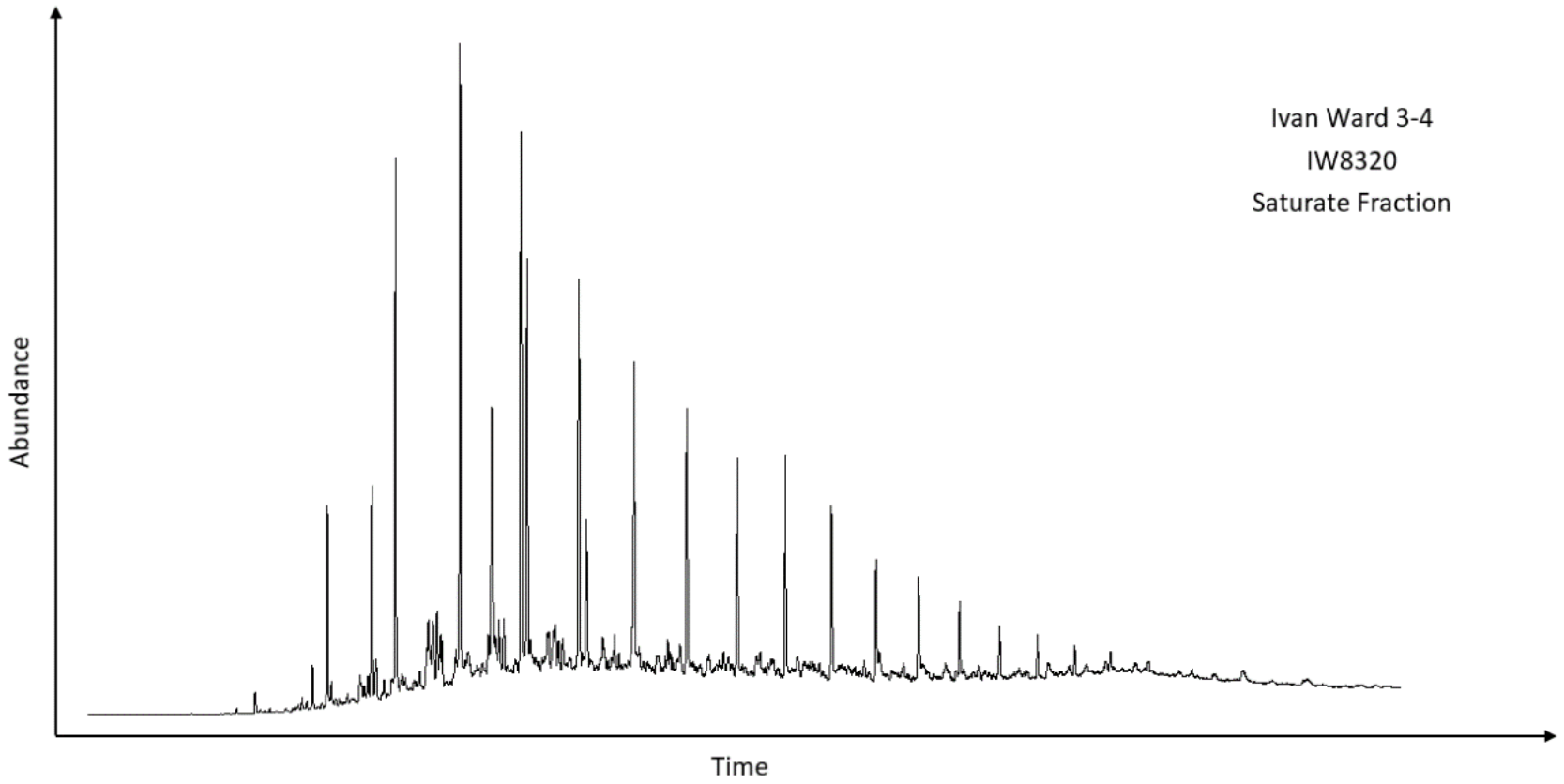
Ivan Ward 3-4
IW8320
Saturate Fraction
Abundance
Time

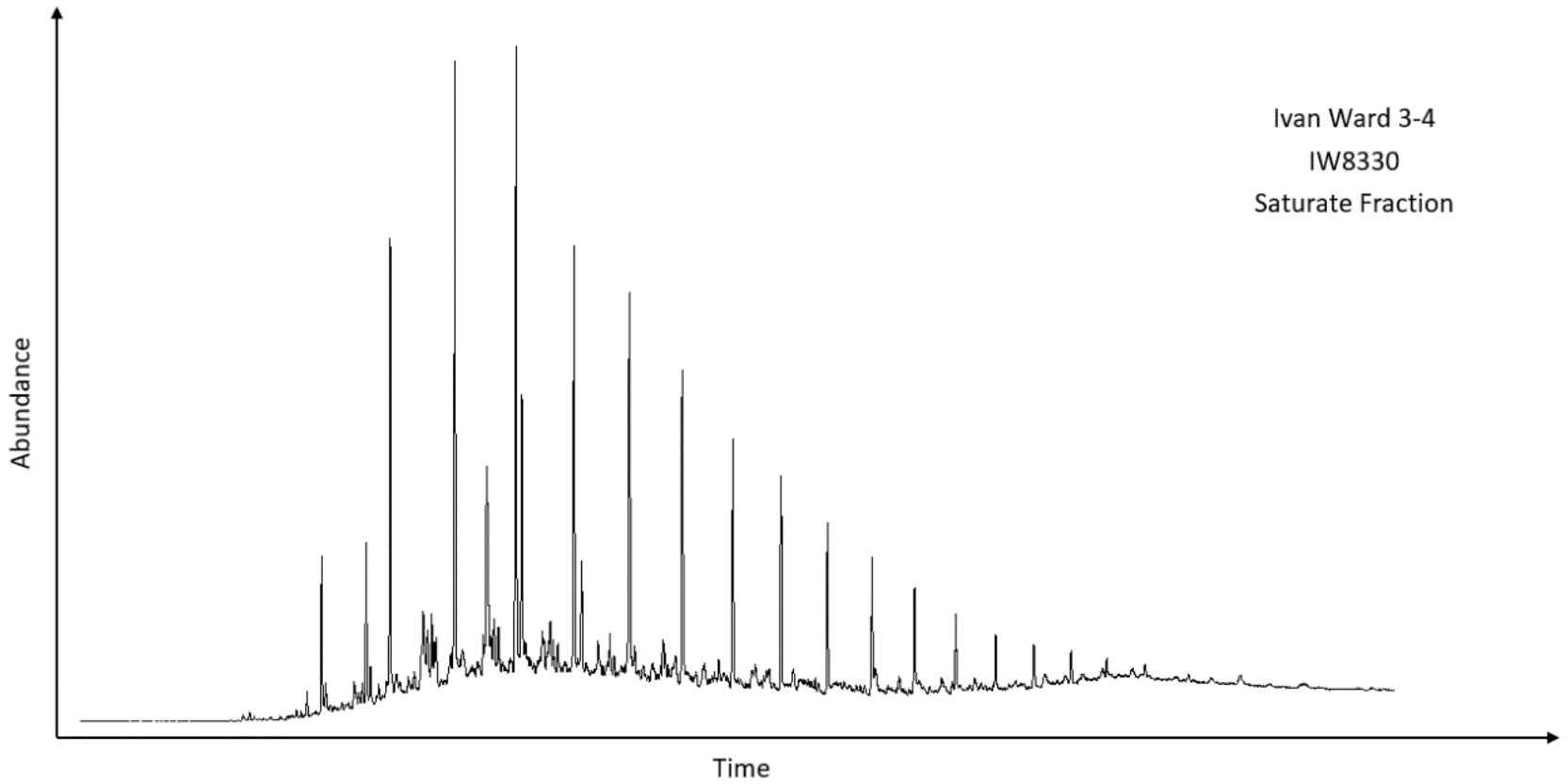
Ivan Ward 3-4
IW8330
Saturate Fraction
Abundance
Time

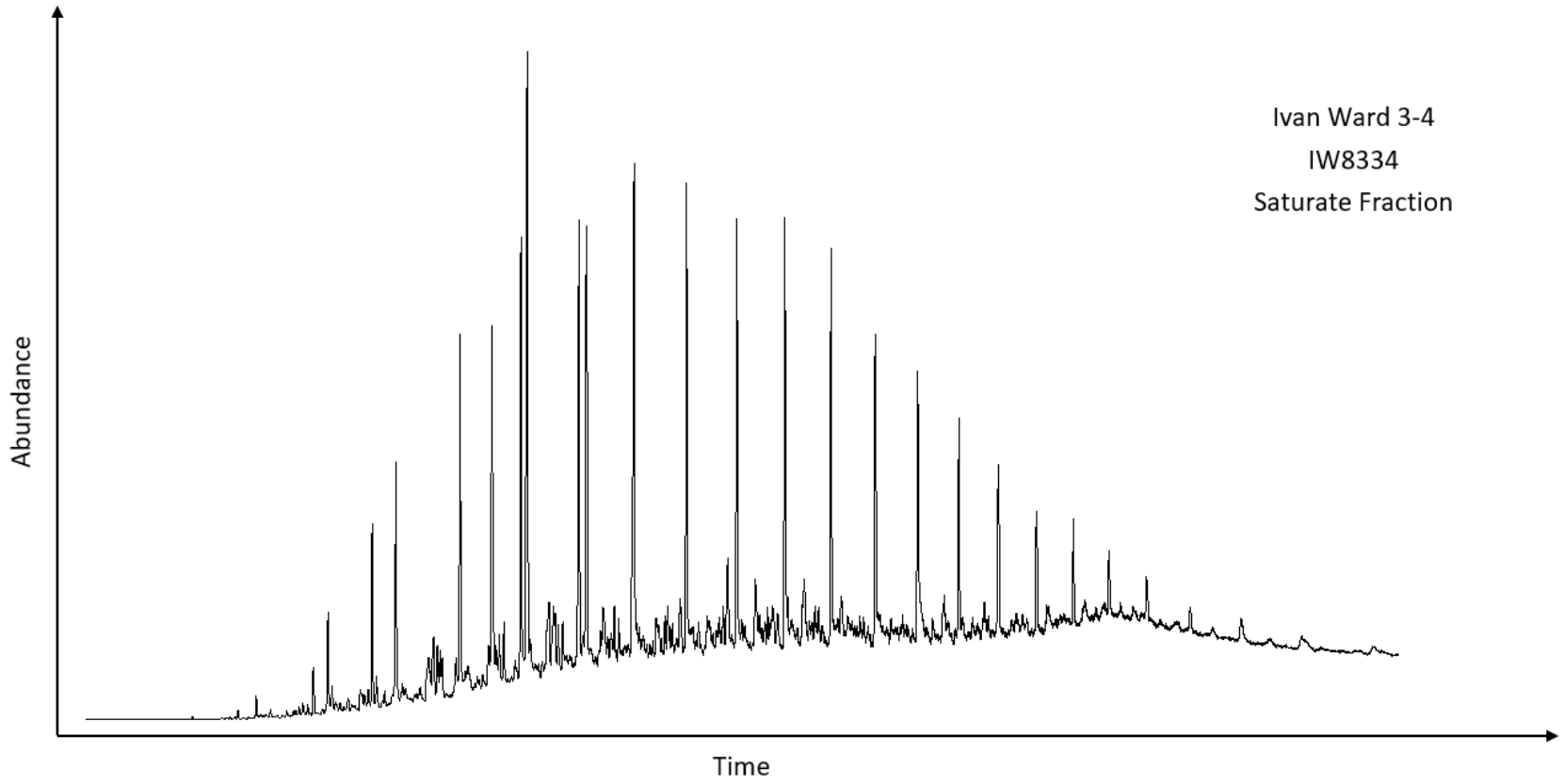
Ivan Ward 3-4
IW8334
Saturate Fraction
Abundance
Time

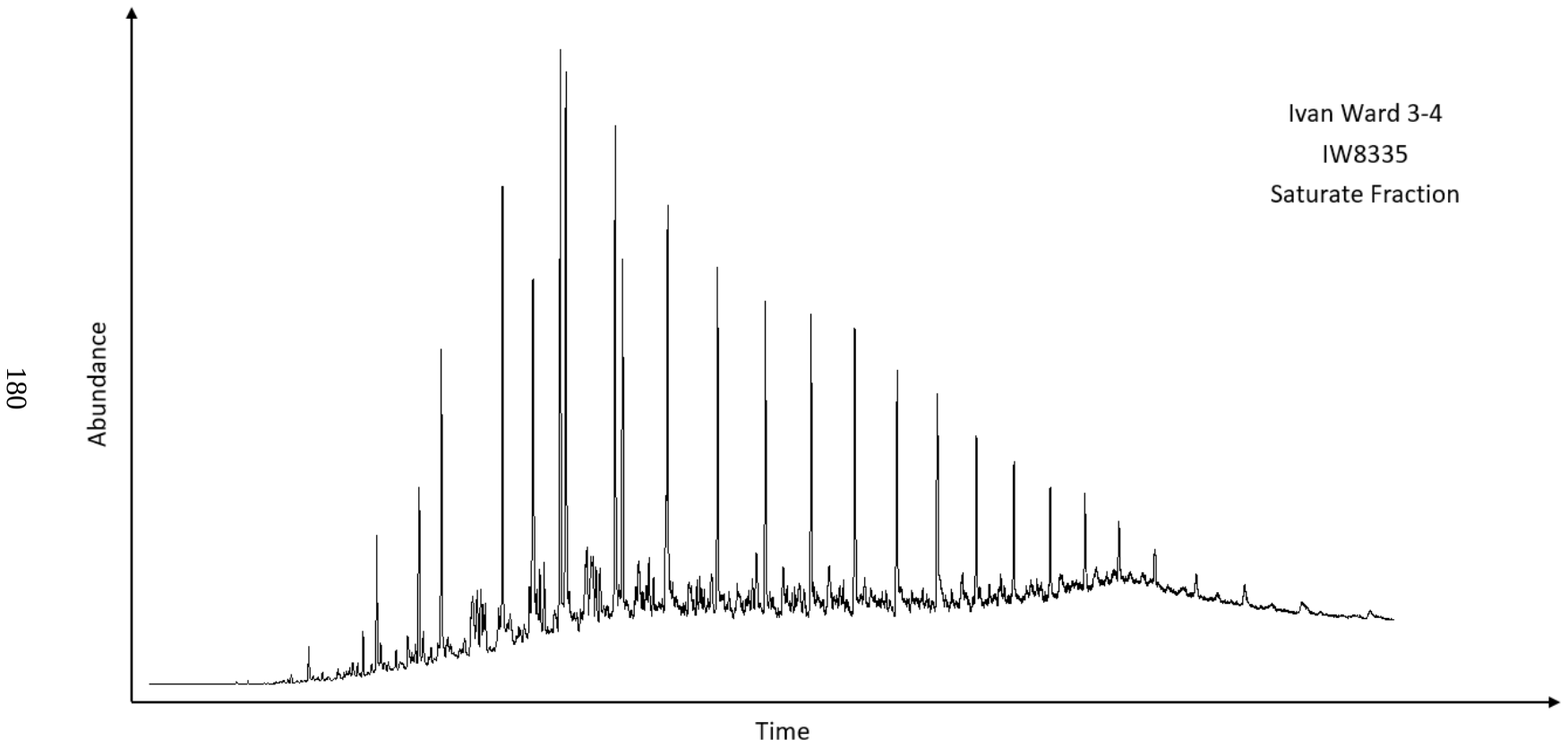
Ivan Ward 3-4
IW8335
Saturate Fraction
Abundance
Time

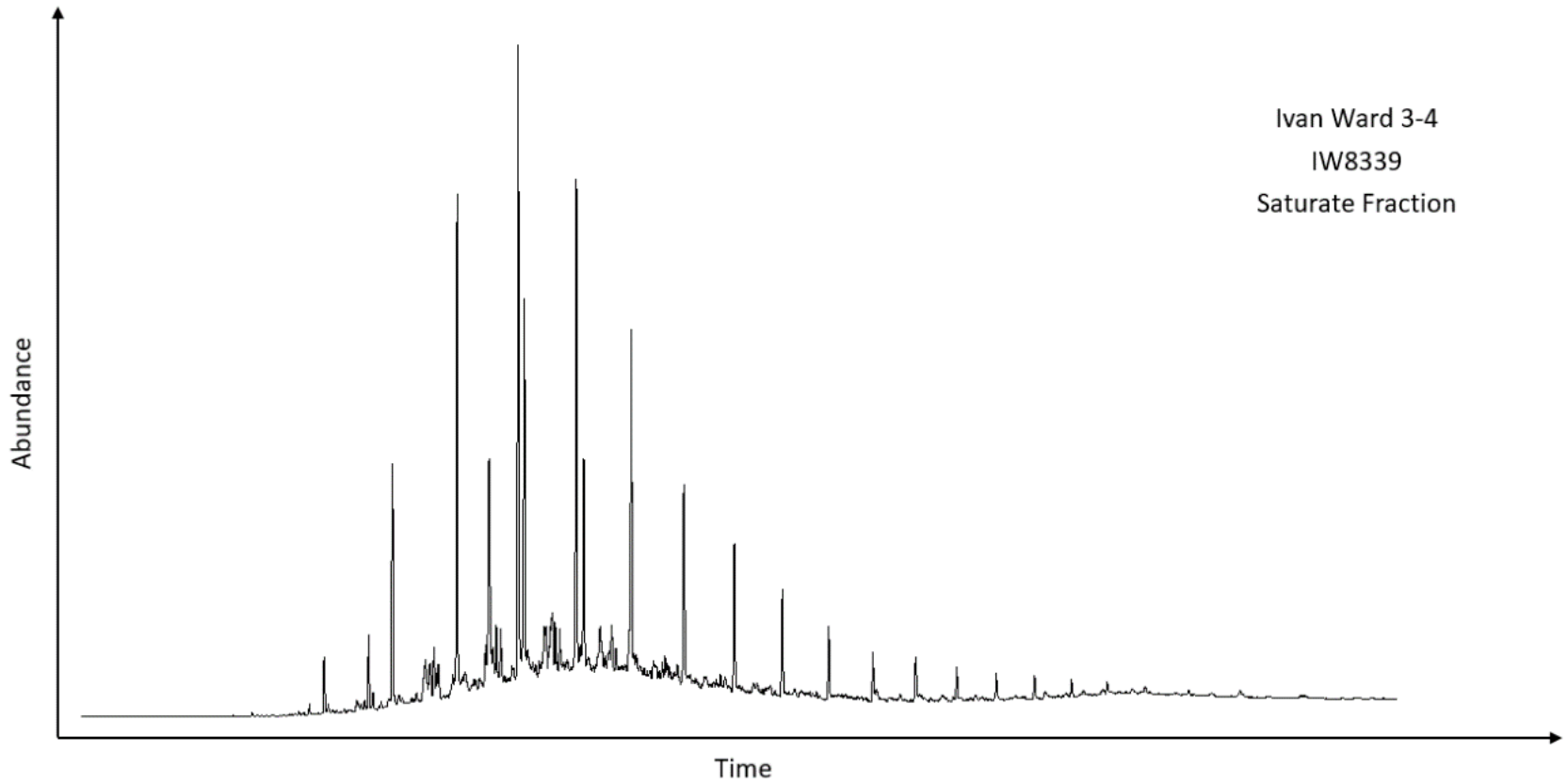
Ivan Ward 3-4
IW8339
Saturate Fraction
Abundance
Time

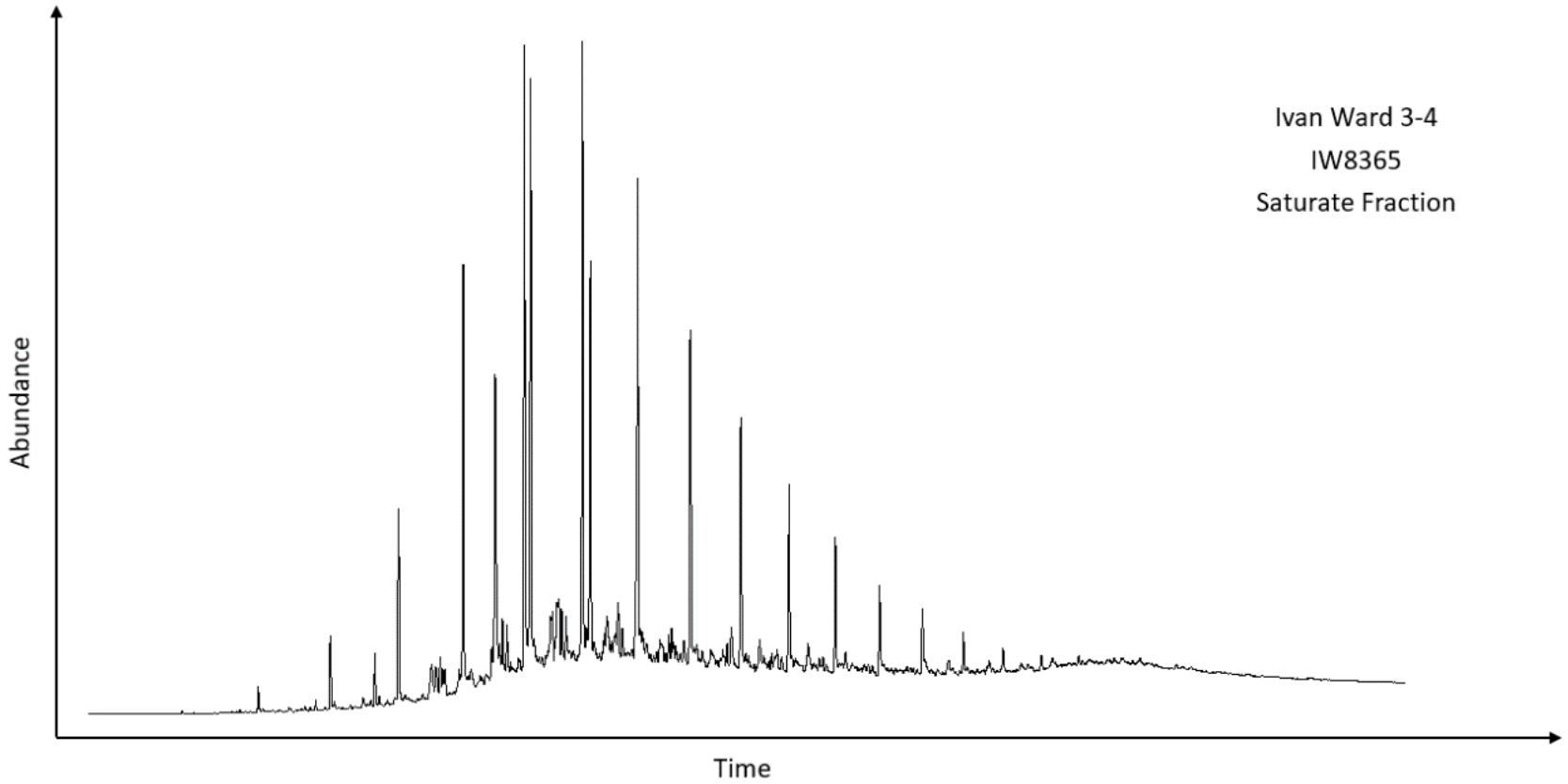
Ivan Ward 3-4
IW8365
Saturate Fraction
Abundance
Time

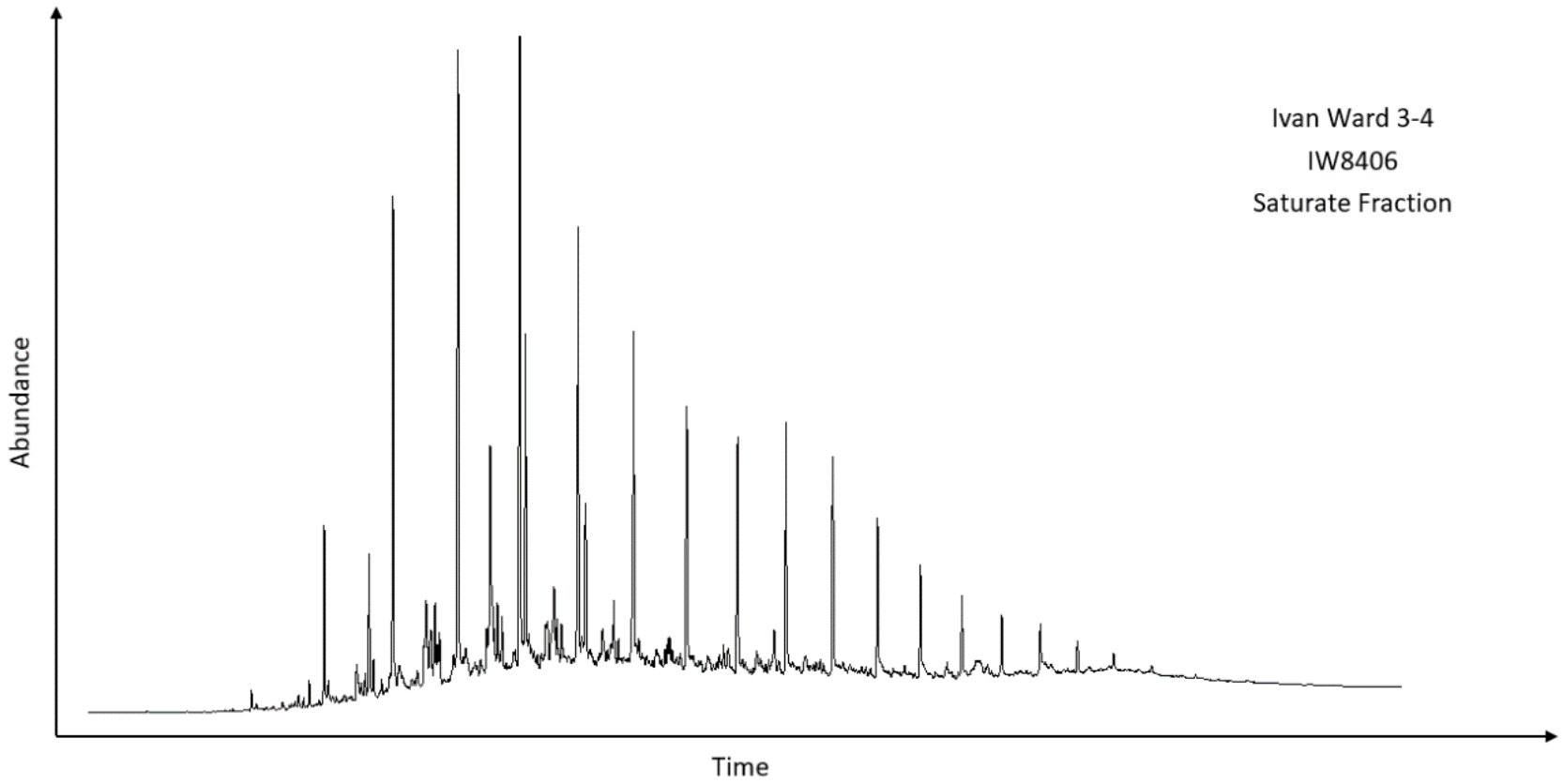
Ivan Ward 3-4
IW8406
Saturate Fraction
Abundance
Time

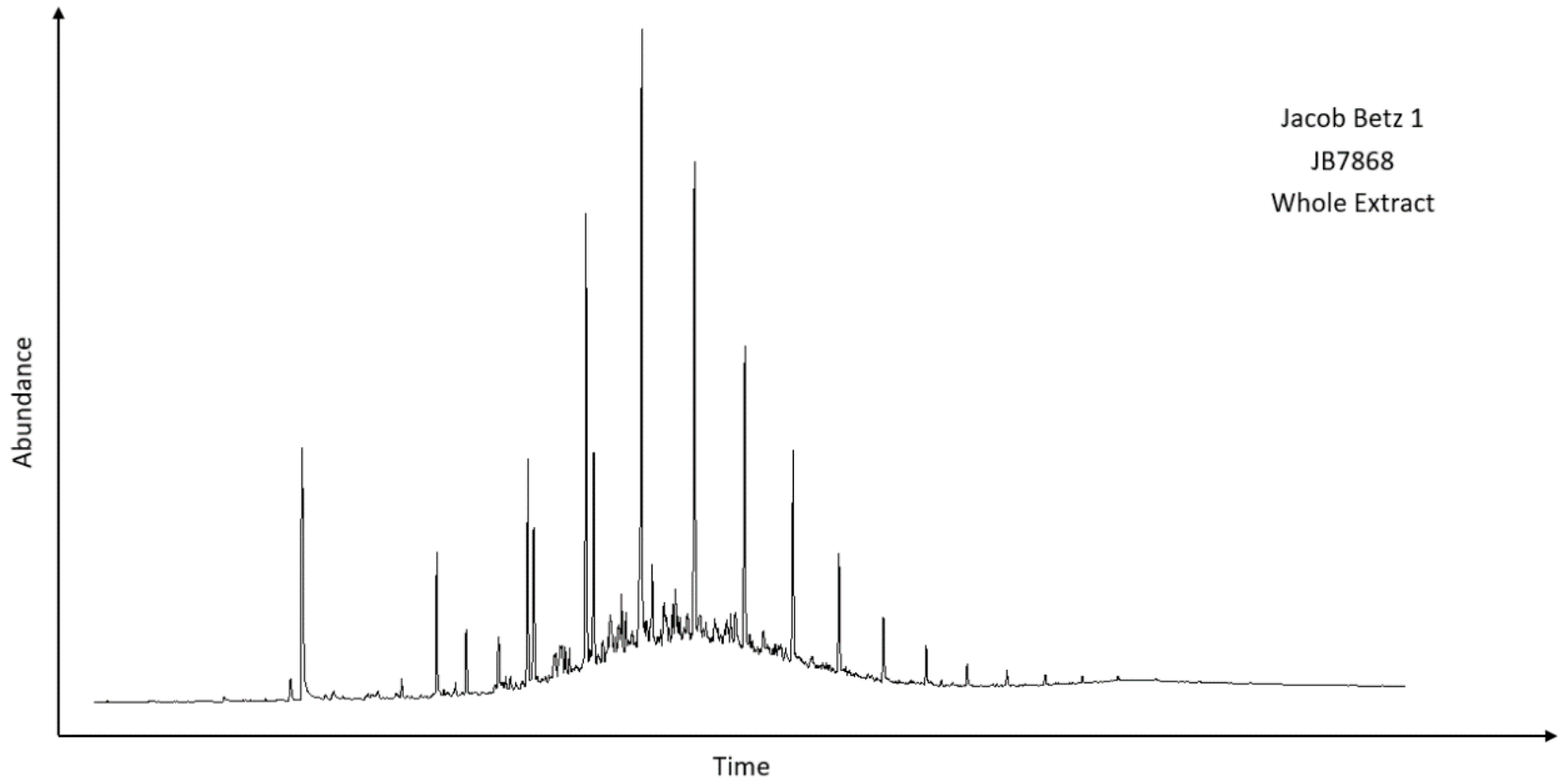
Jacob Betz 1
JB7868
Whole Extract
Abundance
Time

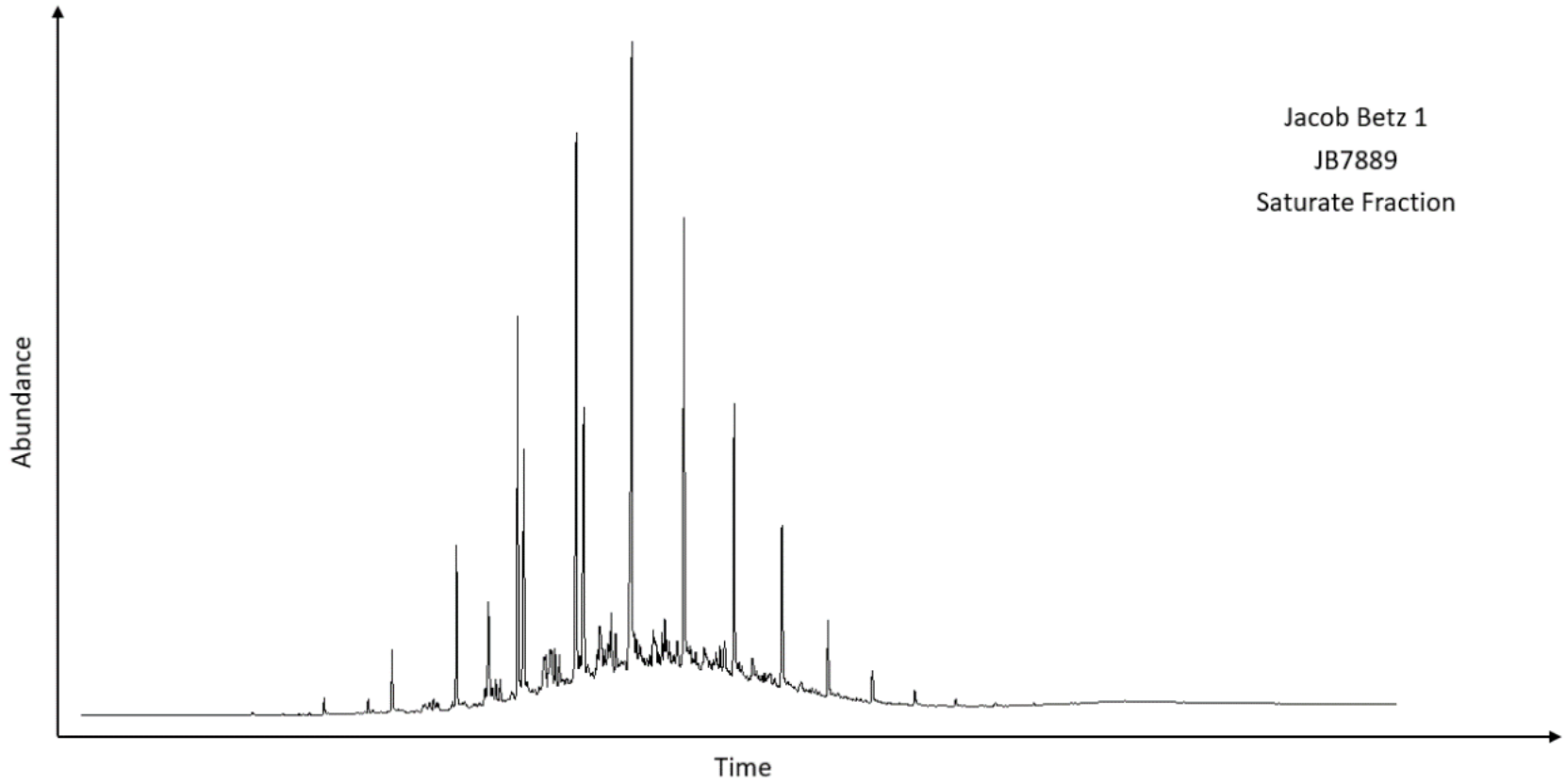
Jacob Betz 1
JB7889
Saturate Fraction
Abundance
Time

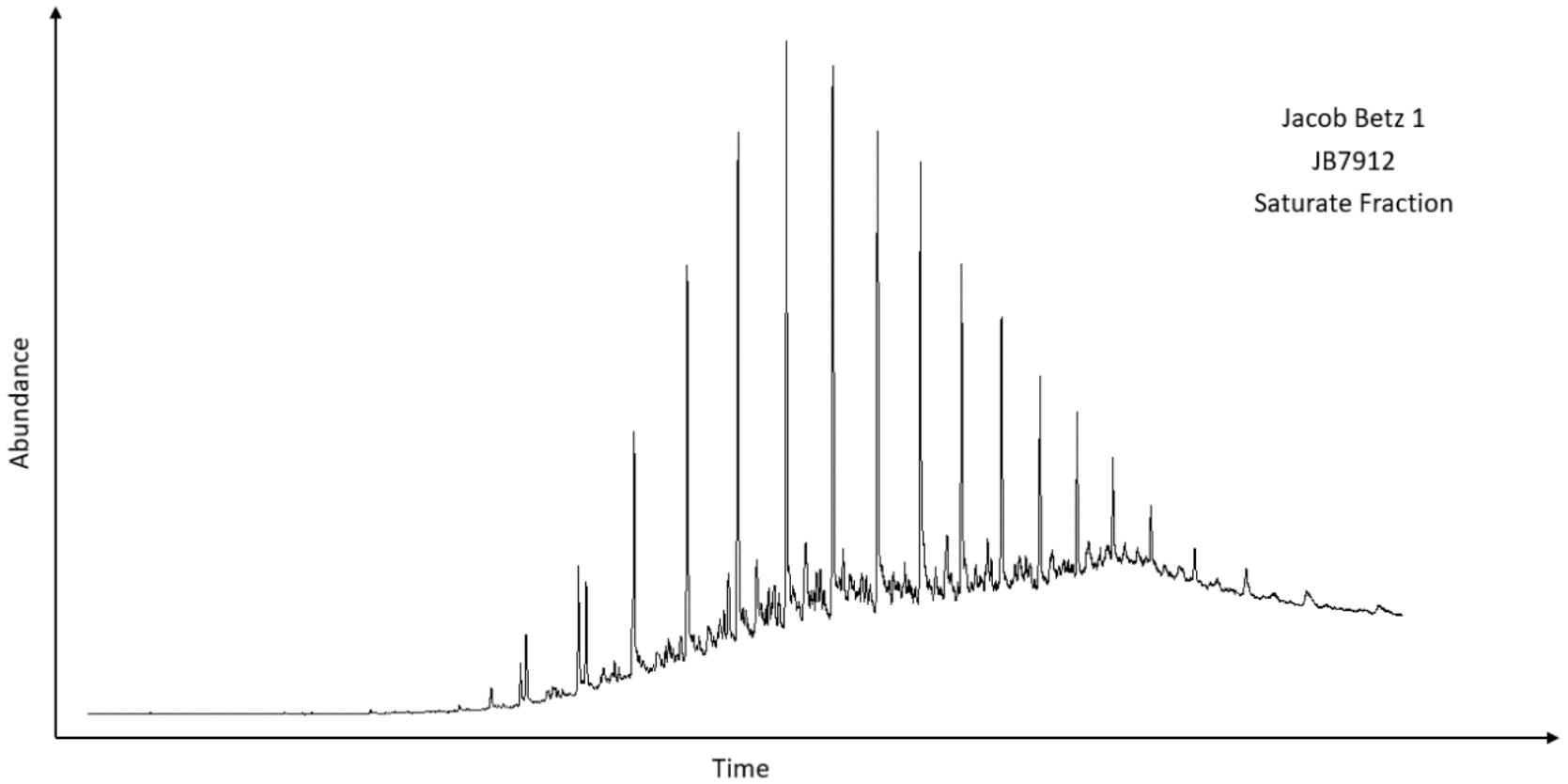
Jacob Betz 1
JB7912
Saturate Fraction
Abundance
Time

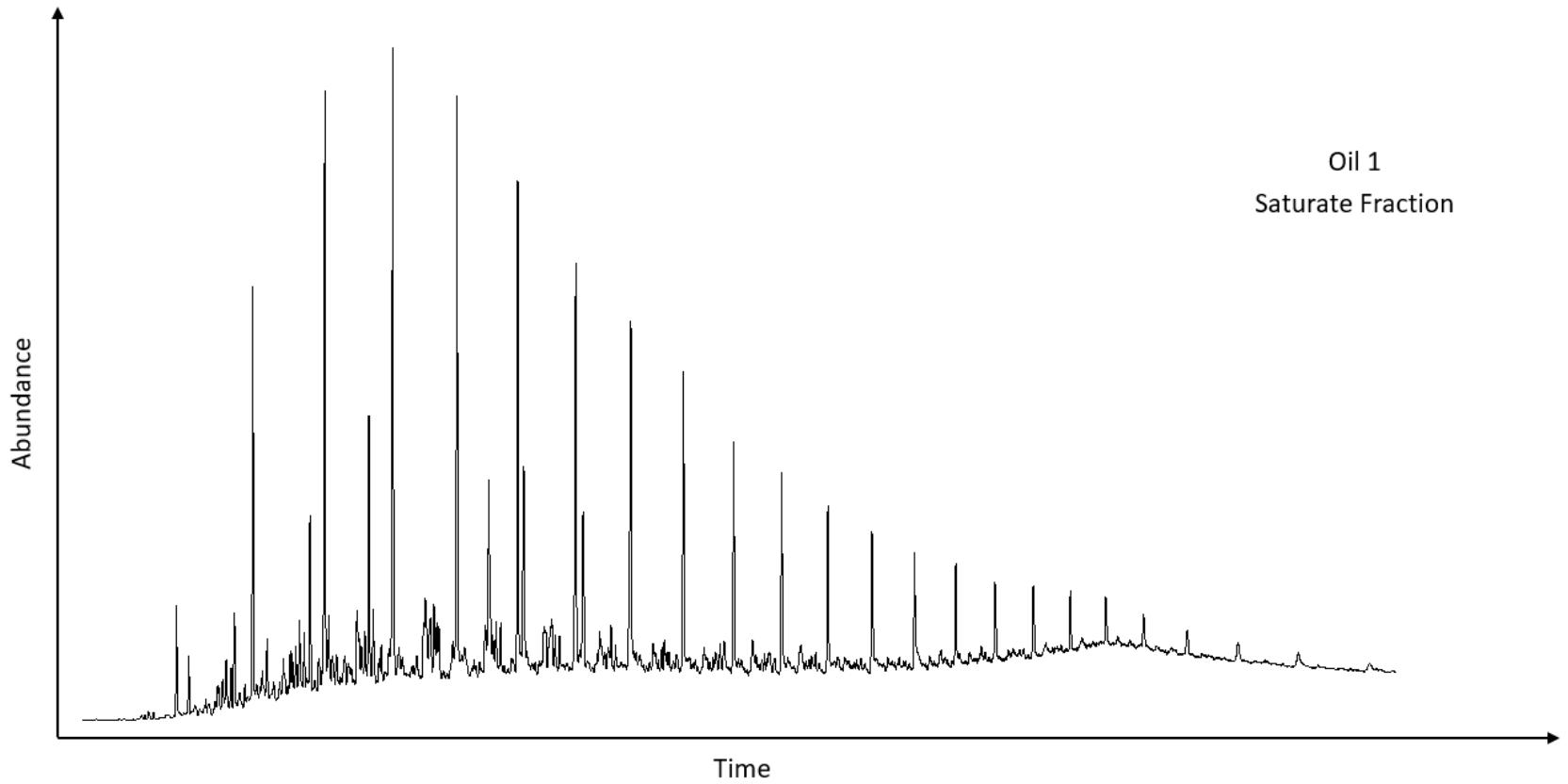
Oil 1
Saturate Fraction
Abundance
Time

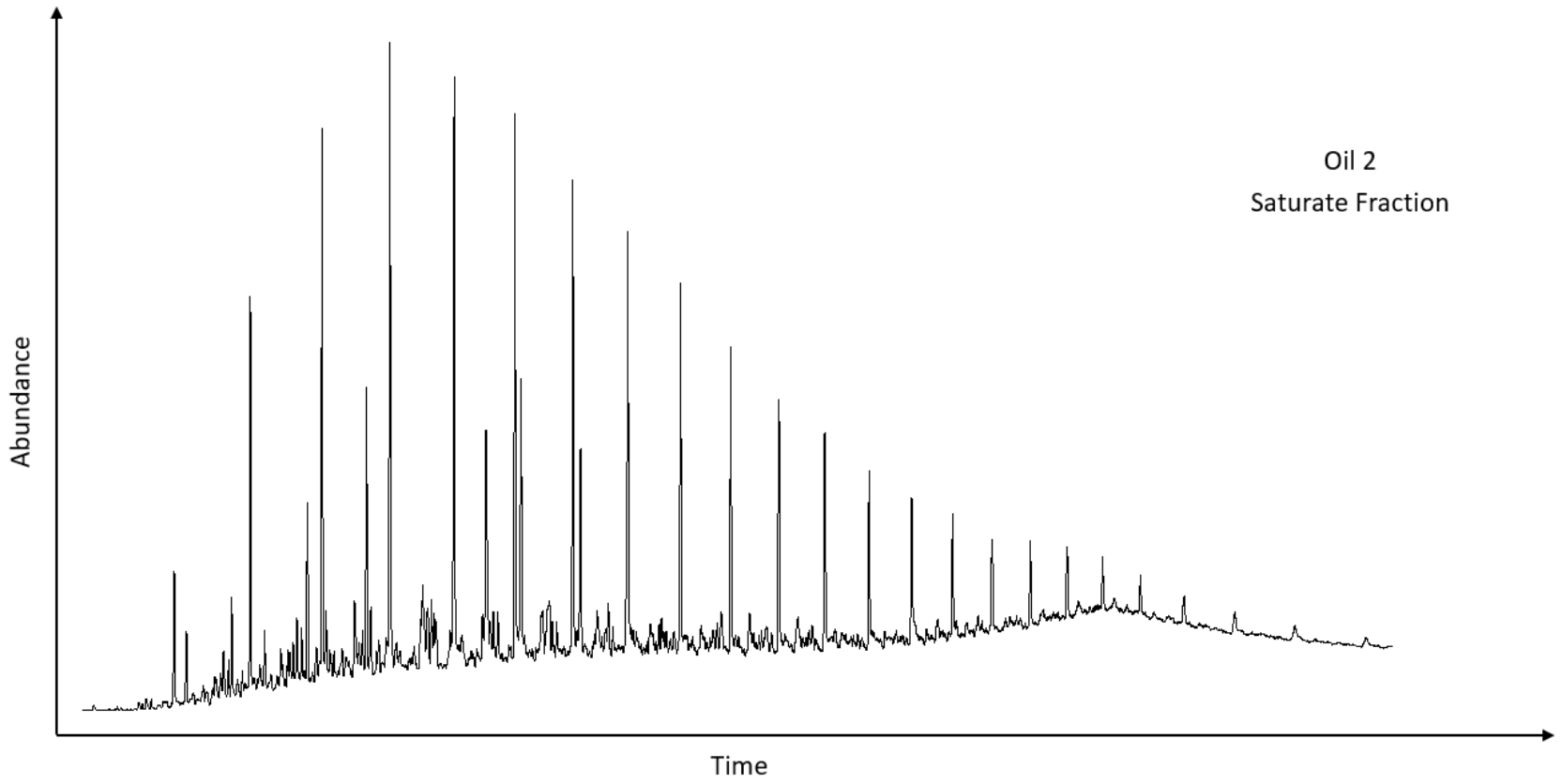
Oil 2
Saturate Fraction
Abundance
Time

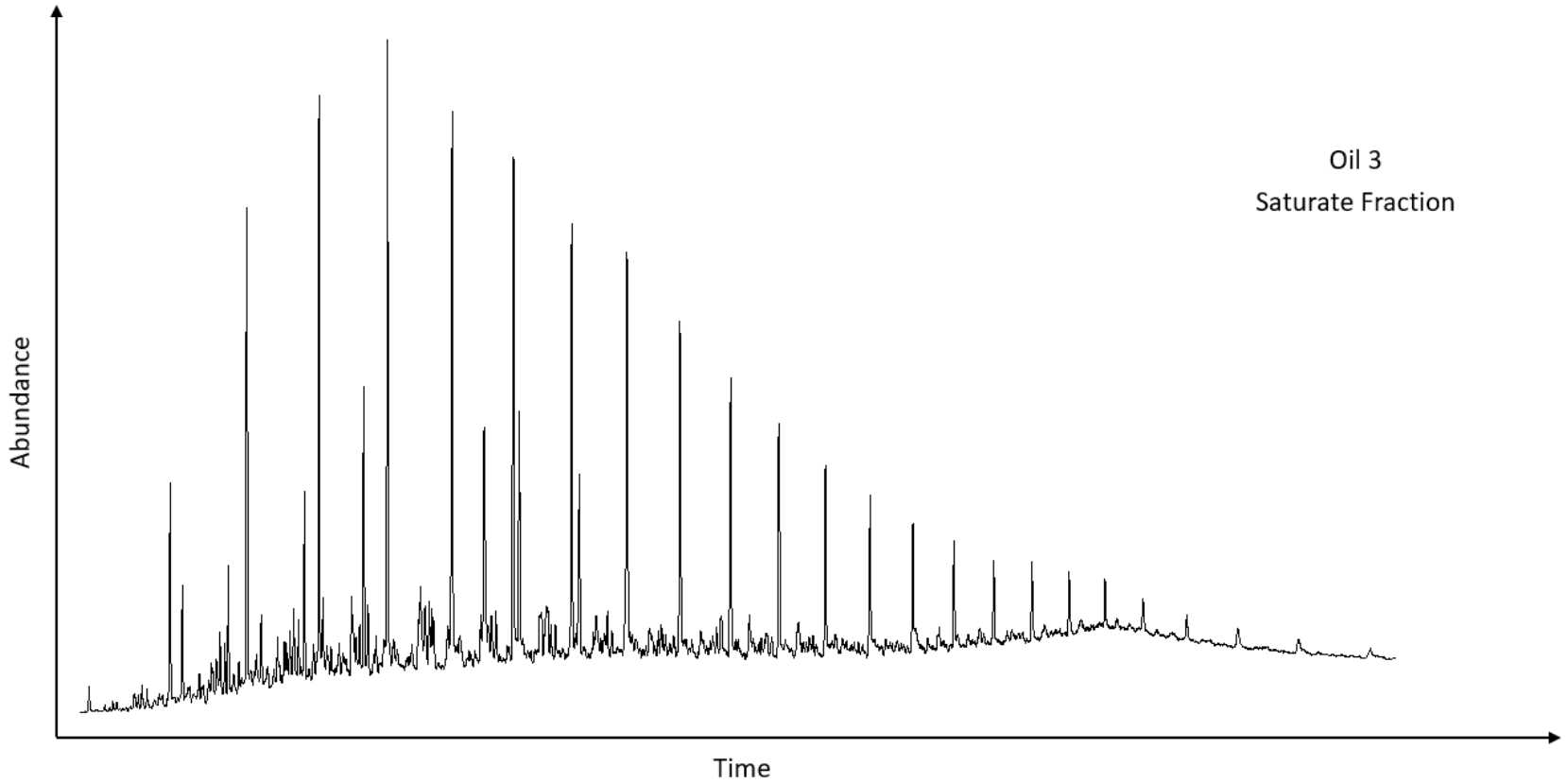
Oil 3
Saturate Fraction
Abundance
Time

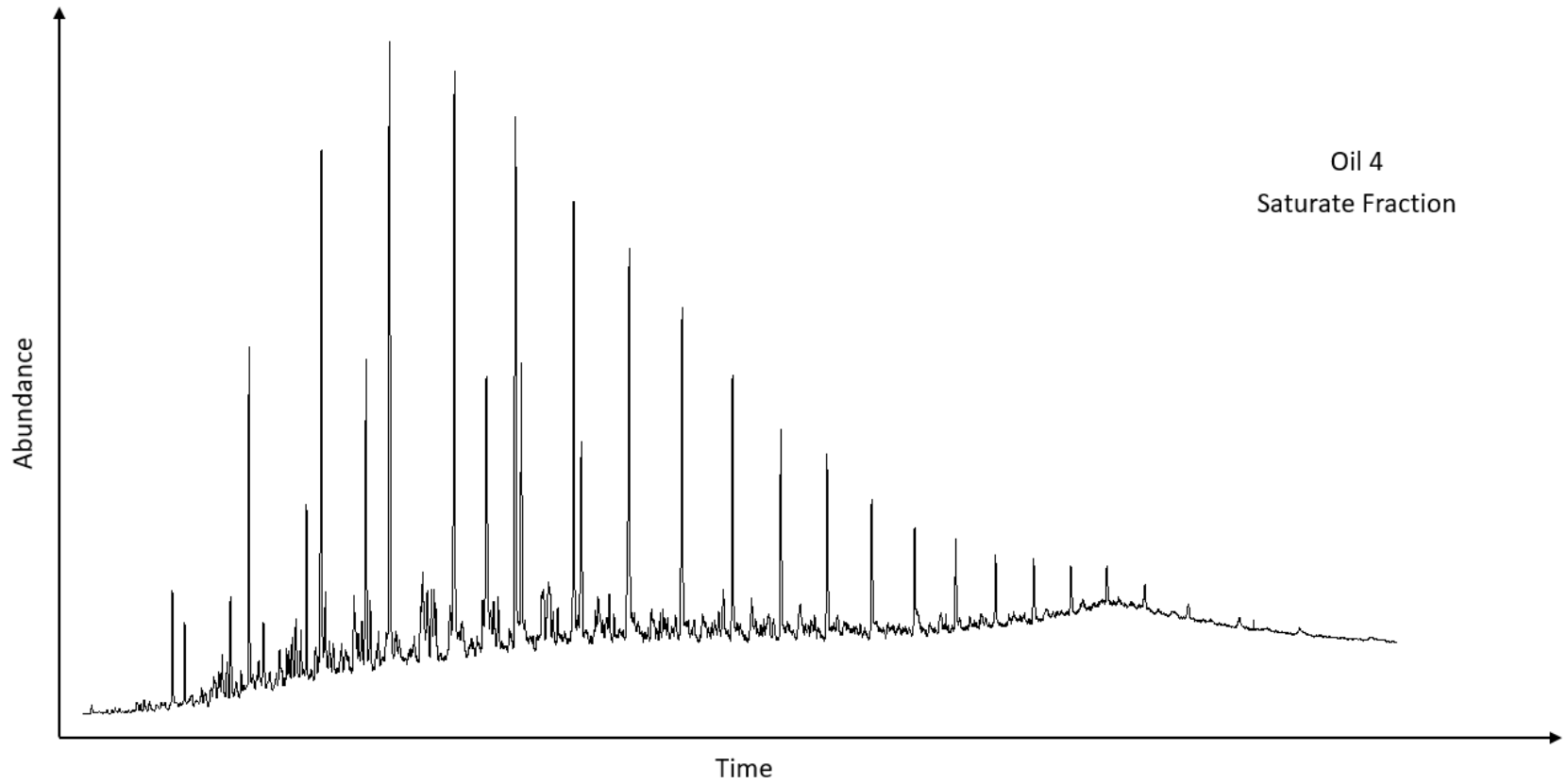
Oil 4
Saturate Fraction
Abundance
Time

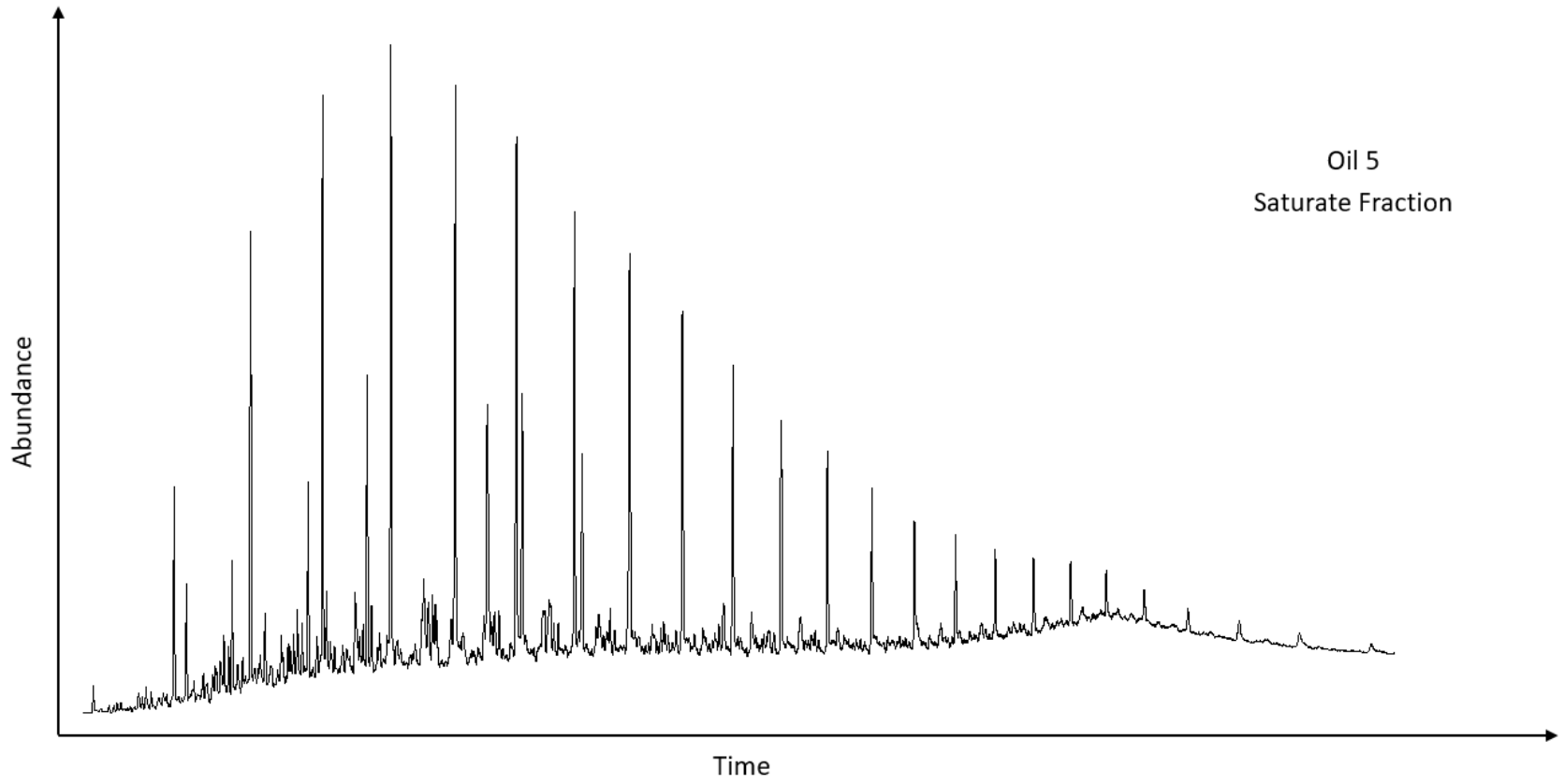
Oil 5
Saturate Fraction
Abundance
Time

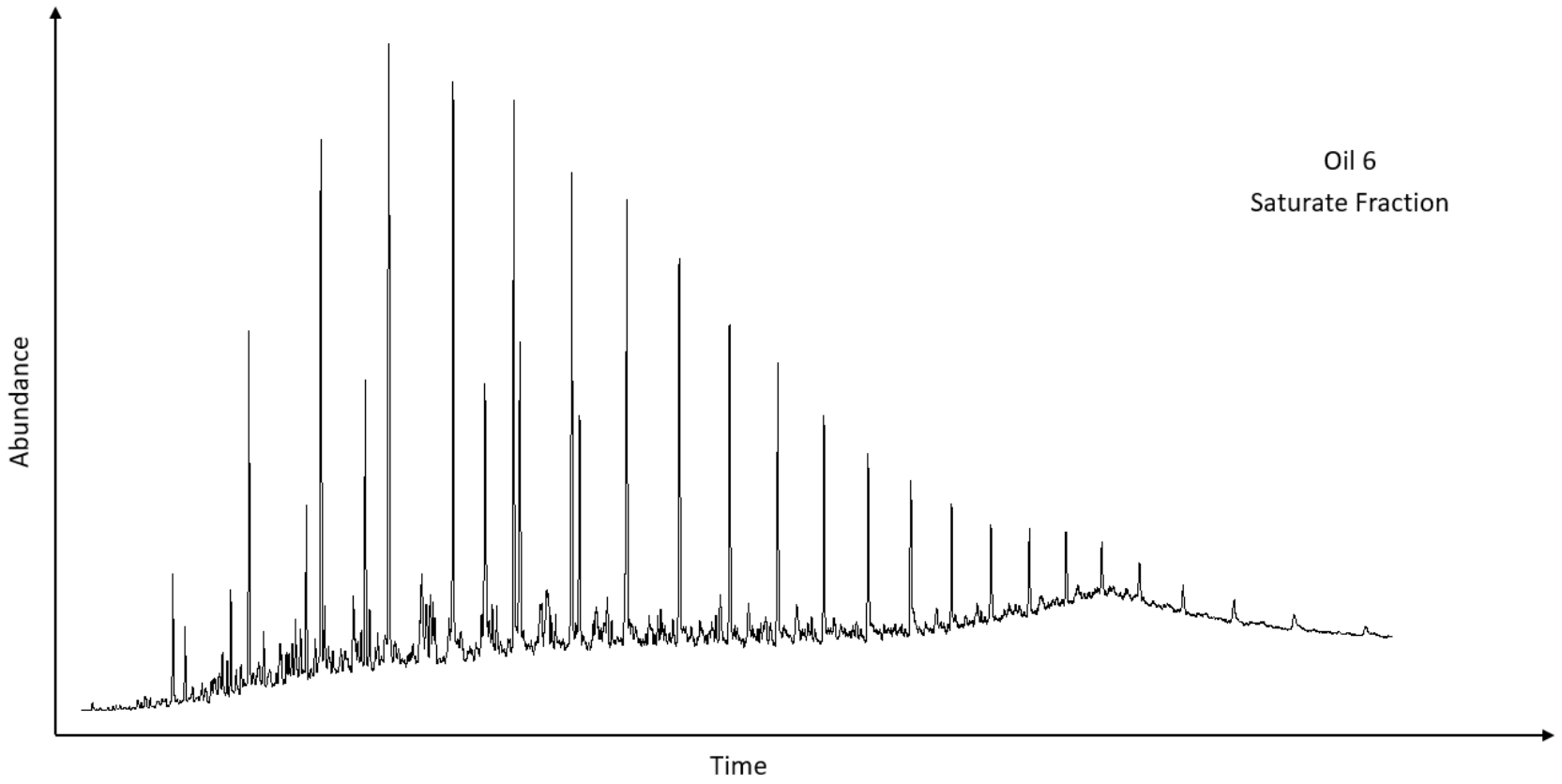
Oil 6
Saturate Fraction
Abundance
Time

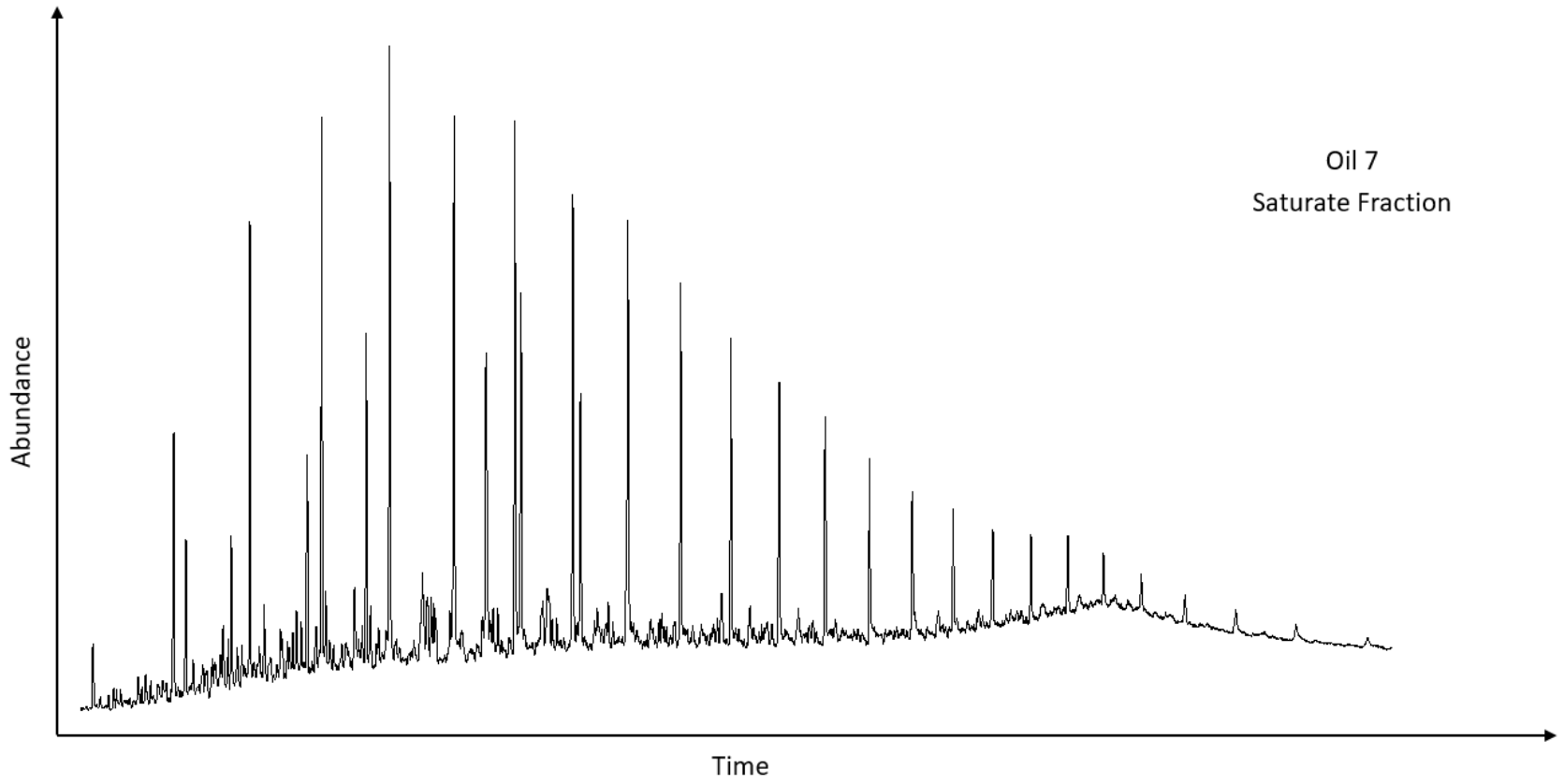
Oil 7
Saturate Fraction
Abundance
Time

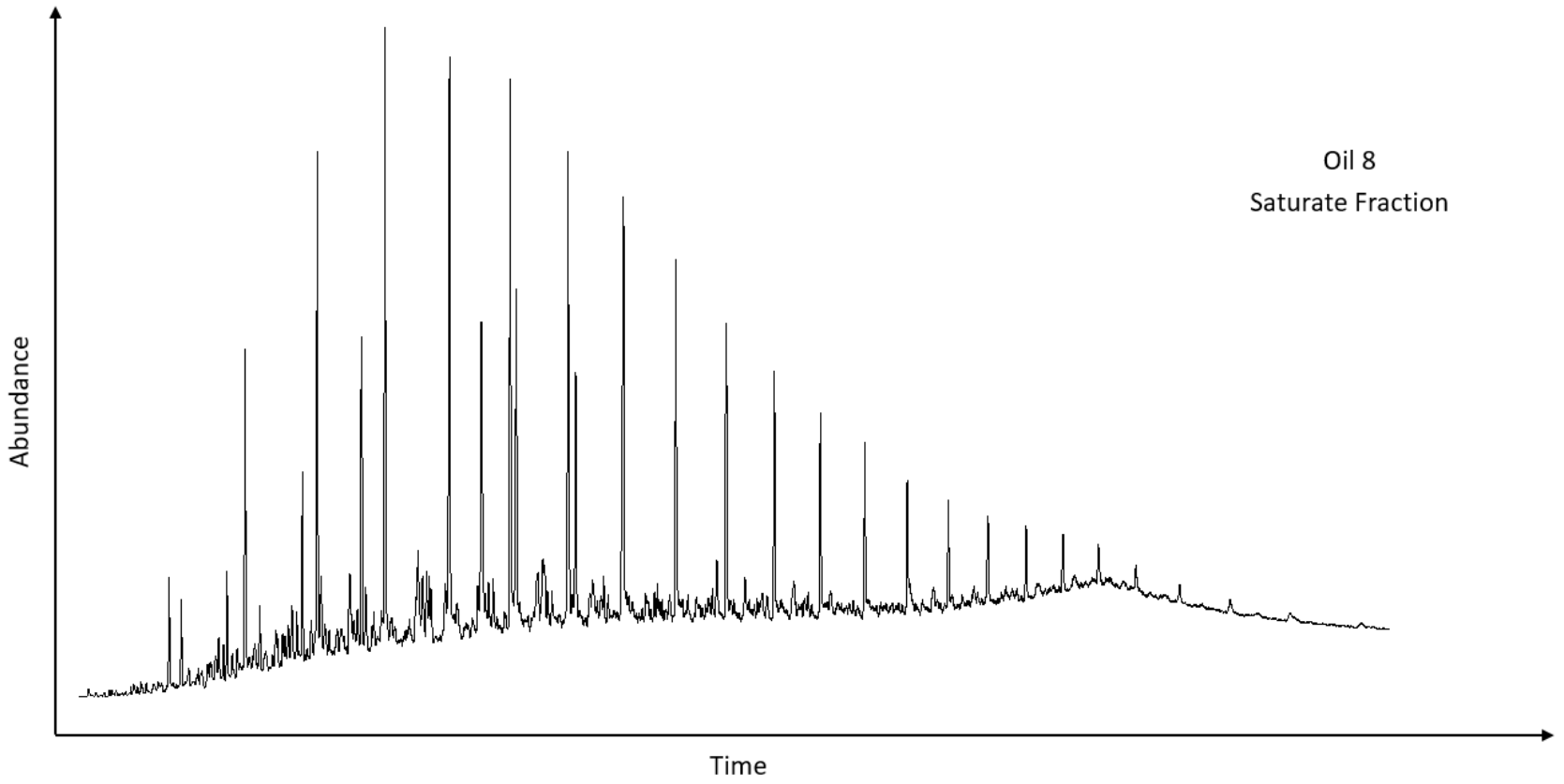
Oil 8
Saturate Fraction
Abundance
Time

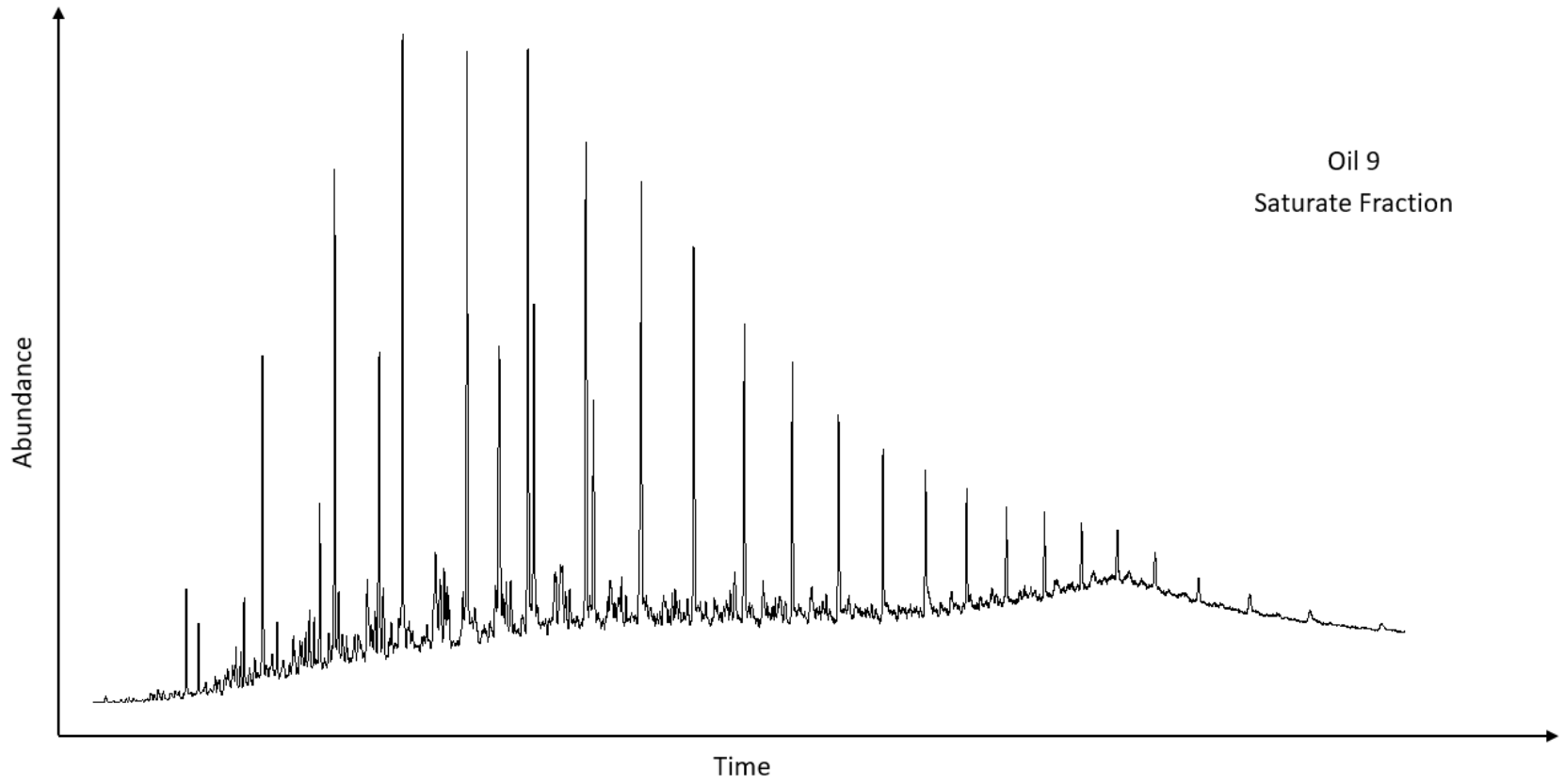
Oil 9
Saturate Fraction
Abundance
Time

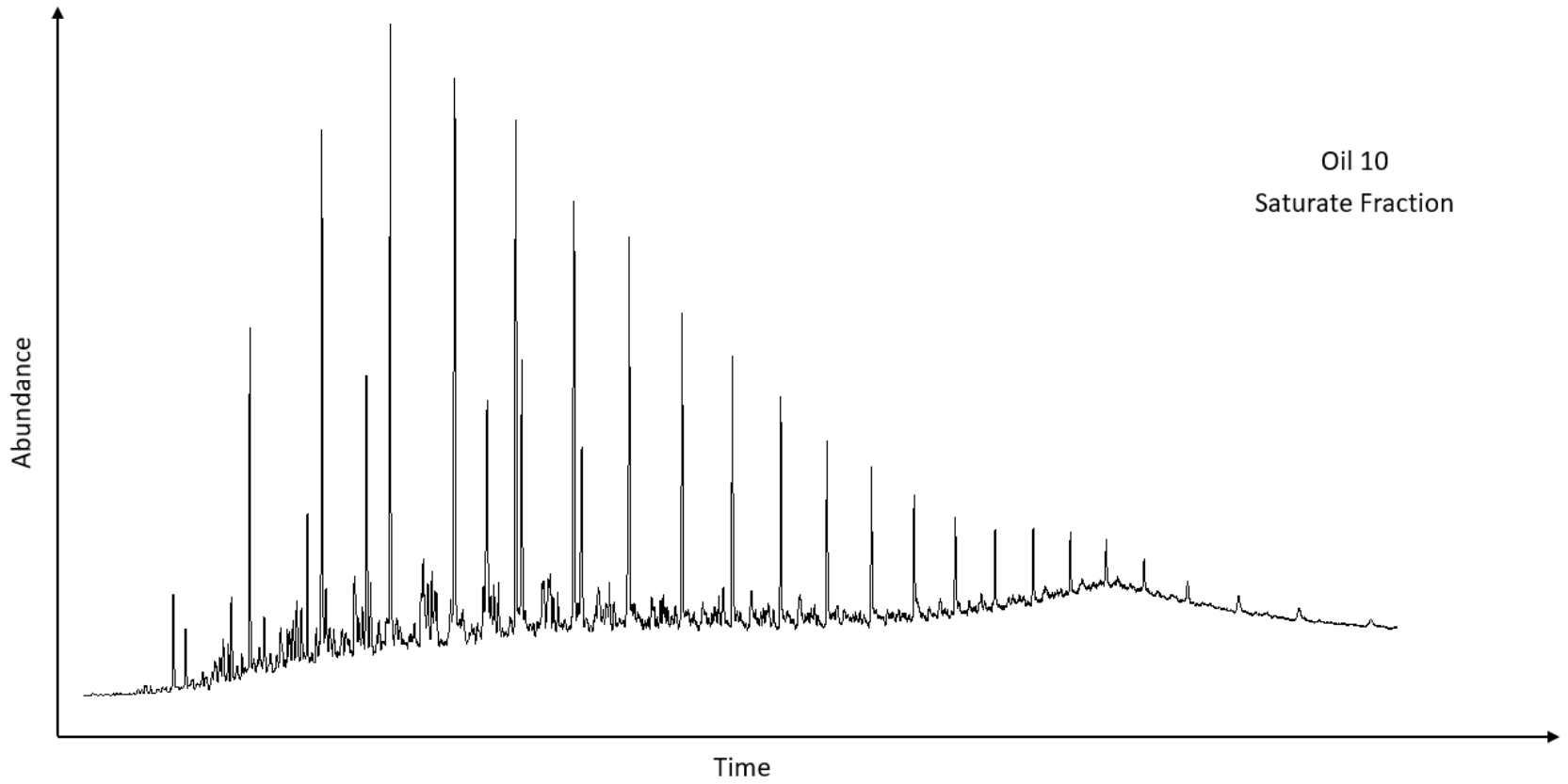
Oil 10
Saturate Fraction
Abundance
Time

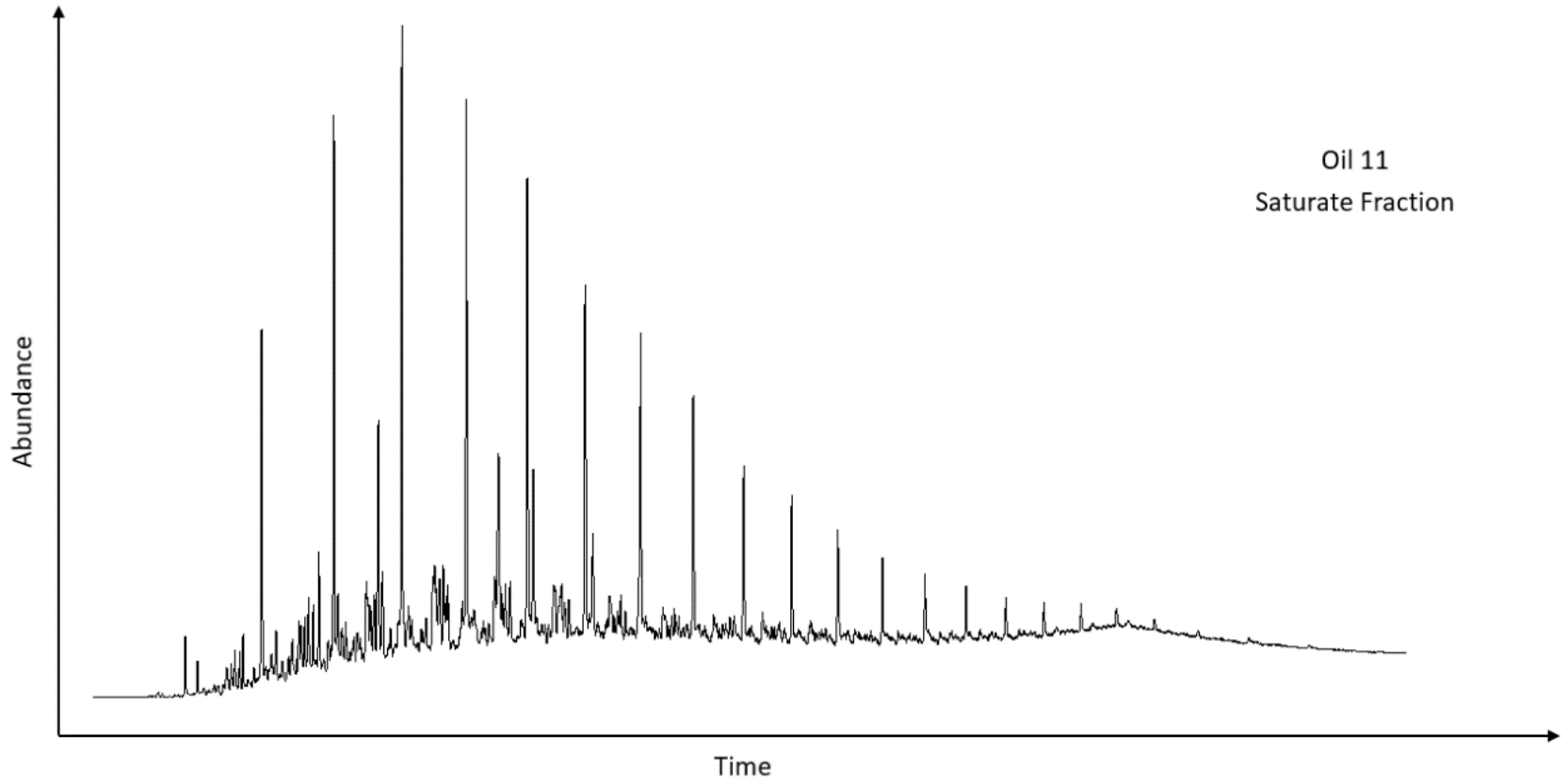
Oil 11
Saturate Fraction
Abundance
Time

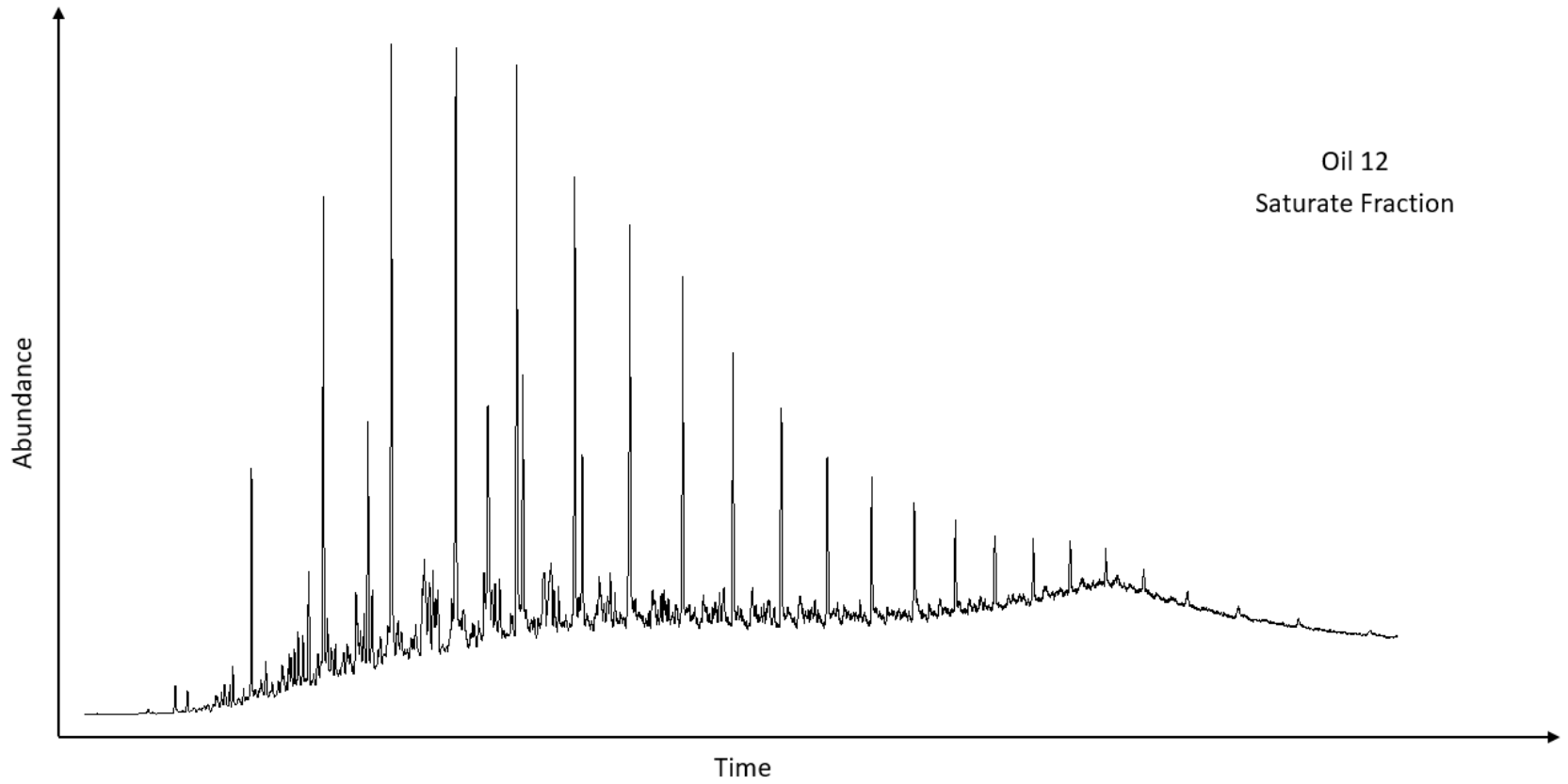
Oil 12
Saturate Fraction
Abundance
Time

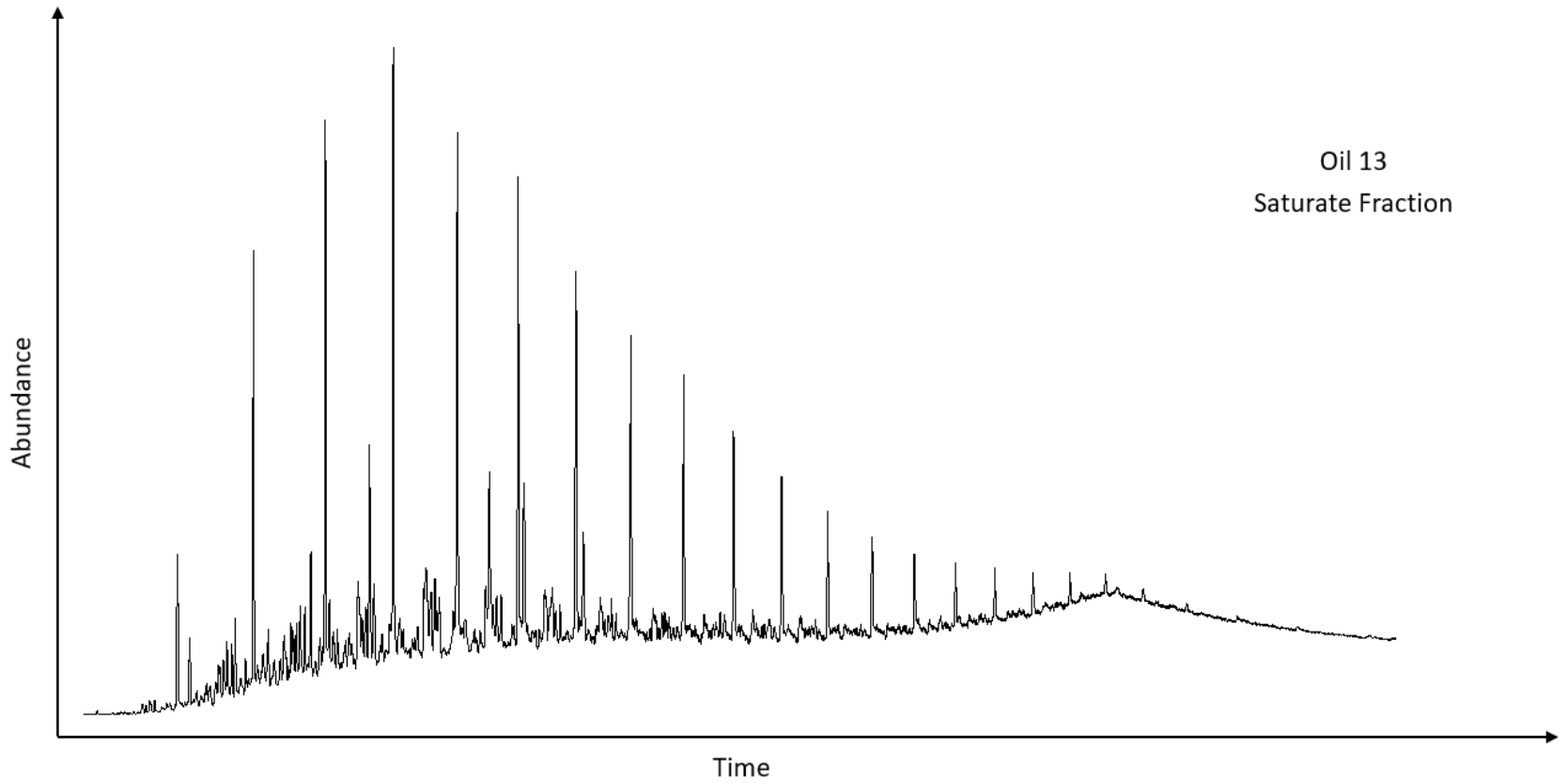
Oil 13
Saturate Fraction
Abundance
Time

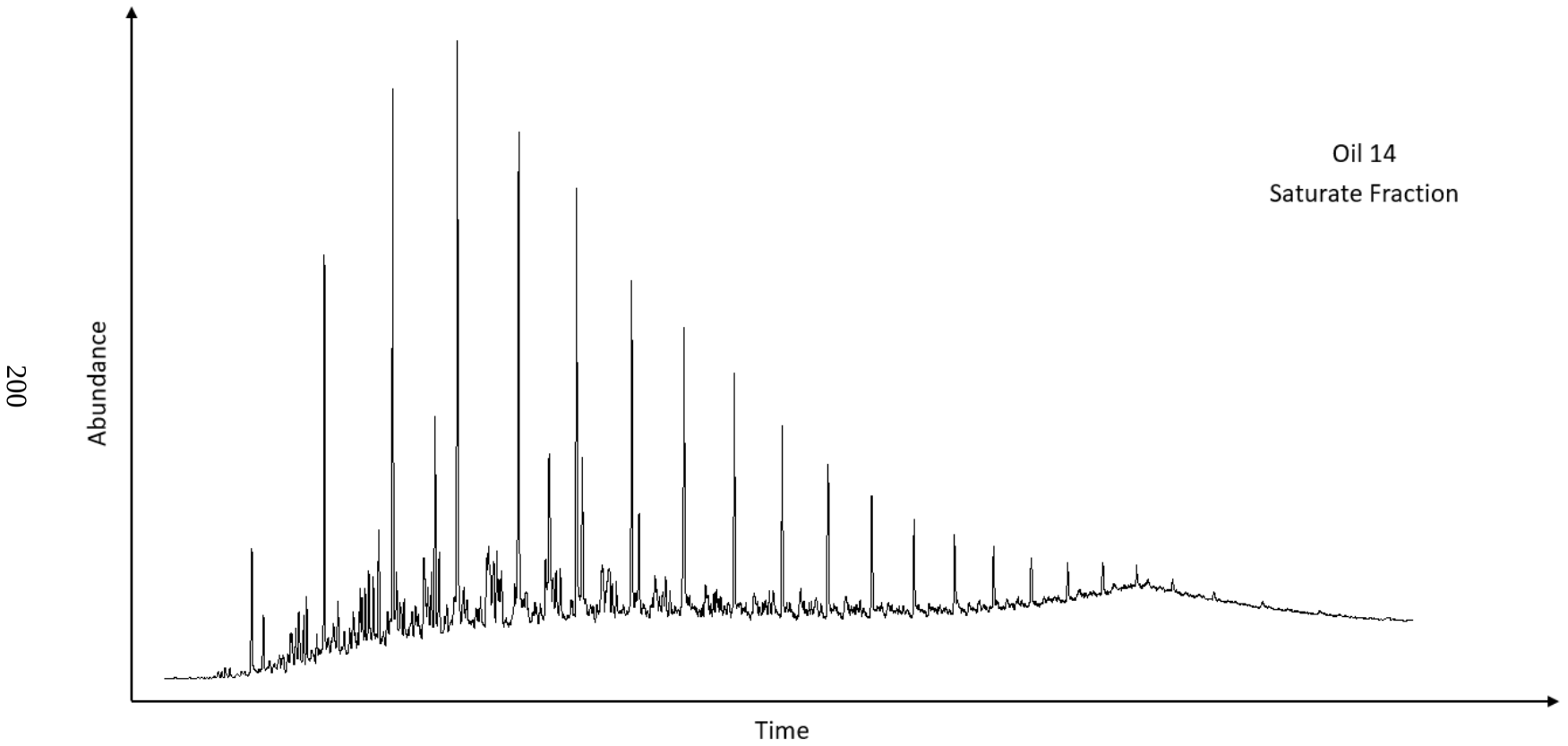
200
Abundance
Time
Oil 14
Saturate Fraction